

**Engineering Kinesthetic Perceptions: The Restoration of Movement Sense in Upper Limb
Prosthetic Use**

By

Jonathon S. Schofield

A thesis submitted in partial fulfillment of the requirements for the degree of

Doctor of Philosophy

Department of Mechanical Engineering
University of Alberta

© Jonathon S. Schofield, 2017

Abstract

Upper limb movement yields rich streams of sensory information that are cortically integrated with motor commands. This is drastically altered in those with upper limb (UL) amputation as sensations of touch and movement are inherently lost. This absence impedes prosthetic control by forcing reliance on visual cues and other indirect means to effectively operate one's prosthesis. This increases the cognitive burden placed on the user as the prosthesis requires continual attention. While advanced prostheses have been developed, 23-39% of users still reject their devices. A major factor is the absence of physiologically relevant sensation. A unique approach to address this challenge is targeted reinnervation (TR) surgery, which reroutes residual nerves that once serviced a patient's amputated hand to strategic muscles in the residual limb (RL). This restores sensation in the missing limb and aids in intuitive control of prostheses. While the return of cutaneous sensations has been reported, an equally vital component to limb control, movement (kinesthetic) sensibility, has yet to be investigated.

In this thesis, we highlight an approach for providing kinesthetic sensory feedback communicated to prosthetic users through the existing sensory channels once present in their missing limb. Our approach leveraged the reinnervated anatomy of participants who had previously undergone TR surgery, and the kinesthetic illusion. The latter is a phenomenon whereby vibration of musculotendinous regions of a limb induces sensations of limb movement. Through able-bodied trials, we developed an applied understanding of the kinesthetic illusion in preparation for translation into an amputee population. In a group of participants who have undergone transhumeral amputation and TR surgery, we demonstrated that we could purposefully elicit sensations of missing hand movement and link these sensations to the

movement of commercially available prosthetic components. Integrating these techniques into functional prostheses required the development of novel prosthetic sockets allowing vibration stimulators access to the RL, while maintaining socket fit, security and suspension. The engineering challenges of this task necessitated the development of foundational information that is largely absent, such as understanding the socket interfaces mechanics of transhumeral prostheses. A novel socket design was fabricated to incorporate our feedback system, and the RL-socket contact pressures were evaluated. Through comparison to the traditional socket data, it was determined that the novel socket not only successfully integrated a kinesthetic feedback system, but allowed investigators to target specific anatomical locations on the RL for the application of contact pressures. Lastly, a numerical predictive model was developed as a foundation for a future clinical socket design tool. Through the application of finite element analysis, we demonstrated a proof-of-concept model that is capable of predicting the locations and magnitudes of contact pressures occurring between the RL and socket. Applications of this model may allow for the evaluation of novel sensory-integrated prosthetic socket prior to their physical fabrication.

Taken together, this work addresses very real, practical challenges associated with UL prosthetic use. It provides foundational information for the advancement of sensory-motor integrated prosthesis and holds the potential to help restore sensation, and improve prosthetic function.

Preface

This thesis is an original work by Jonathon S. Schofield. The research project, of which this thesis is a part, received research ethics approval from the University of Alberta Research Ethics Board, Restoring upper limb movement sense to amputees, REMO: MS6_Pro00034663, and Pro00030709, The Development and Clinical Testing of Advanced Myoelectric Technologies.

The research conducted for this thesis forms part of international research collaboration, led by Dr. Paul Marasco of the Cleveland Clinic, under a National Institutes of Health (NIH) Director's Transformative R01 Research Award, 1R01NS081710-01, with Dr. Jacqueline Hebert being the local principal investigator at the University of Alberta.

This thesis contains information published in four journal articles, with two additional manuscripts currently in peer review:

The majority of Chapter 2 has been published as:

Schofield JS, Evans KR, Carey JP, Hebert JS. (2014). Applications of sensory feedback in motorized upper extremity prosthesis: a review. *Expert Reviews of Medical Devices*. 11(5): 499-511.

A first author role was shared with Evans KR. Contributions included: literature search and review, organization and analysis of literature, figure and table generation, writing and preparing draft manuscripts, writing and preparing revisions during peer review.

The majority of Chapter 3 has been published as:

Schofield JS, Dawson MR, Carey JP, Hebert JS. (2015). Characterizing the effects of amplitude, frequency and limb position on vibration induced movement illusions: Implications in sensory-motor rehabilitation. *Technology and Healthcare*. 23(2): 129-41.

Contributed as a first author: designed experimental protocols, assisted in fabrication of experimental apparatuses, scheduled human participants, collected and analyzed experimental data, generated figures and tables, wrote draft manuscripts, lead the writing and organization of revisions during peer review.

Portions of Chapter 4 are in preparation for publication as:

Marasco PD, Hebert JS, Sensinger JW , Shell CE, **Schofield JS**, Thumser ZC, Nataraj R, Beckler DT, Dawson MR, Blustein DH, Gill S, Mensh BD, Granja-Vazquez R, Newcomb MD, Carey JP, Orzell BM. Engineered illusory movement percepts improve motor control for bionic prosthetic hands. In preparation

Contributed as a coauthor: participated in design of experimental protocol, contributed to data synthesis, assisted in figure generation, participated in the preparation and review of draft manuscripts.

The majority of Chapter 5 has been submitted for publication as:

Schofield JS, Hebert JS, Marasco PD, Carey JP. (2014). Advances in the quantification and prediction of prosthetic socket interface mechanics: A fifteen year review. In preparation

Contributed as a first author: performed literature search and review, organized and analyzed literature, generated figures, prepared draft manuscripts for coauthor review, lead in writing and organizing of revisions.

The majority of Chapter 6 has been published as:

Schofield JS, Evans KR, Hebert JS, and Carey JP. (2016). The Effect of Biomechanical Variables on Force Sensitive Resistor Error: Implications for Calibration and Improved Accuracy. Journal of Biomechanics. 49(5): 786-792

Contributed as the first author: designed experimental protocols, developed and fabricated experimental apparatuses, synthesized and analyzed data, generated figures and tables, authored draft manuscripts for coauthor review, lead the writing and organizing of submissions during peer review.

The majority of Chapter 7 has been published as:

Schofield JS, Schoepp KR, Williams HE, Carey JP, Marasco PD, Hebert JS. (2017).

Characterization of interfacial socket pressure in transhumeral prostheses: a case series. PLOS one. <https://doi.org/10.1371/journal.pone.0178517>

Contributed as a first author: designed experimental protocols, designed and fabricated experimental apparatuses, scheduled human participants, collected and analyzed experimental data, generated figures and tables, wrote draft manuscripts, lead the writing and organization of revisions during peer review.

Acknowledgements

Thank you to all of my supervisors, lab mates, family, and friends that have helped support me over the last four and a half years. It has been an exceptionally rewarding and challenging period in my life, and your encouragement has helped shape me as a researcher, academic, and as a person.

I would like to acknowledge my supervisors Jason Carey and Jacqueline Hebert. Both have been incredibly supportive and sympathetic to my needs as a developing young academic. Jason: thank you for going out of your way to get me into a PhD program. I appreciate all of your calm guidance, and your willingness to be available and help over the last number of years.

Jacqueline, I am very grateful for everything you have done to help me develop. You have provided me with fantastic opportunities to perform independent research, but have always been ready to step in when I needed it. Through my work and your guidance you truly set me up for success, not only as a graduate student, but as I pursue a career in academics. Thank you.

Thank you to my lab mates and co-workers. The lab environment has been incredibly supportive and fun to work in. There are too many people to thank individually. The BLINC lab is an exceptionally talented group of people, and I have learned so much from your diverse expertise.

I would like to thank my wife Jessica. Jessica, you have been especially understanding and sympathetic to my academic pursuits. You have seen me through some of the most stressful moments and celebrated with me during my accomplishments. I truly appreciate the love, encouragement and support.

Finally, thank you to my family and friends. Although I am still not convinced most of you understand what it is that I do, you are always willing to listen (or at least pretend). Thanks to my parents, and my brother. You have been an extremely encouraging and a positive influence. Also thank you to my friends who are always ready to jump in and pull me away when I need an escape from work.

Table of Contents

Abstract	ii
Preface.....	iv
Acknowledgements	vii
List of Tables	xiii
List of Figures	xiv

Part I: Development of our feedback approach

Chapter 1. Introduction	1
1.1 Problem Definition	1
1.2 Objectives	1
1.3 Thesis outline	2
1.4 References	5
Chapter 2. Traditional UL prostheses, prosthetic componentry and sensory feedback systems....	7
2.1 Chapter Preface	7
2.2 Traditional Prostheses	7
2.3 Sensory feedback in upper limb prostheses	8
2.3.1 Introduction.....	8
2.3.2 Search Methods.....	10
2.4 Grasp and Touch Sensory Feedback	10
2.5 Substitution Feedback	12
2.5.1 Vibrotactile Feedback	12
2.5.2 Electrotactile Feedback.....	13
2.5.3 Auditory Feedback.....	15
2.5.4 Other Substitution Methods	16
2.6 Modality Matched Feedback.....	17
2.6.1 Mechanotactile Feedback.....	18
2.6.2 Other Modality Matched Methods.....	19
2.7 Somatotopically Matched Feedback	20

2.7.1	Peripheral Nerve Stimulation.....	20
2.7.2	Phantom Mapping.....	20
2.7.3	Targeted Reinnervation.....	23
2.8	Discussion	25
2.8.1	Grasp and Touch Sensation	25
2.8.2	Future directions	28
2.8.3	Translational Capabilities	29
2.9	Conclusions	31
2.10	References	31
Chapter 3. Sensorimotor integration and kinesthesia in able-bodied individuals.....		42
3.1	Chapter Preface	42
3.2	Intact limbs and sensorimotor integration.....	43
3.2.1	Cutaneous Afferents.....	43
3.2.2	Kinesthesia.....	44
3.3	The kinesthetic illusion in able bodied individuals.....	45
3.3.1	Introduction.....	45
3.3.2	Methods.....	48
3.3.3	Discussion	60
3.4	Conclusions	63
3.4.1	References	64
Chapter 4. The application of the kinesthetic illusion in a population with transhumeral amputation...70		
4.1	Chapter Preface	70
4.2	Introduction	70
4.3	Methods.....	72
4.3.1	Percept Mapping	73
4.3.2	Psychophysical Quantification.....	74
4.3.3	Use of the Kinesthetic Illusion with a Physical Prosthesis	76
4.4	Results	79
4.4.1	Percept Mapping	79

4.4.2	Psychophysical Quantification.....	80
4.4.3	Use of the Kinesthetic Illusion with a Physical Prosthesis	81
4.5	Discussion	83
4.6	Conclusions	86
4.7	References	87

Part II: Translation into functional prostheses

Chapter 5. The mechanical understanding of the interface between prosthetic socket and residual limb...90

5.1	Chapter Preface	90
5.2	Introduction	91
5.2.1	Socket-Limb Interactions.....	92
5.2.2	Poor-fit and Tissue Damage.....	93
5.2.3	Quantification of RL-Socket Mechanics	94
5.2.4	Review Objectives	95
5.3	Lower Limb Quantification and Prediction Methods	95
5.3.1	Lower Limb Experimental Measurement Techniques.....	95
5.3.2	Limb Numerical Predictive Techniques	103
5.4	Upper Limb RL-Socket Mechanics.....	111
5.5	Discussion	112
5.5.1	Experimental Measurement Techniques.....	112
5.5.2	Numerical Prediction Techniques.....	113
5.5.3	Future directions	114
5.6	Conclusions	115
5.7	References	116

Chapter 6. The application of thin film sensors in characterizing biomechanical interfaces.....128

6.1	Chapter Preface	128
6.2	Introduction	128
6.3	Methods.....	129
6.3.1	Experimental Variables.....	129

6.3.2	Setup and Procedure	130
6.3.3	Participant Testing	134
6.4	Results	135
6.4.1	Variable Testing.....	135
6.4.2	Participant Testing	140
6.5	Discussion	141
6.6	Conclusions	142
6.7	References	143
Chapter 7. The characterization of socket-residual limb interface mechanics		147
7.1	Chapter preface	147
7.2	Introduction	147
7.3	Methods.....	150
7.3.1	Socket fit	151
7.3.2	Socket pressure measurements	151
7.3.3	Data treatment	153
7.4	Results	154
7.4.1	Participant 1	154
7.4.2	Participant 2	156
7.4.3	Participant 3	157
7.4.4	Participant 4	159
7.5	Discussion	161
7.5.1	Limitations	164
7.6	Conclusions	164
7.7	References	165
Chapter 8. The integration of kinesthetic feedback in a functional prosthetic system		169
8.1	Chapter Preface	169
8.2	Introduction	169
8.3	Methods.....	171
8.3.1	Design criteria	172
8.3.2	Socket Design	173

8.4	Evaluation.....	178
8.4.1	Pressure measurement methods	178
8.4.2	Pressure Measurement Results	181
8.5	Discussion	184
8.6	Conclusions	185
8.7	References	186
Chapter 9. The prediction and modelling of socket-residual limb interface mechanics.....		188
9.1	Chapter Preface	188
9.2	Introduction	188
9.3	Methods.....	191
9.3.1	Participants.....	191
9.3.2	Model Geometry	192
9.3.3	Material Definitions	194
9.3.4	Meshing.....	194
9.3.5	Contact, Loading, and Boundary Conditions.....	195
9.3.6	Model Validation	197
9.4	Results	198
9.4.1	Participant 1	198
9.4.2	Participant 2	199
9.4.3	Model Validation	200
9.5	Discussion	203
9.6	Conclusions	206
Chapter 10. Conclusions and Future Directions		210
10.1	References	213
References		215
Appendix A: Error data for the fitting of calibration equations.....		240
Appendix B: Modified OPUS survey results.....		242
Appendix C: OPUS survey results prior to modelling.....		243
Appendix D: Model loading calculations		244
Appendix E: Mesh Sensitivity Analysis		246

List of Tables

Table 2-1 Methods of sensory feedback	11
Table 3-1 Summary of mechanoreceptors involved in the sense of touch	44
Table 3-2 Time intervals for participants to first experience the illusion.....	54
Table 3-3 ANOVA results.	55
Table 3-4 Output variables correlation coefficients matrix	60
Table 4-1 Participant information	73
Table 6-1 Combinations of Biomechanical Variables Tested	130
Table 6-2 Mean error based on calibration curve used to fit data	137
Table 6-3 ANOVA Table and Effects Estimates for RMSE-C	139
Table 7-1 Descriptions of participants' prosthetic components	151
Table 8-1 Participant demographics and residual limb characteristics.....	171
Table 8-2 Summary of design criteria	173
Table 8-3 Contact pressure results.....	183
Table 9-1 Participant Information.....	191
Table 9-2 Modelled positions and applied reaction forces	196
Table 9-3 Participant 1 predicted contact pressure results.....	199
Table 9-4 Participant 2 contact pressure results.	200
Table 9-5 Validation of predicted locations of high contact pressure.	202

List of Figures

Figure 2.1 Typical upper limb prosthetic components.....	8
Figure 2.2 Vibrotactile feedback.....	12
Figure 2.3 Electrotactile feedback	14
Figure 2.4 Applied elbow torque	16
Figure 2.5 Rotational skin stretch.	17
Figure 2.6 Mechanotactile feedback	19
Figure 2.7 Hypothetical corresponding regions between location of pressure on residual limb	22
Figure 2.8 Overview of targeted reinnervation procedure	24
Figure 2.9 Schematic of the process used to control a myoelectric prosthetic with sensory feedback.....	27
Figure 2.10 Overview of kinesthetic illusion.....	29
Figure 3.1 Hand held voice coil system.....	49
Figure 3.2 Arm positions for the application of vibratory stimulus.....	50
Figure 3.3 Bicep mean plots of significant variables.....	57
Figure 3.4 Tricep mean plots of significant variables.....	59
Figure 4.1 Psychophysical Quantification Setup	75
Figure 4.2 Volitional Control Setup.....	78
Figure 4.3 Cataloged hand movement percepts	79
Figure 4.4 Vibration properties and perceived strength of kinesthetic illusion	80
Figure 4.5 Limb matching (passive) timing results	81
Figure 4.6 Volitional control (active) timing results.....	83
Figure 4.7 Movement percepts matched to a prosthetic hand.....	84
Figure 5.1 Cross sectional view of a trans-tibial residual limb with prosthetic liner and socket donned. ..	92
Figure 5.2 A hierarchical breakdown of experimental measurement techniques	96
Figure 5.3 A breakdown of the primary definitions necessary in FEM model building.....	104
Figure 5.4 Prominent methods to define modelled component geometries.....	105
Figure 5.5 Prominent meshes used in modelled geometries	106
Figure 5.6 Prominent material definitions subdivided by modelled component	108
Figure 5.7 Prominent boundary conditions defined in FEM models	109
Figure 5.8 A graphical summary of the validation methods from the reviewed literature	110
Figure 5.9 Prosthetic fabrication work flow diagram	114
Figure 6.1 Experimental Setup.....	131

Figure 6.2 Example of the data treatment process for small round sensor 1	133
Figure 6.3 Experimental Setup for Participant Trials	134
Figure 6.4 Baseline Calibration Curves	136
Figure 6.5 RMSE-C Mean Plots for each Experimental Variable	138
Figure 6.6 Participant Testing Data for Individual FSR Sensors.....	140
Figure 7.1 Participant demographics and residual limb characteristics	150
Figure 7.2 Equilibration and calibration apparatuses.....	152
Figure 7.3 Experimental results for Participant 1	155
Figure 7.4 Experimental results for Participant 2	157
Figure 7.5 Experimental results for Participant 3	159
Figure 7.6 Experimental results for Participant 4	160
Figure 8.1 Vibration factor and stimulus location.....	173
Figure 8.2 Prosthetic liner and electrode contacts.	175
Figure 8.3 Prototype socket design.....	176
Figure 8.4 Kinesthetic factor integration and assembly	177
Figure 8.5 The donned prototype prosthesis.	178
Figure 8.6 Equilibration and calibration apparatuses.....	180
Figure 8.7 The four static testing positions.....	181
Figure 9.1 Creation of the residual limb model	193
Figure 9.2 Boundary conditions employed to simulate socket donning	195
Figure 9.3 Boundary and loading conditions employed to simulate prosthetic loading	197

Chapter 1. Introduction

1.1 Problem Definition

Healthy upper limb (UL) movement is a closed loop control system in which rich streams of sensory information are integrated cortically with motor commands. This is drastically altered in those with UL amputation as the mechanisms providing sensory feedback that once encoded touch and movement information are no longer present. While advanced prostheses have been developed to augment lost motor function, 23-39% of users still reject their devices¹. A major factor is the absence of physiologically relevant sensation². This forces the user to rely heavily on vision and significantly increases the conscious attention one must pay to their prosthesis for adequate operation. A unique approach to address this challenge lies in targeted reinnervation (TR) surgery. This reconstructive procedure strategically denervates (surgically disconnects nerves to) muscle sites in the patient's residual limb or chest. The residual nerves that once serviced the patient's amputated hand are then transposed (surgically connected) to these target muscle sites^{3,4}. This technique was initially developed for improved control of prostheses; however, it has also been shown to restore cutaneous sensation of the missing hand⁵. Literature highlights strategies to harness this technique for intuitive touch-based prosthetic feedback⁶. However, kinesthetic (movement) based feedback is a vital contributor to UL motor control and movement accuracy. Techniques communicating relevant kinesthetic information that is intuitive and readily interpreted by the user have yet to be developed or translated into functioning UL prosthetic systems.

1.2 Objectives

This thesis focuses on the exploration and development of a novel sensory feedback technique allowing movement of the prosthesis to be experienced by the user as occurring in the missing limb. Our approach leveraged the reinnervated anatomy of transhumeral participants who have undergone TR surgery, and the kinesthetic illusion; a phenomenon whereby vibration of musculotendinous regions of a limb induces sensations of limb movement⁷. In this thesis we detail the exploration and characterization of the kinesthetic illusion in an able-bodied population and in transhumeral amputees with targeted reinnervation. Bridging the gap between laboratory

and clinical applications, this work integrates our feedback into a functional prosthesis and develops fundamental techniques to measure (using thin-film sensors) and numerically predict (through finite element analyses) the mechanical impact of the feedback system on prosthetic fit.

1.3 Thesis outline

In this thesis we develop an approach for providing kinesthetic sensory feedback communicated to prosthetic users through the existing sensory channels once present in their missing limb. This work crosses a spectrum of development ranging from the applied understanding of the kinesthetic illusion, through the integration in a functional prosthesis, and the quantitative evaluation of the prototyped prosthesis on a user's RL. This work forms the foundations that will enable the transition of our techniques beyond the laboratory and has the potential contribute to UL socket design independent of sensory feedback systems. This work addresses known contributors to prosthetic abandonment by addressing both sensory feedback and evaluation of socket fit. Future development of this work has the potential to provide well-fit sensory integrated prostheses, thereby improving function for those with UL amputation.

This work is developed over a series of chapters and divided into two parts. Part I details the development of our feedback approach. A review of the current state of sensory feedback in UL prostheses is provided in chapter 2. We then developed an applied understanding of vibration induced movement illusions through able-bodied studies in chapter 3, and applied these techniques with an amputee population and prosthetic components in chapter 4. Part II focuses on the translation of our feedback approach into a functional prosthetic system. Chapter 5 provides a review of the mechanical evaluation techniques currently used in the prosthetics field, and highlights significant gaps in UL socket evaluation. Chapters 6 and 7 adapted the techniques described in chapter 5 such that they form the basis for quantitative evaluation of novel UL prosthetic sockets. A novel sensory integrated prosthesis is discussed in chapter 8 and the evaluation techniques developed in subsequent chapters are employed. Finally, chapter 9 describes a numerical prediction tool developed to help facilitate the future design of novel UL prostheses and sensory integrated prosthetic sockets.

Part I: Development of our feedback approach

Chapter 2: Traditional UL prostheses, prosthetic componentry and sensory feedback systems.

In this chapter, a general background is provided that introduces traditional upper limb prostheses, prosthetic componentry and sensory feedback systems. This chapter includes a review paper that highlights the epidemiology of UL amputation and prosthetic use, prevalent techniques employed for providing touch and movement based prosthetic feedback, and discussion around the limitations and future directions of such systems.

Chapter 3: Sensorimotor integration and kinesthesia in able-bodied individuals.

In this chapter, we provide relevant background information in able-bodied individuals around the concept of sensorimotor integration with a specific focus on kinesthesia. We include portions of a manuscript detailing preliminary work with an able-bodied population that explores the kinesthetic illusion in preparation for translation to an amputee population and prosthetic systems.

Chapter 4: The application of the kinesthetic illusion in a population with transhumeral amputation.

Chapter 4 is composed of a selection of material describing and characterizing the application of the kinesthetic illusion in a participant population that has undergone transhumeral amputation and targeted reinnervation surgery. Movement patterns of kinesthetic sensations experienced by participants are characterized, psychophysical measures are employed to quantify illusionary responses to stimulus parameters, and a proof of concept experiment linking experienced kinesthetic sensations to movement of a commercially available prosthetic hand is presented.

Part I: Translation into functional prostheses

Chapter 5: The mechanical understanding of the interface between prosthetic socket and residual limb.

In this chapter we describe the mechanical aspects of the interface between a transhumeral prosthetic socket and the RL; an immediate challenge for translation of our kinesthetic feedback approach into functional prostheses. The importance of understanding this mechanical interface is highlighted in the context of developing novel prosthetic sockets capable of accommodating feedback mechanisms. A review manuscript is included that focuses on empirical and predictive techniques currently employed in prosthetic literature that attempts to understand this interface. Advantages, limitations and the necessary future directions to enable novel socket design are discussed.

Chapter 6: The application of thin film sensors in characterizing biomechanical interfaces.

In this chapter we discuss the application of thin film sensors as a method to address the lack of empirical evidence in UL socket work. Advantages and limitations of use of these sensors are discussed with proposed recommendations for improved sensor accuracy and precision. This work is presented in preparation of employing this sensing technology to empirically characterize UL socket-RL interface mechanics.

Chapter 7: The characterization of socket-residual limb interface mechanics.

A case series is presented in which thin film sensors were used to assess pressure development across the RL resulting from well fit transhumeral prosthetic sockets. Anatomical locations bearing maximum pressure, the size of these areas, and relative magnitudes of the pressure are highlighted. Discussions around the design applications and clinical applicability of these methods and data are provided.

Chapter 8: The integration of kinesthetic feedback in a functional prosthetic system.

A novel prosthetic socket that was developed with the goal of incorporating a kinesthetic feedback device is described in this chapter. Design requirements, solutions and fabrication of

the socket are detailed. Using the techniques presented in chapters 6 and 7, the RL-socket interface mechanics are compared and contrasted between the novel design and a traditional well fit prosthetic socket.

Chapter 9: The prediction and modelling of socket-residual limb interface mechanics.

In this chapter, the preliminary development of a predictive numerical tool is highlighted in the context of novel prosthetic socket design and fabrication. A finite element model with the potential to predict the interfacial mechanics and tissue response of the RL to a socket design prior to fabrication is presented. The limitations and necessary future directions are discussed with specific focus on addressing barriers to potentially enable clinical translation of such a tool.

Chapter 10: Conclusions and future directions.

This chapter includes concluding remarks and frames the work presented in the context of translation from the laboratory into functional prosthetic systems.

1.4 References

1. Biddiss E, Chau T. Upper limb prosthesis use and abandonment: A survey of the last 25 years. *Prosthet Orthot Int*. 2007;31(3):236-257. Accessed 24 January 2014.
2. Biddiss E, Chau T. Upper-limb prosthetics: Critical factors in device abandonment. *Am J Phys Med Rehabil*. 2007;86(12):977-987. Accessed 16 March 2017. doi: 10.1097/PHM.0b013e3181587f6c.
3. Kuiken TA, Dumanian GA, Lipschutz RD, Miller LA, Stubblefield KA. The use of targeted muscle reinnervation for improved myoelectric prosthesis control in a bilateral shoulder disarticulation amputee. *Prosthet Orthot Int*. 2004;28(3):245-253. Accessed 20 December 2013.
4. Hebert J.S., Elzinga K., Chan M., Olson J., Morhart M. Updates in targeted sensory reinnervation for upper limb amputation. *Current Surgery Reports*. 2014;2(45).

5. Kuiken TA, Marasco PD, Lock BA, Harden RN, Dewald JPA. Redirection of cutaneous sensation from the hand to the chest skin of human amputees with targeted reinnervation. *Proc Natl Acad Sci U S A*. 2007;104(50):20061-20066. Accessed 20 December 2013.
6. Schofield JS, Evans KR, Carey JP, Hebert JS. Applications of sensory feedback in motorized upper extremity prosthesis: A review. *Expert Review of Medical Devices*. 2014;11(5):499-511. Accessed 8 April 2015.
7. Goodwin GM, McCloskey DI, Matthews PBC. The contribution of muscle afferents kinaesthesia shown by vibration induced illusions of movement and by the effects of paralyzing joint afferents. *J Physiol (Lond)*. 1972;536:635-647. Accessed 24 May 2013.

Chapter 2. Traditional UL prostheses, prosthetic componentry and sensory feedback systems

The majority of this chapter has been published as:

Schofield JS, Evans KR, Carey JP, Hebert JS. (2014). Applications of sensory feedback in motorized upper extremity prosthesis: a review. *Expert Reviews of Medical Devices*. 11(5): 499-511.

2.1 Chapter Preface

This chapter establishes relevant background information for the subsequent chapters of this thesis. We present a broad overview of upper limb prostheses, prosthetic control and prosthetic sensory feedback as to provide context for the research presented in this thesis. This chapter includes discussions on traditional UL prostheses, prosthetic componentry and sensory feedback systems. Additional information is provided to highlight the epidemiology of upper limb loss, as well as the practical challenges, and future directions of prosthetic sensory feedback systems.

2.2 Traditional Prostheses

Traditional UL prostheses are constructed of a number of key components (Figure 2.1). The prosthesis interfaces with the user at the prosthetic socket. The socket is contoured to utilize the morphology of the user's residual limb for suspension and mechanical stability. The socket is suspended using additional harnessing strapped across the user's chest or other shoulder, and may incorporate an air tight seal on the residual limb to create suspension via passive vacuum pressure. Users may wear optional silicone or gel liners rolled over their residual limb prior to donning the prosthetic socket. These liners help pre-shape residual soft tissues and can increase comfort as well as improve socket fit. Attached distally to the socket are the prosthetic components, which consist of various combinations of commercially available prosthetic shoulders, elbows, wrists and terminal devices (also called the hand or prehensor). Prosthetic components can be controlled mechanically using a system of cables and body movements or

electronically using servo motors actuated through a controller and electrodes placed on residual muscles, termed electromyography (EMG) or myoelectric control.

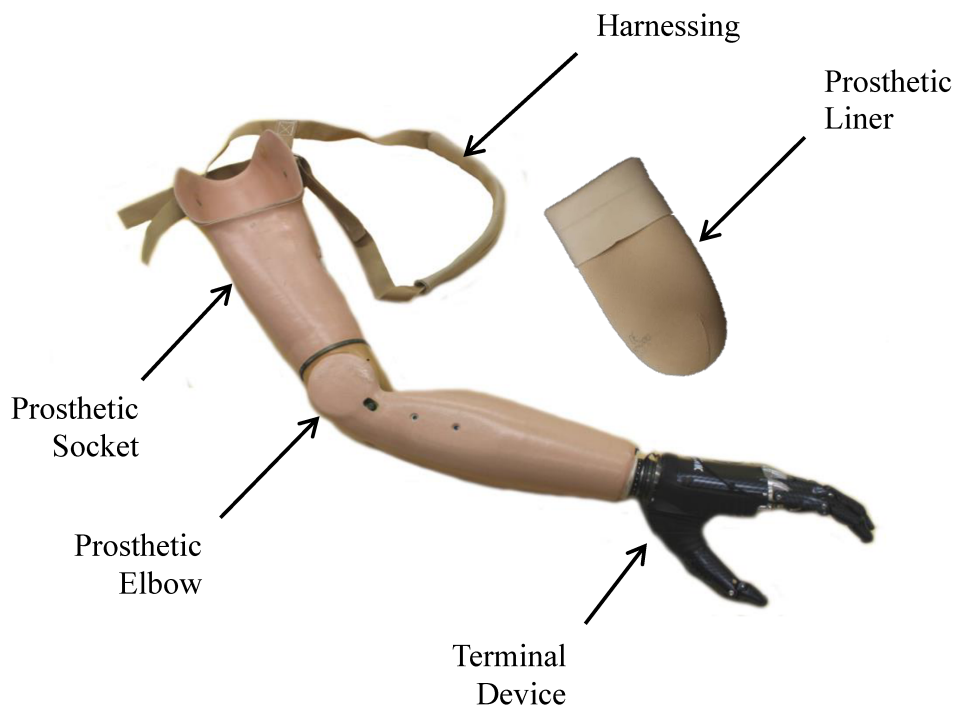


Figure 2.1 Typical upper limb prosthetic components

2.3 Sensory feedback in upper limb prostheses

2.3.1 Introduction

In 2005, there were an estimated 1.6 million people living in the United States with the loss of a limb, 34% of which were upper limb¹. Upper limb loss is one of the most difficult challenges for prosthetic replacement, given the complexity of fine sensory input and dexterous function of a hand. The loss of a hand can significantly reduce quality of life leaving an individual feeling less capable and more dependent¹⁶. Prosthetic arms are designed with the goal of restoring function to those with upper limb loss.

Upper limb prosthetic functionality is ultimately dependent on the user's ability to efficiently control, and comfortably interface with their prosthesis. It follows that having intuitive control

would increase the utility of the device. Yet closely mimicking the performance of a human hand and arm is technically challenging. A normal hand is capable of coordinating movements with 27 degrees of freedom to perform strength based grasping functioning as well as highly coordinated precision movements²⁶. Recently, there have been extensive advances in motorized, multi-articulate prosthetic arms that are capable of a wide range of grasps and movement². These prostheses are controlled using surface EMG signals generated by the muscles. While extensive technical developments are being made in myoelectric (EMG controlled) prostheses, significant barriers remain that prevent them from being as widely accepted as traditional body powered hook-and-pulley systems²⁷.

Execution of dexterous hand movements is highly dependent on both efferent motor control and afferent sensory feedback. Sensory feedback mechanisms relay exteroceptive and proprioceptive information to higher control centers in the brain⁹, and are responsible for detecting grip force and hand position, as well as object shape, compliance, and textures, among others⁸. Therefore, the basis of hand movement is closed loop motor control comprised of a dynamic interplay between motor output and sensory input^{9,28,29}. The loss of an upper extremity significantly alters this closed loop control strategy as sensations of touch and movement are inherently lost. Those with upper limb loss become dependent on their prosthesis to restore lost motor function; however, most myoelectric prostheses are open loop devices and are thus unable to communicate external stimulus acting on the prosthesis to the user. The absence of exteroceptive and proprioceptive sensibility impedes efficient use of the prosthesis. 29% to 39% of upper limb amputees will discontinue use of their prosthesis⁵ with lack of sensory feedback often being highlighted as a major contributing factor^{6,9,16,30}. Typically, prosthetic users adopt a system of strategies to compensate for this lack of sensory information; they rely heavily on visual feedback, as well as indirect feedback mechanisms such as the sound of the motors, vibrations, and changes in pressure on the residual limb⁹. Consequently, the cognitive demand placed on the user is greatly increased as operation of the prosthesis requires high and continuous conscious attention^{10,31}.

A review by Antfolk *et al.* highlighted the need to interface prosthetic limbs with sensory feedback, and reported on numerous strategies to address prosthetic sensibility¹². These systems

have yet to be incorporated in prostheses for long term use or convincingly proven usable outside of a laboratory. Furthermore, no commercially available myoelectric prosthesis actively provides sensory feedback to the user¹². Therefore, a gap currently exists between research prototypes and devices with clinical translational capabilities.

The objectives of this review are to highlight and compare methods for providing amputees with prosthetic sensibility that have been detailed in research based literature. Methodologies for communicating prosthetic grasp and touch information will be discussed, including selected designs and test results within each research area. An overview of future directions including promising methods for grasp and touch feedback, approaches for establishing proprioceptive or kinesthetic feedback, as well as clinical and translational challenges are also provided.

2.3.2 Search Methods

Scopus was used as the primary literature database and cross referenced with PubMed. The literature reviewed has been published prior to June 2016. The following key words were used in the search for literature: *prosthetic sensory feedback*, *haptic prosthetic feedback*, *prosthetic sensory substitution*, *targeted reinnervation*, and *prosthetic tactile display*. This paper focuses on *methods* for providing sensory feedback to upper limb amputees; it is not meant to be an exhaustive review of individual feedback devices.

2.4 Grasp and Touch Sensory Feedback

Sensory feedback systems employ instrumentation (or *sensors*) at the prosthetic level to detect an external stimulus. This instrumentation in turn drives the output of a haptic feedback device (also termed *tactor* in this review) that conveys information about the external stimulus to the prosthetic user. Various types of tactors have been reported in the literature, relying on methods such as vibration, pushing or shear force to communicate the external stimulus to the user. The method used to communicate information through the tactor to the user is defined as the *feedback signal*. This paper categorizes feedback systems in terms of how the user experiences the feedback signal. The sensory feedback systems reviewed in this paper have been divided into three categories: substitution, modality matched and somatotopically matched methods (Table 2-1).

Table 2-1 Methods of sensory feedback

Sensory feedback	Substitution	Vibrotactile
		Electrotactile
		Auditory
		Other methods
	Modality matched	Mechanotactile
		Other methods
	Somatotopically matched	Neural stimulation
		Phantom mapping
		Targeted reinnervation
		Kinesthetic illusion

Sensory substitution categorizes a group of feedback systems that apply a feedback signal that is not matched in modality to the stimulus occurring at the prosthesis. Furthermore, the feedback signal is presented to a location that, physiologically, will not be perceived to the user as in the same corresponding location on their missing limb. Modality matching refers to a feedback signal that is congruent to the external stimulus detected by the prosthetic sensor; however, the feedback signal may not be presented to a location physiologically representative of the missing hand or limb. Somatotopic matching refers to methods in which the feedback signal is perceived as being matched in location to where the stimulus is being applied to the prosthesis. To achieve feedback that is intuitive and perceived as physiologically natural to the user, the sensory feedback system ideally meets both these conditions: modality matching and somatotopic matching⁸.

2.5 Substitution Feedback

Sensory substitution methods communicate the state of the prosthesis to the user through sensory feedback not physiologically representative of what the missing hand or arm would experience. Typically these techniques are the most technically straightforward approaches^{8,32} as they do not consider modality or somatotopic matching. The success of the approach depends on the user's ability to interpret the type and location of the stimulus and associate it with the prosthesis. The most common methodology has been to translate tactile information from the prosthesis to the amputee using vibration, electrocutaneous, or auditory stimuli.

2.5.1 Vibrotactile Feedback

Most commonly reported in prosthetic literature, vibrotactile feedback involves communicating sensory information from the prosthesis to the user through the application of mechanical vibration to a strategic area of the user's skin³³ (Figure 2.2). Mechanical vibration, when introduced to the skin, has been shown to activate numerous cutaneous mechanoreceptors with the response of individual receptor types being a function of vibration frequency, amplitude, and duration of vibration³⁴.

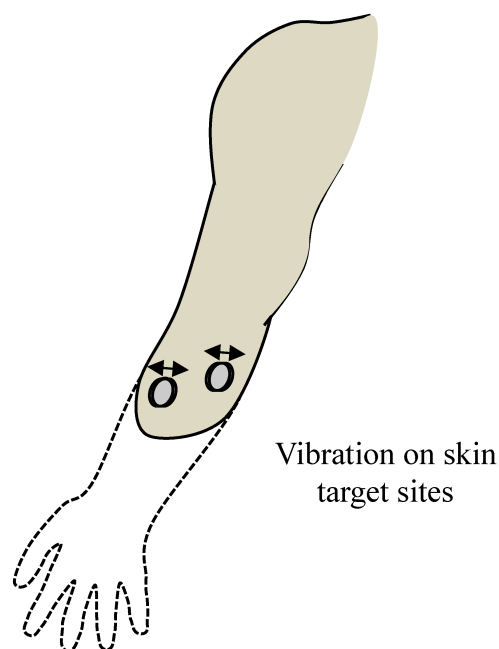


Figure 2.2 Vibrotactile feedback. Where vibration is applied to the skin.

Vibrotactile sensory substitution is most often applied to communicate tactile information during grasping tasks. A tactor will apply continuous vibration, or pulses of vibration when the prosthetic prehensor comes into contact with an object³⁵⁻³⁷. Able-bodied participants are often used to evaluate the efficacy of vibrotactile systems, by manipulating vibration parameters such as amplitude³⁷ and pulse rate^{36,37} to convey grasping force. In three studies, vibratory feedback has been shown to increase confidence and success rates in performing grasping tasks, and compliment visual feedback^{33,38,39}. Conversely, one study has shown that while vibrotactile feedback improved grasp success using complex control strategies, in simplistic control strategies it did not enhance control when visual feedback was already being used⁴⁰. In amputee studies, amplitude and frequency of vibration have been used to communicate grasping forces present in a prosthetic prehensor. This work concluded that vibrotactile feedback may reduce excess prehensor force in experienced users, but negatively influenced those with little previous myoelectric prosthetic experience³⁵.

As a mechanism for providing sensory feedback, vibration is often a baseline standard to which other feedback methods are compared^{37,39,41-44}. Vibrotactile tactors are advantageous in that they are inexpensive, with small size and weight; important factors for prosthetic applications. However, prior to successful implementation it must be demonstrated that the vibration induced into the residual limb tissues does not contaminate the motor control signals. Furthermore, analysis is warranted as to whether the vibration will affect socket movement or cause separation of tissue from the EMG electrodes.

2.5.2 Electrotactile Feedback

Electrotactile feedback communicates sensory information to the prosthetic user via electrodes placed on the user's skin (Figure 2.3). Sensory communication is most often achieved through modulation of the electrical current parameters: amplitude, frequency, and pulse rate to single or multiple electrode sites^{12,41,45-49}. These parameters are mapped such that a touch or force stimulus introduced to the prosthesis corresponds to a specific electrical signal presented to the user's skin.

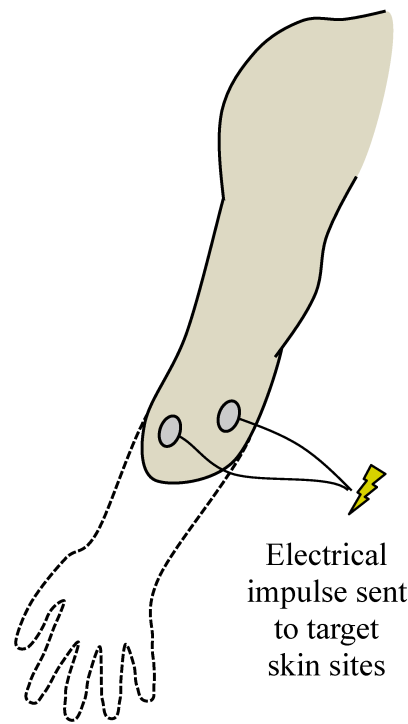


Figure 2.3 Electrotactile feedback. Where electrodes are placed over the skin.

Electrocutaneous stimulation can evoke a range of sensations that have been qualitatively described by participants as a tingling, itch, vibration, buzz, touch, pressure, pinch, and sharp or burning pain⁵⁰. One study reports participants describing the sensation as similar to small bubbles bursting on the skin⁴¹. Some studies do not report the specific sensations experienced by the participants as a result of the electrocutaneous feedback; rather, they identify the range between initial sensation and pain^{51,52}. Despite the mismatched modality, testing in able-bodied participants has shown that electrotactile feedback may improve participants' ability to reach and maintain specific grasp force values⁵¹, while requiring similar amounts of time to integrate both electrocutaneous and visual information to the use of visual feedback alone⁴⁷. In testing with amputee populations, improvements in user confidence, control, and grasp force discrimination have also been demonstrated with electrotactile feedback^{45,48,49}.

A benefit to electrocutaneous systems is that they often require less power than mechanical systems (for example vibrotactile devices). Yet overall, electrotactile feedback is less accepted

than vibrotactile feedback by populations using myoelectric devices^{41,50}. Perhaps a reason for these lower acceptance rates lies in the limitations of electrotactile feedback. Elicited sensations have been shown to be dependent on many stimulation parameters such as voltage, current, wave form, electrode size, material and contact force, as well as physiological factors such as skin location, thickness and electrochemistry⁵⁰. Therefore the ability to repeatedly isolate and elicit a specific sensation becomes an involved task. In a prosthetics context, sensory feedback devices should have long term stability and consistency of the prosthetic-to-user communication channel. Without stability in the elicited sensations the user may face substantial challenges in learning to interpret feedback. To further complicate these issues, participants often demonstrate adaptation to electrocutaneous stimulus over time. Research to minimize adaptation for use in a prosthetic environment is ongoing⁵². Finally, incorporating electrocutaneous feedback into a myoelectric prosthesis may require spatial consideration, as electrical signals from the sensory feedback system should not contaminate the myoelectric motor control signals to the prosthesis.

2.5.3 Auditory Feedback

Auditory feedback has been demonstrated as a technique to convey contact of a robotic hand to an object⁵³, as well as the position of the hand's digits and intended grasping pattern^{10,54,55}. Methods of auditory feedback provide information on the state of a robotic or prosthetic hand through varying frequencies of tones or sounds. For example, Gonzalez *et al.* conducted able-bodied testing with an auditory scheme that utilized the sounds of a cello to signify thumb movement and a violin for index finger movement. During the grasping task these two instruments would play a specific starting note and a final note to signify successful completion of the task. Errors in finger trajectory were signified by a separate unique note for each finger to inform the user of the need to correct the movement^{10,54,55}. When compared to the absence of auditory feedback (strictly visual feedback), participants demonstrated improved grasping task performance and reduced cognitive burden during the operation of a robotic hand^{10,54,55}. One amputee study indicated that auditory feedback could be useful for identifying which prosthetic fingers are being touched at any given time⁵³.

Audio-based sensory substitution systems inherently require training for effective use. The user must learn to interpret auditory stimulation as tactile stimulation and associate these audio cues

with specific prosthetic limb states. Although with training an amputee may be able to utilize this feedback system, the substitutive challenge may create excessive cognitive burden and a significant barrier to effective use.

2.5.4 Other Substitution Methods

Other methods have been investigated to achieve sensory substitution. One such method involves using a motorized elbow brace to apply extension torques to the elbow proportional to grasp force^{44,56} (Figure 2.4). This method has been tested on able-bodied and trans-radial amputee participants. In able-bodied users, the use of elbow torques was found to be equivalent to using vibration feedback to adapt to unpredicted weight change⁴⁴, and showed improvement in the ability to identify different object stiffness or weights when compared to visual feedback only^{44,56}. Amputee participants have shown similar results regarding coordination, task performance, and adaption⁴⁴. However, as this technique relies on intact function of the elbow joint, it would only be useful for amputation below the elbow.

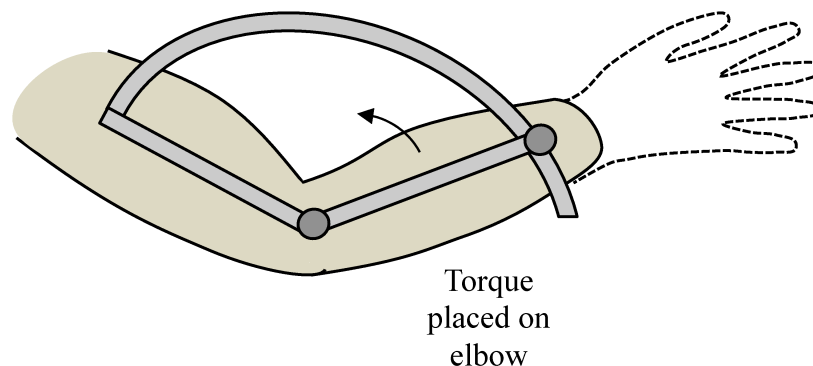


Figure 2.4 Applied elbow torque. Where torque is proportional to grip force.

Rotational skin stretch has also been investigated, in which a feedback mechanism is attached to the skin with adhesive and then rotated to stretch the skin proportional to grasp strength (Figure 2.5). Tested with able-bodied participants in a virtual environment, this method decreased the number of errors and amount of visual attention required when compared to visual feedback alone⁵⁷. However, the temporary nature of this adhesive may be a drawback as its effectiveness has yet to be evaluated beyond 2 hours of usage⁵⁷ and consistency in reapplication may be an important consideration prior to incorporation in prostheses.

Many of these non-traditional feedback methods have yet to be studied extensively with amputee participants; to justify their use, further research is required. In particular, results must be compared to different methods including vibrational and mechanotactile feedback in order to understand their potential as sensory feedback mechanisms. Additionally, comparisons regarding cost, weight, size, and longevity should be considered.

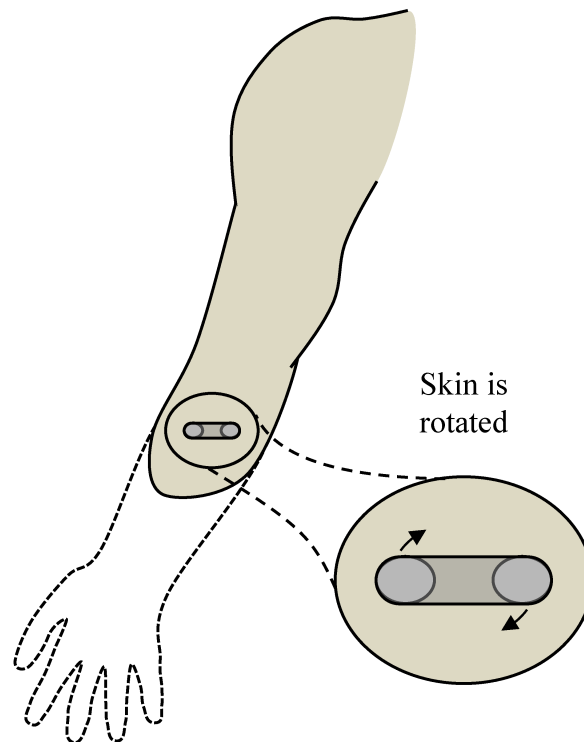


Figure 2.5 Rotational skin stretch. Where tactor ends are attached to the skin using adhesive then rotated proportional to grip force.

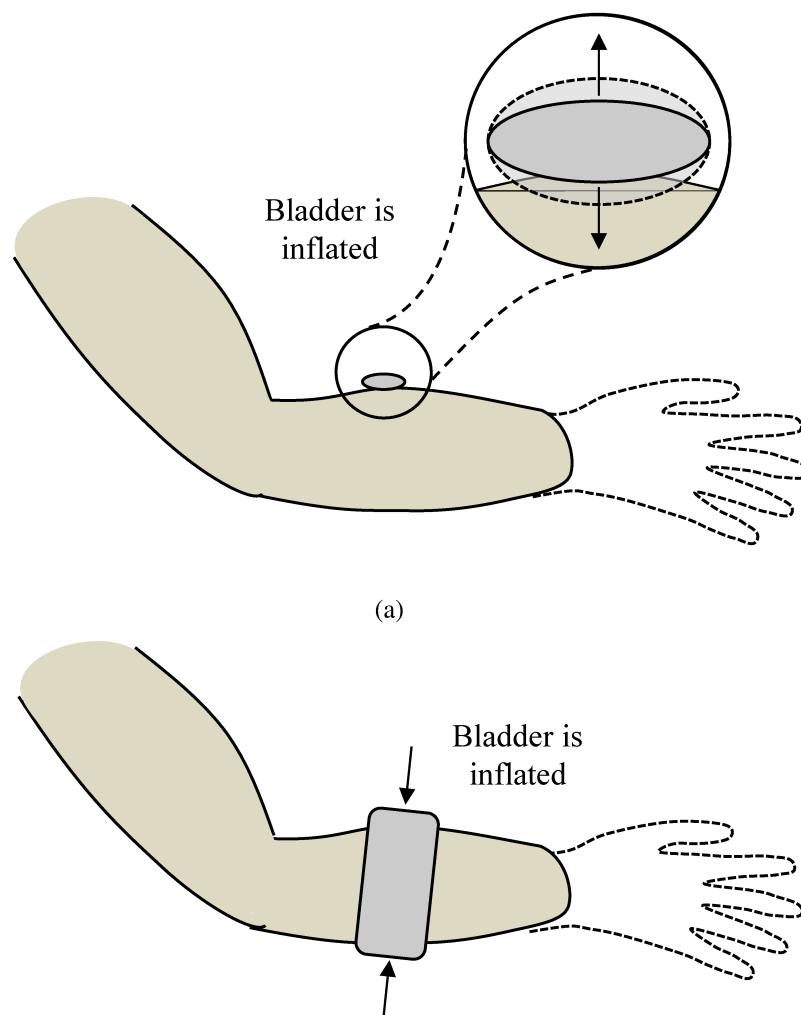
2.6 Modality Matched Feedback

In modality matched methods, the information communicated to the user is matched in sensation, for example touch to the prosthesis is felt as touch to the skin, although mismatched in location. As a result, the user must still dedicate conscience attention to interpret the feedback signal. In some applications, modality-matched feedback may be preferable to sensory substitution. These systems potentially require a lower cognitive demand as the modality of the feedback signal does not require interpretation by the user. Most often, modality matched feedback methods

communicate tactile information to the amputee using force or pressure applied perpendicular to the skin, although other methods being investigated include tangential forces and thermal devices.

2.6.1 Mechanotactile Feedback

Mechanotactile feedback is commonly used to communicate conditions of touch and grasp occurring at the prosthetic prehensor to the user. Most systems will translate touch or grasp force information from the prehensor as a perpendicular force or pressure applied to a strategic location on the amputee's residual limb or body¹². To achieve this task, numerous tactor designs are present in literature, utilizing pneumatics^{39,43,58,59}, servo-motors^{42,60-62}, and voice coils³¹ to generate force (Figure 2.6).



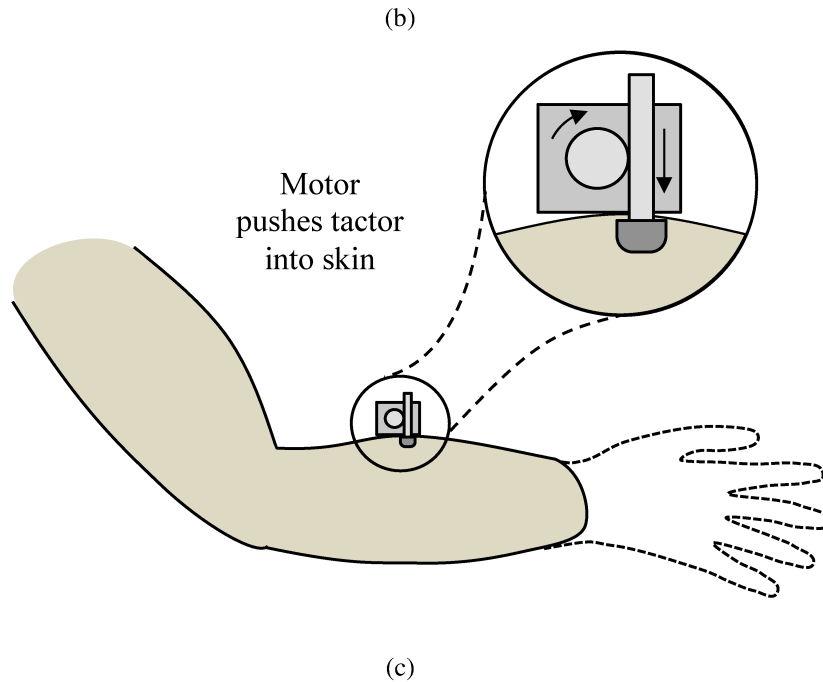


Figure 2.6 Mechanotactile feedback. (a) pneumatic bladder, (b) pneumatic pressure cuff, and (c) servo-motor or voice coil.

Studies conducted in able-bodied populations have demonstrated participants being able to incorporate these types of feedback signals into their control strategy of a robotic^{31,43} or virtual hand^{13,39}, as well as reduce error in replicating grasping pressure to a consistent value⁴³. In amputee studies, incorporation of mechanotactile feedback has been shown to improve performance during object manipulation tasks⁶⁰. Additionally, as a feedback signal, mechanotactile tactors can provide graduated levels of force (or pressure), and typically enable the user to discriminate between various levels^{13,59}. These systems have demonstrated improved multi-site force and spatial discrimination over vibration^{42,59}.

When compared to other feedback systems, mechanotactile systems typically consume more power and are often larger and heavier than vibrotactile or electrotactile devices; development into minimizing these drawbacks is ongoing^{63,64}.

2.6.2 Other Modality Matched Methods

Although perpendicular force is presently the most common form of mechanotactile feedback, advances in tactile systems have led to a broad range of mechanical feedback modalities. Two

separate multi-modal factors have been described, capable of providing perpendicular force, tangential force, vibration, and temperature^{8,63,65,66}. Armiger *et al.* further describe a system to incorporate a multi-modal device into a prosthetic socket⁶³.

Although multi-modal factors have the ability to deliver significantly more information than a traditional single-mode feedback device, the utility of providing additional signals needs to be further evaluated. Investigation must be conducted on the ability of participants to effectively utilize multiple feedback modalities, as it has been demonstrated in two amputee participants that providing multiple kinds of feedback simultaneously actually degrades grip force control⁶⁶. This may result from a greater degree of conscious attention being required to interpret multiple sensory signals applied to a single location. Although these devices represent technological strides in design challenges inherent to feedback devices, demonstration of clinical practicality will be needed to validate their effectiveness.

2.7 Somatotopically Matched Feedback

Somatotopically matched methods deliver feedback such that an amputee senses the stimulus as though it were applied to the same corresponding location of their missing limb. Compared to substitution or modality matching methods, somatotopically matched feedback may reduce the cognitive burden placed on the user as the stimulus applied to the prosthetic sensor will be perceived as occurring at a physiologically matched location in the user's missing limb. As a result the user may require less training and conscious attention to interpret feedback signals. Somatotopic matching techniques have been investigated with direct neural stimulation; by exploiting the effects of nerve remapping that occurs following amputation; and by purposefully rerouting sensory nerves using Targeted Reinnervation (TR).

2.7.1 Peripheral Nerve Stimulation

As the nervous system functions on electrical voltage potentials, perhaps the most obvious solution is to electrically stimulate physiological channels to simulate sensory feedback. Peripheral nerve stimulation relies on the principle that, following upper limb amputation, the original afferent neural pathways are preserved proximally and can be exploited for interfacing with prostheses⁵². This principle suggests that *natural* physiological feedback can be restored, through strategic electrical stimulation of nerve afferents using invasive neural electrodes. To

date, peripheral nerve stimulation has been investigated in amputees using a number of electrode designs: nerve-cuff electrodes⁵³ (such as Flat Interface Nerve Electrodes –FINE), longitudinal intrafascicular electrodes (LIFE electrodes)⁵⁴⁻⁵⁸, and Utah slant array electrodes^{59,60}. Amputee participants have reported referred sensations to the missing limb including touch and pressure, as well as proprioceptive sensations such as position sense or movement^{52,58}, single digit flexion⁶¹, and sensation of the hand closing⁵⁵. Through manipulation of the electrical frequency and current, investigators are able to influence the location, magnitude, and modality of these elicited sensations^{56,58}. These studies support that tactile and proprioceptive pathways are accessible following limb amputation, and can be exploited as sensory feedback strategy.

As a technique for sensory feedback, peripheral nerve stimulation techniques hold limitations. Ultimately the success of eliciting a particular sensation in a certain location is dependent on the system's ability to selectively stimulate specific sensory afferents in a particular fascicle, a function dependent on the stimulating waveform. Current reported techniques lack this selectivity and as a result spatial resolutions of referred sensations are often large, encompassing entire fingers or areas as large as the palm^{68,69}. Beyond spatial discrimination, this lack of selectivity often results in a loss of *naturalness* in elicited sensations. Although participants do report tactile or proprioceptive sensations, they are frequently accompanied by foreign sensations resembling vibration, tapping, or fluttering on the skin^{21,68}. In the penetrating intrafascicular electrodes, such as the LIFE or Utah array electrodes, the long term stability of has yet to be comprehensively studied in human participants^{58,70}, with limited numbers of patients implanted with chronic electrodes^{67,71}. Therefore, whether the body acclimates to the stimuli or if the system requires adjustments of the stimulus parameters over time remains unknown. However, recent studies with chronically implanted FINE electrodes have demonstrated promising long term results in studies with limited population sizes^{67,71}. Peripheral nerve stimulation as a method of sensory feedback is a promising and rapidly evolving field. Challenges around the longevity, and clinical feasibility of such systems are being actively investigated; however, this emerging technology still remains in its infancy.

2.7.2 Phantom Mapping

Phantom sensation is defined as occurring when an amputee feels sensation of the missing limb. Phantom mapping relies on the ability to intentionally elicit these phantom sensations as a result of stimulation of the residual limb. This feedback technique requires the identification of areas on an amputee's residual limb that consistently elicit sensations referring to the missing hand (Figure 2.7). Tactors that elicit this illusion are positioned in the locations where the sensations are experienced, and are mapped to the input from the prosthetic digits. When activated, the tactors provide somatotopically matched sensations experienced in the amputees missing digits. Thus far, mechanotactile^{42,77} or vibrotactile⁷⁷ systems have been studied with transradial amputee participants.

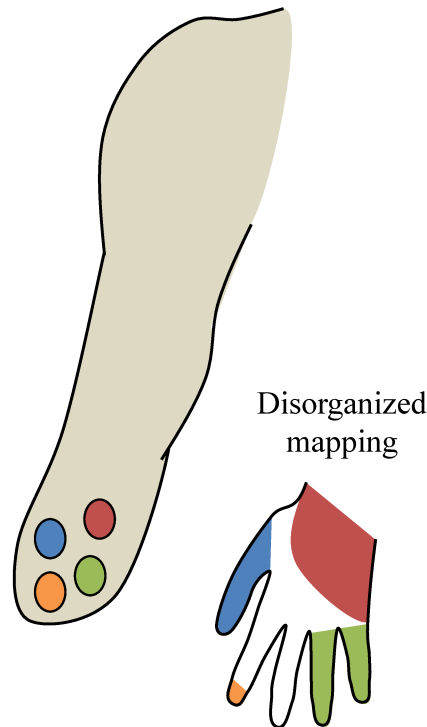


Figure 2.7 Hypothetical corresponding regions between location of pressure on residual limb and sensation on phantom hand.

As a mechanism for sensory feedback to multiple sites on an amputee's residual limb, phantom mapping has been shown to improve feedback site discrimination beyond the capabilities of able-bodied participants⁴². Additionally, when comparing vibrotactile to mechanotactile devices,

participants demonstrated better discrimination results using mechanotactile devices⁴². Although literature has only reported use of mechanotactile and vibrotactile devices for somatotopic matching, there may be potential to apply other feedback methods such as electrotactile or skin stretch. Investigation is warranted to further identify feedback signals that effectively exploit phantom mapping techniques.

Although phantom mapping enables the possibility of both somatotopic and modality matching, it relies exclusively on participants having a consistent phantom representation of their digits. However, phantom mapping is not experienced by all upper-extremity amputees, and often dissipates with time following the amputation surgery⁷⁸. Furthermore, elicited phantom sensations may range from a *natural* feeling of touch to *unnatural* itching, tingling, or pain. These sensations will vary from individual to individual as well as over time. Phantom mapping has the potential to provide somatotopically matched feedback to amputees; however is limited by the reliability and level of sensations experienced in the individual's phantom map. As a result, phantom mapping techniques may only be an option for a limited population of prosthetic users.

2.7.3 Targeted Reinnervation

Targeted reinnervation (TR) is a surgical procedure that moves the motor and sensory nerves that previously innervated the amputated limb to muscle and skin target sites⁷⁹ (Figure 2.8). This surgery was initially performed to increase the number of motor control sites for myoelectric prostheses and allow for intuitive control^{15,79,80}. However, it was found that the redirected sensory afferents also reinnervate overlying skin. This reinnervation creates an expression of the hand map, such that when touched, the patients feel as if they are being touched on the missing limb⁸¹⁻⁸³. Cutaneous sensations such as vibration, temperature, and skin stretch have been introduced to participants' reinnervation sites and experienced as a referred sensation in their missing hand, although one participant has described paresthetic sensations⁸¹. Unlike phantom mapping, TR allows the reinnervated sites to be selectively placed¹⁵. The experienced sensations have also been shown to be repeatable and discrete. In other words, participants may develop an organized, detailed, and consistent hand map capable of receiving stimuli in multiple modalities⁸¹.

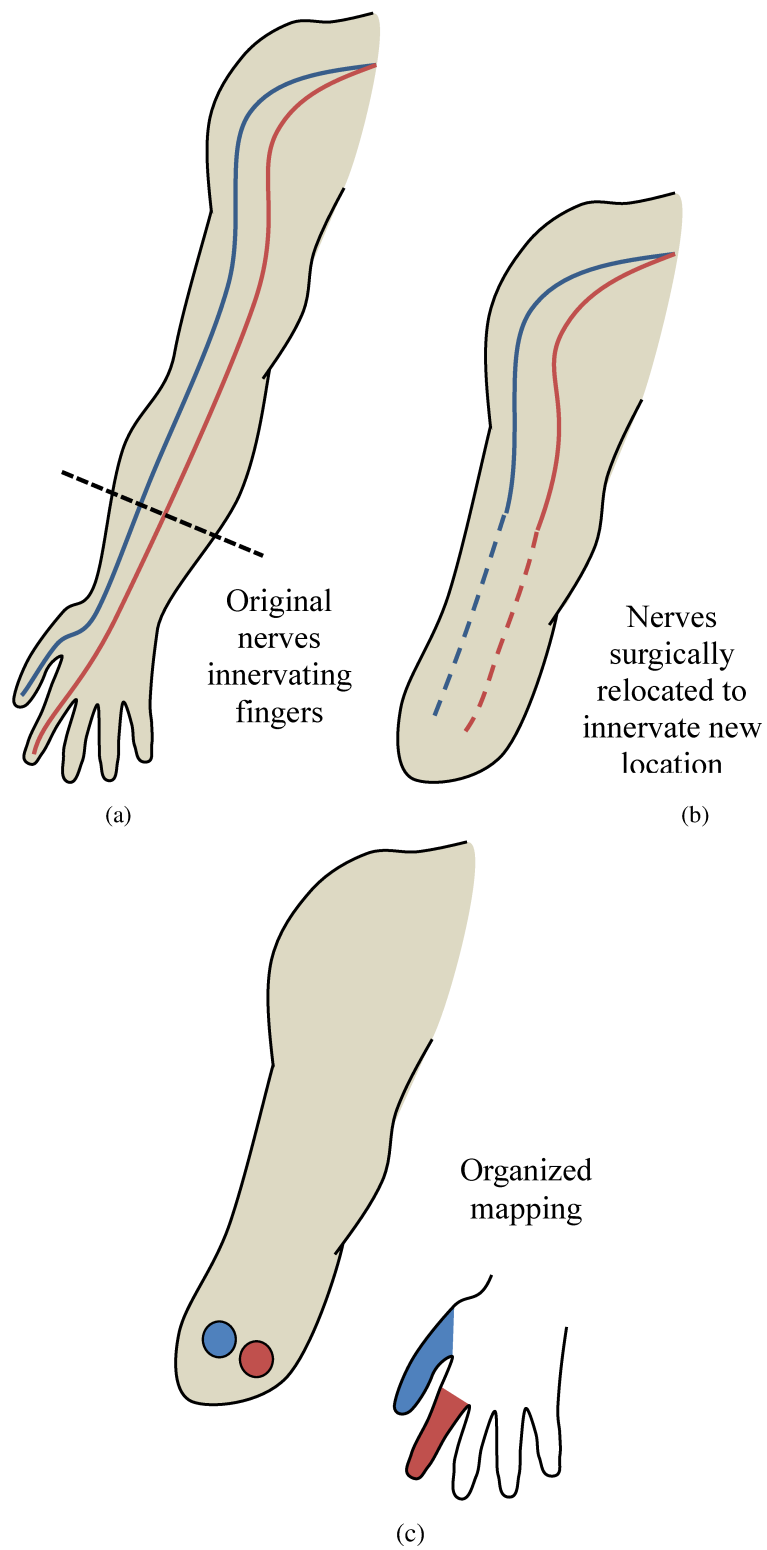


Figure 2.8 Overview of targeted reinnervation procedure, showing (a) original nerves innervating the fingers, (b) the transfer of the nerves to new sites, and (c) the ideal resultant final mapping.

Consequently, patients who have undergone TR surgery may have the ability to receive prosthetic feedback that is intuitive, feels *natural*, and utilizes the same physiological channels that were lost with their missing limb. While using somatotopically and modality matched sensory feedback systems, TR amputees have shown an enhanced ability to detect force gradation⁸⁴, and improved grip force control in a virtual environment⁶⁶. Furthermore, a TR participant demonstrated the ability to distinguish object stiffness⁸⁵, and discriminate between two spatially separated tactors while using motor control sites to operate a robotic hand¹⁵. Another participant improved simple task completion speed using a new prosthesis developed to read signals from her reinnervated chest muscle⁸². Clinical translation of these findings to a prosthetic device might be achieved by linking the sensors from the prosthetic hand to strategically positioned tactors on the residual limb to stimulate the relevant area of the hand map. This may allow the participant to experience sensations matched in modality and somatotopy simultaneous to a stimulus occurring at the prosthetic device.

Although promising, TR feedback techniques, first published in 2004, are in their relative infancy compared with other feedback methods^{79,83}. Research is still ongoing to develop means of effectively utilizing the reinnervated skin sites. A further limitation lies in the need for surgery to utilize TR feedback techniques. There are a limited number of institutions performing TR surgeries and as of 2013, just over 40 patients have been reported to have received TR surgery⁸⁶.

2.8 Discussion

2.8.1 Grasp and Touch Sensation

In moving toward sensory systems capable of being implemented for long term use, a number of factors must be considered. The concept of providing “natural, physiological feedback” should be considered. Neither substitution nor modality matched methods provide input through the original sensory pathways of the amputee⁷⁰. Thus, the corresponding sensory information may be perceived as *unnatural* and may require additional time, training, and attention to effectively exploit^{87,88}. The ideal system would combine the benefits of modality and somatotopic matching systems to allow the participant to feel a relevant stimulus at the correct location on their missing limb^{83,89}.

Another consideration is that methods of evaluating feedback systems have occurred in controlled laboratory environments where participants are asked to perform simple object grasping and manipulating tasks. As the complexity of the task is often low, most of the participant's concentration can be dedicated to interpreting the feedback signals provided. In reality, day-to-day activities incorporate varying levels of complexity with corresponding concentration required of the user. Feedback signals requiring high levels of concentration to decode will ultimately increase the cognitive burden of the users or be perceived as extraneous and distracting from the given task. Many systems proposed in literature require training and sensory adaptation to interpret a non-physiological signal as exteroceptive or proprioceptive information⁵⁰. This additional processing of information increases the cognitive burden and has the potential to negate one of the largest benefits of sensory feedback; reduced conscious attention (Figure 2.9). Therefore an effective feedback signal must first input the correct stimulus, and secondly ensure that the feedback signal is received as natural, and not a distraction. In the future, it will be important for researchers to develop better measures for evaluating the usability of sensory feedback systems in day-to-day life, such as reporting on the naturalness of measured sensations as well as the amount of cognitive burden required. Furthermore, to sufficiently address a feedback system's efficacy, the device must be integrated in to a prosthetic system, and functional tasks beyond grip force or simple object manipulation must be performed. Participant testing should occur over multiple sessions to enable evaluation of the training and time required for the feedback system to improve prosthetic use.

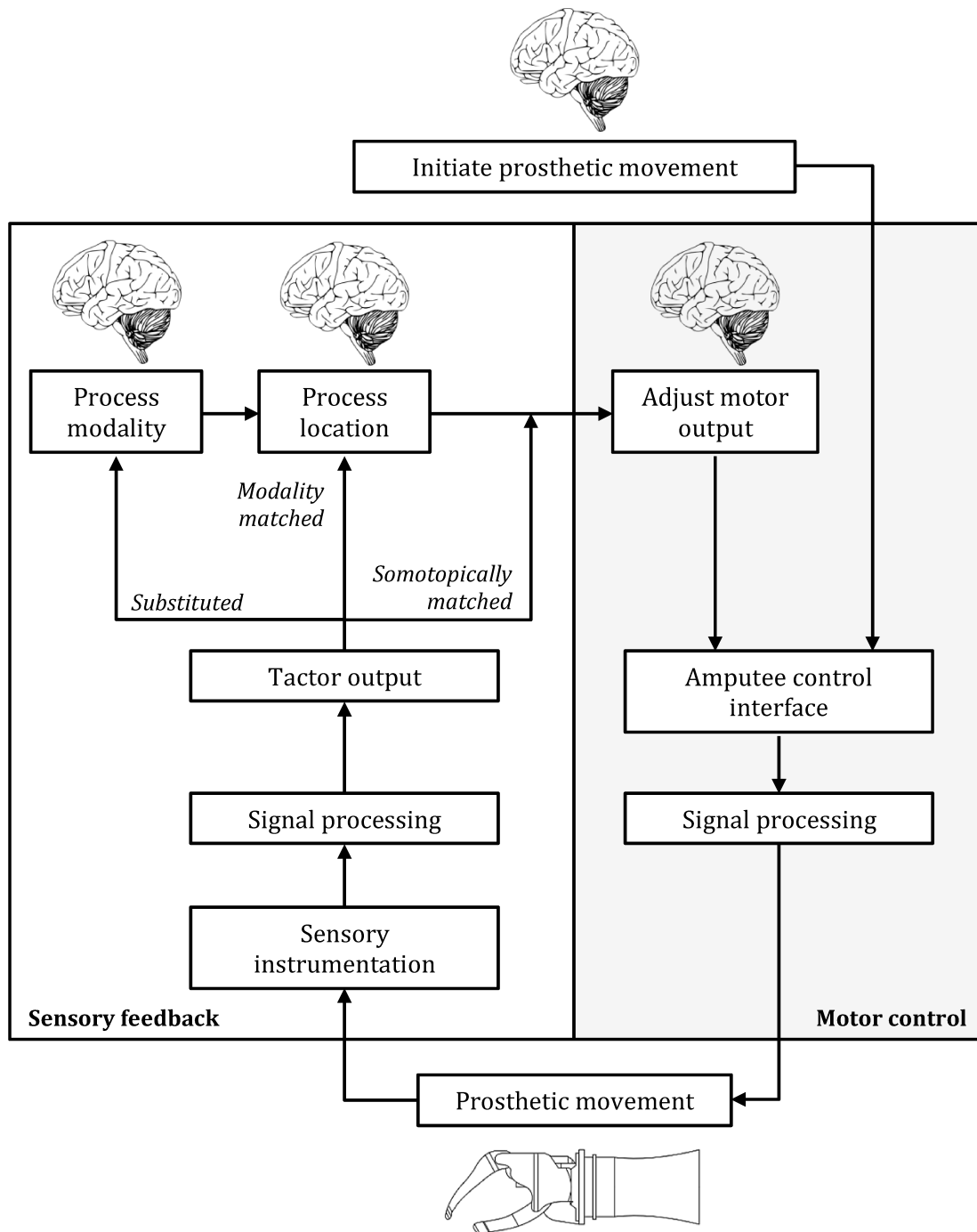


Figure 2.9 Schematic of the process used to control a myoelectric prosthetic with sensory feedback.

2.8.2 Future directions

While systems providing cutaneous sensation have been studied extensively, providing the user with a sense of joint position and movement has been less studied. However, allowing an individual to sense the position of their prosthesis in space without requiring visual attention has the potential to greatly improve dynamic prosthetic control.

Vibrotactile feedback has been implemented to establish proprioceptive communication between the user and prosthesis through substitution^{77,90}. In a case study Mann *et al.* introduced vibratory tactors to the residual limb of a single participant with above elbow amputation. The amplitude of vibration was manipulated to provide the user with information on the state of elbow flexion and extension in the prosthesis. The participant demonstrated improvements in positional control of the prosthesis during reaching tasks⁹⁰. Although this area has not been studied extensively, there is potential for vibrotactile sensory substitution (or other substitution methods) to be implemented to communicate the positional state of prosthetic joints or the prehensor.

An alternative possibility to providing kinesthetic sensibility would be to exploit vibration induced movement illusions. Also termed the *kinesthetic illusion*, this unique physiological phenomenon possesses the ability to provide somatotopically matched kinesthetic feedback. In able-bodied individuals, vibration introduced to musculotendinous regions of a limb can induce sensations that the limb is moving^{91,92}. It is believed that the vibratory stimulus induces muscle spindle activity⁹³; consequently the direction of illusory movement will be experienced as though the stimulated muscle group is being stretched (Figure 2.10). However, the kinesthetic illusion has yet to be tested with amputee participants or implemented as a method of prosthetic sensory feedback. As a potential unique solution to kinesthetic sensibility it warrants further investigation.

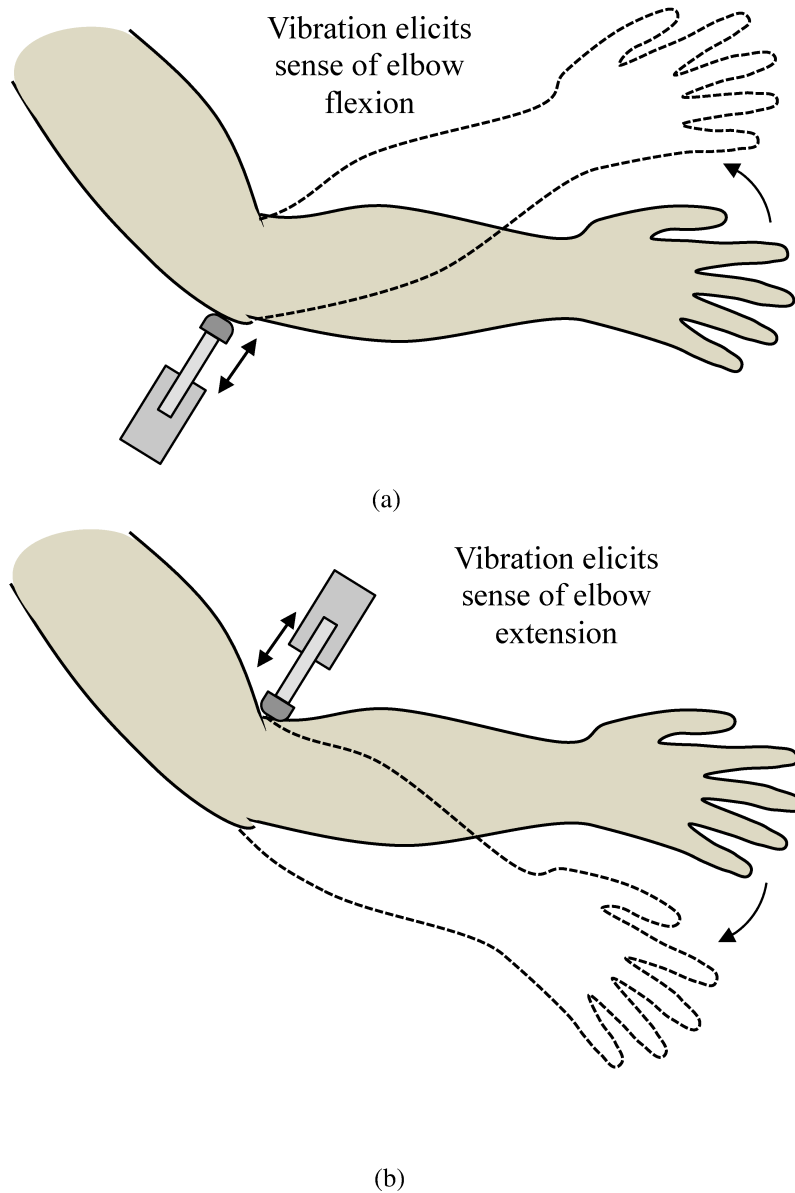


Figure 2.10 Overview of kinesthetic illusion. Showing (a) elbow flexion, and (b) elbow extension.

2.8.3 Translational Capabilities

In moving towards clinical or commercial use, it is important to consider several future directions related to sensory feedback methods, socket integration challenges, and overall system usability.

One current challenge involves integrating these feedback systems into the prosthetic socket. Sockets are used to attach the prosthesis to the residual limb, and different designs may include combinations of roll-on suction suspension liners, flexible materials, and an anatomically contoured casing^{16,94}. Suction attachments are typical in myoelectric arms⁹⁵; and therefore it is imperative that implementing a sensory feedback system does not compromise this suction seal. Currently, electrodes are connected to the body by embedding them into a fabric liner that fits between the socket and the body⁹⁶ or embedding the electrodes directly into the socket wall for a skin suction fit. Most literature concerning current tactor designs do not address the socket integration issue, instead tactors are simply placed directly on the skin for testing without regards to the vacuum seal that must be maintained for prosthetic use. One exception is the work by Armiger *et al.* in which a tactor has been mounted in the interface between the user and the prosthetic device, within the socket⁶³. However, the vacuum seal issue is not directly addressed, and specific details of the integration are not provided. Therefore, it will be important to address this subject in future research.

Another potential difficulty facing amputees is misalignment of tactors during the donning process, when they attach the prosthesis over their residual limb. It is hypothesized that misalignment of tactors could result in feedback that is neither intuitive nor useful (similar to misalignment of myoelectric sensors used to record muscle signals⁹⁷). For this reason it will be important to consider methods and designs to consistently align the tactors.

Other general aims in the design of sensory feedback systems are to make the system robust enough to reliably provide feedback over extended periods of time, have a small enough profile to allow freedom of movement, ensure a reduced footprint to allow ample spacing for sensors and other features, and consume low enough amounts of power to ensure function throughout an entire day. It will be important to continue to investigate different feedback methods, as it is possible that a better method for communication between a person and their prosthesis has yet to be comprehensively tested. As is the nature of prosthetic limb replacement, each intervention is unique and tailored to the individual user. Individual patients may want varying degrees of sensory feedback, with specific modalities and somatotopy dependent on preference and application; therefore, patient specificity will ultimately drive an individual's ideal solution.

2.9 Conclusions

The state of upper limb prostheses can be characterized by rapid technological advancements limited by an inability to provide a reliable sensory interface with the amputee. State-of-the-art prostheses are capable of mimicking the multiple degrees of freedom possessed by the human hand and arm, and can be equipped with instrumentation to measure position, temperature, and grasping forces⁶³. For decades the lack of sensory feedback from prosthetic-to-user has been highlighted as a major barrier hampering upper limb prosthetic utility. Today this issue has become even more significant due to the rapid developments in multi-function prosthetic terminal devices. Various sensory feedback systems have been proposed, and most have shown that a user can improve their ability to manipulate the prostheses with feedback. However, few sensory feedback systems have been translated and integrated with functional commercially available prosthetic components. This paradox can perhaps be attributed to two factors crucial to a feedback systems success: the ability to provide relevant feedback that does not demand attention from the user, and the ability to incorporate the system into prostheses without compromising fit or function. If a feedback device is to be successfully incorporated into prostheses for clinical or long-term use, these two issues will be pivotal in the device's success.

2.10 References

1. Ziegler-Graham K, MacKenzie EJ, Ephraim PL, Travison TG, Brookmeyer R. Estimating the prevalence of limb loss in the united states: 2005 to 2050. *Arch Phys Med Rehabil*. 2008;89(3):422-429. doi: <http://dx.doi.org/10.1016/j.apmr.2007.11.005>.
2. Lake C, Dodson R. Progressive upper limb prosthetics. *Phys Med Rehabil Clin N Am*. 2006;17(1):49-72. Accessed 5 April 2013.
3. A.M.R.Agur MJL. *Grant's atlas of anatomy*. 10th ed. Lippincott Williams and Wilkins; 1999.

4. Belter JT, Segil JL, Dollar AM, Weir RF. Mechanical design and performance specifications of anthropomorphic prosthetic hands: A review. *Journal of Rehabilitation Research and Development*. 2013;50(5):599-618. Accessed 27 February 2014.
5. Cloutier A, Yang J. Design, control, and sensory feedback of externally powered hand prostheses: A literature review. *Crit Rev Biomed Eng*. 2013;41(2):161-181. Accessed 27 February 2014.
6. Lundborg G, Rosén B. Sensory substitution in prosthetics. *Hand Clin*. 2001;17(3):481-488. Accessed 24 May 2013.
7. Kim K, Colgate JE, Santos-Munné JJ, Makhlin A, Peshkin MA. On the design of miniature haptic devices for upper extremity prosthetics. *IEEE/ASME Transactions on Mechatronics*. 2010;15(1):27-39. Accessed 5 April 2013.
8. Vallbo AB, Johansson RS. Properties of cutaneous mechanoreceptors in the human hand related to touch sensation. *Hum Neurobiol*. 1984;3(1):3-14. Accessed 3 December 2013.
9. Johansson RS. Sensory and memory information in the control of dexterous manipulation. In: *Neural basis of motor behaviour*. Kluwer Academic Publishers; 1996:205.
10. Biddiss E, Chau T. Upper limb prosthesis use and abandonment: A survey of the last 25 years. *Prosthet Orthot Int*. 2007;31(3):236-257. Accessed 24 January 2014.
11. Wright TW, Hagen AD, Wood MB. Prosthetic usage in major upper extremity amputations. *J Hand Surg*. 1995;20(4):619-622. Accessed 24 May 2013.
12. Biddiss E, Beaton D, Chau T. Consumer design priorities for upper limb prosthetics. *Disability and Rehabilitation: Assistive Technology*. 2007;2(6):346-357. Accessed 5 April 2013.
13. Panarese A, Edin BB, Vecchi F, Carrozza MC, Johansson RS. Humans can integrate force feedback to toes in their sensorimotor control of a robotic hand. *IEEE Transactions on Neural Systems and Rehabilitation Engineering*. 2009;17(6):560-567. Accessed 2 December 2013.

14. Gonzalez J, Soma H, Sekine M, Yu W. Psycho-physiological assessment of a prosthetic hand sensory feedback system based on an auditory display: A preliminary study. *Journal of NeuroEngineering and Rehabilitation*. 2012;9(1). Accessed 27 March 2013.
15. Antfolk C, D'Alonzo M, Rosén B, Lundborg G, Sebelius F, Cipriani C. Sensory feedback in upper limb prosthetics. *Expert Review of Medical Devices*. 2013;10(1):45-54. Accessed 2 December 2013.
16. Bach-y-Rita P. Tactile sensory substitution studies. *Annals of the New York Academy of Sciences*. 2004;1013:83-91. Accessed 3 December 2013.
17. Cipriani C, Dalonzo M, Carrozza MC. A miniature vibrotactile sensory substitution device for multifingered hand prosthetics. *IEEE Transactions on Biomedical Engineering*. 2012;59(2):400-408. Accessed 5 April 2013.
18. Jones LA, Sarter NB. Tactile displays: Guidance for their design and application. *Hum Factors*. 2008;50(1):90-111. Accessed 30 October 2013.
19. Pylatiuk C, Kargov A, Schulz S. Design and evaluation of a low-cost force feedback system for myoelectric prosthetic hands. *Journal of Prosthetics and Orthotics*. 2006;18(2):57-61. Accessed 30 October 2013.
20. Chatterjee A, Chaubey P, Martin J, Thakor N. Testing a prosthetic haptic feedback simulator with an interactive force matching task. *Journal of Prosthetics and Orthotics*. 2008;20(2):27-34. Accessed 30 October 2013.
21. Stepp CE, Matsuoka Y. Vibrotactile sensory substitution for object manipulation: Amplitude versus pulse train frequency modulation. *IEEE Transactions on Neural Systems and Rehabilitation Engineering*. 2012;20(1):31-37. Accessed 20 December 2013.
22. Saunders I, Vijayakumar S. The role of feed-forward and feedback processes for closed-loop prosthesis control. *Journal of NeuroEngineering and Rehabilitation*. 2011;8(1). Accessed 3 December 2013.

23. Tejeiro C, Stepp CE, Malhotra M, Rombokas E, Matsuoka Y. Comparison of remote pressure and vibrotactile feedback for prosthetic hand control. *Proceedings of the IEEE RAS and EMBS International Conference on Biomedical Robotics and Biomechatronics*. 2012:521-525. Accessed 20 December 2013.
24. Cipriani C, Zaccone F, Micera S, Carrozza MC. On the shared control of an EMG-controlled prosthetic hand: Analysis of user-prosthesis interaction. *IEEE Transactions on Robotics*. 2008;24(1):170-184. Accessed 3 December 2013.
25. Shannon GF. A comparison of alternative means of providing sensory feedback on upper limb prostheses. *Med.Biol.Engineering*. 1976;14(3):289-294. Accessed 3 December 2013.
26. Antfolk C, D'Alonzo M, Controzzi M, et al. Artificial redirection of sensation from prosthetic fingers to the phantom hand map on transradial amputees: Vibrotactile versus mechanotactile sensory feedback. *IEEE Transactions on Neural Systems and Rehabilitation Engineering*. 2013;21(1):112-120. Accessed 27 March 2013.
27. Patterson PE, Katz JA. Design and evaluation of a sensory feedback system that provides grasping pressure in a myoelectric hand. *Journal of Rehabilitation Research and Development*. 1992;29(1):1-8. Accessed 2 December 2013.
28. Brown JD, Paek A, Syed M, et al. Understanding the role of haptic feedback in a teleoperated/prosthetic grasp and lift task. *2013 World Haptics Conference, WHC 2013*. 2013:271-276. Accessed 20 December 2013.
29. Lundborg G, Rosen B, Lindstrom K, Lindberg S. Artificial sensibility based on the use of piezoresistive sensors. *J Hand Surg*. 1998;23 B(5):620-626. Accessed 3 December 2013.
30. Wang G, Zhang X, Zhang J, Gruver WA. Gripping force sensory feedback for a myoelectrically controlled forearm prosthesis. *Proceedings of the IEEE International Conference on Systems, Man and Cybernetics*. 1995;1:501-504. Accessed 3 December 2013.

31. Tupper CN, Gerhard GC. Improved prosthesis control via high resolution electro-tactile feedback. *Bioengineering, Proceedings of the Northeast Conference*. 1989:39-40. Accessed 3 December 2013.
32. Shannon GF. A myoelectrically-controlled prosthesis with sensory feedback. *Medical and Biological Engineering and Computing*. 1979;17(1):73-80. Accessed 20 December 2013.
33. Rohland TA. Sensory feedback for powered limb prostheses. *Med.Biol.Engineering*. 1975;13(2):300-301. Accessed 20 December 2013.
34. Kaczmarek KA, Webster JG, Bach-y-Rita P, Tompkins WJ. Electrotactile and vibrotactile displays for sensory substitution systems. *IEEE Transactions on Biomedical Engineering*. 1991;38(1):1-16. Accessed 30 October 2013.
35. Zafar M, Van Doren CL. Effectiveness of supplemental grasp-force feedback in the presence of vision. *Medical and Biological Engineering and Computing*. 2000;38(3):267-274. Accessed 3 December 2013.
36. Buma DG, Buitenweg JR, Veltink PH. Intermittent stimulation delays adaptation to electrocutaneous sensory feedback. *IEEE Transactions on Neural Systems and Rehabilitation Engineering*. 2007;15(1):435-441. Accessed 3 December 2013.
37. Lundborg G, Rosén B, Lindberg S. Hearing as substitution for sensation: A new principle for artificial sensibility. *J Hand Surg*. 1999;24(2):219-224. Accessed 2 December 2013.
38. Gonzalez J, Soma H, Sekine M, Yu W. Auditory display as a prosthetic hand biofeedback. *Journal of Medical Imaging and Health Informatics*. 2011;1(4):325-333. Accessed 3 December 2013.
39. Gonzalez J, Yu W. Multichannel audio aided dynamical perception for prosthetic hand biofeedback. *2009 IEEE International Conference on Rehabilitation Robotics, ICORR 2009*. 2009:240-245. Accessed 3 December 2013.

40. Gillespie RB, Contreras-Vidal JL, Shewokis PA, et al. Toward improved sensorimotor integration and learning using upper-limb prosthetic devices. *2010 Annual International Conference of the IEEE Engineering in Medicine and Biology Society, EMBC'10*. 2010:5077-5080. Accessed 20 December 2013.
41. Wheeler J, Bark K, Savall J, Cutkosky M. Investigation of rotational skin stretch for proprioceptive feedback with application to myoelectric systems. *IEEE Transactions on Neural Systems and Rehabilitation Engineering*. 2010;18(1):58-66. Accessed 20 December 2013.
42. Childress DS. Closed-loop control in prosthetic systems: Historical perspective. *Ann Biomed Eng*. 1980;8(4-6):293-303. Accessed 2 December 2013.
43. Antfolk C, Björkman A, Frank S-, Sebelius F, Lundborg G, Rosen B. Sensory feedback from a prosthetic hand based on airmediated pressure from the hand to the forearm skin. *J Rehabil Med*. 2012;44(8):702-707. Accessed 2 December 2013.
44. Meek SG, Jacobsen SC, Goulding PP. Extended physiologic taction: Design and evaluation of a proportional force feedback system. *Journal of Rehabilitation Research and Development*. 1989;26(3):53-62. Accessed 2 December 2013.
45. Antfolk C, Cipriani C, Carrozza MC, et al. Transfer of tactile input from an artificial hand to the forearm: Experiments in amputees and able-bodied volunteers. *Disability and Rehabilitation: Assistive Technology*. 2013;8(3):249-254. Accessed 2 December 2013.
46. Antfolk C, Balkenius C, Lundborg G, Rosén B, Sebelius F. A tactile display system for hand prostheses to discriminate pressure and individual finger localization. *Journal of Medical and Biological Engineering*. 2010;30(6):355-360. Accessed 5 April 2013.
47. Stepp CE, Matsuoka Y. Relative to direct haptic feedback, remote vibrotactile feedback improves but slows object manipulation. *Conference proceedings : ...Annual International Conference of the IEEE Engineering in Medicine and Biology Society.IEEE Engineering in Medicine and Biology Society.Conference*. 2010;2010:2089-2092. Accessed 3 December 2013.

48. Armiger RS, Tenore FV, Katyal KD, et al. Enabling closed-loop control of the modular prosthetic limb through haptic feedback. *Johns Hopkins APL Technical Digest (Applied Physics Laboratory)*. 2013;31(4):345-353. Accessed 29 April 2013.
49. HDT Robotics. Robotics research. <http://www.hdtglobal.com/services/robotics/Research/>. Updated 2013. Accessed 12/2013, 2013.
50. Kim K, Colgate JE, Peshkin MA, Santos-Munné JJ, Makhlin A. A miniature tactor design for upper extremity prosthesis. *Proceedings of the Frontiers in the Convergence of Bioscience and Information Technologies, FBIT 2007*. 2007:537-542. Accessed 5 April 2013.
51. Kim K, Colgate JE. Haptic feedback enhances grip force control of sEMG-controlled prosthetic hands in targeted reinnervation amputees. *IEEE Transactions on Neural Systems and Rehabilitation Engineering*. 2012;20(6):798-805. Accessed 18 December 2013.
52. Micera S, Carpaneto J, Raspopovic S. Control of hand prostheses using peripheral information. *IEEE Reviews in Biomedical Engineering*. 2010;3:48-68. Accessed 30 December 2013.
53. Clippinger FW, Avery R, Titus BR. A sensory feedback system for an upper-limb amputation prosthesis. *Bull Prosthet Res*. 1974:247-258. Accessed 30 December 2013.
54. Benvenuto A, Raspopovic S, Hoffmann KP, et al. Intrafascicular thin-film multichannel electrodes for sensory feedback: Evidences on a human amputee. *2010 Annual International Conference of the IEEE Engineering in Medicine and Biology Society, EMBC'10*. 2010:1800-1803. Accessed 20 December 2013.
55. Horch K, Meek S, Taylor TG, Hutchinson DT. Object discrimination with an artificial hand using electrical stimulation of peripheral tactile and proprioceptive pathways with intrafascicular electrodes. *IEEE Transactions on Neural Systems and Rehabilitation Engineering*. 2011;19(5):483-489. Accessed 27 March 2013.

56. Rossini PM, Micera S, Benvenuto A, et al. Double nerve intraneural interface implant on a human amputee for robotic hand control. *Clinical Neurophysiology*. 2010;121(5):777-783. Accessed 20 December 2013.
57. Dhillon GS, Horch KW. Direct neural sensory feedback and control of a prosthetic arm. *IEEE Transactions on Neural Systems and Rehabilitation Engineering*. 2005;13(4):468-472. Accessed 27 March 2013.
58. Dhillon GS, Krüger TB, Sandhu JS, Horch KW. Effects of short-term training on sensory and motor function in severed nerves of long-term human amputees. *J Neurophysiol*. 2005;93(5):2625-2633. Accessed 30 December 2013.
59. Davis TS, Wark HAC, Hutchinson DT, et al. Restoring motor control and sensory feedback in people with upper extremity amputations using arrays of 96 microelectrodes implanted in the median and ulnar nerves. *J Neural Eng*. 2016;13(3). Accessed 8 August 2017. doi: 10.1088/1741-2560/13/3/036001.
60. Clark GA, Wendelken S, Page DM, et al. Using multiple high-count electrode arrays in human median and ulnar nerves to restore sensorimotor function after previous transradial amputation of the hand. *Conf Proc IEEE Eng Med Biol Soc*. 2014;2014:1977-1980. Accessed 8 August 2017. doi: 10.1109/EMBC.2014.6944001.
61. Tan DW, Schiefer MA, Keith MW, Anderson JR, Tyler DJ. Stability and selectivity of a chronic, multi-contact cuff electrode for sensory stimulation in human amputees. *J Neural Eng*. 2015;12(2). Accessed 8 August 2017. doi: 10.1088/1741-2560/12/2/026002.
62. Riso RR. Strategies for providing upper extremity amputees with tactile and hand position feedback - moving closer to the bionic arm. *Technology and Health Care*. 1999;7(6):401-409. Accessed 27 March 2013.
63. Anani A, Korner L. Discrimination of phantom hand sensations elicited by afferent electrical nerve stimulation in below-elbow amputees. *Med Prog Technol*. 1979;6(3):131-135. Accessed 2 January 2014.

64. Micera S, Citi L, Rigosa J, et al. Decoding information from neural signals recorded using intraneural electrodes: Toward the development of a neurocontrolled hand prosthesis. *Proc IEEE*. 2010;98(3):407-417. Accessed 30 December 2013.
65. Polasek KH, Hoyen HA, Keith MW, Kirsch RF, Tyler DJ. Stimulation stability and selectivity of chronically implanted multicontact nerve cuff electrodes in the human upper extremity. *IEEE Transactions on Neural Systems and Rehabilitation Engineering*. 2009;17(5):428-437. Accessed 30 December 2013.
66. Alles DS. Information transmission by phantom sensations. *IEEE Trans Man-Mach Syst*. 1970;MMS-11(1):85-91. Accessed 15 January 2014.
67. Kooijman CM, Dijkstra PU, Geertzen JHB, Elzinga A, Van Der Schans CP. Phantom pain and phantom sensations in upper limb amputees: An epidemiological study. *Pain*. 2000;87(1):33-41. Accessed 14 January 2014.
68. Kuiken TA, Dumanian GA, Lipschutz RD, Miller LA, Stubblefield KA. The use of targeted muscle reinnervation for improved myoelectric prosthesis control in a bilateral shoulder disarticulation amputee. *Prosthet Orthot Int*. 2004;28(3):245-253. Accessed 20 December 2013.
69. Hijjawi JB, Kuiken TA, Lipschutz RD, Miller LA, Stubblefield KA, Dumanian GA. Improved myoelectric prosthesis control accomplished using multiple nerve transfers. *Plast Reconstr Surg*. 2006;118(7):1573-1578. Accessed 20 December 2013.
70. Hebert JS, Olson JL, Morhart MJ, et al. Novel targeted sensory reinnervation technique to restore functional hand sensation after transhumeral amputation. *IEEE Transactions on Neural Systems and Rehabilitation Engineering*. 2014;22(4):765.
71. Kuiken TA, Marasco PD, Lock BA, Harden RN, Dewald JPA. Redirection of cutaneous sensation from the hand to the chest skin of human amputees with targeted reinnervation. *Proc Natl Acad Sci U S A*. 2007;104(50):20061-20066. Accessed 20 December 2013.

72. Kuiken TA, Miller LA, Lipschutz RD, et al. Targeted reinnervation for enhanced prosthetic arm function in a woman with a proximal amputation: A case study. *Lancet*. 2007;369(9559):371-380. Accessed 20 December 2013.
73. Sensinger JW, Schultz AE, Kuiken TA. Examination of force discrimination in human upper limb amputees with reinnervated limb sensation following peripheral nerve transfer. *IEEE Transactions on Neural Systems and Rehabilitation Engineering*. 2009;17(5):438-444. Accessed 5 April 2013.
74. Dawson MR, Fahimi F, Carey JP. The development of a myoelectric training tool for above-elbow amputees. *Open Biomedical Engineering Journal*. 2012;6(1):5-15. Accessed 20 December 2013.
75. Kung TA, Bueno RA, Alkhalefah GK, Langhals NB, Urbanchek MG, Cederna PS. Innovations in prosthetic interfaces for the upper extremity. *Plast Reconstr Surg*. 2013;132(6):1515-1523. Accessed 14 January 2014.
76. Johansson RS, Westling G. Signals in tactile afferents from the fingers eliciting adaptive motor responses during precision grip. *Experimental Brain Research*. 1987;66(1):141-154. Accessed 30 December 2013.
77. Westling G, Johansson RS. Responses in glabrous skin mechanoreceptors during precision grip in humans. *Experimental Brain Research*. 1987;66(1):128-140. Accessed 30 December 2013.
78. Hernandez-Arieta A, Dermitzakis K, Damian D, Langarella M, Pfeifer R. Sensory-motor coupling in rehabilitation robotics. In: Takahashi Y, ed. *Service robot applications*. Rijeka: InTech Europe; 2008:21-36.
79. Mann RW, Reimers SD. Kinesthetic sensing for the EMG controlled "Boston arm". *IEEE Trans Man-Mach Syst*. 1970;MMS-11(1):110-115. Accessed 30 October 2013.

80. Goodwin GM, McCloskey DI, Matthews PBC. The contribution of muscle afferents kinaesthesia shown by vibration induced illusions of movement and by the effects of paralyzing joint afferents. *J Physiol (Lond)*. 1972;536:635-647. Accessed 24 May 2013.
81. Eklund G. Position sense and state of contraction: The effects of vibration. *J Neurol Neurosurg Psychiatr*. 1972;35:606-611. Accessed 24 May 2013.
82. Proske U, Gandevia SC. The proprioceptive senses: Their roles in signaling body shape, body position and movement, and muscle force. *Physiol Rev*. 2012;92(4):1651-1697. Accessed 30 September 2013.
83. Lake C. The evolution of upper limb prosthetic socket design. *Journal of Prosthetics and Orthotics*. 2008;20(3):85-92. Accessed 20 December 2013.
84. Daly W. Upper extremity socket design options. *Phys Med Rehabil Clin N Am*. 2000;11(3):627-638. Accessed 20 December 2013.
85. Moran CW. Revolutionizing prosthetics 2009 modular prosthetic limb-body interface: Overview of the prosthetic socket development. *Johns Hopkins APL Technical Digest (Applied Physics Laboratory)*. 2011;30(3):240-249. Accessed 5 April 2013.
86. Hargrove L, Englehart K, Hudgins B. A training strategy to reduce classification degradation due to electrode displacements in pattern recognition based myoelectric control. *Biomedical Signal Processing and Control*. 2008;3(2):175-180. Accessed 4 February 2014.

Chapter 3. Sensorimotor integration and kinesthesia in able-bodied individuals

The majority of this chapter has been published as:

Schofield JS, Dawson MR, Carey JP, Hebert JS. (2015). Characterizing the effects of amplitude, frequency and limb position on vibration induced movement illusions: Implications in sensory-motor rehabilitation. *Technology and Healthcare*. 23(2): 129-41.

3.1 Chapter Preface

This chapter introduces the concept of sensorimotor integration and kinesthesia in intact healthy limbs. An overview of the anatomy and physiological principles involved in upper limb sensorimotor control are provided. In this thesis, we present the development and integration of a novel prosthetic sensory feedback technique for upper limb prostheses; the work in this chapter was used to support these objectives in two ways. 1) The concepts presented provide the reader with the necessary background information in preparation for subsequent chapters detailing the development of our kinesthetic sensory feedback technique. 2) This chapter describes the process by which we developed an applied understanding of kinesthetic illusion prior to implementing it in prosthetic sensory feedback. The work presented helped characterize the illusion and optimize feedback parameters in preparation for the translation of our feedback techniques into an amputee population.

The study described in this chapter is presented in the broader context of sensorimotor rehabilitation. In literature investigating kinesthesia through vibration induced movement illusions, vibratory parameters and body position show little agreement across studies or are not reported. This chapter consolidates practical factors that may impact illusionary movement sensations by evaluating their effects and relation to perceived movement sensations. The results and findings are directly transferable to the study presented in chapter 4 that utilized the same techniques in an amputee population.

3.2 Intact limbs and sensorimotor integration

Sensorimotor integration is the process by which the central nervous system utilizes sensory input to update and modulate motor output¹. Movement of an intact upper limb results in the stimulation of numerous afferent sensory organs embedded in the skin, muscles, joints and tendinous tissues, among many others. The central nervous system is dependent on the information provided through these channels and forms internal cognitive models that predict and compare sensory outcomes of an action². In the sections below, two categories of sensory information are highlighted, cutaneous and kinesthetic information. These sections provide a brief overview of these sensory systems in healthy intact limbs to provide context for subsequent chapters discussing the particular relevance in upper limb prosthetic control.

3.2.1 Cutaneous Afferents

Cutaneous afferents help shape the way we interact with objects in our environment. During object manipulation peripheral tactile information is relayed from afferent sensory organs to the central nervous system, providing real-time updates¹. Mechanistically, when an intact hand interacts with an object, the contacting and surrounding soft tissues are deformed which stimulates embedded mechanoreceptors. Encoded within the afferent signals of these receptors is information relaying the magnitude, direction and spatial distribution of contact forces, friction, slip, and others that are vital to the planning and control of object manipulation³. Four distinct mechanoreceptors types are contained either superficially within the skin (Meissner corpuscles and Merkel cells) or embedded within the deeper tissues of the dermis (Pacinian corpuscles and Ruffini corpuscles)⁴. Table 3-1 provides a summary of individual mechanoreceptors, response characteristics, locations in hand tissue, and the mechanical stimuli to which they respond.

Table 3-1 Summary of mechanoreceptors involved in the sense of touch^{1,4}

Mechanoreceptor	Location	Response	Stimuli
Meissner corpuscles FA-I (fast adapting type I)	Superficial skin (epidermis)	Dynamic deformation in the ~5-50Hz range	Touch, pressure, texture
Merkel cells SA-I (slow adapting type I)	Superficial skin (epidermis)	Dynamic deformation < ~5Hz	Light touch, flutter
Pacinian corpuscles FA-II (fast adapting type II)	Deeper tissue (dermis)	Mechanical transients and vibration in the ~40-400Hz range	Deep pressure, vibration, touch
Ruffini corpuscle SA-II (slow adapting type II)	Deeper tissue (dermis)	Low dynamic sensitivity	Skin stretch

3.2.2 Kinesthesia

Throughout literature authors define varying distinctions to separate the two broad concepts of kinesthesia and proprioception, yet a consistent distinguishing definition has yet to be adopted. In this work kinesthesia will be defined as the summation of sensory signals resulting in a sense of movement⁵. Proprioception will refer to a higher order sense that incorporate systems (including kinesthetic contributions) participating in the awareness of one's limb or body position in space. Although proprioception and kinesthesia both play important roles in the awareness of one's limbs and body, this work focuses more specifically on kinesthesia as it holds important implications in UL prosthetic movement control.

A number of sensory receptors contribute to kinesthesia. During limb movement, muscles, tendons, skin and other tissues surrounding the involved joints will undergo deformation. Each tissue is innervated with mechanically sensitive receptors that likely play a role in kinesthetic sensation. For example, the stretching of skin provides information about specific phalange joint movements during digit flexion and extension⁶. However, there is strong evidence to suggest that muscle spindles embedded within the muscle tissue are the chief contributors to kinesthetic sensation⁵.

Muscle spindles are sensory receptors with the primary role of detecting muscle length. The receptors are composed of intrafusal muscle fibers and are embedded in the muscle belly parallel

to the extrafusal fibers. Muscle spindles provide sensory information to the central nervous system through two types of afferent fibers, group 1A (primary afferents) and group II (secondary afferents). The primary afferents are rapidly adapting and sensitive to changes in muscle length and the rate of change⁷, therefore contributing to movement sense and perceived movement velocity, whereas the secondary afferents are sensitive to static muscle position⁴. The role of muscle spindles in kinesthetic sensation is significant. In fact, vibration of specific frequencies and amplitudes introduced to a muscle can activate muscle spindles and yield illusionary sensations of limb movement⁸. These strong and robust sensations can lead to misjudgments in limb position and even sensations of the limb moving to impossible body positions^{5,9}. This phenomenon forms the basis of much of the work discussed in this thesis.

3.3 The kinesthetic illusion in able bodied individuals

3.3.1 Introduction

The kinesthetic illusion is a physiological phenomenon by which the introduction of vibration to a musculotendinous region of a limb will induce sensations that the limb is moving although it remains stationary. In fact these sensations can be so strong that participants have reported experiencing joints bending beyond physiological limits¹⁰, or experienced illusionary distortion of objects or body parts in contact with the stimulated limb¹¹. First published in 1972, Goodwin *et al.*, reported participants experiencing sensations of elbow extension with the introduction of vibration to their distal biceps tendon; and elbow flexion with vibration of the distal triceps tendon⁸. They hypothesized that this phenomenon is a result of the vibrational stimulus exciting muscle spindle receptors. These afferent sensory organs, located in the belly of the muscle, are primarily responsible for detecting changes in muscle length. Most literature reports focusing vibration on the muscle tendon or musculotendinous regions^{5,9} as strong vibration of these locations will induce small rapid cyclical changes in muscle length. When introduced at appropriate frequencies, this rapid physical stretching of the muscle produces a powerful excitatory response in muscle spindle activity¹². Since first being published in 1972, these movement illusions have been incorporated in numerous rehabilitative and research applications.

The kinesthetic illusion elicits sensations of limb movement without dependence on a patient's motor abilities. This has shown particular utility in research applications and treatment of those affected by neuromuscular disorders. For example, Rinderknecht *et al.*, found that the kinesthetic illusion paired with virtual reality enhances the positive effects of motor imagery therapies in patients with upper limb paralysis following stroke¹³. The aim of their work was to induce and support plastic processes in affected brain regions to promote the ability to perform basic gestures like grasping. They suggest that virtual reality to visualize movement of a patient's paralyzed hand, couple with illusionary sensations of movement, may provide a feasible rehabilitative technique for improved hand motor control^{13,14}. In children with cerebral palsy, Redon-Zouiteni *et al.* found that proprioceptive stimulation, through tendon vibration, resulted in improved upper body posture¹⁵. The kinesthetic illusion has also shown promise in the treatment of patients with spasticity. Krueger-Beck *et al.* found that the induction of movement illusions in a particular muscle group can reduce the level of involuntary activity¹⁶. Further applications of the kinesthetic illusion can be found in literature on the research and treatment of those suffering from complex-regional pain syndrome¹⁷, treatment of lower back pain¹⁸ and dystonia or essential tremor¹⁹⁻²², among others²³⁻²⁶.

However, the effective use of the kinesthetic illusion in a rehabilitative or research setting is fundamentally dependent on understanding how to introduce vibration such that this phenomenon can be consistently elicited and manipulated. The vibratory stimulus is most often presented to the participants in a sinusoidal waveform, with some exceptions²⁷⁻²⁹. Therefore this stimulus can be defined by two parameters, frequency and amplitude. However, the effects that frequency and amplitude have on experienced movement sensations are not always clear in previous reports. Early research by Roll *et al.*, attempted to evaluate the effect of vibration frequency on the perceived movement velocity. By systematically manipulating frequency, they determined that perceived velocity increased when vibratory frequency was increased from 10 to 70Hz. A further frequency increase in the range of 80 to 120 Hz resulted in a reduction of perceived velocity²⁹. However, this study did not investigate amplitude effects, and allowed amplitude to vary between 0.2 to 0.5mm. As this variation was not statistically blocked, it may have functioned as a confounding variable in their findings. Regardless, this work has led to the

suggestion that 80Hz produces the “optimal” illusion⁹. Yet, Clark argued that amplitude has a strong influence on the kinesthetic illusion and that decreasing amplitude results in a decreased velocity of the movement illusion³⁰. Little follow up research has been conducted to investigate these claims; and arguably, amplitude effects have yet to be studied thoroughly.

As a result, literature shows little consistency in the vibratory values used to achieve the kinesthetic illusion. The original work performed by Goodwin *et al.* was successful in eliciting movement sensations using a hand held vibrator producing a frequency of 100Hz and 1 mm amplitude (neutral-to-peak)⁸. Subsequent literature has reported eliciting the kinesthetic illusion with frequencies ranging from 10 Hz^{29,31} to 160Hz³². Studies not specifically focusing on the effects of low frequency have conducted testing with values as low as 60 Hz³³ and a high as 160 Hz³². The second parameter defining sinusoidal vibration is amplitude. In previous literature, this parameter also varies widely ranging from 0.2 mm^{27,29,34} to 6 mm³⁵ (neutral-to-peak); although most often, 0.2 mm thru 1 mm (neutral to peak). It may also be noted that, numerous authors neglect to define the vibration amplitude used in their studies^{11,28,30,36-39}. As sinusoidal vibration is defined by both frequency and amplitude, it is difficult to state the importance of one variable without fully defining the other. A comprehensive study of the effects of vibratory parameters would require systematic manipulation of both frequency and amplitude. Incorporation of both parameters would allow assessment of individual effects, and would identify if frequency and amplitude interact with each other or hold a co-dependent relationship.

Beyond amplitude and frequency, the experimental setup an investigator or clinician chooses may also impact the perceived movement illusions. It has been shown that the position of a limb and state of muscle relaxation may impact movement sensations. Craske *et al.* have shown that limb positions which increase stretch in a muscle may make the limb more sensitive to perceptions of movement¹⁰. McCloskey demonstrated that contraction and fatigue of a muscle reduced perceived movement velocity⁴⁰. It has also been reported that when participants are able to view their stimulated limb they will experience either no illusion or significantly reduced motion and velocity of illusion⁴¹⁻⁴⁴. Furthermore, tactile feedback^{45,46} as well as movement of the contralateral arm^{43,44} may also reduce illusory movement sensations.

Given the inconsistency of vibratory parameters found in the literature, it becomes a challenging task for a clinician or researcher to select the optimal vibratory parameters for a given experimental setup, and to fully understand the impact their choices may have on the resulting movement illusions. Therefore, this study aims to more comprehensively investigate the vibratory parameters affecting the kinesthetic illusion. Specifically, the effects of three fundamentally important independent variables: amplitude, frequency, and arm position, are quantified in relation to the strength of illusion (SOI), range of motion (ROM) and perceived velocity of the illusion. Consistent with past literature, it is hypothesized that all three independent variables will affect the kinesthetic illusion. The analysis performed will quantify the degree to which each variable affects the illusion, thereby facilitating future choice of parameters to most consistently elicit and manipulate the kinesthetic illusion.

3.3.2 Methods

Twelve able-bodied participants were recruited (9 male, 3 female; mean age: 24 SD 1.7 years). All participants reported right hand dominance, and no current (or previous) neurological or muscular conditions that may affect experimental results. Informed consent was obtained prior to participation; ethics was approved through our institute's review board.

3.3.2.1 Experimental Setup

Vibration was introduced to the participants using a hand held⁸ voice coil system (VCS1010, EquipSolutions, Sunnyvale, USA) attached to a flat faced probe tip (1.8 cm diameter)(Figure 3.1). The probe tip was depressed perpendicularly into the tissue of each participant with approximately 2.5 to 4 Newtons force as measured by an inline load cell (iLoad Pro, Loadstar Sensors, Fremont, USA). Video and audio footage of participant trials was digitally recorded (Pro9000, Logitech, Morges, Switzerland).

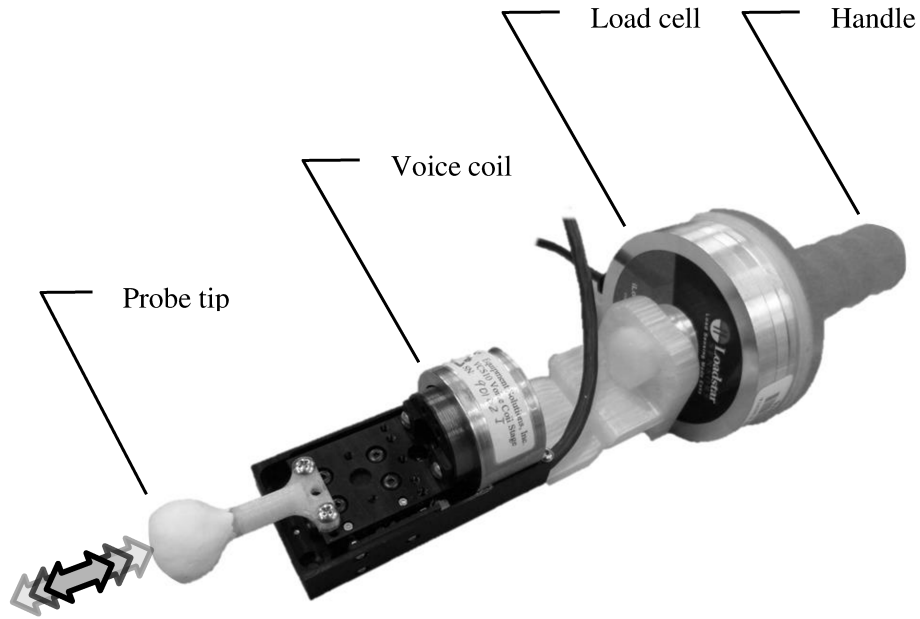


Figure 3.1 Hand held voice coil system

Participants were seated in front of a table with moveable arm supports. The supports were configured to achieve the arm positions described below in the ‘Testing Procedure’ section. Specific care was given to minimize contact of the participants forearm with the table or support structure thus minimizing tactile feedback. Further consideration was given to position the limb such that relaxation of the tested muscle group was promoted. Both factors have been shown to influence the kinesthetic illusion^{10,40}.

3.3.2.2 Testing Procedure

Vibration testing was conducted on each participant’s dominant-side (right) biceps and triceps. For each muscle group, the participant’s arm was tested in two elbow joint positions. These positions were selected to induce a state of muscle stretch in one position and relative slack in the next. For the biceps, *stretch* was achieved by fully extending the elbow and *relative slack* by positioning the elbow at approximately 90° flexion. For the triceps, *stretch* and *relative slack* were achieved by positioning the elbow to approximately 120° and 90° elbow flexion,

respectively (Figure 3.2). Joint angles were verified using a goniometer prior to testing. The order that each muscle group and position was tested in was selected at random.

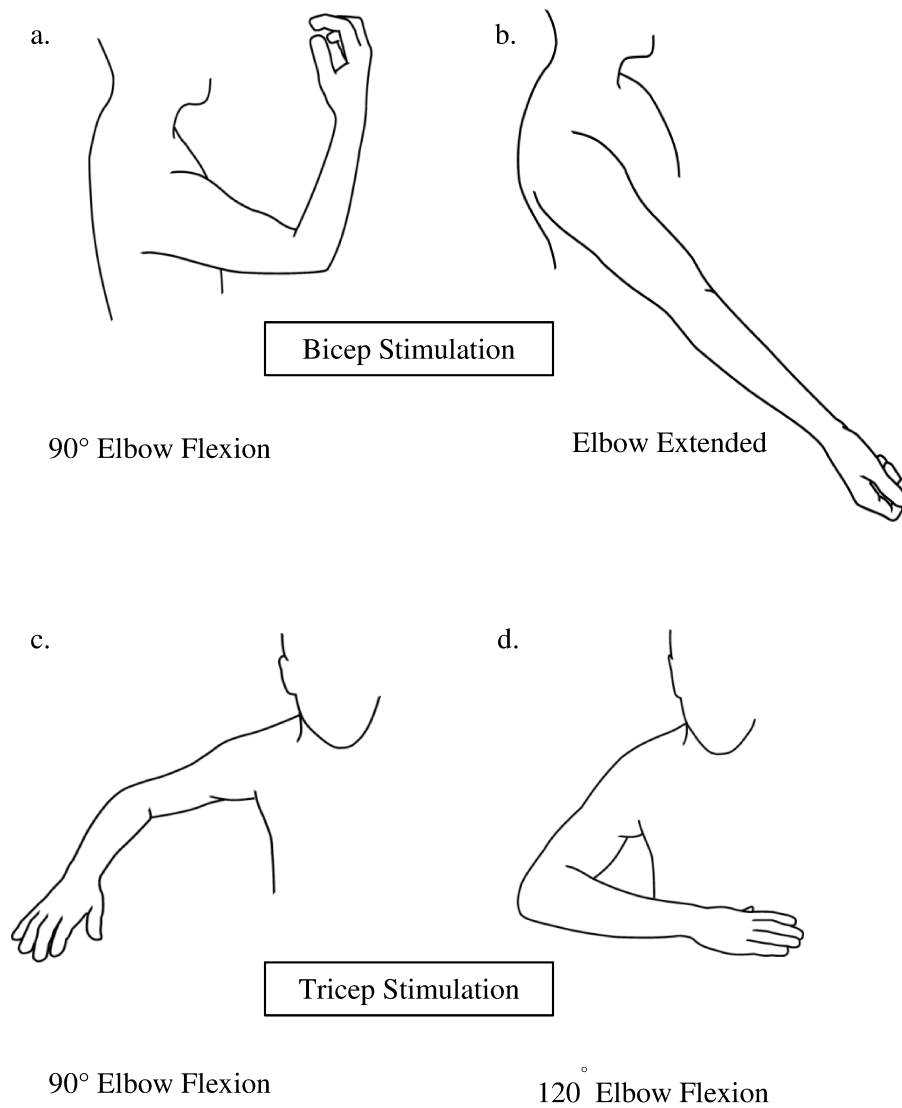


Figure 3.2 Arm positions for the application of vibratory stimulus. Bicep stimulation provided at two positions, a. approximately 90° flexion (relative muscle slack) b. elbow fully extended (muscle stretch), Tricep stimulation provided at two positions, c. approximately 90° flexion (relative muscle slack) d. approximately 120° flexion (relative muscle stretch)

3.3.2.3 Initial Testing

Prior to varying the parameters of amplitude and frequency, it was necessary to identify a location, that when vibrated, consistently elicited the kinesthetic illusion.

Before testing, participants were informed that they may experience a variety of sensations and one of these sensations may, or may not be, movement. Specific details such as when one may expect to feel movement, and at which joint or in which direction, were withheld. The participants' vision was occluded and they were asked to report "any sensations beyond simple vibration." Vibration with parameters shown effective at eliciting the kinesthetic illusion in prior pilot testing (90 Hz and 0.5mm amplitude) was systematically introduced to various locations of the participant's distal musculotendinous tissue. Each location was tested for approximately 10 seconds prior to moving to the next. If after 5 minutes of continuous testing a participant failed to experience movement sensations, they would be provided with the information "some participants report feeling movement in their elbow." Testing would then continue for another 5 minutes. If the participant again failed to experience movement illusions, they would be seeded with the information, "participants often report sensations that their elbow is flexing (or extending)." Testing would then continue until the participant experienced movement illusions or until 10 additional minutes passed at which point testing would be discontinued if no illusion was induced.

Once a participant reported sensations consistent with the kinesthetic illusion, probing of the surrounding tissue was conducted to precisely identify a location most consistently producing a strong kinesthetic sensation. The participant would be asked to compare stimulus locations in close proximity, with the investigator prompting, "Which one gives the strongest sensation of movement, number one or number two?" Vibration would be applied to location one or location two simultaneous with the investigator's verbal cue. This was continued until a location consistently producing a stronger illusion than the surrounding tissue was identified. The final stimulus location was marked on the participant's skin with a felt-tipped marker. This initial testing procedure was repeated for each muscle group in each arm position (as described in the experimental setup section).

3.3.2.4 Vibration Parameter Testing

To evaluate the effects of amplitude, frequency and muscle stretch (elbow joint position) on the kinesthetic illusion, a full factorial design was used. The manipulated variables, amplitude and frequency were introduced at three levels (0.1, 0.3, 0.5mm neutral to peak and 70, 90 and 110Hz, respectively). The third manipulated variable, muscle stretch, was introduced according to the elbow joint positions described in Figure 3.2. In total each muscle site would be exposed to 18 unique combinations of amplitude, frequency and joint position. These combinations were randomly presented to each muscle for 10 seconds, at the corresponding location determined in the initial testing.

Following each combination, three output variables were quantified to characterize the induced kinesthetic illusion: SOI, ROM, and illusionary velocity. SOI was quantified on a 5 point Likert Scale. The participant was prompted, “We want you to describe the realism of the illusion. How strong or convincing was the illusion that your arm was moving?” A score of zero would be assigned to the absence of an illusion, and integers from one to five would represent: Not at all, Slightly, Somewhat, Very, and Extremely, respectively. ROM was quantified by asking the participant to manipulate a two-dimensional sagittal arm model to indicate the range they felt their joint moving, and then measuring the angular change in elbow position. Similar memory and recall methods have been used in previous literature^{8,29,40}. Finally illusionary velocity was quantified by having the participants manipulate the two dimensional model “at the same velocity they felt their arm moving.” The time duration to complete each movement was taken from digital video footage. Velocity was calculated as the ROM divided by the movement duration.

3.3.2.5 Data Treatment and Analysis

To address the possible subjectivity and inter-participant error introduced as a result of manipulating the 2D sagittal model; ROM and velocity results were normalized. For example, the largest ROM value occurring in a specific muscle group of a participant would be identified. The remaining ROM values for that participant’s muscle group would then be normalized (divided) by the corresponding maximum ROM value. This procedure was repeated for each muscle group of each participant individually. Therefore ROM and velocity results fell between

zero and one. A value of zero represents the absence of an illusion and therefore no motion or no velocity, and one representing the largest value experienced by the participant's muscle group.

ANOVAs were performed to evaluate the significance of the three manipulated variables (amplitude, frequency, muscle stretch) on SOI, ROM and velocity independently.

Correspondingly three ANOVAs were performed for each muscle group. Each ANOVA evaluated both main effects and two-way interactions effects with $p < 0.05$ assumed significant.

To characterize the nature of the relationships between significant manipulated variables and corresponding output variables, mean plots were utilized. From the ANOVA results, a mean plot was created for each manipulated variable having a significant effect on one of the measured output variables. Finally correlation matrices were created to quantify the linear-dependence of the three output variables (SOI, ROM, and velocity).

3.3.3 Results

The initial testing was performed to identify locations on a participant's limb, that when vibrated, consistently elicited the kinesthetic illusion. However, it was found that only four of twelve participants were able to experience movement sensations while uninformed of the specifics of the kinesthetic illusion. After five minutes of testing, 8 participants were seeded with further information intending to lead them to experience the illusion. An additional 3 participants described sensations consistent with vibration induced movement illusions following this information. However, five participants still failed to experience the illusion after ten minutes of testing. At this stage, information was provided explicitly describing the kinesthetic illusion. These five participants all described consistent movement sensation shortly thereafter (Table 3-2).

Table 3-2 Time intervals for participants to first experience the illusion. Conditions for participants to first experience the kinesthetic illusion, categorized by time interval and the corresponding number of participants to first experience during each interval

Testing Time (minutes)	Information Provided	Participants first experiencing illusion
0-5	None (Participants Uninformed)	4
6-10	“Some participants report feeling movement in their elbow.”	3
11-15	“Participants often report sensations that their elbow is flexing (or extending).”	5

ANOVAs were conducted to identify variables having a significant effect on SOI, ROM or perceived velocity. In the biceps, amplitude was found to have a significant effect on all three output measures, SOI, ROM and velocity ($p < 0.05$). It was also shown that the perceived velocity was affected by the initial arm position of participants. No interaction effects were shown to be significant (Table 3-3a.).

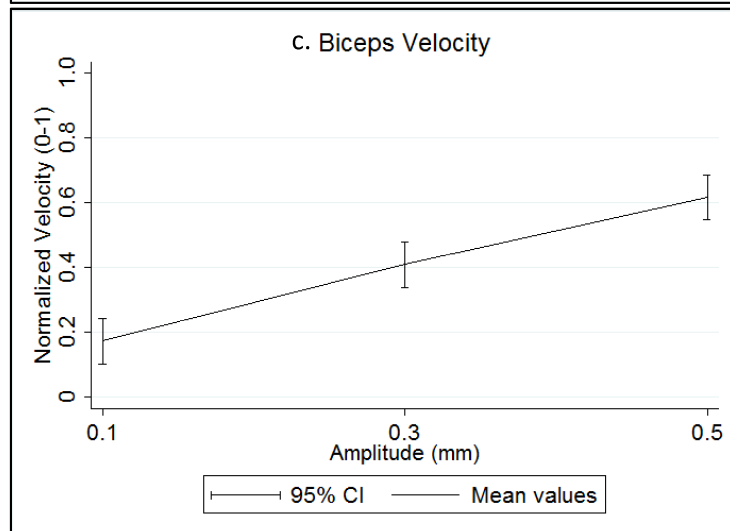
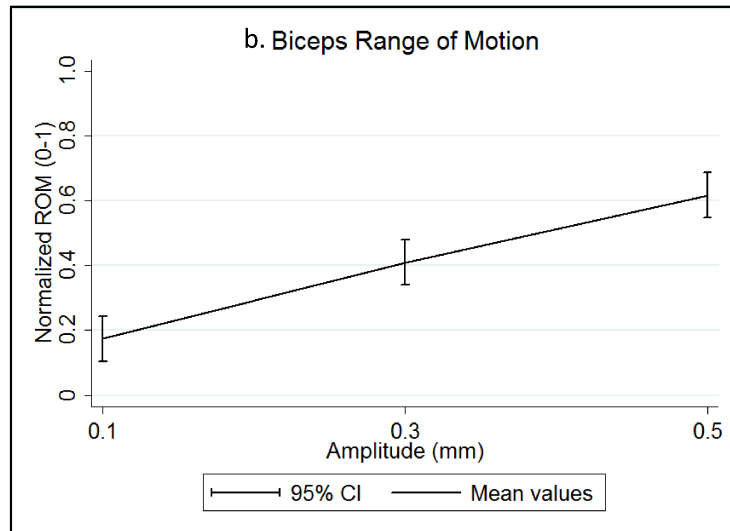
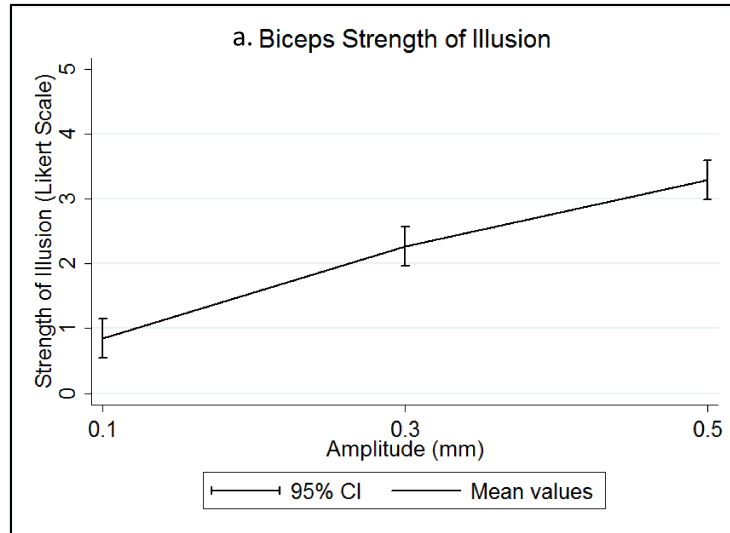
Similarly in the triceps, amplitude was found to have a significant effect on all three output measures, SOI, ROM and velocity ($P < 0.05$). It was also shown that the ROM and perceived velocity was affected by the initial arm position of participants. No interaction effects were shown significant (Table 3-3 b.).

Table 3-3 ANOVA results. a. Bicep results, p-values for both main effects and interaction effects shown b. Tricep results, p-values for both main effects and interaction effects shown *Indicates statistically significant values (p<0.05)

a. Bicep Results		P-Value		
		SOI	ROM	Velocity
Main Effects	Amplitude	<0.010*	<0.010*	<0.010*
	Frequency	0.700	0.886	0.969
	Position	0.366	0.120	0.012*
Interaction Effects	Position/Amplitude	0.648	0.710	0.467
	Position/Frequency	0.917	0.482	0.924
	Amplitude/Frequency	0.915	0.990	0.863

b. Triceps Results		P-Value		
		SOI	ROM	Velocity
Main Effects	Amplitude	<0.010*	<0.010*	<0.010*
	Frequency	0.404	0.537	0.936
	Position	0.611	0.009*	0.033*
Interaction Effects	Position/Amplitude	0.669	0.535	0.767
	Position/Frequency	0.596	0.440	0.860
	Amplitude/Frequency	0.777	0.504	0.902

Mean plots were created to characterize the nature of the relationship between significant variables and corresponding output variables. In the biceps, as amplitude was increased SOI, ROM and perceived velocity were also found to increase (Figure 3.3 a-c). At 0.5mm amplitude the mean plots predicted the average participant will experience the strongest, largest and fastest illusion when compared to 0.1 and 0.3mm amplitude. Furthermore, from the ANOVA results, muscle stretch (joint position) was also determined to have a significant effect on perceived velocity. It can be seen that in joint positions creating more muscle stretch, perceived velocity also increased such that the fastest illusion can be predicted to occur when the elbow is fully extended (Figure 3.3d).



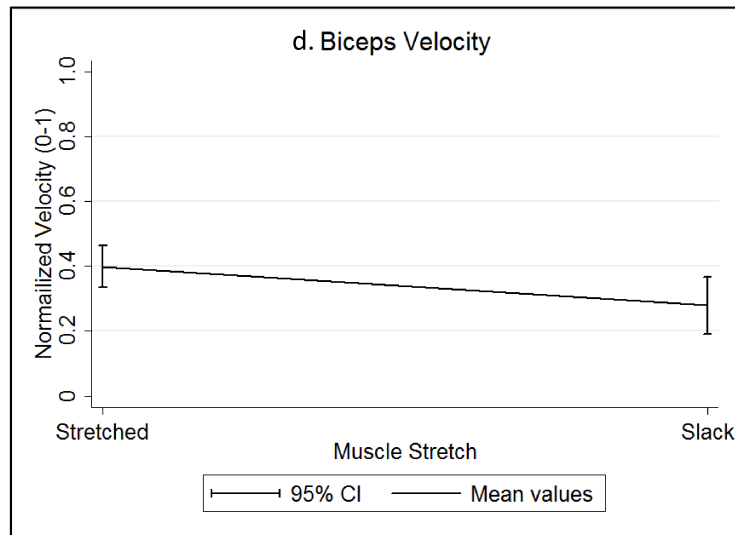
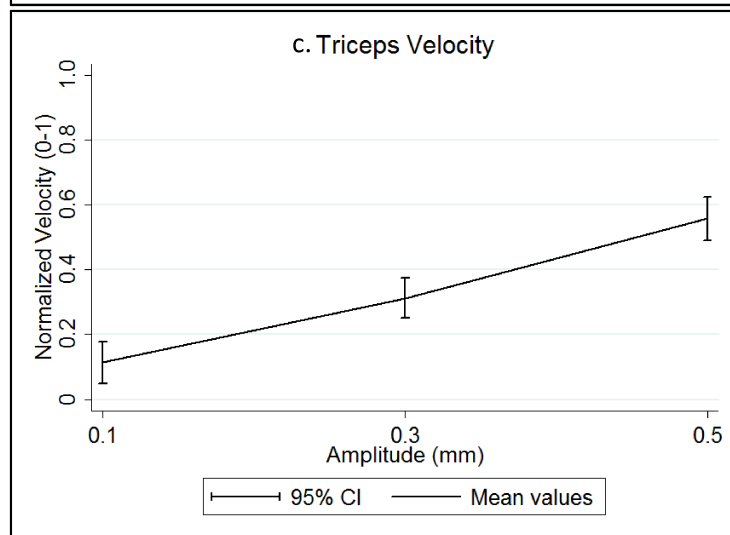
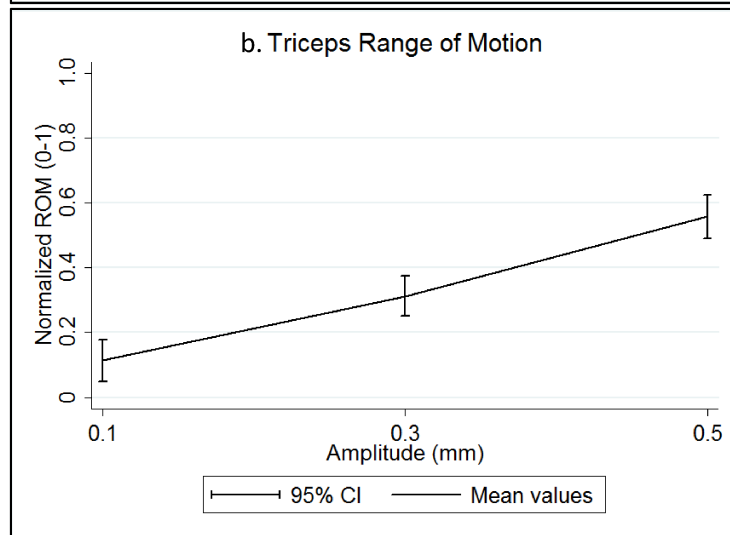
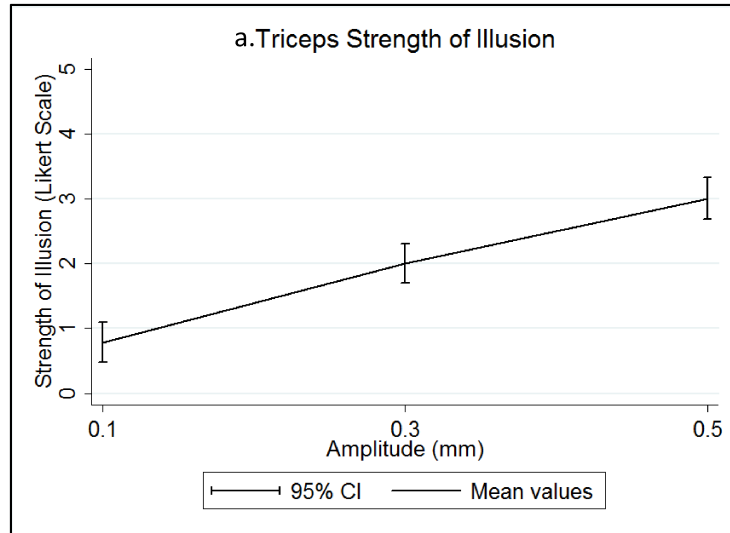


Figure 3.3 Bicep mean plots of significant variables. Mean values and 95% confidence intervals (CI) for each significant manipulated variable plotted at the levels specified in the vibration parameter testing section above. a. Strength of illusion as a function of amplitude b. Normalized range of motion as a function of amplitude c. Normalized velocity as a function of amplitude d. Normalized velocity as a function of muscle stretch.

Similarly, in the triceps, as amplitude increased SOI, ROM and perceived velocity also increased (Figure 3.4 a-c). Again, at 0.5mm amplitude the mean plots predict the average participant will experience the strongest, largest and fastest illusion when compared to 0.1 and 0.3mm amplitude. Furthermore, from the ANOVA results, muscle stretch (joint position) was also determined to have a significant effect on ROM and perceived velocity. However, inverse to the bicep finding, it can be seen that in joint positions creating less muscle stretch, ROM and perceived velocity increased (Figure 3.4 d-e).



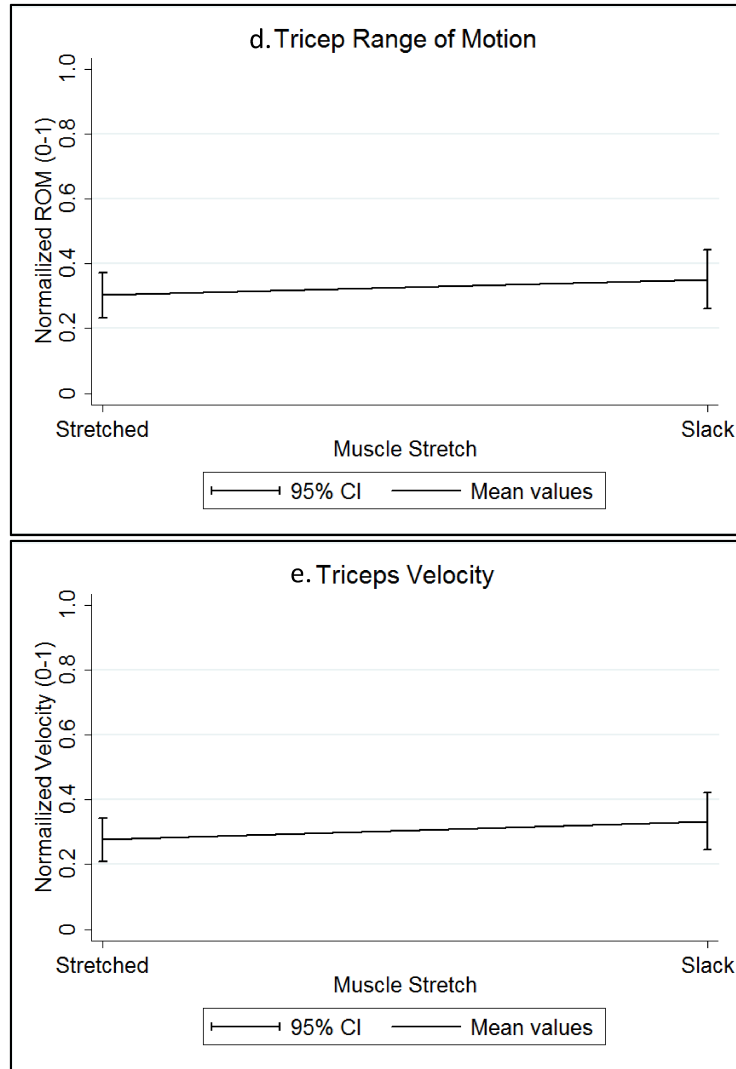


Figure 3.4 Tricep mean plots of significant variables. Mean values and 95% confidence intervals (CI) for each significant manipulated variable plotted at the levels specified in the vibration parameter testing section above. a. Strength of illusion as a function of amplitude b. Normalized range of motion as a function of amplitude c. Normalized velocity as a function of amplitude d. Normalized range of motion as a function of muscle stretch e. Normalized velocity as a function of muscle stretch

Finally it can be seen in the correlation matrices that the three output variables (SOI, ROM and perceived velocity) all strongly correlate with each other. In the biceps correlation coefficients range from 0.749 through 0.871 and in the tricep values coefficients range from 0.711 to 0.859 (Table 3-4).

Table 3-4 Output variables correlation coefficients matrix. Pearson correlation coefficients (R) for the output variables strength of illusion (SOI), range of motion (ROM) and perceived velocity. Table divided by bicep and tricep results

		Correlation (R)		
		SOI	ROM	Velocity
Biceps	SOI	1.000	0.806	0.749
	ROM		1.000	0.871
	Velocity			1.000
Triceps	SOI	1.000	0.763	0.711
	ROM		1.000	0.859
	Velocity			1.000

3.3.4 Discussion

When vibration of certain amplitude and frequency ranges is introduced to musculotendinous regions of a limb, illusory sensation that the limb is moving may occur. Throughout literature, this kinesthetic illusion has been used in the research and rehabilitation of numerous affected populations. Early work to understand this illusion suggests that the vibrational parameters amplitude and frequency may affect the velocity and ROM of these illusions^{29,30}. However, little agreement exists when characterizing the extent and nature to which frequency and amplitude play a role. Beyond vibration parameters, research suggests that physiological factors such as joint position (or muscle stretch)¹⁰, and visual feedback⁴¹⁻⁴³, among others^{40,43-46}, also play a role. Ultimately, this lack of agreement on vibration parameter effects, and abundance of information addressing physiological confounding factors, may present an obstacle to researchers and clinicians wanting to utilize the kinesthetic illusion in a laboratory or clinic.

With the goal of addressing this limitation, this study examined the effects of manipulating three fundamentally important variables (amplitude, frequency, and limb position) on the illusory traits SOI, ROM and perceived velocity. It was found that amplitude was the one vibratory parameter that had the most prominent effect on the experience of the kinesthetic illusion.

In prior literature, it is rarely reported if participants were informed of the kinesthetic illusion prior to testing and the duration of time necessary to first experience the illusion. Our data suggest that movement illusions are not necessarily experienced immediately in first time

participants. Only 4 out of our 12 participants experienced these sensations during the first 5 minutes of testing in the absence of explicit information describing the kinesthetic illusion (Table 3-2). There are a few possible explanations for these results. The first is the tonic vibration reflex. This is a natural reflex that results in the contraction of a muscle with sustained vibration⁴⁷. As contraction of the vibrated muscle has been shown to weaken or abolish the kinesthetic illusion⁴⁰, it is possible these two physiological phenomena may have competed⁸. Some participants had to be repeatedly asked to relax their vibrated muscle and resist the impulse to contract. Anecdotally some participants demonstrated a higher sensitivity to the tonic vibration reflex and consequently took longer to first experience the kinesthetic illusion. A second explanation may lie in how each participant interpreted the sensations experienced. It was common for participants to have difficulty articulating the sensations or to first describe the sensations as “strange.” Although providing these participants with small amounts of information may have lead them to the kinesthetic illusion, this process may have also helped them form clearer mental imagery of how to interpret the sensations they were experiencing. However, once participants began to experience the kinesthetic illusion, regardless of how much or how little information was initially provided, the subsequent description of illusionary movement and response to altering vibration parameters was very consistent across participants. Therefore, using the kinesthetic illusion in rehabilitative applications may require a degree of participant training, especially in populations with limited sensory capacity. In research applications, investigators must be aware that achieving illusionary movements may require time and a strategy to reveal enough information without biasing results. Regardless of the applications, eliciting the kinesthetic illusion may require more than the simple introduction of vibration to muscles or tendons.

In past studies, vibratory frequency has been more often manipulated, and its effects generally more studied, than amplitude. However, from our factorial analysis, we found that amplitude significantly affected the SOI, ROM and perceived velocity of illusions in both the bicep and tricep groups; whereas frequency was found to have no significant effect. This suggests that in the experimental ranges examined (0.1-0.5mm and 70-110Hz) amplitude was the vibratory parameter ultimately governing the kinesthetic illusion. According to Roll *et al*, a decline in

perceived velocity should have been present from 80 through 120Hz²⁹. However, our data suggest that the effects of amplitude so greatly outweighed any frequency phenomenon, that it was neither statistically distinguishable nor was it experienced by the participant group.

The amplitude mean plots in both the biceps and triceps show that increasing the amplitude in the range of 0.1 to 0.5mm resulted in a corresponding increase in all three output variables (SOI, ROM, perceived velocity)(Figure 3.3 a-c, and Figure 3.4 a-c). Therefore, if a researcher or clinician wishes to manipulate the SOI, ROM, or velocity, experienced by an individual, this can be achieved through manipulation of vibrational amplitude. However it must be noted that this relationships can only be expected in the experimental amplitude range (0.1mm to 0.5mm). The mean plots did not show signs of ‘levelling-off’ or ‘plateauing.’ Therefore it cannot be concluded that the strongest, largest or fastest illusion will occur at 0.5mm, as it may occur beyond this amplitude value. Consequently, further work may be warranted to address the amplitude intervals in which the kinesthetic illusion can occur, and values inducing maximum illusions of SOI, ROM or velocity.

The mean plots (Figure 3.3 and Figure 3.4) and correlation matrices (Table 3-4) also illustrated a dependency between output variables. In both the biceps and triceps strong correlation was found between all three outputs (SOI, ROM, Perceived velocity). Ultimately this suggests that these variables cannot be uncoupled and manipulated independently. For example a clinician or researcher wishing to increase the velocity of movement will achieve this by increasing the amplitude. Inherently this amplitude increase will also increase the amount of movement and strength of illusion the subject experiences. As a result of this dependency it does not appear that the illusion can be elicited such that one of the output variables is low while the other remains high. As an example, it would not be possible to elicit a very strong illusion with large ROM, but feel as though it is moving with a slow velocity. The implications of this relationship suggest that researcher or clinician must be willing to achieve a balance of these three variables while designing experiments or therapeutic intervention using the kinesthetic illusion.

It may also be noted that muscle stretch (arm position) was found to have a significant impact on the velocity of illusion in the biceps, as well as ROM and velocity in the triceps. When evaluating their corresponding mean plots, the slope of the muscle stretch graphs is notably less than that of the corresponding amplitude effects graphs (Figure 3.3 and Figure 3.4). Therefore, the conclusion can be drawn that amplitude has a more prominent effect on the kinesthetic illusion than that of muscle stretch. However, clinicians and researchers should be aware that altering initial body posture prior to testing may have the potential to influence the experienced illusion.

3.3.4.1 Limitations

This study was conducted on able-bodied individuals to understand this kinesthetic illusion as it may apply to rehabilitation and research applications. Therefore the results and analysis performed may not directly extrapolate to the selection of vibratory parameters for populations with sensory motor impairment; the nature of the experienced illusion may vary across injury type and individual. Furthermore this study was conducted within specific experimental ranges (0.1-0.5mm amplitude, 70-110 Hz Frequency, 2 arm positions). As a result, the findings and suggestions discussed are limited to illusionary movements elicited within these constraints.

3.4 Conclusions

As a rehabilitation technique, vibration induced movement illusions have demonstrated beneficial results for numerous sensory-motor disorders. However, literature shows little consistency in the vibration parameters or body positioning used, and their effects have yet to be comprehensively investigated. Our work demonstrated amplitude significantly affected the illusionary SOI, ROM and velocity in the biceps and triceps. Increasing amplitude resulted in an increase of all three output variables. Limb position showed an effect on illusionary velocity in the biceps as well as ROM and velocity in the triceps. Frequency in the experimental range demonstrated no statistical effect. This work will help guide clinicians and researchers in selecting appropriate vibratory parameters and body positions to consistently elicit and manipulate the kinesthetic illusion. More specifically, in the context of prosthetic sensory

feedback, this work helped build a baseline understanding such that the kinesthetic illusion can be applied for movement feedback. It helped narrow an effective range of vibration parameters. From a practical perspective it enable our further understanding of how one may experience illusory movement sensations and how best to characterize their perceptions. As we move forward toward employing the kinesthetic illusion in prosthetic sensory feedback, this work provided baseline data for comparison with an amputee population in subsequent chapters.

3.4.1 References

1. Ackerley R, Kavounoudias A. The role of tactile afference in shaping motor behaviour and implications for prosthetic innovation. *Neuropsychologia*. 2015;79:192-205. Accessed 10 February 2017. doi: 10.1016/j.neuropsychologia.2015.06.024.
2. Bays PM, Wolpert DM. Computational principles of sensorimotor control that minimize uncertainty and variability. *J Physiol*. 2007;578(2):387-396. Accessed 13 February 2017. doi: 10.1113/jphysiol.2006.120121.
3. Johansson RS, Flanagan JR. Coding and use of tactile signals from the fingertips in object manipulation tasks. *Nat Rev Neurosci*. 2009;10(5):345-359. Accessed 24 January 2017. doi: 10.1038/nrn2621.
4. Kandel ER, Schwartz JH, Jessell TM. Ch.23 touch. In: *Principles of neuroscience*. 4th ed. McGraw-Hill, Health Professions Division; 2000.
5. Proske U, Gandevia SC. The proprioceptive senses: Their roles in signaling body shape, body position and movement, and muscle force. *Physiol Rev*. 2012;92(4):1651-1697. Accessed 30 September 2013.
6. Collins DF, Refshauge KM, Gandevia SC. Sensory integration in the perception of movements at the human metacarpophalangeal joint. *J Physiol*. 2000;529(2):505-515. Accessed 14 February 2017. doi: 10.1111/j.1469-7793.2000.00505.x.

7. Cooper S. The responses of the of the primary and secondary endings of muscle spindles with intact motor innervation during applied stretch. *Exp Physiol*. 1961;46(4):389-398. Accessed 14 February 2017. doi: 10.1113/expphysiol.1961.sp001558.
8. Goodwin GM, McCloskey DI, Matthews PBC. The contribution of muscle afferents kinaesthesia shown by vibration induced illusions of movement and by the effects of paralyzing joint afferents. *J Physiol (Lond)*. 1972;536:635-647. Accessed 24 May 2013.
9. Jones LA. Motor illusions: What do they reveal about proprioception? *Psychol Bull*. 1988;103(1):72-86. Accessed 5 April 2013.
10. Craske B. Perception of impossible limb positions induced by tendon vibration. *Science*. 1977;196(4285):71-73. Accessed 16 December 2013.
11. Lackner JR. Some proprioceptive influences on the perceptual representation of body shape and orientation. *Brain*. 1988;111(2):281-297. Accessed 18 December 2013.
12. Kandel ER. Part VI: Movement. In: *Principles of neural science*. 5th ed. New York: McGraw-Hill; 2013:743.
13. Rinderknecht MD, Kim Y, Santos-Carreras L, Bleuler H, Gassert R. Combined tendon vibration and virtual reality for post-stroke hand rehabilitation. *2013 World Haptics Conference, WHC 2013*. 2013:277-282. Accessed 20 December 2013.
14. Rinderknecht MD. Device for a novel hand and wrist rehabilitation strategy for stroke patients based on illusory movements induced by tendon vibration. *Proceedings of the Mediterranean Electrotechnical Conference - MELECON*. 2012:926-931. Accessed 20 December 2013.
15. Redon-Zouiteni, C. Roll, JP. Lacert, P. Proprioceptive postural reprogramming in childhood cerebral palsy validation of tendon vibration as a therapeutic tool. *Motricité cérébrale*. 1994;15(2):57.

16. Krueger-Beck E, Nogueira-Neto GN, Nohama P. Vibrational stimulus in spasticity - A perspective of treatment. *Revista Neurociencias*. 2010;18(4):523-530. Accessed 29 January 2014.
17. Gay A, Parratte S, Salazard B, et al. Proprioceptive feedback enhancement induced by vibratory stimulation in complex regional pain syndrome type I: An open comparative pilot study in 11 patients. *Joint Bone Spine*. 2007;74(5):461-466. Accessed 16 December 2013.
18. Willigenburg NW, Kingma I, Hoozemans MJM, van Dieën JH. Precision control of trunk movement in low back pain patients. *Human Movement Science*. 2013;32(1):228-239. Accessed 20 December 2013.
19. Frima N, Nasir J, Grünewald RA. Abnormal vibration-induced illusion of movement in idiopathic focal dystonia: An endophenotypic marker? *Movement Disorders*. 2008;23(3):373-377. Accessed 5 February 2014.
20. Frima N, Grünewald RA. Abnormal vibration induced illusion of movement in essential tremor: Evidence for abnormal muscle spindle afferent function. *Journal of Neurology, Neurosurgery and Psychiatry*. 2005;76(1):55-57. Accessed 5 February 2014.
21. Frima N, Rome SM, Grünewald RA. The effect of fatigue on abnormal vibration induced illusion of movement in idiopathic focal dystonia. *Journal of Neurology Neurosurgery and Psychiatry*. 2003;74(8):1154-1156. Accessed 5 February 2014.
22. Rome S, Grünewald RA. Abnormal perception of vibration-induced illusion of movement in dystonia. *Neurology*. 1999;53(8):1794-1800. Accessed 5 February 2014.
23. Han J, Jung J, Lee J, Kim E. Effects of vibration stimuli on the knee joint reposition error of elderly women. *Journal of Physical Therapy Science*. 2013;25(1):93-95. Accessed 20 December 2013.
24. Roll R, Kavounoudias A, Albert F, et al. Illusory movements prevent cortical disruption caused by immobilization. *Neuroimage*. 2012;62(1):510-519. Accessed 29 January 2014.

25. Quercia P, Demougeot L, Dos Santos M, Bonnetblanc F. Integration of proprioceptive signals and attentional capacity during postural control are impaired but subject to improvement in dyslexic children. *Experimental Brain Research*. 2011;209(4):599-608. Accessed 5 February 2014.
26. Vaugoyeau M, Hakam H, Azulay J-. Proprioceptive impairment and postural orientation control in parkinson's disease. *Human Movement Science*. 2011;30(2):405-414. Accessed 5 February 2014.
27. Roll JP, Vedel JP, Ribot E. Alteration of proprioceptive messages induced by tendon vibration in man: A microneurographic study. *Experimental Brain Research*. 1989;76(1):213-222. Accessed 16 December 2013.
28. Gilhodes JC, Roll JP, Tardy-Gervet MF. Perceptual and motor effects of agonist-antagonist muscle vibration in man. *Experimental Brain Research*. 1986;61(2):395-402. Accessed 16 December 2013.
29. Roll JP, Vedel JP. Kinaesthetic role of muscle afferents in man, studied by tendon vibration and microneurography. *Experimental Brain Research*. 1982;47(2):177-190. Accessed 16 December 2013.
30. Clark FJ, Matthews PB, Muir RB. Effect of the amplitude of muscle vibration on the subjectively experienced illusion of movement [proceedings]. *J Physiol (Lond)*. 1979;296:14P-15P. Accessed 18 December 2013.
31. Meek SG, Jacobsen SC, Goulding PP. Extended physiologic taction: Design and evaluation of a proportional force feedback system. *Journal of Rehabilitation Research and Development*. 1989;26(3):53-62. Accessed 2 December 2013.
32. Eklund G. Position sense and state of contraction: The effects of vibration. *J Neurol Neurosurg Psychiatr*. 1972;35:606-611. Accessed 24 May 2013.

33. Verschueren SMP, Brumagne S, Swinnen SP, Cordo PJ. The effect of aging on dynamic position sense at the ankle. *Behav Brain Res*. 2002;136(2):593-603. Accessed 16 December 2013.
34. Calvin-Figuière S, Romaiguère P, Roll J-. Relations between the directions of vibration-induced kinesthetic illusions and the pattern of activation of antagonist muscles. *Brain Res*. 2000;881(2):128-138. Accessed 5 April 2013.
35. Kito T, Hashimoto T, Yoneda T, Katamoto S, Naito E. Sensory processing during kinesthetic aftereffect following illusory hand movement elicited by tendon vibration. *Brain Res*. 2006;1114(1):75-84. Accessed 20 December 2013.
36. White O, Proske U. Illusions of forearm displacement during vibration of elbow muscles in humans. *Experimental Brain Research*. 2009;192(1):113-120. Accessed 18 December 2013.
37. Seizova-Cajic T, Smith JL, Taylor JL, Gandevia SC. Proprioceptive movement illusions due to prolonged stimulation: Reversals and aftereffects. *PLoS ONE*. 2007;2(10). Accessed 20 December 2013.
38. Lackner J. Human sensory-motor adaptation to the terrestrial force environment. *Brain Mechanisms and Spatial Vision*. 1985;21:175.
39. Capaday C, Cooke JD. The effects of muscle vibration on the attainment of intended final position during voluntary human arm movements. *Experimental Brain Research*. 1981;42(2):228-230. Accessed 18 December 2013.
40. McCloskey DI. Differences between the senses of movement and position shown by the effects of loading and vibration of muscles in man. *Brain Res*. 1973;61:119-131. Accessed 23 December 2013.
41. Guerraz M, Provost S, Narison R, Brugnion A, Virolle S, Bresciani J-. Integration of visual and proprioceptive afferents in kinesthesia. *Neuroscience*. 2012;223:258-268. Accessed 5 April 2013.

42. Seizova-Cajic T, Azzi R. Conflict with vision diminishes proprioceptive adaptation to muscle vibration. *Experimental Brain Research*. 2011;211(2):169-175. Accessed 5 February 2014.
43. Izumizaki M, Tsuge M, Akai L, Proske U, Homma I. The illusion of changed position and movement from vibrating one arm is altered by vision or movement of the other arm. *J Physiol (Lond)*. 2010;588(15):2789-2800. Accessed 5 April 2013.
44. Lackner JR, Taublieb AB. Influence of vision on vibration-induced illusions of limb movement. *Exp Neurol*. 1984;85(1):97-106. Accessed 18 December 2013.
45. Blanchard C, Roll R, Roll J-, Kavounoudias A. Combined contribution of tactile and proprioceptive feedback to hand movement perception. *Brain Res*. 2011;1382:219-229. Accessed 5 April 2013.
46. Rabin E, Gordon AM. Prior experience and current goals affect muscle-spindle and tactile integration. *Experimental Brain Research*. 2006;169(3):407-416. Accessed 5 February 2014.
47. Eklund G. HK. Motor effects of vibratory muscle stimuli in man. *Electroenceph clin Neurophysiol*. 1965;19:619.

Chapter 4. The application of the kinesthetic illusion in a population with transhumeral amputation

Portions of this section have been submitted as:

Marasco PD, Hebert JS, Sensinger JW , Shell CE, Schofield JS, Thumser ZC, Nataraj R, Beckler DT, Dawson MR, Blustein DH, Gill S, Mensh BD, Granja-Vazquez R, Newcomb MD, Carey JP, Orzell BM. Engineered illusory movement percepts improve motor control for bionic prosthetic hands. In preparation

4.1 Chapter Preface

In this chapter, we build on the work presented in chapter 3 by transitioning the techniques developed in able-bodied participants into a population that had undergone transhumeral amputation and targeted reinnervation surgery. Herein is described experiments characterizing the kinesthetic illusion in an amputee population, and demonstrating its application in the movement feedback of physical prosthetic components. The techniques developed provide movement feedback matched to prosthetic movement, and experienced in the missing limb. Here we argue that this provides intuitive, relevant feedback information, thus addressing a major barrier present with many other feedback techniques. The data presented in this chapter helped identify key challenges as we worked toward the integration of our feedback approach into functional prosthetic sockets, a major focus of the subsequent chapters.

4.2 Introduction

Kinesthesia is the inherent sense of movement of one's body position or limbs. It plays a key role in the coordination of dexterous upper limb (UL) movements as the encoded information informs higher centers in the brain, and helps in motor planning^{1,2}. For those using UL prostheses, kinesthesia is largely absent as artificial limbs do not actively relay movement information to the user. Therefore, the user is fitted with a numb tool, requiring constant visual monitoring to perform even simple tasks. This results in an increased cognitive burden associated with prosthetic use as high and continuous attention must be paid to the prosthesis. The lack of

meaningful sensory feedback is often highlighted as a major contributor to abandonment of motorized prostheses³ and is a fundamental barrier to their acceptance and use. In fact, cable-actuated, hook style prosthesis see lower rates of abandonment than their dexterous robotic counter parts. A key reason lays in the ability of the user to indirectly sense prosthetic joint movement through tension and resistance in the cable system⁴. Unfortunately, traditional cable powered prostheses lack the potential multi-grip dexterity that can be provided with modern motorized prostheses.

The potential functional implications of providing sensory feedback for UL prostheses are well recognized^{5,6}. Significant advances have been made in cutaneous (touch) based prosthetic feedback through the application of surgical techniques and implantable devices; including through targeted reinnervation (TR) surgery⁷⁻⁹. This reconstructive procedure strategically denervates muscle sites in the patient's residual limb (RL) or chest. The residual nerves that once serviced the patient's amputated hand are then reinnervated to these target muscle sites¹⁰. This technique was initially developed for improved control of prostheses; however, it also been shown to restore cutaneous sensations of the missing hand⁹. With stimulation of the skin on the RL, participants have reported matched sensations mapped to their missing hand in response to vibration, pressure, heat, cold and pain⁹. Experimental strategies that harness these sensations to provide intuitive touch-based prosthetic feedback have been highlighted in literature⁵. Additionally, participants who underwent TR surgery have reported sensations of wanting to move or reach out when deep pressure was applied to the reinnervated skin and underlying musculature¹¹. These reported sensation holds important implications in UL prosthetic feedback as kinesthesia, like cutaneous sensation, plays a vital role in the control and function of the upper limb. Yet, techniques that access and communicate relevant kinesthetic information through intuitive sensory channels remain elusive.

In this chapter, we describe a technique to purposefully elicit kinesthetic sensations experienced in the missing limb of four transhumeral participants who had previously undergone TR surgery. Psychophysical measures were employed to characterize the illusionary sensations, showing the similarity to the kinesthetic illusion experienced in able bodied individuals. We demonstrate the

application of our technique in providing real-time kinesthetic feedback during the physical operation of prosthetic components.

Our approach aimed to take advantage of the physiological phenomenon known as the kinesthetic illusion that we had investigated in able-bodied participants. The kinesthetic illusion occurs when vibration of specific frequencies (~70-110Hz) and amplitudes (~0.1-0.5mm) is introduced to musculotendinous regions of a limb^{12,13}. The vibration activates muscle spindles; afferent sensory receptors responsible for detecting muscle stretch. This activation results in illusionary sensations of limb movement while the limb itself physically remains stationary¹³. Paired with the reinnervated anatomy of those who have undergone TR surgery, the kinesthetic illusion holds exciting possibilities to provide prosthetic movement feedback. We theorized that hand movement sensations could be purposefully elicited as it was believed that the native muscle spindle receptors present in the limb become cortically associated with the reinnervated hand and forearm nerves. In turn, these sensations could be characterized and linked to the movement of robotic prostheses to provide real time kinesthetic feedback. To investigate, our work had three objectives:

- 1) **Percept mapping:** To elicit and catalog hand and arm movement sensations present with the vibration of reinnervated musculature in the amputated limb.
- 2) **Psychophysical quantification:** To characterize and optimize the illusionary sensations through manipulation of vibratory stimulus parameters.
- 3) **Use of the kinesthetic illusion with a physical prosthesis:** To demonstrate the application of the kinesthetic illusion in providing real-time movement feedback using prosthetic components.

4.3 Methods

Four participants with unilateral transhumeral amputation were recruited. All participants had previously received TR surgery^{8,10}. Participant information is provided in Table 4-1. Ethics approval was received through the University of Alberta's institutional review board and written informed consent was obtained from the participants prior to enrollment in the study.

Table 4-1 Participant information

Participant	Amputation	Targeted Reinnervation
1	Left Transhumeral	Median nerve to medial biceps; Distal radial nerve to lateral triceps
2	Left Transhumeral	Median nerve to medial biceps and to brachialis; Distal radial nerve to lateral triceps
3	Right Transhumeral	Median nerve to medial biceps; Distal radial nerve to lateral triceps
4	Right Transhumeral	Median nerve to clavicular head of pectoralis; Ulnar nerve to superior sternal head of pectoralis

4.3.1 Percept Mapping

For each participant, vibration testing was conducted to explore possible movement percepts and identify locations within the reinnervated muscle that, when vibrated, consistently elicited strong kinesthetic sensations. Participants were seated with their RL supported by an adjustable arm rest. Using a hand held vibrator (Vibrasens, Techno Concept, Mane, FR), vibration at 90Hz frequency and 0.5mm (neutral to peak) amplitude was introduced to each participant's RL. Participants were directed to report "any sensations beyond simple vibration." Participants were not informed that the intent of the study was to investigate kinesthetic sensations nor provided with specific information describing the kinesthetic illusion. The hand held vibrator was systematically pressed into various locations of the reinnervated musculature with enough pressure to blanch the skin (2-5N). Each location was tested for approximately 10 seconds prior to moving to the next. Once a participant reported a kinesthetic sensation, probing of the surrounding tissue was conducted to precisely identify a location most consistently producing the strongest kinesthetic sensations. The participant would be asked to compare stimulus locations in close proximity, with the investigator prompting, "Which one gives the strongest sensation of movement, number one or number two?" This was continued until a location consistently producing an illusion stronger than the surrounding tissue was identified. At each stimulus location in which a sensation of movement was elicited, participants were instructed to use their intact hand to match what they felt in configuration, velocity and duration, similar to the

techniques employed in able-bodied literature^{12,14} and Chapter 3. A digital video recorder was used to capture hand and upper limb movements and corresponding percepts were schematically rendered. The final stimulus location most consistently eliciting strong movement percept was marked on the participant's skin with a felt-tipped marker. This procedure was repeated to capture movement percepts present with stimulation of the reinnervated biceps, triceps and brachialis (when a residual brachialis was present and accessible).

4.3.2 Psychophysical Quantification

With the anticipation of translating the kinesthetic illusion into a prosthetic sensory feedback system, the objectives of the psychophysical quantification (PPQ) testing was twofold. First it was used to help optimize the mechanical vibratory parameters (amplitude and frequency) such that the strongest percepts of missing hand movement could be elicited. Secondly by comparing the response of our amputee population to that of able-bodied, it served to verify that muscle spindles (and the kinesthetic illusion) were in fact the primary mechanism of the movement percepts elicited.

Participants were seated with their RL supported by an adjustable arm rest. Participants were blindfolded with hearing occluded to remove external audio or visual clues. Vibration was introduced to the participants using a voice coil system (VCS1010, EquipSolutions, Sunnyvale, USA) attached to a flat faced probe tip (18 mm diameter). The voice coil system was held in position using a swing arm (S8 APO, Lecia, Concord, CAN) and micromanipulator system (MM-3, Narishige Group, Tokyo JA). Voice coil control was achieved using custom software developed using Simulink Real-Time software (Mathworks XPC Target) that was capable of manipulating vibration amplitude and frequency. In the locations identified by the perceptual mapping procedures (above) the probe tip was depressed perpendicularly into the reinnervated muscle tissue with approximately 2 to 5 Newtons force; as measured by an inline load cell (LCM703-10, Omegadyne, Sunbury, USA) (Figure 4.1).

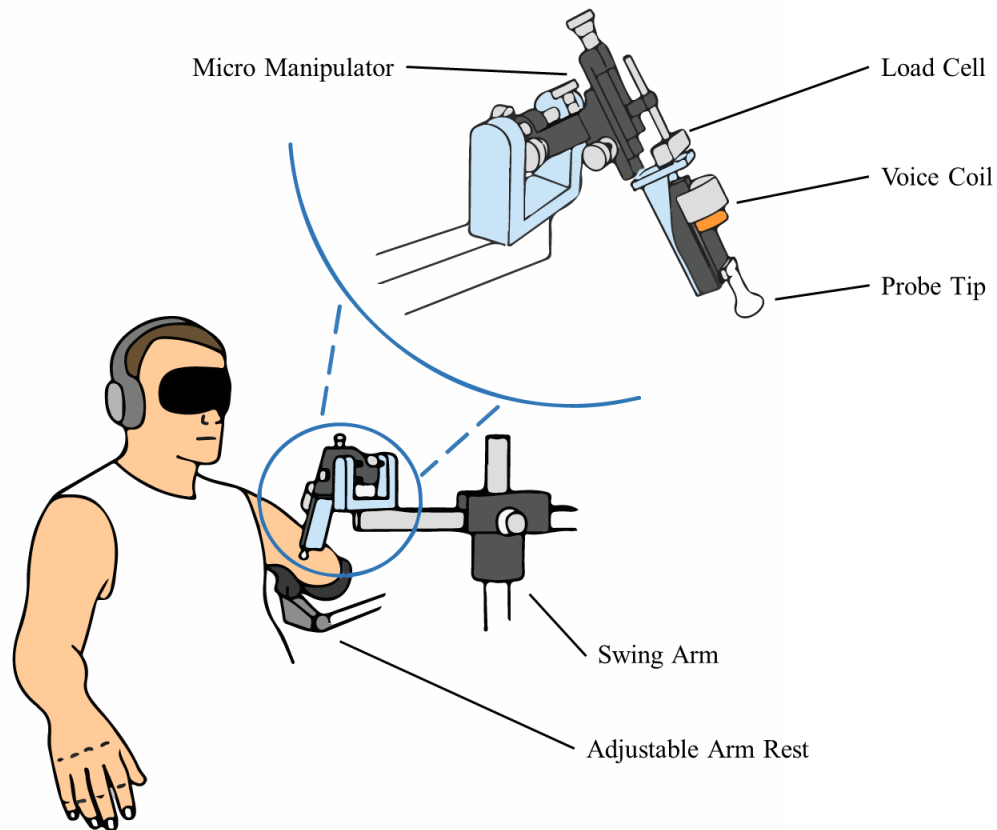


Figure 4.1 Psychophysical Quantification Setup

Sinusoidal vibration defined by randomized combinations of amplitude (at 0.1, 0.3 and 0.5mm) and frequency (at 10, 30, 50, 70, 90 and 110 Hz) were introduced to the reinnervated muscle tissue according to a full factorial, design-of-experiments (DOE) protocol¹⁵. Each combination was presented to the participant for 10 seconds. In total, each muscle site was exposed to 18 unique combinations of amplitude and frequency, with 4 repetitions performed (72 trials in total for each site).

Following each trial, the psycho-physical strength of illusion was quantified using a 5 point Likert Scale. The participant was prompted, “On a scale of 0 to 5, we want you to describe how strong the sensation of hand movement is; with 0 being no movement and 5 being an extremely strong movement sensation.” Additionally, in combinations resulting in a movement illusion, the participant was asked to pantomime the experienced percept using their intact limb. Following

completion of the 72 vibration trials, the ‘optimal’ combination of amplitude and frequency, most consistently eliciting strong movement sensations across all participants, was identified.

4.3.3 Use of the Kinesthetic Illusion with a Physical Prosthesis

Participant 2 most consistently demonstrated strong perceptual sensations of hand movement and therefore was selected to take part in further experiments aimed at pairing the kinesthetic illusion with a physical prosthetic device. The aim of these experiments was to demonstrate the use of the kinesthetic illusion to provide real-time movement feedback from commercially available prosthetic components. A multi-articulate prosthetic hand (Robolimb, Touch Bionics, Mansfield, MA, USA) was integrated with a Desktop Delsys electromyography system (Bagnoli, Natick, MA, USA), and the voice coil implemented in the PPQ testing. The voice coil was positioned over the participant’s residual biceps in the location most consistently eliciting strong sensations of illusionary movement, as determined from the PPQ testing. Custom software was developed using Simulink Real-Time (MathWorks, Natick, MA, USA) and C Sharp (Microsoft, Redmond, WA, USA) allowing the voice coil to be linked in real-time to prosthetic hand movement. The software provided additional functionality to adjust prosthetic digit trajectories; as well as allow actuation of the prosthesis through one of two modes: remotely triggered by the investigator (“passive”), or triggered using traditional myoelectric prosthetic control (“active”).

4.3.3.1 Limb Matching (Passive) Experiment

This experiment aimed to demonstrate that not only can percepts of missing hand movements be triggered through vibration inducing the kinesthetic illusion, but this can be linked to the matched movement of a prosthetic hand. Prosthetic hand movement was remotely triggered by the investigator and digit actuation was matched to the participant’s movement sensations, as determined from the prior PPQ testing. The participant and voice coil system were positioned as described in the PPQ testing setup (Figure 4.1). When the prosthesis was actuated, the voice coil would produce vibration with the optimal frequency and amplitude identified in the PPQ testing. Therefore, the vibration would induce the kinesthetic illusion in time with prosthetic hand

movement, and thus communicate prosthetic movement through matched sensations in the participant's missing limb.

Participants were prompted: "In this test we will be moving the prosthetic hand closed at random time intervals, and will stimulate your arm simultaneously using the voice coil. We ask that you pantomime the movement you feel in your missing limb with your intact limb in real time."

The investigator would trigger prosthetic movement and correspondingly the voice coil would deliver vibrational stimulus. Once initiated, the prosthetic digits would actuate through their preprogrammed trajectories, independent of the voice coil and/or participant. Once the participant's intact hand reached a static position, the investigator would allow the vibration to continue for approximately 1-2s prior to ceasing the stimulation and resetting the prosthetic hand's position. This additional stimulation was intended to prevent the participant from inferring termination of prosthetic hand movement through sensory substitution of the cutaneous sensation. Digital video recorders were used to capture digit movement data of the participant's intact hand and the prosthetic hand. Movement durations and timing data were extracted from analysis of this video footage. This procedure was repeated for 9 trials in total.

4.3.3.2 Volitional Control (Active) Experiment

The goal of this experiment was to demonstrate a system providing kinesthetic sensory feedback in real time with the volitional motor control of the prosthesis, and to demonstrate that the sensory system would not interfere with active prosthetic control that is dependent on the muscles in the residual limb. The same experimental setup as described in the limb matching test was utilized, with exception of the prosthetic hand control (Figure 4.2). To achieve volitional control of the prosthesis, EMG electrodes were placed on the participant's RL at locations corresponding to their hand open and hand close signals. Signal gains and thresholds were adjusted consistent with conventional myoelectric prosthetic control. Similar to the limb matching experiments, when the prosthetic hand was actuated, the voice coil would simultaneously introduce vibration to the participant's RL with parameters adjusted to induce the kinesthetic illusion.

The prosthetic hand was set to actuate the same perceptual hand conformation as was experienced by the participant in the PPQ experiment. The voice coil was setup up such that when prosthetic-hand close was volitionally initiated via EMG signals, the voice coil would begin to vibrate with the goal of inducing a kinesthetic illusion closely matching in digit trajectory. When the prosthetic hand ceased movement, the voice coil would cease after approximate 1-2s delay. The hand could then be reset to its starting position through remote triggering by the investigator, or through EMG control via the participant.

Participants were prompted: “Initiate hand close at your leisure. Please demonstrate in real time sensations of movement you are experiencing.” A digital video recorder was used to capture digit movement of the participant’s intact hand and the prosthetic hand. Movement durations and timing data were extracted from analysis of this video footage. This procedure was repeated for 19 trials in total.

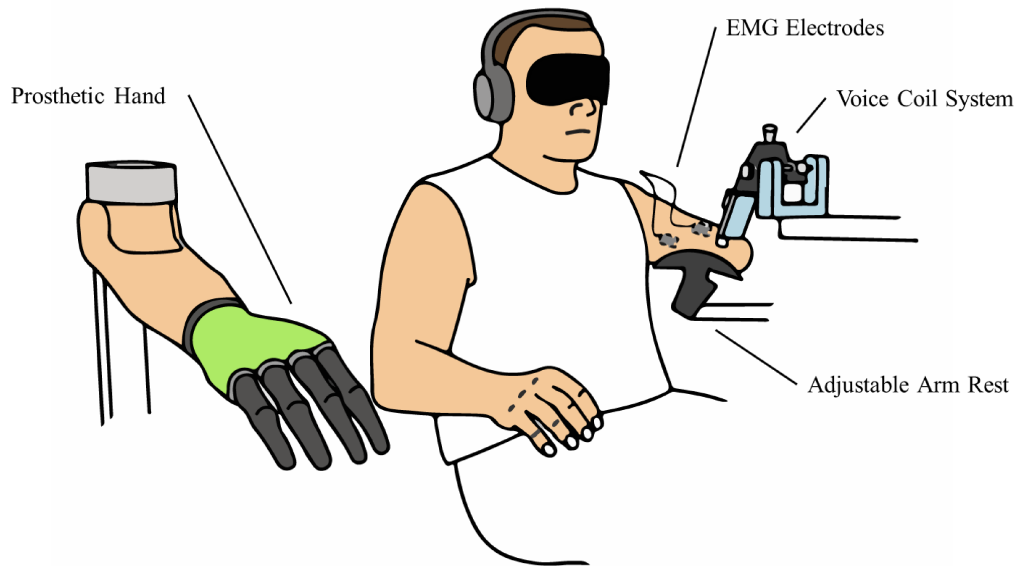


Figure 4.2 Volitional Control Setup

4.4 Results

4.4.1 Percept Mapping

While blind to the investigators' intent of inducing movement illusions, all four participants spontaneously reported complex movement percepts projected to their missing hand, wrist and/or elbow (Figure 4.3). With continued vibration, 12 percepts were isolated across the four participants. These movement sensations often involved multiple digits travelling through functional hand conformations such as cylinder grip, flat pinch, and fine pinch. Individual digits were sensed and participants were able to clearly articulate the trajectory and velocities of the individual digits. Muscles reinnervated by the median nerve most often provided sensations of digit flexion; whereas, muscles reinnervated by the radial nerve provided percepts of extension.

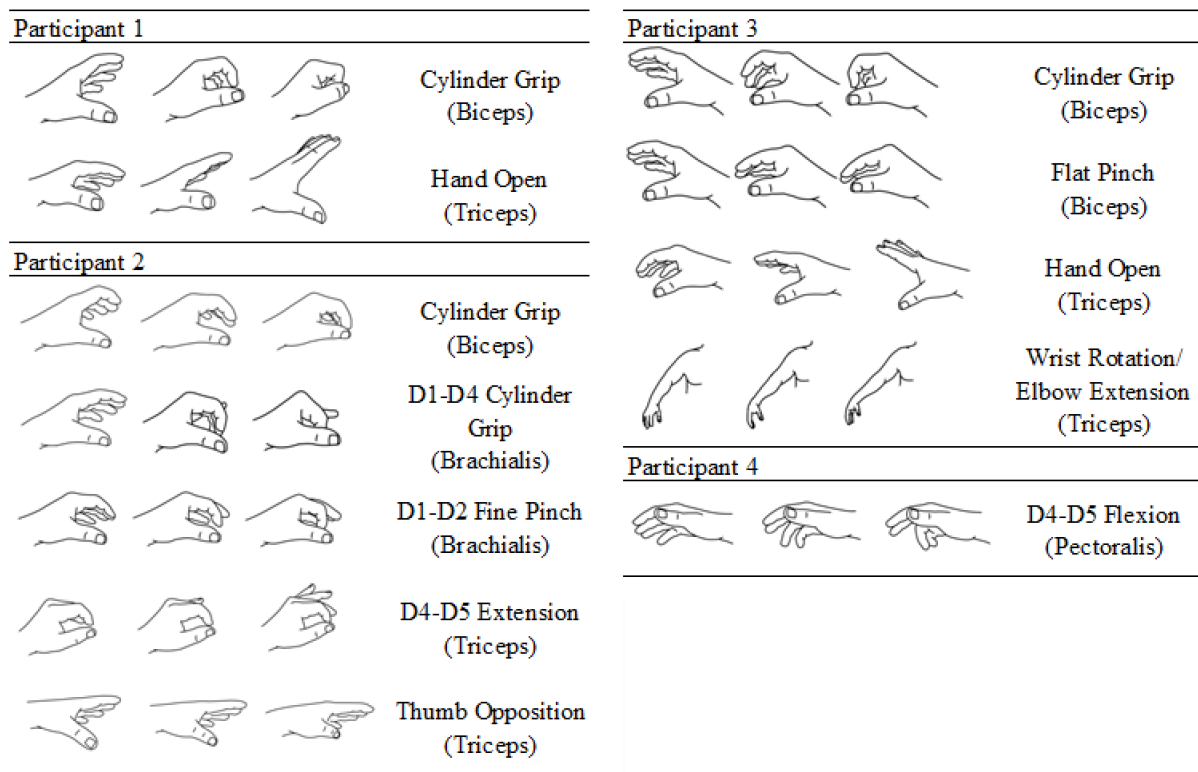


Figure 4.3 Cataloged hand movement percepts. Rendering of each kinesthetic movement percept projected to the missing hand/arm. For each percept the perceived start, middle, and end points are rendered from left to right. The residual muscle group stimulated to achieve each percept is noted in parentheses.

4.4.2 Psychophysical Quantification

The psychophysical strength of illusion was plotted relative to the input vibratory parameters of frequency and amplitude. The results indicate the strongest responses to the kinesthetic illusion at frequencies between 70 and 110 Hz (Figure 4.4). These values closely match the reported range of the kinesthetic illusion reported in able bodied participants^{12,13,16} in chapter 3. Furthermore, the largest stimulator displacement (500 μm) also provided the strongest responses across all frequencies^{12,17}.

It may be noted that the high amplitude and frequency demands placed on the voice coil motor while loaded onto the soft tissue heavily taxed the mechanical system. At higher frequency and amplitude values, the actual stimulus parameters were unable to be fully achieved. True frequency values presented to the participant were 10, 30, 50, 66.7, 83.3 and 100 Hz at amplitudes of 0.08, 0.27 and 0.45mm (neutral-peak).

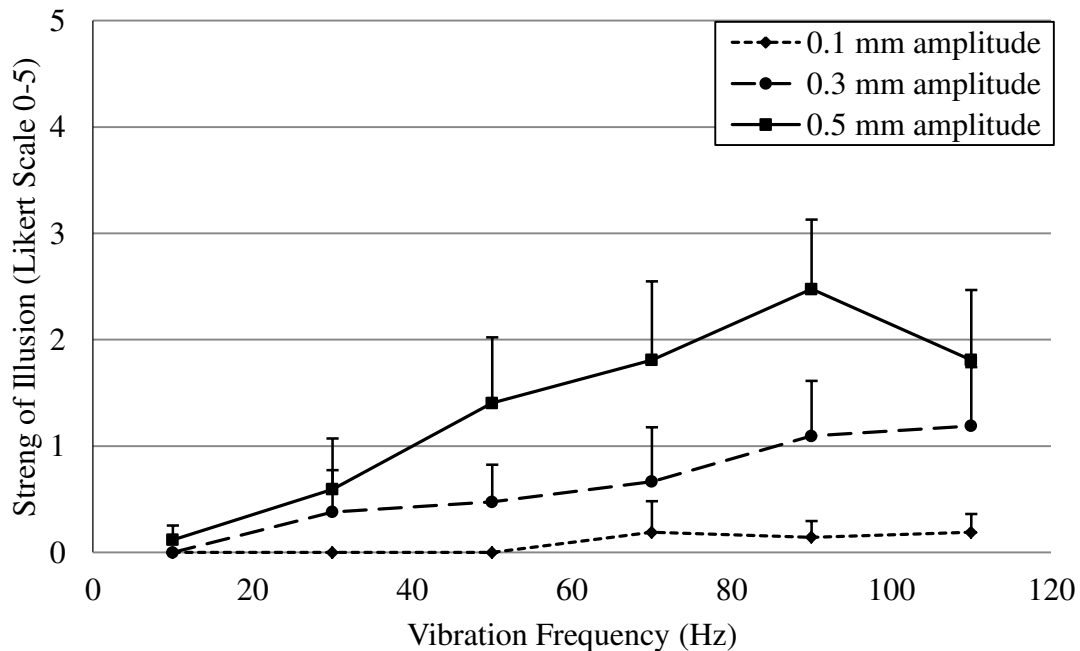


Figure 4.4 Vibration properties and perceived strength of kinesthetic illusion. Strength of movement illusions (as indicated by participants on a five point Likert scale) plotted against vibration frequency and vibration amplitude (neutral to peak). Note, due to the high mechanical demands placed on the hardware, true frequency and amplitude values deviated from their target values. True values presented to the participants were 10, 30, 50, 66.7, 83.3 and 100 Hz frequency and 0.08, 0.27 and 0.45mm (neutral-peak) amplitude.

4.4.3 Use of the Kinesthetic Illusion with a Physical Prosthesis

4.4.3.1 Limb Matching (Passive) Experiment

The limb matching experiment was conducted using the participant's most consistent hand movement percept (D1-D4 Cylinder Grip). This functional grip conformation was able to be communicated to the participant through vibration of the reinnervated muscle and the corresponding kinesthetic illusion. Closing of the prosthetic hand (triggered by the investigator) was time locked with the initiation of vibration stimulus. An average percept lag of 1.08s (± 0.70 s) was present between the initiation of vibration and the initiation of the kinesthetic illusion. This lag represents a mismatch in timing between illusionary movement (kinesthetic feedback) and physical movement of the prosthesis. The average duration of the illusion was 6.10s (± 2.41 s) while the prosthetic hand averaged 0.54s (± 0.31 s) to perform the preprogrammed movement. Figure 4.5 depicts the sequence and duration of events.

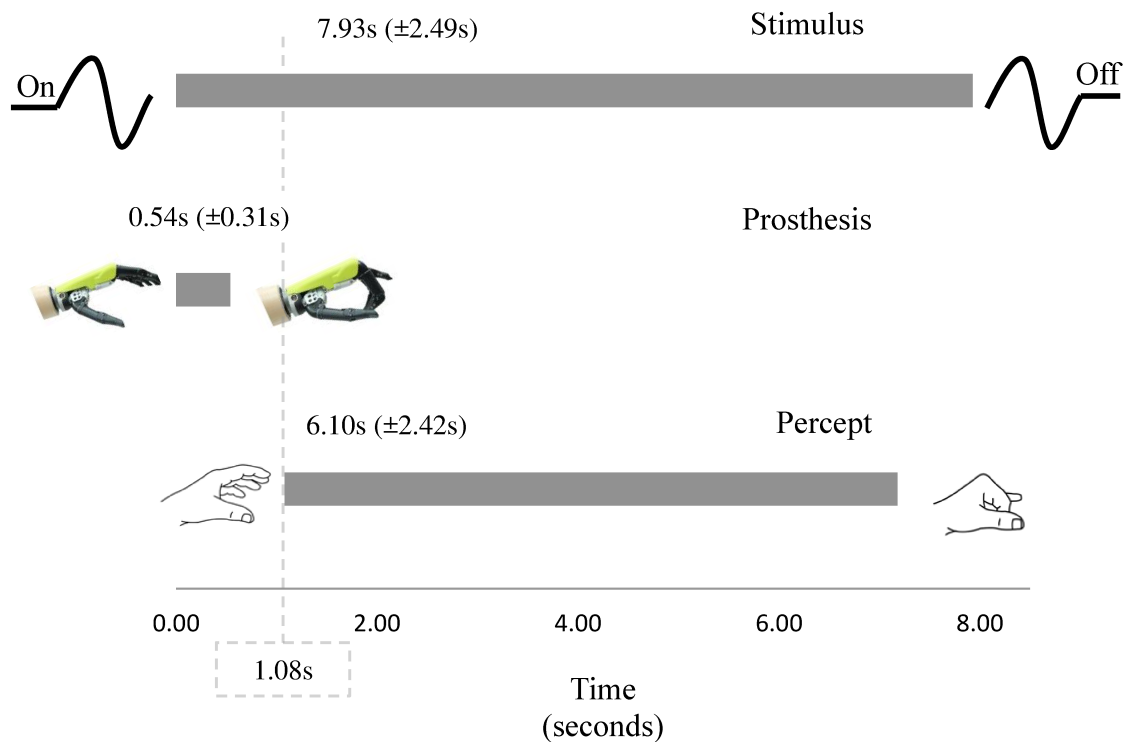


Figure 4.5 Limb matching (passive) timing results. Stimulus, prosthesis, and percept timing are presented in units of seconds. The dashed line signifies the onset of the illusionary percept. The time value present above each grey time bar represents the duration of the event and \pm denotes standard deviation of that duration.

4.4.3.2 Volitional Control (Active) Experiment

During the volitional control experiment the participant was given direct EMG control of the prosthetic hand-close function. The stimulus location and EMG control site were spatially separated on the participant's RL. Therefore, the EMG control of the prosthesis and vibration feedback could be performed simultaneously. No interference between the EMG and vibration feedback system was observed. Both the stimulus location on the participants RL and the trajectory of the prosthetic hand were the same as in the limb matching experiments described above.

In addition to the kinesthetic illusion, the participant also experienced an intrinsic motor percept that corresponded to volitional contraction of the hand-close muscle site, in which the TR participant uses imagery of hand movement to initiate contraction of the reinnervated muscle. This concept is further explored in the discussion section. When the participant used the intrinsic motor percept to actively control the prosthetic hand, the lag in the onset of the movement illusion was reduced such that the participant began to anticipate prosthetic movement on average 0.04s (± 0.62 s) prior to the initiation of prosthetic movement. The duration of movement illusion was reduced relative to the passive limb matching experiments, yielding a time of 0.62s (± 0.62 s); a value more reflective of the 0.54s (± 0.31 s) movement duration of the prosthetic hand. It was also clear that the participant was not simply using the vibration as a substitutive haptic feedback as the vibration duration averaged 2.46s (± 2.67 s), which was longer than the movement illusion and actual movement duration. In other words the vibration duration did not provide any secondary information for the participant to infer when the prosthesis ceased motion as vibration continued well beyond (Figure 4.6).

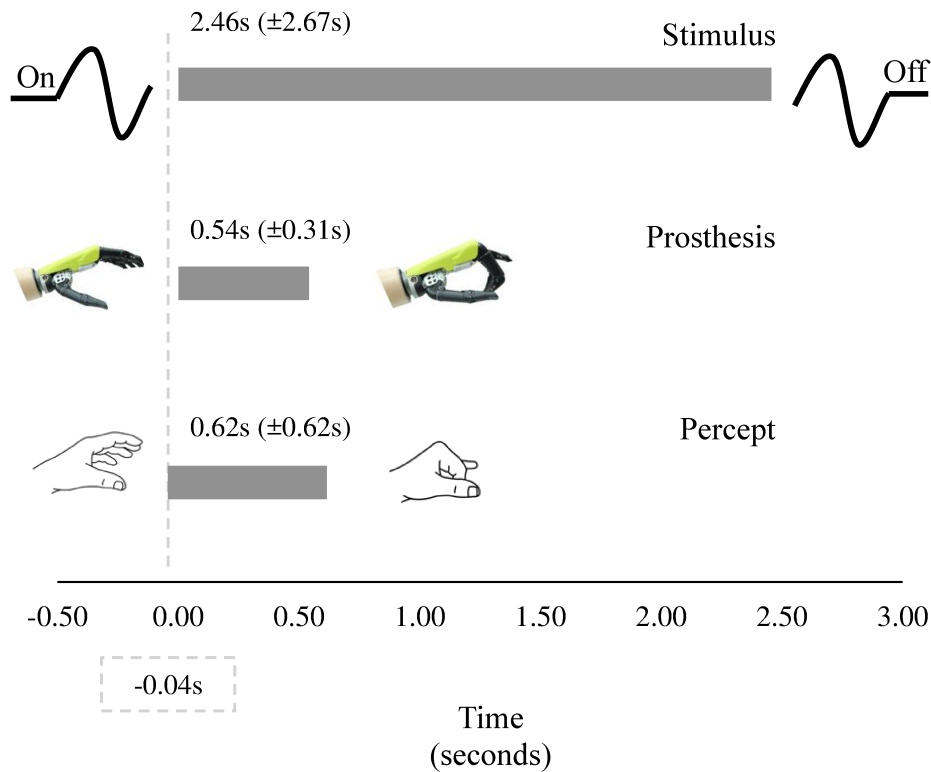


Figure 4.6 Volitional control (active) timing results. Stimulus, prosthesis, and percept timing are presented in units of seconds. The dashed line signifies the onset of the illusory percept. The time value present above each grey time bar represents the duration of the event and \pm denotes standard deviation of that duration.

4.5 Discussion

In this chapter, we present a technique that utilizes the reinnervated sensory pathways in participants who have undergone targeted reinnervation surgery to purposefully elicit perceptual movement illusions projected to their missing hand. We characterized the behavior of these kinesthetic illusions, identified key stimulus parameters, and demonstrated the application in real time bi-directional control of prosthetic components.

All four participants reported sensations of illusory movement in their missing hand. In participants that experienced multiple perceptual hand conformations, the different movement sensations were consistent over the duration of testing, and accessible by stimulation of the unique discrete locations on their RL. All the illusions described by our participants were

synergistic movement patterns of multiple digits. Most were highly relevant hand conformations such as cylinder grip or pinch grip, which are common grasp patterns in many daily activities. From the percept mapping experiments, it became apparent that a dexterous prosthetic hand with individual digit control would be necessary to facilitate the illusionary movement sensations describe by the participants. Figure 4.7 illustrates the 9 unique grasp patterns described in the Perceptual Mapping Experiments as a schematic rendering and the corresponding pattern achieved using the robotic prosthetic hand.

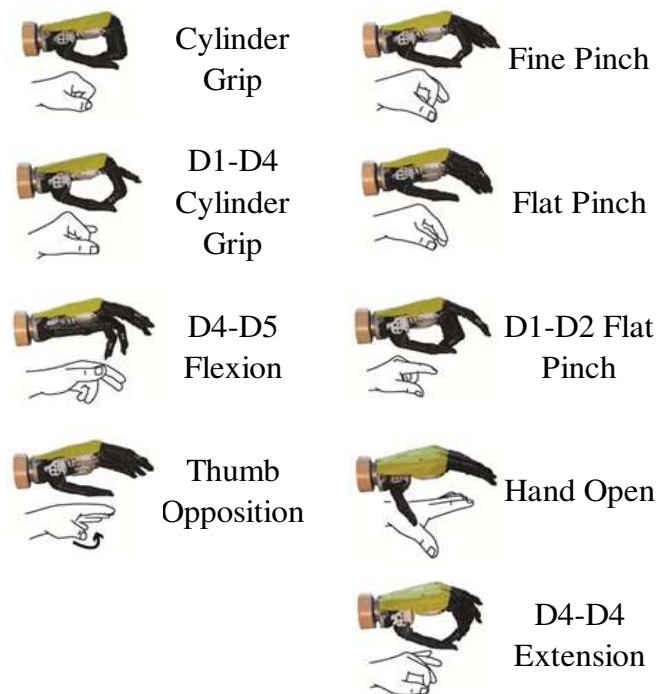


Figure 4.7 Movement percepts matched to a prosthetic hand. Each unique hand movement percept described across all participants schematically represented and matched with the i-limb Robolimb.

Results from the PPQ trials had strong similarities to the able-bodied kinesthetic illusion experiments in Chapter 3 and past literature^{12,13,16}. The strongest, most consistent kinesthetic illusions were found at values of 90Hz frequency and 0.5mm neutral-to-peak amplitude. Therefore, these data supported that we were in fact eliciting the kinesthetic illusion. They also suggested that as a byproduct of targeted reinnervation surgery, native stretch receptors in the

reinnervated muscle (muscle spindles) became cortically associated with the reinnervated neural pathways and interpreted as the missing hand.

In translating these techniques into functional prostheses, these data highlighted target vibration parameters (90Hz frequency and 0.5mm amplitude) to effectively elicit the kinesthetic illusion as a means of prosthetic sensory feedback. However, a practical challenge presented itself. The electrical and mechanical requirements of achieving these frequency and amplitude values became demanding on many miniaturized motors. Consequently, the size of the vibration feedback device may become a challenge for integration. Especially in a system where the prosthetic socket, control electrodes, and feedback devices will require strategic contact of specific locations on the RL, the physical dimensions and locations of each component must be carefully considered. Therefore, prosthetic socket design also becomes a crucial barrier in accommodating the components vital to bidirectional prosthetic control. Additionally, eliciting a reliable kinesthetic percept will be dependent on consistently stimulating the same anatomical location on the RL. The sensitivity of the kinesthetic percepts to stimulus location necessitates well fit sockets, as slip or displacement of the prosthesis on the RL may be detrimental to the experienced kinesthetic sensations. Therefore, the development of prosthetic sockets to both accommodate novel feedback devices and ensure socket suspension and security are pivotal barriers that must be addressed prior to translating these techniques beyond the laboratory.

The limb matching experiments largely served as a proof of concept demonstrating the application of the kinesthetic illusion as prosthetic sensory feedback. A dramatic difference in the timing characteristics between the passive and active prosthetic control conditions was observed. Unique to the active control condition, the participant described an intrinsic motor percept when initiating hand close. In other words, the intent to close the prosthetic hand was linked to muscle contraction through motor imagery of movement. In a traditional prosthesis this would be performed without movement feedback. The increased speed of illusionary movement and reduction in percept lag may therefore be attributed to a number of factors. By assigning the participant active EMG control of the prosthetic hand, both motor control and sensory feedback were present. The intent to initiate hand close, the participant's intrinsic motor percept, and the

feedback provided through the kinesthetic illusion provided three channels of congruent information that appeared to reinforce the perception of missing hand movement. These findings strongly support the potential utility of our technique if integrated into a functional prosthetic arm.

4.6 Conclusions

As advanced myoelectric prostheses become increasingly available, so too will the importance of intuitive sensory feedback in the effective control of these advanced dexterous systems. In this work, we demonstrated that we can intentionally elicit perceptual sensations of missing hand movement in participants who have previously undergone targeted reinnervation surgery. We further demonstrated that these sensations can be leveraged to relay prosthetic movement information enabling bidirectional control of the prosthesis. This work represents significant strides toward the realization of sensate upper limb prostheses as it provides intuitive, relevant feedback that is readily interpreted by the users as occurring in their missing limb. For the practical utility of our technique to be achieved, it must be translated beyond the laboratory into a fully functional prosthesis and tested to determine if it improves function with daily activity. Yet, a number of technical design barriers exist that encumber the integration of such a system. Positioning and location considerations with other necessary prosthetic components present a significant issue in moving forward; as does the integration of feedback device without compromising prosthetic fit or function. Therefore novel prosthetic sockets designs that address these challenges must be developed; a major focus of the remaining thesis chapters.

4.7 References

1. Gordon J, Ghilardi MF, Ghez C. Impairments of reaching movements in patients without proprioception. I. spatial errors. *J Neurophysiol.* 1995;73(1):347-360. Accessed 24 May 2017.
2. Ghez C, Gordon J, Ghilardi MF. Impairments of reaching movements in patients without proprioception. II. effects of visual information on accuracy. *J Neurophysiol.* 1995;73(1):361-372. Accessed 24 May 2017.
3. Biddiss E, Chau T. Upper-limb prosthetics: Critical factors in device abandonment. *Am J Phys Med Rehabil.* 2007;86(12):977-987. Accessed 16 March 2017. doi: 10.1097/PHM.0b013e3181587f6c.
4. Childress DS. Control strategy for upper-limb prostheses. *Annu Int Conf IEEE Eng Med Biol Proc.* 1998;5:2273-2275. Accessed 23 May 2017.
5. Schofield JS, Evans KR, Carey JP, Hebert JS. Applications of sensory feedback in motorized upper extremity prosthesis: A review. *Expert Review of Medical Devices.* 2014;11(5):499-511. Accessed 8 April 2015.
6. Antfolk C, D'alonzo M, Rosén B, Lundborg G, Sebelius F, Cipriani C. Sensory feedback in upper limb prosthetics. *Expert Review of Medical Devices.* 2013;10(1):45-54. Accessed 2 December 2013.
7. Raspopovic S, Capogrosso M, Petrini FM, et al. Bioengineering: Restoring natural sensory feedback in real-time bidirectional hand prostheses. *Sci Transl Med.* 2014;6(222). Accessed 24 May 2017. doi: 10.1126/scitranslmed.3006820.
8. Hebert JS, Olson JL, Morhart MJ, et al. Novel targeted sensory reinnervation technique to restore functional hand sensation after transhumeral amputation. *IEEE Transactions on Neural Systems and Rehabilitation Engineering.* 2014;22(4):765.

9. Kuiken TA, Marasco PD, Lock BA, Harden RN, Dewald JPA. Redirection of cutaneous sensation from the hand to the chest skin of human amputees with targeted reinnervation. *Proc Natl Acad Sci U S A*. 2007;104(50):20061-20066. Accessed 20 December 2013.
10. Kuiken TA, Dumanian GA, Lipschutz RD, Miller LA, Stubblefield KA. The use of targeted muscle reinnervation for improved myoelectric prosthesis control in a bilateral shoulder disarticulation amputee. *Prosthet Orthot Int*. 2004;28(3):245-253. Accessed 20 December 2013.
11. Marasco PD, Kim K, Colgate JE, Peshkin MA, Kuiken TA. Robotic touch shifts perception of embodiment to a prosthesis in targeted reinnervation amputees. *Brain*. 2011;134(3):747-758. Accessed 24 May 2017. doi: 10.1093/brain/awq361.
12. Schofield JS, Dawson MR, Carey JP, Hebert JS. Characterizing the effects of amplitude, frequency and limb position on vibration induced movement illusions: Implications in sensory-motor rehabilitation. *Technology and Health Care*. 2015;23(2):129-141. Accessed 8 April 2015.
13. Goodwin GM, McCloskey DI, Matthews PBC. The contribution of muscle afferents kinaesthesia shown by vibration induced illusions of movement and by the effects of paralyzing joint afferents. *J Physiol (Lond)*. 1972;536:635-647. Accessed 24 May 2013.
14. McCloskey DI. Differences between the senses of movement and position shown by the effects of loading and vibration of muscles in man. *Brain Res*. 1973;61:119-131. Accessed 23 December 2013.
15. Montgomery D.C. Factorials with mixed levels. In: *Design and analysis of experiments*. 8th ed. Wiley; 2012:412.
16. Proske U, Gandevia SC. The proprioceptive senses: Their roles in signaling body shape, body position and movement, and muscle force. *Physiol Rev*. 2012;92(4):1651-1697. Accessed 30 September 2013.

17. Clark FJ, Matthews PB, Muir RB. Effect of the amplitude of muscle vibration on the subjectively experienced illusion of movement [proceedings]. *J Physiol (Lond)*. 1979;296:14P-15P. Accessed 18 December 2013.

Chapter 5. The mechanical understanding of the interface between prosthetic socket and residual limb

The majority of this chapter is under review as:

Schofield JS, Evans KR, Carey JP, Hebert JS. (2017). Advances in the quantification and prediction of prosthetic socket interface mechanics: A fifteen year review. In preparation

5.1 Chapter Preface

An immediate barrier limiting the use of sensory feedback systems, including our kinesthetic feedback approach, is the integration of these systems beyond the laboratory into functional wearable prostheses¹. There are a number of physiological and engineering challenges to overcome. For a user to accept a feedback system, the information provided must be relevant, non-distracting and simple as to not overwhelm the user. Once such a system is identified, incorporating the system into a user's prosthesis without compromising biomechanical function or comfort must then be accomplished. Our kinesthetic feedback approach addressed the challenge of providing intuitive, relevant, non-distracting information to the user; however, incorporation of our system into a functional prosthesis still needed to be addressed.

Implementation of most non-implantable sensory feedback systems, including our kinesthetic system, requires a haptic communication device (tactor) be appropriately positioned on the user's residual limb (RL) and thereby be incorporated or pass through the prosthetic socket. This positioning must be reliable and comfortable to maximize the effectiveness of the system and facilitate user acceptance. Traditional prosthetic sockets do not allow for these requirements as they encapsulate the RL without considerations for the non-traditional incorporation of sensory feedback components. Therefore, development of non-traditional prosthetic sockets is inherently required. Consequently, an in depth understanding of how the prosthetic socket mechanically interacts with the user's residual limb is imperative to enable informed design decisions and an appreciation for the functional implications of non-traditional sockets. In current UL prosthetic literature, these socket-soft tissue interactions have yet to be comprehensively characterized.

In lower limb prostheses, a biomechanical understanding of the socket-RL interface has been approached through measurement of contact pressures and FE modelling². In this chapter we review techniques previously employed to quantitatively describe the mechanical interactions between the prosthetic socket and the RL. Although most of the work reviewed in this chapter relates to lower limb prostheses, a brief description of the state of upper limb prostheses is included with the anticipation of adapting lower limb techniques to the upper limb in subsequent chapters.

5.2 Introduction

Each year in the United States, an estimated 185,000 people undergo the amputation of a limb³. In 1996 estimates of prevalence suggested that 1.2 million Americans were living with limb loss⁴, and in 2005 these estimates raised to 1.6 million⁵. These numbers are steadily increasing and are expected to more than double by 2050 as a result of the aging population and increases in the incidence of diabetes mellitus and dysvascular disease⁵. For many of these individuals, a prosthesis will be prescribed to aid in the performance of daily activities.

The functional role of upper limb (UL) and lower limb (LL) prostheses are fundamentally different. UL prostheses are designed to assist during the many dexterous movements performed with the hands and arms while interacting with the daily environment. In contrast, LL prostheses are designed for more predictable cyclical applications such as weight bearing and balance during ambulatory activities. Although the functional goals are different, the prosthetic socket is the universal component that acts as the interface between the limb and the various prosthetic components, regardless of the limb or level of amputation.

Hence, one of the most influential factors for the use of a prosthesis is the design of the prosthetic socket⁶. The socket functions as the point of attachment of the prosthesis to the user's residual limb (RL). It is at this crucial junction where the soft tissue of the user's RL must serve as the connection between the bone and rigid materials of the prosthesis. Traditional sockets are designed to strategically compress specific areas of the user's limb while relieving contact pressures in others. The overall goal of the socket is to utilize the individual's morphology to achieve suspension and mechanical stability of the prosthesis while avoiding tissue irritation,

damage or general discomfort. Some users may wear optional silicone or gel liners rolled over their residual limb prior to donning the socket (Figure 5.1). These liners help pre-shape residual soft tissues and can increase comfort and suspension. Regardless of the interface used, the socket must be custom designed for each patient to achieve appropriate geometry for an effective interfacial pressure distribution between the RL and socket.

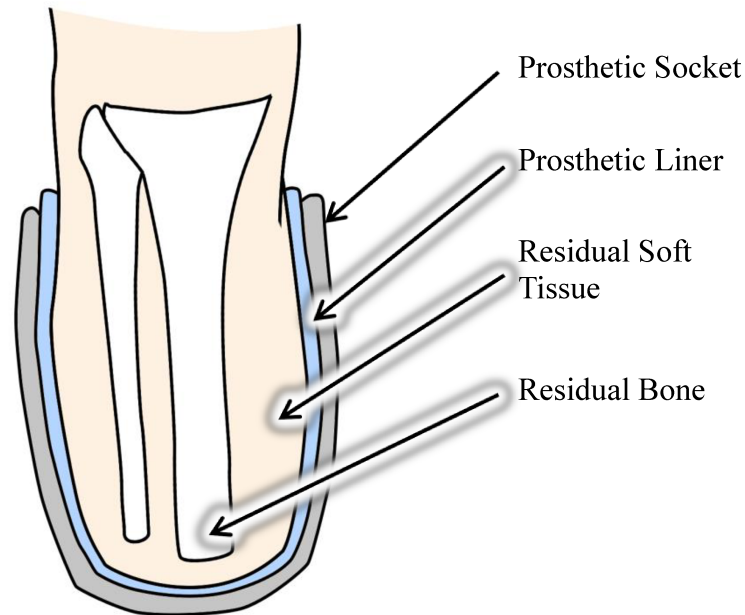


Figure 5.1 Cross sectional view of a trans-tibial residual limb with prosthetic liner and socket donned.

5.2.1 Socket-Limb Interactions

The general term “socket fit” can be used to encompass both the quantitative and qualitative factors that have influence on comfort, suspension, and the security of the prosthesis while worn on the RL. Socket fit and specifically comfort have substantial implications on user satisfaction⁷⁻⁹. At its core, socket fit is a fundamentally biomechanical concept that is highly dependent on the interaction between RL and socket. Movement and loading of the prosthesis is translated through the surrounding soft tissue onto a patient’s residual skeletal structure via the socket. Therefore, the prosthesis is coupled to the user’s skeletal system through an intermediate layer of highly

deformable soft tissue. In practice, the socket utilizes prominent bony structures in the RL for stability while using total contact with the residual soft tissue to counter-stabilize resultant loads. Yet overly high pressures focally applied to tissue can significantly decrease comfort and increase the risk of tissue irritation or damage¹⁰. Additionally the RL hosts a number of areas that are more physiologically tolerant to higher loading, such as the patellar tendon and popliteal fossa on transtibial amputees¹¹, as well as areas more sensitive to loading such as the distal end of the bone of the RL¹⁰. Therefore the challenge to the prosthetist lays in designing a socket that balances stability, suspension and corresponding contact pressures, all while accommodating the anatomy and locations on the limb to which interfacial pressures are being distributed. In clinical practice, the implications of proper design are well acknowledged and much of a prosthetist's effort will be specifically dedicated to the design and fabrication of the socket¹⁰.

5.2.2 Poor-fit and Tissue Damage

In both UL and LL prosthetic applications, soft tissue irritation of the RL is a common complication. Numerous dermatologic problems related to prosthetic use have been reported including pressure ulcers, blisters, cysts, edema, skin irritation, and dermatitis^{12,13}. Tissue damage can be present in two forms, surface or deep tissue. Damage at the surface epidermis of the skin will typically result from shear loads imparted on the skin as a result of repetitive socket displacement. Slip between the skin's surface and the prosthetic socket results in a friction-shearing that can mechanically separate layers in the epidermis resulting in friction blisters¹⁴. Other common complications may include epidermal abrasion, as well as general irritation and redness.

Beyond surface tissue damage, more severe tissue injuries can occur. Typically, these injuries are a consequence of higher load applications, and therefore deep tissue injuries are more commonly reported with LL prosthetic use¹⁵⁻¹⁷. Deep tissue damage and wound formation may result from physiologically inappropriate compression and deformation of soft tissue between the residual skeletal structure and the rigid surfaces of the prosthetic socket. These conditions may occlude blood flow, as well as nutrient, oxygen and lymphatic transport in the affected tissues. Furthermore these conditions may promote ischemic reperfusion, all of which are conditions supporting pressure wound formation and deep tissue injury¹⁵. Additionally, a poor fitting socket

may lead to mechanical damage of the residuum resulting in bruising, and general soreness of affected areas.

Tissue damage resulting from poor socket fit is a physiological consequence of the biomechanical conditions imparted on the RL via the socket. This has direct implications on a user's prosthetic use¹² as injuries often require time to be treated and heal prior to resuming use of the prosthesis. Comfort is commonly identified as a crucial factor affecting the use and user satisfaction of a prosthetic device^{7,9,18}. Additionally, many patients experience compromised sensory capacity in their residual limb as a result of nerve damage associated with their initial injury and amputation, or related to associated disease processes such as diabetes mellitus. This further emphasizes the importance of a well-designed socket as damage to the residuum may not be detected by these populations until more severe tissue injury occurs.

5.2.3 Quantification of RL-Socket Mechanics

In socket design and fabrication, a comprehensive understanding of RL-socket biomechanics is fundamentally important. This quantitative knowledge holds the potential not only to identify anatomical locations bearing high normal and shearing loads, but can facilitate the prediction of how a socket may interact with the residuum. This has important implications on the improvement of comfort, risk of tissue injury, as well as the satisfaction and usage of the prosthesis.

In literature, this biomechanical understanding has been achieved in 2 ways, through experimental measurement techniques such as instrumented prosthetic sockets, or numerical modelling techniques such as finite element methods (FEM). A number of review papers have been published prior to the year 2000 highlighting measurement techniques specifically in LL prostheses^{19,20} as well as more recent reviews^{2,21} focusing solely on transtibial prostheses. Additionally, the most recent reviews on numerical modelling techniques predicting interfacial stresses in LL prostheses have been published in 1998^{22,23}. It can be argued that numerical modelling techniques are highly theoretical in nature and must be validated against experimental data to ensure accuracy of results; a concept further discussed in this review. Therefore, the most

comprehensive understanding of RL-socket biomechanics can be derived through the paring of numerical modelling and experimental measurement techniques. The most recent review encompassing both of these concepts was published in 2001²⁴.

5.2.4 Review Objectives

In the last 15 years, substantial advances have been made in sensor technologies to facilitate experimental techniques, and computational power to facilitate numerical techniques. The goal of this narrative review is therefore to highlight prominent recent methods found in scientific literature that quantify and predict RL-socket interface mechanics in both UL and LL prostheses. Therefore, this review is not meant to be an exhaustive summary of individual sensors, socket studies or numerical studies. Prominent techniques reported in scientific literature between January 2001 and May 2017 will be discussed with a specific focus on clinical translation and applicability in a prosthetic fabrication context.

5.3 Lower Limb Quantification and Prediction Methods

5.3.1 Lower Limb Experimental Measurement Techniques

Experimental measurement techniques utilize a variety of force and pressure sensors to capture the mechanics at the interface between RL and socket. Existing measurement techniques can be divided into two groups, based on sensor placement²⁰. Sensors can either be installed directly in (or passed through) the socket wall, or inserted between the RL and socket. In the latter, if a liner is worn, the sensors may be positioned between the liner and RL or between the socket and liner. A hierarchical breakdown of measurement techniques discussed in this section is shown in Figure 5.2.

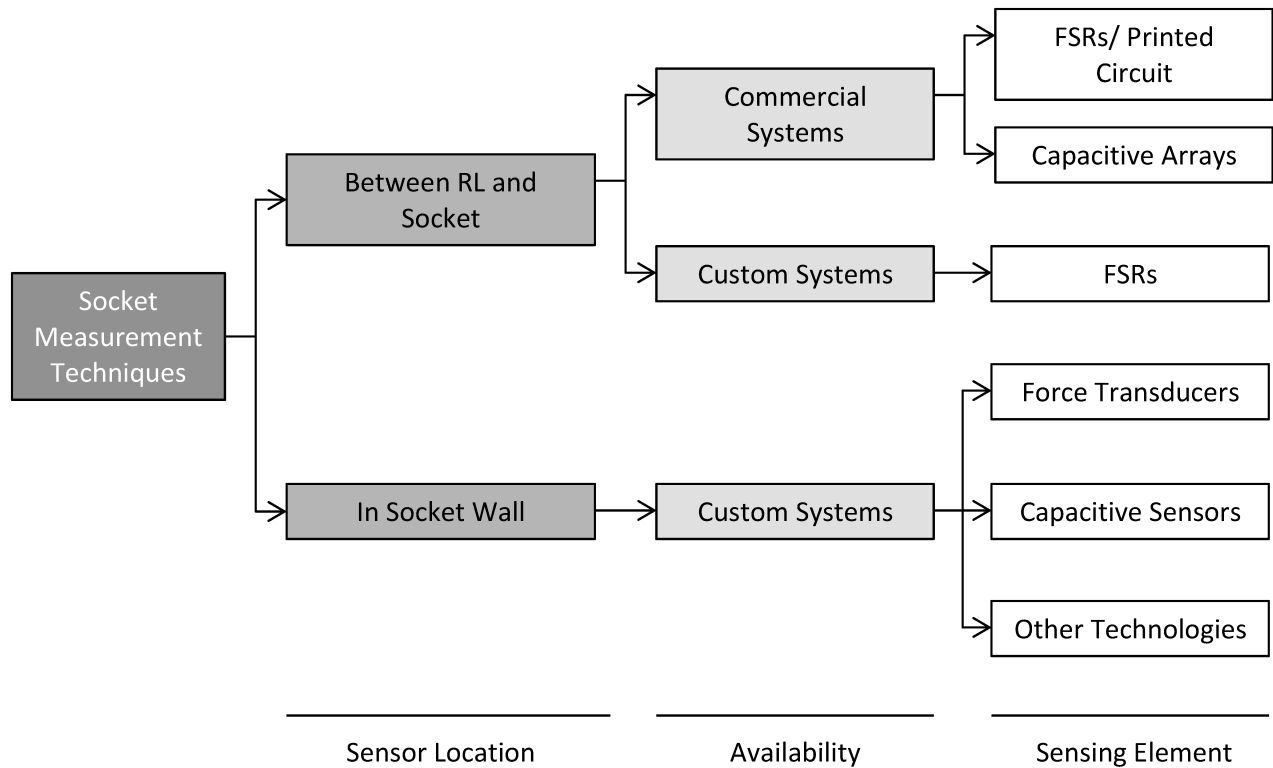


Figure 5.2 A hierarchical breakdown of experimental measurement techniques. Where FSR denoted force sensitive resistor

A number of criteria must be satisfied to ensure the sensor ability to sufficiently capture the biomechanical interactions of the RL and socket. The sensor must be able to accurately capture forces (or pressures) applied to the tissue while being minimally intrusive. In other words, the presence of the sensor itself must not change the biomechanics of the system. Care must be taken to ensure the physical geometry of the sensor does not significantly displace, deform or otherwise alter the mechanical response of the soft tissue and prosthetic socket²⁵. Additionally, sensors must be accurate for repeated measures, demonstrating stability over the variable biological conditions in which it will be used, such as temperature, physical geometries, and interface compliances²⁵. A summary of prominent experimental measurement techniques and applications are provided below. Technical advantages and limitations of these technologies are addressed with the clinical implications highlighted in discussion section of this review.

5.3.1.1 Sensors inserted between RL and socket

Custom systems that can be inserted between the RL and socket are typically based on Force sensitive resistors (FSRs). FSRs are constructed of thin-film polymers and change resistance with the application of force²⁵. FSR-based approaches can be found throughout prosthetic literature. El-Sayed et al. implemented a system of FSRs and piezoelectric sensors in a transfemoral prosthetic socket²⁶. Their work with a single participant concluded that RL-socket interface mechanics can be used during ambulation to identify events during the gait cycle²⁶. Mai, et al. strategically placed 6 FSRs in the prosthetic socket of a single transtibial amputee. The application of these sensors characterized the effect of 3 different prosthetic feet on the pressure introduced to the RL-socket interface²⁷. Beil et al. instrumented a urethane prosthetic liner with 5 FSRs, and investigated 9 transtibial participants with the aim to quantify RL-socket interface pressures in sockets suspended via suction and vacuum assist. They were able to use sensor reading to characterize significant differences in peak pressures and impulse across the two suspension techniques²⁸.

A number of studies utilized commercially available systems that were specifically designed to quantify LL socket interface forces (or pressures). By far the most popular system used in clinical literature is the Tekscan VersaTek or F-Socket systems (Tekscan, Boston, MA, USA)^{2,29-31}. Other systems found in literature also include the TACTILUS tactile pressure sensor system (Sensor Products Inc., Madison, NJ, USA)³², Rincoe socket fitting system (RG Rincoe and Associates, Golden, CO, USA)³³, and Novel pliance pressure sensor system (Novel gmbH, Munich, Germany)^{34,35}. With the exception of the Novel pliance system, which uses an array of capacitive sensing elements, most commercially available systems employ pressure sensors comprised of FSR arrays or printed circuits. These sensors are typically flexible and thin-profile, with thickness as little as 0.2mm³⁶, making them ideal to be inserted between the RL and socket. They are tethered directly to a manufacturer provided data acquisition system with accompanying software to perform calibration, data collection and analysis. These systems are designed specifically for ease of use in a clinical or socket fabrication setting and consequently include features such as real-time visualization of pressures and automatic report generation.

FSRs and printed circuit technologies are an attractive option for clinicians and researchers as they have a thin profile, low monetary cost^{36,37} and often require minimal signal processing prior to extracting data. While effective for measuring normal pressures, these technologies (in either custom or commercial systems) have a number of known limitations including hysteresis^{36,38}, drift error³⁹, and sensitivities to shearing forces, temperature, curvature, substrate compliances, and loading rates^{25,37,40,41}. Compensatory strategies to minimize sensor error may be taken such as calibrating sensors in an environment as close to their intended use as possible²⁵. These low cost, widely available sensors are a very attractive option for many prosthetic applications; however, due to inherent limitations they may come at the expense of reduced measurement accuracy and repeatability.

5.3.1.2 Sensors placed in the socket wall

As the sensors discussed in this section must be custom installed into the individual prosthetic socket, the development of a commercially available system is largely unfeasible. With most of the custom sensor technologies highlighted, sensor profiles are too large to be practically inserted between the socket and RL without disrupting or deforming the natural biomechanical state of the residuum. Therefore, the most common approach is to drill holes in the prosthetic socket and pass the sensor through the socket wall such that it sits flush with the interior of the socket surface. Care must be taken during this installation process as protrusion of the sensors into residual tissue may falsely inflate the force values captured by the sensor^{10,42}. Sensors examined for this application include force transducers, capacitive sensors, and other emerging technologies such as optical and fluid filled devices.

Force Transducers

Force transducer is a general term that represents a large category of force sensing technologies. The most common subset of force transducer is the elastic element load-cell. In these sensors, strain gauges are mounted to a deformable element with known geometry and modulus of elasticity. The force applied to the sensor is then determined through integration of the strain gauge readings and physical calculations to infer the applied load.

The application of force transducers has been reported in literature as early as the 1970s⁴³⁻⁴⁵. However, significant advancements were made in the 1990s when research groups from the King's College School of Medicine in London and the University of Washington developed a series of force transducer socket measurement systems⁴⁶⁻⁴⁹. Unlike FSRs, printed circuits, or other previous prosthetic force transducer systems, which were only capable of measuring normal forces, these newly developed systems allow for measurement of both normal and shear forces experienced at the surface of LL prosthetic sockets^{46,49}. Since then, a number of novel force transducer sensors have been developed and integrated into LL prosthetic sockets. Goh et al. developed a custom force transducer system that inserted 16 sensors into the prosthetic socket to capture normal forces acting on the socket of 5 transtibial participants⁵⁰. Of clinical relevance, in a later study they used the same system to contrast the normal forces acting on the transtibial residuum of 4 participants who were fit with prosthetic sockets fabricated using two different techniques (patellar-tendon-bearing and pressure cast sockets)⁵¹. In the past 15 years numerous force transducers capable of measuring orthogonal forces (normal and shearing forces) have been reported⁵²⁻⁵⁴. Most often, multiple sensors were installed in an experimental LL prosthesis. The sensors were tethered to a data acquisition system and captured forces acting on the prosthetic socket at specific locations of interest. Typical experimental design used the sensor readings to quantify forces during activities of daily living as a means of contrasting the biomechanical impact of prosthetic components^{55,56} or fabrication techniques^{50,51}.

The application of force transducers holds many practical advantages over FSR or printed circuit technologies. For example, this technology is inherently more accurate, exhibits less hysteresis, and is capable of capturing orthogonal force values (normal and shearing). However, the force transducers are only capable of measuring forces at a point. Installing multiple sensors in a prosthetic socket is possible, however the spatial resolution of such a system may still remain limited¹⁹. Additionally, the added weight and bulk of a multiple sensor system may alter the natural biomechanics of a participant's movements²¹.

Capacitive Sensors

In the simplest form, a capacitive sensor is comprised of two conductive substrate layers separated by a deformable dielectric layer. Compression of the sensor results in a change of distance between the two conductive players and thus a change in capacitance proportional to the displacement. The change in capacitance can be used to infer the applied load⁵⁷.

A number of studies can be found reporting on capacitive sensor design and applications in prosthetic sockets. Zheng et al. report a novel sensor that uses capacitance signal from the soft tissue of a RL contacting the prosthetic socket wall⁵⁸. They performed experiments with 6 transtibial participants and demonstrated that the sensor information can be used to identify contact of tissue with the socket wall⁵⁸. Vandeparre et al. developed a capacitive sensor made from elastomeric foam, dielectric films and stretchable metallic electrodes. They evaluated sensor response and stability in a laboratory environment under large deformations and temperature differentials⁵⁹. They suggest the stability of their readings and robust construction make these sensors ideal for prosthetic applications⁵⁹. Sundara et al. developed a capacitive sensor that can be incorporated into a prosthetic liner. They performed a series of bench tests to demonstrate the sensors ability to capture shear and normal stresses and discuss the possible application of these sensors in prosthetic sockets^{60,61}. Polliack et al. developed a capacitive sensor to capture normal forces acting on a prosthetic socket. They performed bench testing to characterize sensor accuracy, hysteresis and drift responses in a flat configuration. Additionally, they integrated 9 sensors into two transtibial prosthetic sockets and worn by participants for 3 hours and demonstrated minimal sensor drift⁶². Finally, Laszczak et al. developed a 3D printed capacitive sensor. They bench top tested their device and suggest its possible utility in evaluation of interface stresses during prosthetic socket fittings⁶³.

Largely speaking, it is evident why researchers may gravitate towards developing and applying novel capacitive sensors to prosthetic environments. Typically they achieve higher sensitivity, lower temperature dependency, more robust structure, lower power consumption, better frequency response, and a larger dynamic range than FSR or printed circuit technology²¹. However, using multiple capacitive sensors in close proximity on a prosthetic socket may

increase the sensors' susceptibility to crosstalk noise, field interactions and fringing capacitance⁶⁴. As a result more advanced electronics and filtering may be necessary to ensure the accuracy of the system. Additionally, many of these sensors have yet to be applied directly to a prosthetic socket, tested with an amputee participant or validated against other 'more standard' technologies.

Other Sensing Technologies

As instrumentation technology has continued to advance, so has the innovation of novel prosthetic force and pressure sensors. In recent years a number of sensors have been designed and proposed for incorporation in prosthetic socket systems. One such innovation involves sensors using Fiber Bragg grating elements. Conceptually, these sensors use an optical fiber that transmits nearly all wavelengths of light with negligible attenuation. Only light around a specific wavelength will be reflected; known as the Bragg wavelength. Perturbations introduced to the fiber, such as strain or changes in temperature will result in a shifting of the Bragg wavelength. This shift can then be used to infer the nature of the perturbation⁶⁵.

The application of fiber optic sensors such as Fiber Bragg grating has been suggested in numerous medical and biomedical applications including prosthetic sockets⁶⁶⁻⁶⁸. Fiber optic sensors offer many advantages including high sensitivity, high resolution, small size, and low weight⁶⁶. Additionally this sensor technology provides minimal hysteresis in sensor readings⁶⁹. Tsiokos et al. discussed the development of a novel Fiber Bragg sensor with possible application in prosthetic sockets as well as pressure monitoring in medical beds and seats⁶⁶. Although not implemented in a medical environment, they highlighted a series of bench top tests that supported the use of their novel sensor. Al-Fakih et al. embedded Fiber Bragg elements in a thin layer of epoxy material, which was in turn embedded in a silicone polymer material to form a pressure sensor⁷⁰. This sensor was inserted in the patellar tendon area of a trans-tibial prosthetic socket. An inflatable bladder was then used to simulate the RL of a participant. They highlighted favorable results with respect to the sensors hysteresis, sensitivity and reliability. In a later study, design parameters were evaluated and tested in a single transtibial amputee and compared to sensor reading of a Tekscan system (printed circuit system) (Boston, MA, USA). They suggest

favorable results of their design with it yielding slightly higher values than the standard Tekscan system. Although Fiber Bragg sensing systems show promising potential, the experimental nature of this technology in prosthetic systems warrants further investigation to determine the efficacy in a clinical environment.

Another technology that has been proposed for use with prosthetic sockets is fluid filled (bubble) sensors. These sensors infer applied loads through the measurement of pressure changes in a fluid filled compartment of the sensor^{36,71}. In bench top testing and under cyclical loading, these sensors have been shown to outperform other technologies such as FSRs when evaluating sensor drift and hysteresis³⁶. Similar to the Fiber Bragg sensor discussed previously, this technology has demonstrated favorable results for incorporation into a prosthetic socket³⁶; yet, it is largely experimental and has only been bench top tested. Further investigation of sensor performance while exposed to the environmental variables of a prosthetic socket is still necessary to evaluate sensor efficacy.

5.3.1.3 Summary of Findings

The vast majority of experimental measurement studies characterize the pressures developed in transtibial prosthetic sockets. A range of pressures (or stresses) have been reported. Normal pressures up to approximately 415kPa and shear stresses to approximately 65kPa have been reported^{10,20,62,72}. Only one experimental measurement study was found characterizing transfemoral prosthetic socket pressures with maximum values of 27 kPa and greater than 30kPa being reported on the anterior proximal side and anterior distal side of a single patient's RL. Variation in these values can be expected across patients resulting from individual anatomy, socket fit, prosthetic components used and activities being performed during testing. Additional technical variation may be introduced by factors such as sensor accuracy, sensitivity, hysteresis and drift as well as the calibration, signal conditioning and data acquisition techniques.

5.3.2 Limb Numerical Predictive Techniques

An inherent limitation of experimental measurement techniques is that they exclusively measure surface interactions of the RL and socket. This information can begin to inform clinicians of how a socket is interacting with the RL; however it does not capture the behavior of deeper RL tissues. It may be argued that correlation exists between empirically measured surface forces and deeper tissue stresses, however it is difficult predict the mechanical interactions of one's bone and soft tissues from surface forces alone. An understanding of mechanical stresses occurring in deep soft tissue could lead to improved socket design, and the reduction or prevention of deep tissue injuries and subsequent wound formation. To infer the mechanics of the internal RL tissues, most literature relies on Finite Element Methods (FEM). FEM employs commercially available software to produce a 3-dimensional simulation of the prosthetic socket and residual tissues of the limb. Imaging techniques will typically be used to define the *geometry* of the prosthetic socket and tissue being considered in the model. These geometries will be subdivided into a number smaller elements (*meshing*) to approximate the overall behavior of the system, *material properties* for each modelled component will be input and forces acting on each component (*boundary conditions*) will be mathematically defined. The software will solve for the physical response of each individual element which allows for an approximation of the behavior of the RL-prosthetic system as a whole. A breakdown of the primary definitions necessary to develop an FEM model are highlighted in Figure 5.3 and further discussed below.

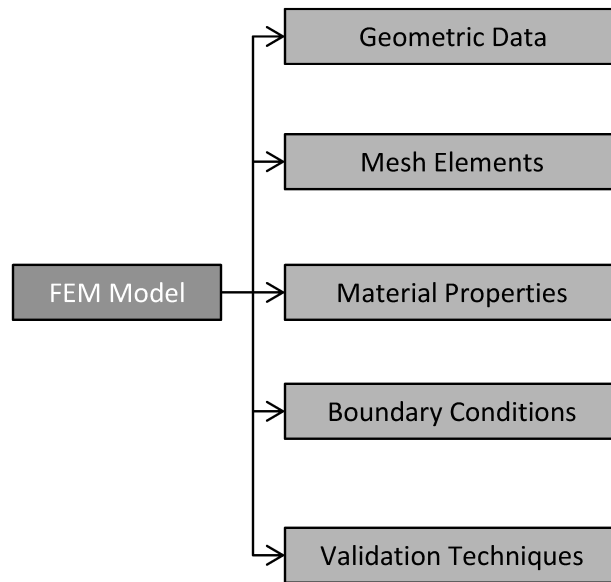


Figure 5.3 A breakdown of the primary definitions necessary in FEM model building

5.3.2.1 Geometry

Most FEM literature considers the prosthetic socket, residual bone, and soft tissue socket as three separate components⁷³⁻⁷⁶, with a number of studies also accounting for the presence of prosthetic liners⁷⁷⁻⁸³. More detailed models may also account for specific features of the RL's anatomy including specific soft tissues such as muscle, fat and skin^{17,84,85}.

Capturing the individual geometry of a patient's RL has been performed using a number of strategies. The internal and external anatomy of the residual limb is most commonly captured using magnetic resonance imaging (MRI)^{77,81-83,86-88}, computerized tomography (CT) scans^{74,76,78,79} or a combination of both^{17,84}. However other strategies do exist, for example Goh et al. describe a technique in which an optical scanner was used to define the exterior geometry of a RL's soft tissue and a 3d anthropometric bone model was scaled, cropped and positioned in the model based on anatomical landmarks⁷³.

Socket geometry has also been derived using a number of techniques. MRI and CT strategies can allow for the geometry of the prosthetic socket to be captured. If the socket is worn while the imaging technique is being performed, the prosthesis is typically visible in the 3D image and can

therefore be easily digitized for analysis⁷⁹. Yet, this technique should be used with caution as discussed below. Computer aided design (CAD) techniques can be used to create 3D digitized models of prosthetic sockets. Such systems are available commercially for clinical use during socket fabrication, and the resulting digitized socket geometry can be exported for use in FE models^{73,77,82,88-91}. Optical and laser scanning techniques have also been used. Typically this requires a prosthetist creating a plaster positive of the interior socket surfaces and using a scanner to digitize this geometry^{74,89}. Prominent methods to define modelled component geometries are highlighted in Figure 5.4.

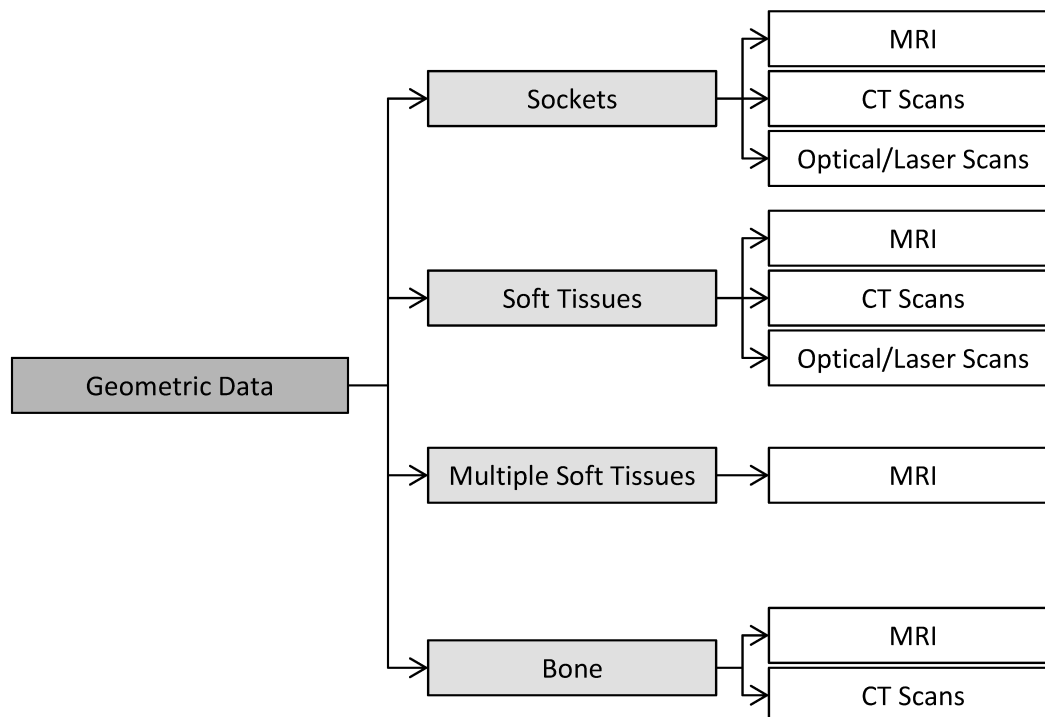


Figure 5.4 Prominent methods to define modelled component geometries. Where MRI denotes magnetic resonance imaging and CT denotes computerized tomography

The geometric definitions of each modelled component form the foundation on which the remainder of the model is built. Regardless of the employed imaging technique, it is vital that geometry be sufficiently representative of the system being modelled and that it is captured in an initial undeformed state. For example, if a socket was worn during the MRI or CT imaging of a RL, an initial preload is physically imparted on these tissues and inevitably impacts the stresses

and pressures present. Many models perform imaging in the absence of the socket compression on the RL^{73,82,83,88}, while others have attempted to compensate using initial boundary condition definitions^{17,84}; however, some studies neglect this preload⁷⁹.

5.3.2.2 Meshing

FEM models will represent the geometry of each component through a series of connected nodes (elements). Together the set of elements, representative of components geometry, are defined as its mesh. In the FEM software the mesh will be paired with the material properties of each component (discussed below), resulting in a physical definition of how the structure deforms with the application of load.

The geometry of the elements defining a modeled component holds important implications in the ability of the model to predict deformation and corresponding stresses. Tetrahedral elements are typically used to define soft tissues and bone; as they can readily accommodate irregular geometries. Linear tetrahedral^{75,77,81,88} or non-linear^{73,79} tetrahedral elements are typically used, although the linearity of the elements used is often not reported^{17,74,76,84,87,91}. In many studies the socket is meshed using tetrahedral elements as well^{73-76,79,82,88,91}. In addition, components of thin cross section and large surface area, such as the prosthetic socket or skin, are mathematically amenable to meshing with 2D shell elements^{17,77,84,90}. Prominent meshes used in modelled geometries are highlighted in Figure 5.5.

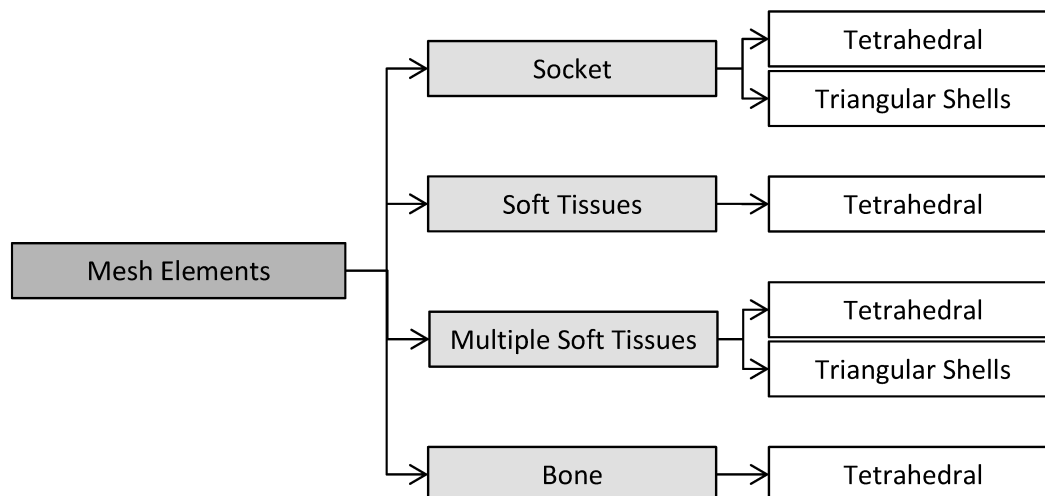


Figure 5.5 Prominent meshes used in modelled geometries

Consideration must be given to appropriate element selection. In most commercially available software, meshing is an automated procedure based on user inputs and definitions. It is possible to achieve a sufficient mesh quality from a geometric perspective, while neglecting other important mathematical factors. For example, many models use a linear tetrahedral mesh to define the soft tissues of the residual limb^{75,77,81,88}. Yet in incompressible materials, such as those expected in human soft tissues, this mesh is subject to a mathematical phenomenon known as locking. This numerical error may result in material displacements being under predicted. A non-linear tetrahedral mesh may help overcome this limitation at the cost of increased computational resources and time. Additionally, the use of shell elements (rather than tetrahedral) to mesh the prosthetic socket can significantly reduce the number of elements required. Shell elements can provide accurate results, reduce the risk of excessive element distortion and reduce the required computational resources to mathematically converge on results.

5.3.2.3 Material Property Definitions

Material definitions are a crucially important aspect in FEM models. They provide the FEM software with a mathematical description of the underlying physics for each material. This allows for computation of how a material responds to the application of force. In nearly all the reviewed literature, the prosthetic socket material properties were defined as isotropic, linear elastic and homogeneous, with exception of two studies modelling the socket as rigid non-deformable structure^{73,77}. Similar definitions were also found for defining residual bone. However, the most variation in material definitions can be found in the modelling of soft tissue. Isotropy and homogeneity are fairly common assumptions for soft tissue. The division in literature comes in assignment elastic properties; how the material deforms under a given load. Many models assume linear elasticity^{73,75,77,79,81,85,87,88,91}. Inherent to this assumption is the mathematical requirement that each element in the model's mesh undergoes infinitesimally small deformations (strain) and that a linear relationship exists between material deformation and the stress developed. The second approach assigns a non-linear definition to the material. In reality, the soft tissue of a residual limb can demonstrate large deformations as well as non-linear and viscoelastic behaviors^{92,93}; a significant departure from a linear elastic continuum. Most models incorporating non-linear, large deformation behaviors will opt to use a hyperelastic Mooney-

Rivlin material definition ^{17,74,76,84}, although Portnoy et al. have also defined skin as a neo-Hookean solid ⁸⁴. Prominent material definitions subdivided by modelled component are highlighted in Figure 5.6.

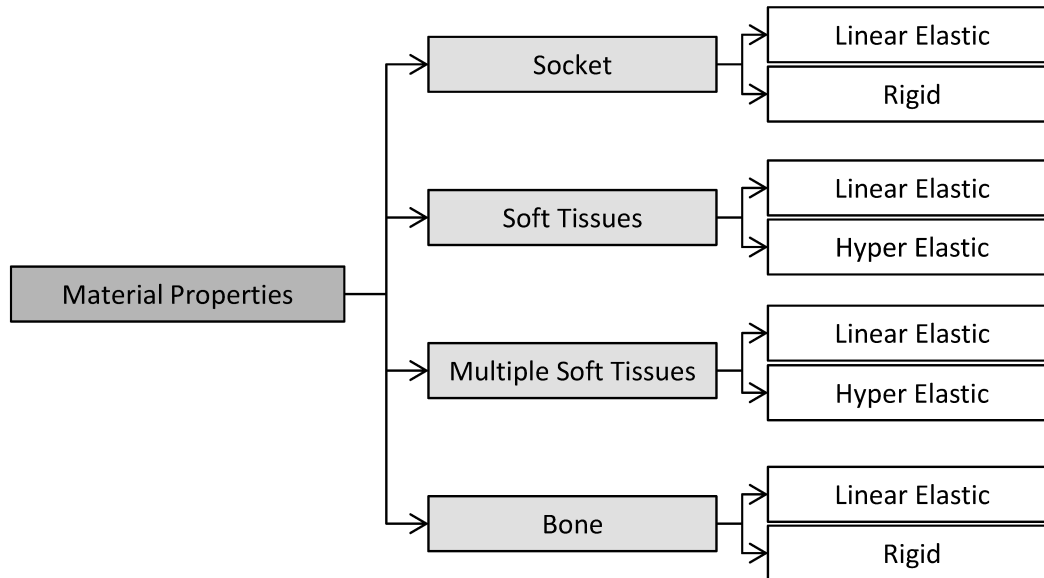


Figure 5.6 Prominent material definitions subdivided by modelled component

A hyperelastic definition requires significantly more computational resources; however in the past 15 years advances in computing power have enabled nonlinear models to be more readily adopted. The appropriateness of material properties has the ability to significantly impact the model's ability to accurately predict results, and the length of time required to run. Analysis comparing predicted values to those measured experimentally ultimately serves as the best validation for appropriate material definitions.

5.3.2.4 Boundary Conditions

Boundary conditions are added to FEM models to describe the physical interaction of modelled components with each other and their external environments. Typically the contacting surfaces of the residual skeletal structure and soft tissues will be mathematically bonded to represent a zero-displacement boundary condition. In nearly all studies reported in this review, the contact surface of the residual soft tissues and prosthetic sockets were allowed to displace with an assigned friction coefficient (with exception of the bonded (no slip) conditions implemented in

the Goh et al. study⁷³). The boundary conditions applied to the external surfaces of the prosthetic socket were representative, in location, magnitude, and direction, of the loads associated with the specific activity being model (for example gait reaction forces). These boundary conditions were determined either through physical and mathematical calculations^{75,77,81,82} or from experimental data such as gait analysis techniques^{73,78,79,81,91} or socket instrumentation^{17,84,85}; although some studies used loading define in previous literature^{76,89}. Figure 5.7 summarizes the prominent boundary conditions defined in FEM models.

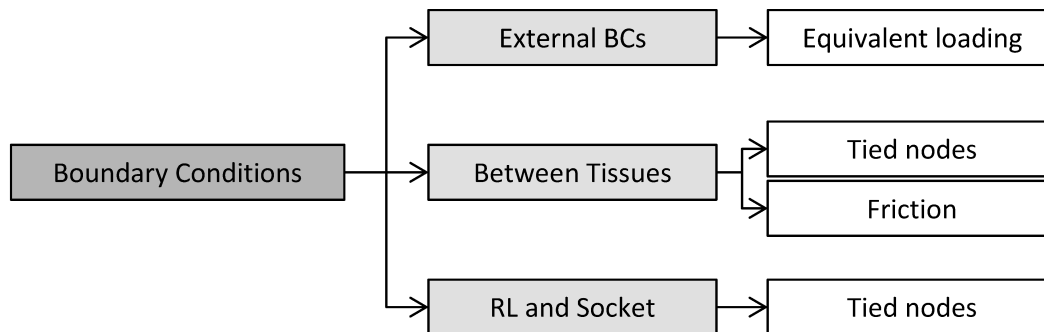


Figure 5.7 Prominent boundary conditions defined in FEM models

5.3.2.5 Model Validation

The ability for a model to sufficiently predict the behavior of a physical system is dependent on appropriate geometry, meshes, material definitions and boundary conditions being defined. The numerous variations of techniques, in the literature, defining these crucial inputs necessitates the need to validate that the model is accurately predicting and representing the physics of the numerically simulated system. This establishes confidence in the model's performance and allows the end user (the researcher or clinician) to understand the inherent error and limitations of the model. This is typically accomplished through comparing modelled results to those measured empirically at the RL-socket interface^{73,78,85}, or comparing results to those reported in previous literature^{75,76,79,81,82,87,88}; although some studies do not explicitly report the validation techniques used to develop their model^{77,89,90}. Yet FEM models have the ability to report the magnitudes of interfacial forces, stresses, strains and/or pressures as well as their anatomical locations. A comprehensive validation of a model will include error reporting in a model's

ability to predict both the magnitude and location of these values. Validation methods highlighted in the literature are summarized in Figure 5.8.

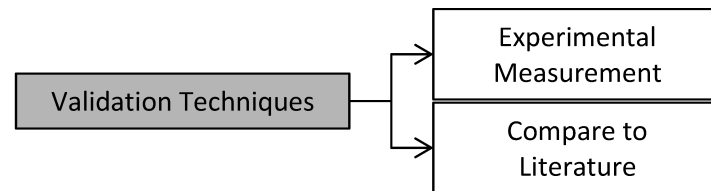


Figure 5.8 A graphical summary of the validation methods from the reviewed literature

Validation through comparison to previous literature needs to be exercised with caution. The individual anatomy of a patient's RL and the specific prosthetic components may introduce substantial biomechanical variation across patients and studies. Additionally the modeling choices in terms of geometric derivation, meshes, material definitions, and boundary conditions may drastically impair the ability to compare model predictions across studies. A typical study employing this method of validation will contrast obtained pressure or stress results relative to the spectrum of ranges report in literature. For example Faustini et al. reported stress values predicted at the patellar tendon (250 kPa) and the popliteal depression (109 kPa) to fall within values reported in prior FEM and empirical measurement literature (380–200kPa and 80–175 kPa, respectively)⁷⁹. Additionally, a number of studies validated against literature, which, in turn, had also validated against prior existing literature⁷⁴⁻⁷⁶. This practice can propagate the inaccuracy and uncertainty of a previous model throughout numerous subsequent studies.

Ideally a comprehensive model employs experimental measurement techniques to validate the numerically predicted values. This allows for empirical quantification of interface mechanics while accommodating for the unique factors surrounding each patient's RL and socket. This empirical definition can then be the benchmark against which the numerical model is validated. This has been employed^{73,78,85} however the increased requirement for equipment and resources has likely resulted in few studies following this route.

5.4 Upper Limb RL-Socket Mechanics

In the United States, UL loss accounts for an estimated 35% of those living with limb amputation⁵. Although, the prevalence is less than that of the LL, there are disproportionately fewer studies quantifying RL-socket mechanics. Similar to the LL, prosthetic comfort and function are closely tied to the mechanics of prosthetic fit in the UL. Current UL socket fabrication processes rely heavily on heuristic practices; and remarkably, the distribution of pressure onto the residual limb has yet to be comprehensively investigated or quantitatively defined. To date, two pieces of literature have been published that provided a rudimentary understanding of socket interface biomechanics. Daly et al. placed a TekScan pressure sensor system (Boston, MA, USA) between the RL and prosthetic socket of 9 UL amputee participants. They attempted to correlate discomfort with the mean pressure developed across the residual limb⁹⁴. They found the relationship to be participant specific and variable, ranging from low to high correlation. Mean normal pressure values of 3.3 - 4.0psi, 2.6 – 7.6psi, and 2.9 – 3.9psi were reported in 3 transradial, 3 transhumeral and 3 shoulder disarticulation amputee participants, respectively. However, limiting the utility of this study, Daley et al. reported mean pressures exclusively. They did not report pressures to anatomical locations on the participants' residual limbs, impeding the transfer of their results to socket design decisions. Sensinger et al. developed a linear-elastic Finite Element (FE) model to evaluate sagittal rotational stiffness of the socket on the residual limb in the context of impedance based prosthetic control systems⁹⁵. Although this work provides the first FE model of an UL prosthetic system, its scope was not focused on establishing transitional information for the design of prosthetic sockets, therefore limiting its utility to inform design and fabrication practices. It is evident that many of the experimental and numerical techniques developed for LL prostheses can be adapted to describe the UL. Yet these techniques may not translate directly as there is much more complexity in requirements for UL movement in contrast to the highly cyclical loading in the LL. Applying experimental measurement and numerical modeling techniques to UL sockets holds the potential to characterize these unique physical differences and develop a fundamental mechanical understanding to aid in socket design and fabrication processes.

5.5 Discussion

The ability to understand and predict the mechanical interactions of the RL and socket ideally would help to quantitatively inform clinical socket design decisions and fabrication practices. There are two reoccurring objectives in the literature regarding investigations of socket fit; the first being the characterization of forces, stresses or pressures developed in the RL soft tissues as a result of the prosthetic socket during various activities of daily living (such as gait or sitting), and the second being the characterization of these values to evaluate prosthetic components, socket designs or fabrication techniques. Although decades of research have been conducted around prosthetic fit and interface mechanics, socket fabrication is still largely experience based-with minimal quantitative fabrication guidelines. Although many studies characterize the interactions of the RL-socket interface for a limited patient sample, a clinician cannot confidently rely on literature to address the unique challenges of an individual patient. Furthermore, variability in terms of patient anatomy and potential prosthetic components inhibits the findings of a single study being applied across multiple patients. Therefore clinical deployment of interface measurement techniques or FEM requires data that is derived from the individual patient at hand. Largely speaking, advanced sensors and numerical simulations, such as FEM, lack accessibility for the clinician. In bridging this gap, two key issues must be addressed. First the system must be accurate and reliable enough that the clinician will have confidence in the result being presented. Secondly, the system must be packaged for ease of use; the system must be able to be operated effectively without over burdening the user with excessive training requirements and complexity. The clinician could then rely on this analytical data to help inform the design and fabrication of the prosthetic socket.

5.5.1 Experimental Measurement Techniques

For researchers and clinicians, selection of the appropriate measurement system has important implications on the possible data that can be collected. Commercially available pressure measurement systems, such as the Tekscan F-Socket (Boston, MA, USA), have seen the most use in clinical literature relative to the other quantification techniques reviewed in this chapter. A possible explanation is the ease of use of these systems. Unlike pressure sensors that need to be installed through the socket wall, most commercially available systems can be inserted between the RL and socket. This allows the clinician to evaluate socket fit without permanently altering

the socket to install sensors. Therefore such systems can be readily employed, in a non-destructive fashion, in a patient's existing (or newly fabricated) socket to aid in evaluation of socket fit. Additionally such systems typically include user interfaces that require minimal technical knowledge; alleviating another significant barrier to custom sensor systems. Yet, many commercially available technologies possess inherent limitations in terms of accuracy, hysteresis, sensor drift, or sensitivity to their environment; the impact of which must be recognized by the clinician. Many of these limitations may be minimized through implementing a custom sensor system. However, this process often first requires sensor integration with a data acquisition system, with custom software developed for the calibration, signal conditioning and data collection; a significant barrier to those lacking the required technical expertise.

In this review we categorized sensors relative to their location in the RL-socket system. The data that can be captured is influenced by whether a sensor is placed directly against the user's residual soft tissue (inserted between RL and socket), or installed in the wall of the socket. If a sensor is inserted such that it is in direct contact with the residual limb, it holds the advantage of being able to capture resultant forces (or pressures) applied directly to the soft tissues. In systems where sensors must be installed into the socket wall, the forces being applied to the socket wall are captured. In the event a patient uses a prosthetic liner interface, the socket mounted strategy will not capture the true forces acting on the user's soft tissue. However, most sensors thin enough to be inserted between the RL and socket with minimal protrusion cannot capture shear stresses acting on that tissue; a crucial consideration during the sensor selection process.

5.5.2 Numerical Prediction Techniques

Experimental measurement techniques are solely capable of measuring the interface mechanics of prosthetic systems after they have been fabricated. However, if implemented clinically, numerical prediction techniques have the ability to forecast RL-socket interactions prior to a socket being fabricated. A workflow diagram of this procedure can be found in Figure 5.9. With the emergence of CAD based socket design programs, sockets can be created virtually prior to fabrication. Conceptually, socket designs could then be imported into an FEM to evaluate the interface mechanics of the socket on a patient's virtual RL. From the corresponding results the prosthetist could then decide whether to fabricate or redesign the socket^{23,77}. Theoretically, such

a system could drastically impact current socket fabrication practices; however, such systems remain largely absent in the clinic today. The development of a comprehensive FEM model requires a working knowledge of specialized areas in physics, mathematics and solid mechanics. Therefore a user interface allowing a non-expert to utilize such a tool without impacting the accuracy of results is necessary. Additionally, although more complex FEMs may closely resemble the physical RL-socket system, it may take hours, and in extreme cases days, to compute results (depending on the computational resources available). This time frame can be a major barrier to adoption in clinical setting. Efforts need to be made to simplify models and reduce computational time. Through rigorous model validation an appropriate balance between reduced complexity (resulting in reduced computational time) and model accuracy may be achieved.

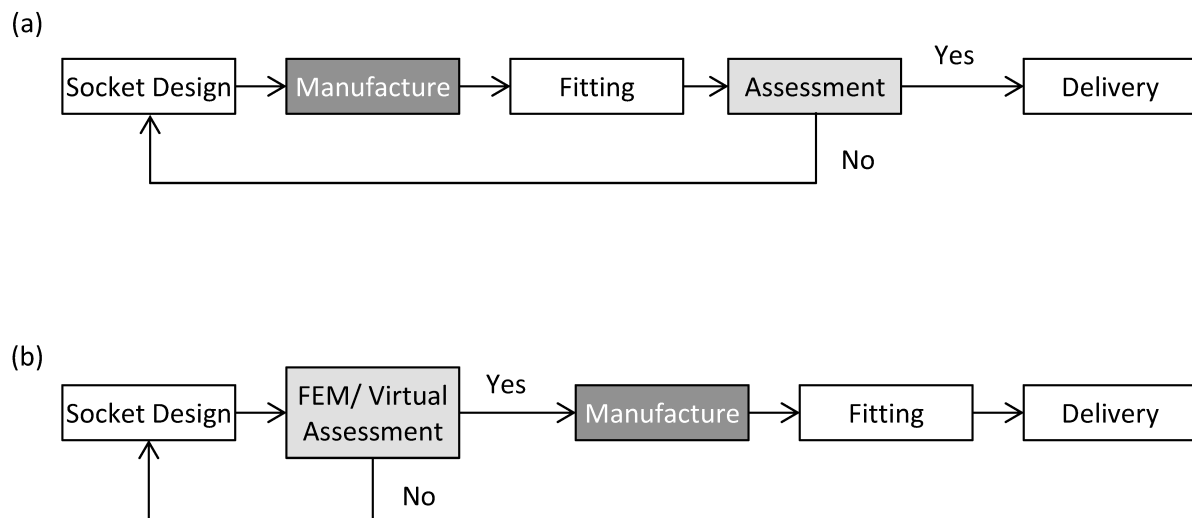


Figure 5.9 Prosthetic fabrication work flow diagram. (a) Current prosthetic socket fabrication practices. (b) Prosthetic socket fabrication practices utilizing FEM. Figure adapted from Zachariah et al.²² permission to reproduce obtained through the original publisher.

5.5.3 Future directions

The last 15 years of studies characterizing RL-socket interface mechanics have leveraged advancements in instrumentation technology and computing power, as well as provided a

substantial body of knowledge. However, significant gaps still remain between the laboratory and clinic. For these advanced techniques to be adopted clinically, future work must be performed to address accessibility for the clinical end user.

A number of recent studies highlight novel sensing systems with advantages over existing commercially available systems. Continued development toward clinical applications requires validation of these technologies in actual prosthetic limbs worn by patients. In doing so, limitations specific to prosthetic use can be captured and addressed. Considerations for ease of use in a clinical setting must also be pursued. Significant barriers such as the requirement for highly specialized training or intrusive installation procedures must be addressed.

Predictive modelling techniques will need to take a similar trajectory. As discussed previously, many current models lack comprehensive validation of their accuracy. Without this vital step, very little confidence can be gained from the results. In both scientific and clinical contexts, this weakness fundamentally limits the utility of such studies. As finite element modelling is a technically rigorous process, appropriately simplified, yet accurate, models will need to be developed prior to clinical adoption. Preliminary work can already be found in literature that aims to develop automated FEM modelling software to be used in tandem with clinical expertise⁷⁷. It can be anticipated that similar work will be conducted in the near future and will continue to pursue the pairing of CAD and automated FEM modelling. Ultimately this work can drastically simplify the FEM procedures; packaging this powerful numerical technique in a more clinically amenable format.

5.6 Conclusions

Prosthetic sockets directly impact prosthetic comfort, use, user satisfaction, and tissue health of the RL. Fabrication of this vitally important component is dependent on an appropriate understanding of the interface mechanics between the RL and socket. Substantial advancements in instrumentation technology and computational power have unlocked the possibility of advanced systems providing quantitative data that may work in tandem with a clinician's experience during socket fabrication. However, both advanced instrumentation and predictive modelling techniques are still largely absent in the clinic, as current systems described in the literature lack clinical accessibility. It is suggested that two key barriers exist. First, experimental

systems must be rigorously validated to lend confidence to the quantitative information provided to the clinician. Second, clinically amenable user-interfaces need to be created that minimize system complexity and the need for highly specialized technical training of the user. By addressing these two factors the gap between advanced engineering technology and clinical translation can begin to be reduced.

In the context of sensory integrated UL prostheses, the application of quantitative measurement and prediction techniques will be necessary. As sensory integrated prostheses inherently require non-traditional prosthetic components and sockets, analytical tools to help inform the design process are imperative. Adapting and developing many of the empirical techniques employed in the LL will enable appreciate of how non-traditional prostheses interact with RLs, and provide insight into critical factors such as fit and comfort. Furthermore predictive techniques such as finite element approaches may serve as tools to help inform socket design through virtual analysis prior to fabrication. The subsequent chapters (chapters 6 and 7) further develop and adapt empirical techniques to facilitate the evaluation of the sensory integrated prosthesis developed in chapter 8.

5.7 References

1. Schofield JS, Evans KR, Carey JP, Hebert JS. Applications of sensory feedback in motorized upper extremity prosthesis: A review. *Expert Review of Medical Devices*. 2014;11(5):499-511. Accessed 8 April 2015.
2. Pirouzi G, Abu Osman NA, Eshraghi A, Ali S, Gholizadeh H, Wan Abas WAB. Review of the socket design and interface pressure measurement for transtibial prosthesis. *Scientific World Journal*. 2014;2014. Accessed 22 April 2015.
3. Owings MF, Kozak LJ. Ambulatory and inpatient procedures in the united states, 1996. *Vital and health statistics.Series 13, Data from the National Health Survey*. 1998(139):1-119. Accessed 25 January 2016.

4. Adams PF, Hendershot GE, Marano MA, eds. *Current estimates from the national health interview survey, 1996.* ; 1999; No. 10.
5. Ziegler-Graham K, MacKenzie EJ, Ephraim PL, Travison TG, Brookmeyer R. Estimating the prevalence of limb loss in the united states: 2005 to 2050. *Arch Phys Med Rehabil.* 2008;89(3):422-429. doi: <http://dx.doi.org/10.1016/j.apmr.2007.11.005>.
6. Lake C, Dodson R. Progressive upper limb prosthetics. *Phys Med Rehabil Clin N Am.* 2006;17(1):49-72. Accessed 5 April 2013.
7. Biddiss E, Chau T. Upper limb prosthesis use and abandonment: A survey of the last 25 years. *Prosthet Orthot Int.* 2007;31(3):236-257. Accessed 24 January 2014.
8. Biddiss E, Beaton D, Chau T. Consumer design priorities for upper limb prosthetics. *Disability and Rehabilitation: Assistive Technology.* 2007;2(6):346-357. Accessed 5 April 2013.
9. Schultz AE, Baade SP, Kuiken TA. Expert opinions on success factors for upper-limb prostheses. *Journal of Rehabilitation Research and Development.* 2007;44(4):483-489. Accessed 5 April 2013.
10. Sanders J. Stump-socket interface conditions. In: *Pressure ulcer research: Current and future perspectives.* Heidelberg Germany: Springer-Verlag Berlin; 2005:129-147. Accessed 25 January 2016.
11. Hachisuka K, Dozono K, Ogata H, Ohmine S, Shitama H, Shinkoda K. Total surface bearing below-knee prosthesis: Advantages, disadvantages, and clinical implications. *Arch Phys Med Rehabil.* 1998;79(7):783-789. Accessed 25 January 2016.
12. Li W, Pang Q, Lu M, Liu Y, Zhou ZR. Rehabilitation and adaptation of lower limb skin to friction trauma during friction contact. *Wear.* 2015;332-333:725-733. Accessed 25 January 2016. doi: 10.1016/j.wear.2015.01.045.

13. Levy W. Chapter 26: Skin problems of the amputee. In: Bowker JH, Michael JW, eds. *Atlas of limb prosthetics: Surgical, prosthetic, and rehabilitation principles*. 2nd ed. Mosby Year Book; 1992.
14. Knapik JJ, Reynolds KL, Duplantis KL, Jones BH. Friction blisters: Pathophysiology, prevention and treatment. *Sports Med*. 1995;20(3):136-147. Accessed 25 January 2016. doi: 10.2165/00007256-199520030-00002.
15. Mak AFT, Zhang M, Tam EWC, eds. *Biomechanics of pressure ulcer in body tissues interacting with external forces during locomotion*. ; 2010Annual Review of Biomedical Engineering; No. 12.
16. Salawu A, Middleton C, Gilbertson A, Kodavali K, Neumann V. Stump ulcers and continued prosthetic limb use. *Prosthet Orthot Int*. 2006;30(3):279-285. Accessed 26 January 2016.
17. Portnoy S, Siev-Ner I, Shabshin N, Gefen A. Effects of sitting postures on risks for deep tissue injury in the residuum of a transtibial prosthetic-user: A biomechanical case study. *Comput Methods Biomech Biomed Engin*. 2011;14(11):1009-1019. Accessed 26 January 2016.
18. Dillingham TR, Pezzin LE, MacKenzie EJ, Burgess AR. Use and satisfaction with prosthetic devices among persons with trauma-related amputations: A long-term outcome study. *American Journal of Physical Medicine and Rehabilitation*. 2001;80(8):563-571. Accessed 31 January 2014.
19. Silver-Thorn MB, Steege JW, Childress DS. A review of prosthetic interface stress investigations. *Journal of Rehabilitation Research and Development*. 1996;33(3):253-266. Accessed 9 February 2014.
20. Sanders JE. Interface mechanics in external prosthetics: Review of interface stress measurement techniques. *Med Biol Eng Comput*. 1995;33(4):509-516. Accessed 13 May 2015.

21. Al-Fakih EA, Abu Osman NA, Mahmad Adikan FR. Techniques for interface stress measurements within prosthetic sockets of transtibial amputees: A review of the past 50 years of research. *Sensors*. 2016;16(7). Accessed 13 September 2016. doi: 10.3390/s16071119.
22. Zachariah SG, Sanders JE. Interface mechanics in lower-limb external prosthetics: A review of finite element models. *IEEE Trans Rehabil Eng*. 1996;4(4):288-302. Accessed 26 January 2016. doi: 10.1109/86.547930.
23. Zhang M, Mak AFT, Roberts VC. Finite element modelling of a residual lower-limb in a prosthetic socket: A survey of the development in the first decade. *Medical Engineering and Physics*. 1998;20(5):360-373. Accessed 31 January 2014.
24. Mak AFT, Zhang M, Boone DA. State-of-the-art research in lower-limb prosthetic biomechanics-socket interface: A review. *Journal of Rehabilitation Research and Development*. 2001;38(2):161-173. Accessed 9 February 2014.
25. Schofield JS, Evans KR, Hebert JS, Marasco PD, Carey JP. The effect of biomechanical variables on force sensitive resistor error: Implications for calibration and improved accuracy. *J Biomech*. 2016;49(5):786. doi: <http://dx.doi.org/10.1016/j.jbiomech.2016.01.022>.
26. El-Sayed AM, Hamzaid NA, Tan KYS, Abu Osman NA. Detection of prosthetic knee movement phases via in-socket sensors: A feasibility study. *Sci World J*. 2015;2015. Accessed 2 February 2016. doi: 10.1155/2015/923286.
27. Mai A, Commuri S, Dionne CP, Day J, Ertl WJJ, Regens JL. Effect of prosthetic foot on residuum-socket interface pressure and gait characteristics in an otherwise healthy man with transtibial osteomyoplastic amputation. *J Prosthet Orthot*. 2012;24(4):211-220. Accessed 2 February 2016. doi: 10.1097/JPO.0b013e31826fdaf8.
28. Beil TL, Street GM, Covey SJ. Interface pressures during ambulation using suction and vacuum-assisted prosthetic sockets. *J Rehabil Res Dev*. 2002;39(6):693-700. Accessed 3 February 2016.

29. Kahle JT, Jason Highsmith MJ. Transfemoral sockets with vacuum-assisted suspension comparison of hip kinematics, socket position, contact pressure, and preference: Ischial containment versus brimless. *Journal of Rehabilitation Research and Development*. 2013;50(9):1241-1252. Accessed 2 February 2016.
30. Dumbleton T, Buis AWP, McFadyen A, et al. Dynamic interface pressure distributions of two transtibial prosthetic socket concepts. *Journal of Rehabilitation Research and Development*. 2009;46(3):405-415. Accessed 2 February 2016.
31. Rogers B, Bosker G, Faustini M, Walden G, Neptune RR, Crawford R. Case report: Variably compliant transtibial prosthetic socket fabricated using solid freeform fabrication. *Journal of Prosthetics and Orthotics*. 2008;20(1):1-7. Accessed 2 February 2016.
32. Rajtukova V, Hudak R, Zivcak J, Halfarova P, Kudrikova R. Pressure distribution in transtibial prostheses socket and the stump interface. *Procedia Engineering*. 2014;96:374-381. Accessed 2 February 2016.
33. Polliack AA, Sieh RC, Craig DD, Landsberger S, McNeil DR, Ayyappa E. Scientific validation of two commercial pressure sensor systems for prosthetic socket fit. *Prosthet Orthot Int*. 2000;24(1):63-73. Accessed 22 April 2015.
34. Boutwell E, Stine R, Hansen A, Tucker K, Gard S. Effect of prosthetic gel liner thickness on gait biomechanics and pressure distribution within the transtibial socket. *Journal of Rehabilitation Research and Development*. 2012;49(2):227-240. Accessed 22 April 2014.
35. Wolf SI, Alimusaj M, Fradet L, Siegel J, Braatz F. Pressure characteristics at the stump/socket interface in transtibial amputees using an adaptive prosthetic foot. *Clin Biomech*. 2009;24(10):860-865. Accessed 3 February 2016. doi: 10.1016/j.clinbiomech.2009.08.007.
36. Dabbling JG, Filatov A, Wheeler JW. Static and cyclic performance evaluation of sensors for human interface pressure measurement. *Proceedings of the Annual International Conference of the IEEE Engineering in Medicine and Biology Society, EMBS*. 2012:162-165. Accessed 22 April 2015.

37. Lebosse C, Renaud P, Bayle B, De Mathelin M. Modeling and evaluation of low-cost force sensors. *IEEE Transactions on Robotics*. 2011;27(4):815-822. Accessed 22 April 2015.
38. Herbert-Copley AG, Sinitski EH, Lemaire ED, Baddour N. Temperature and measurement changes over time for F-scan sensors. *MeMeA 2013 - IEEE International Symposium on Medical Measurements and Applications, Proceedings*. 2013:265-267. Accessed 22 April 2015.
39. Polliack AA, Sieh RC, Craig DD, Landsberger S, McNeil DR, Ayyappa E. Scientific validation of two commercial pressure sensor systems for prosthetic socket fit. *Prosthet Orthot Int*. 2000;24(1):63-73. Accessed 22 April 2015.
40. Hall RS, Desmoulin GT, Milner TE. A technique for conditioning and calibrating force-sensing resistors for repeatable and reliable measurement of compressive force. *J Biomech*. 2008;41(16):3492-3495. Accessed 11 December 2015. doi: 10.1016/j.jbiomech.2008.09.031.
41. Buis AWP, Convery P. Calibration problems encountered while monitoring stump/socket interface pressures with force sensing resistors: Techniques adopted to minimise inaccuracies. *Prosthet Orthot Int*. 1997;21(3):179-182. Accessed 22 April 2015.
42. Patterson RP, Fisher SV. The accuracy of electrical transducers for the measurement of pressure applied to the skin. *IEEE Trans Biomed Eng*. 1979;BME-26(8):450-456. Accessed 10 February 2016. doi: 10.1109/TBME.1979.326570.
43. Sonck WA, Cockrell JL, Koepke GH. Effect of liner materials on interface pressures in below-knee prostheses. *Arch Phys Med Rehabil*. 1970;51(11):666-669. Accessed 10 February 2016.
44. Rae JW, Cockrell JL. Interface pressure and stress distribution in prosthetic fitting. *U S, Veterans Adm, Dep Med Surg*. 1971(10-16):64-111. Accessed 10 February 2016.
45. Pearson JR, Holmgren G, March L, Oberg K. Pressures in critical regions of the below knee patellar tendon bearing prosthesis. *Bull Prosthet Res*. 1973;No.19:52-76. Accessed 10 February 2016.

46. Williams RB, Porter D, Roberts VC, Regan JF. Triaxial force transducer for investigating stresses at the stump/socket interface. *Med Biol Eng Comput*. 1992;30(1):89-96. Accessed 10 February 2016. doi: 10.1007/BF02446199.
47. Smith LM, Sanders JE, Spelman FA. Portable signal conditioning and data acquisition system for prosthetic triaxial force transducers. *Proc Annu Conf Eng Med Biol*. 1993;15(pt 3):1288-1289. Accessed 10 February 2016.
48. Sanders JE, Smith LM, Spelman FA, Warren DJ. A portable measurement system for prosthetic triaxial force transducers. *IEEE Trans Rehab Eng*. 1995;3(4):366-373. Accessed 10 February 2016. doi: 10.1109/86.481977.
49. Sanders JE, Miller RA, Berglund DN, Zachariah SG. A modular six-directional force sensor for prosthetic assessment: A technical note. *Journal of Rehabilitation Research and Development*. 1997;34(2):195-202. Accessed 9 February 2014.
50. Goh JCH, Lee PVS, Chong SY. Stump/socket pressure profiles of the pressure cast prosthetic socket. *Clin Biomech*. 2003;18(3):237-243. Accessed 3 February 2016. doi: 10.1016/S0268-0033(02)00206-1.
51. Goh JCH, Lee PVS, Sook YC. Comparative study between patellar-tendon-bearing and pressure cast prosthetic sockets. *J Rehabil Res Dev*. 2004;41(3 B):491-501. Accessed 3 February 2016.
52. Xin Z. Design of a new type six-axis force sensor. *Int Conf Intelligent Comput Technol Autom , ICICTA*. 2009;2:446-449. Accessed 10 February 2016. doi: 10.1109/ICICTA.2009.343.
53. Zhang X. Development of a novel three-axis force sensor. *IET Conf Publ*. 2009;2009(556 CP). Accessed 10 February 2016. doi: 10.1049/cp.2009.1440.
54. Abu Osman NA, Spence WD, Solomonidis SE, Paul JP, Weir AM. Transducers for the determination of the pressure and shear stress distribution at the stump-socket interface of trans-

tibial amputees. *Proc Inst Mech Eng Part B J Eng Manuf.* 2010;224(8):1239-1250. Accessed 10 February 2016. doi: 10.1243/09544054JEM1820.

55. Neumann ES, Yalamanchili K, Brink J, Lee JS. Transducer-based comparisons of the prosthetic feet used by transtibial amputees for different walking activities: A pilot study. *Prosthet Orthot Int.* 2012;36(2):203-216. Accessed 10 February 2016. doi: 10.1177/0309364612436408.

56. Sanders JE, Jacobsen AK, Fergason JR. Effects of fluid insert volume changes on socket pressures and shear stresses: Case studies from two trans-tibial amputee subjects. *Prosthet Orthot Int.* 2006;30(3):257-269. Accessed 10 February 2016. doi: 10.1080/03093640600810266.

57. Siegel DM, Drucker SM, Garabieta I. Performance analysis of a tactile sensor. . 1987:1493-1499. Accessed 10 February 2016.

58. Zheng E, Wang L, Wei K, Wang Q. A noncontact capacitive sensing system for recognizing locomotion modes of transtibial amputees. *IEEE Transactions on Biomedical Engineering.* 2014;61(12):2911-2920. Accessed 2 February 2016.

59. Vandeparre H, Watson D, Lacour SP. Extremely robust and conformable capacitive pressure sensors based on flexible polyurethane foams and stretchable metallization. *Appl Phys Lett.* 2013;103(20). Accessed 12 February 2016. doi: 10.1063/1.4832416.

60. Sundara-Rajan K, Bestick A, Rowe GI, et al. An interfacial stress sensor for biomechanical applications. *Measurement Science and Technology.* 2012;23(8). Accessed 2 February 2016.

61. Sundara-Rajan K, Rowe GI, Simon AJ, Klute GK, Ledoux WR, Mamishev AV. Shear sensor for lower limb prosthetic applications. *2009 1st Annual ORNL Biomedical Science and Engineering Conference, BSEC 2009.* 2009. Accessed 2 February 2016.

62. Polliack AA, Craig DD, Sieh RC, Landsberger S, McNeal DR. Laboratory and clinical tests of a prototype pressure sensor for clinical assessment of prosthetic socket fit. *Prosthet Orthot Int.* 2002;26(1):23-34. Accessed 2 February 2016.

63. Laszczak P, Jiang L, Bader DL, Moser D, Zahedi S. Development and validation of a 3D-printed interfacial stress sensor for prosthetic applications. *Med Eng Phys*. 2015;37(1):132-137. Accessed 13 September 2016. doi: 10.1016/j.medengphy.2014.10.002.
64. Tiwana MI, Redmond SJ, Lovell NH. A review of tactile sensing technologies with applications in biomedical engineering. *Sens Actuators A Phys*. 2012;179:17-31. Accessed 22 September 2016. doi: 10.1016/j.sna.2012.02.051.
65. Meltz G, Dunphy JR, Glenn WH, Farina JD, Leonberger FJ. Fiber optic temperature and strain sensors. *Proc SPIE Int Soc Opt Eng*. 1987;798:104-114. Accessed 10 February 2016. doi: 10.1117/12.941093.
66. Tsiokos D, Kanellos G, Papaioannou G, Pissadakis S. Fiber optic-based pressure sensing surface for skin health management in prosthetic and rehabilitation interventions. In: *Biomedical engineering - technical applications in medicine*. InTech; 2012. 10.5772/50574.
67. Mishra V, Singh N, Tiwari U, Kapur P. Fiber grating sensors in medicine: Current and emerging applications. *Sens Actuators A Phys*. 2011;167(2):279-290. Accessed 12 February 2016. doi: 10.1016/j.sna.2011.02.045.
68. Mignani AG, Baldini F. Fibre-optic sensors in health care. *Phys Med Biol*. 1997;42(5):967-979. Accessed 12 February 2016. doi: 10.1088/0031-9155/42/5/015.
69. Mignani AG, Baldini F. Biomedical sensors using optical fibres. *Rep Prog Phys*. 1996;59(1):1-28. Accessed 12 February 2016. doi: 10.1088/0034-4885/59/1/001.
70. Al-Fakih EA, Osman NA, Eshraghi A, Adikan FR. The capability of fiber bragg grating sensors to measure amputees' trans-tibial stump/socket interface pressures. *Sensors (Basel)*. 2013;13(8):10348-10357. Accessed 10 February 2016.
71. Wheeler JW, Dabling JG, Chinn D, et al. MEMS-based bubble pressure sensor for prosthetic socket interface pressure measurement. *Proc Annu Int Conf IEEE Eng Med Biol Soc EMBS*. 2011:2925-2928. Accessed 2 February 2016. doi: 10.1109/IEMBS.2011.6090805.

72. Sanders JE, Lam D, Dralle AJ, Okumura R. Interface pressures and shear stresses at thirteen socket sites on two persons with transtibial amputation. *J Rehabil Res Dev.* 1997;34(1):19-43. Accessed 12 February 2016.
73. Goh JCH, Lee PVS, Toh SL, Ooi CK. Development of an integrated CAD-FEA process for below-knee prosthetic sockets. *Clin Biomech.* 2005;20(6):623-629. Accessed 2 February 2014.
74. Lacroix D, Ramírez Patiño JF. Finite element analysis of donning procedure of a prosthetic transfemoral socket. *Ann Biomed Eng.* 2011;39(12):2972-2983. Accessed 23 February 2016.
75. Ramírez JF, Vélez JA. Incidence of the boundary condition between bone and soft tissue in a finite element model of a transfemoral amputee. *Prosthet Orthot Int.* 2012;36(4):405-414. Accessed 23 February 2016.
76. Zhang L, Zhu M, Shen L, Zheng F. Finite element analysis of the contact interface between trans-femoral stump and prosthetic socket. *Proceedings of the Annual International Conference of the IEEE Engineering in Medicine and Biology Society, EMBS.* 2013:1270-1273. Accessed 2 March 2014.
77. Colombo G, Facoetti G, Morotti R, Rizzi C. Physically based modelling and simulation to innovate socket design. *Computer-Aided Design and Applications.* 2011;8(4):617-631. Accessed 9 February 2014.
78. Peng H-, Hsu LH, Huang GF, Hong DY. The analysis and measurement of interface pressures between stump and rapid prototyping prosthetic socket coated with a resin layer for transtibial amputee. *IFMBE Proceedings.* 2009;23:1720-1723. Accessed 22 April 2014.
79. Faustini MC, Neptune RR, Crawford RH. The quasi-static response of compliant prosthetic sockets for transtibial amputees using finite element methods. *Medical Engineering and Physics.* 2006;28(2):114-121. Accessed 23 February 2016.

80. Jia X, Zhang M, Li X, Lee WCC. A quasi-dynamic nonlinear finite element model to investigate prosthetic interface stresses during walking for trans-tibial amputees. *Clin Biomech.* 2005;20(6):630-635. Accessed 13 May 2015.
81. Jia X, Zhang M, Wang R, Jin D. Dynamic investigation of interface stress on below-knee residual limb in a prosthetic socket. *Tsinghua Science and Technology.* 2004;9(6):680-683. Accessed 23 February 2016.
82. Jia X, Zhang M, Lee WCC. Load transfer mechanics between trans-tibial prosthetic socket and residual limb - dynamic effects. *J Biomech.* 2004;37(9):1371-1377. Accessed 2 February 2014.
83. Lee WCC, Zhang M, Jia X, Cheung JTM. Finite element modeling of the contact interface between trans-tibial residual limb and prosthetic socket. *Medical Engineering and Physics.* 2004;26(8):655-662. Accessed 2 February 2014.
84. Portnoy S, Yizhar Z, Shabshin N, et al. Internal mechanical conditions in the soft tissues of a residual limb of a trans-tibial amputee. *J Biomech.* 2008;41(9):1897-1909. Accessed 23 February 2016.
85. Portnoy S, Yarnitzky G, Yizhar Z, et al. Real-time patient-specific finite element analysis of internal stresses in the soft tissues of a residual limb: A new tool for prosthetic fitting. *Ann Biomed Eng.* 2007;35(1):120-135. Accessed 23 February 2016.
86. Sengeh DM, Herr H. A variable-impedance prosthetic socket for a transtibial amputee designed from magnetic resonance imaging data. *Journal of Prosthetics and Orthotics.* 2013;25(3):129-137. Accessed 11 March 2014.
87. Lee WCC, Zhang M. Using computational simulation to aid in the prediction of socket fit: A preliminary study. *Medical Engineering and Physics.* 2007;29(8):923-929. Accessed 23 February 2016.

88. Jia X, Zhang M, Li X, Lee WCC. A quasi-dynamic nonlinear finite element model to investigate prosthetic interface stresses during walking for trans-tibial amputees. *Clin Biomech.* 2005;20(6):630-635. Accessed 23 February 2016.
89. Lenka P, Choudhury A. Analysis of trans tibial prosthetic socket materials using finite element method. *J. Biomedical Science and Engineering.* 2011;4:762.
90. Nehme G, Dib M. Impact of pressure distribution on the relief areas of prosthetic sockets for transtibial amputees using design of experiment and finite element analysis. *Journal of Prosthetics and Orthotics.* 2011;23(4):170-183. Accessed 23 February 2016.
91. Lee WCC, Zhang M, Jia X, Cheung JTM. Finite element modeling of the contact interface between trans-tibial residual limb and prosthetic socket. *Medical Engineering and Physics.* 2004;26(8):655-662. Accessed 23 February 2016.
92. Tönük E, Silver-Thorn MB. Nonlinear viscoelastic material property estimation of lower extremity residual limb tissues. *J Biomech Eng.* 2004;126(2):289-300. Accessed 6 October 2013.
93. Tonuk E, Silver-Thorn MB. Nonlinear viscoelastic material property estimation for lower extremity residual limbs. *Annual International Conference of the IEEE Engineering in Medicine and Biology - Proceedings.* 1999;1:645. Accessed 6 October 2013.
94. Daly W, Voo L, Rosenbaum-Chou T, Arabian A, Boone D. Socket pressure and discomfort in upper-limb prostheses: A preliminary study. *Journal of Prosthetics and Orthotics.* 2014;26(2):99-106. Accessed 22 April 2014.
95. Sensinger JW, Weir RFF. Modeling and preliminary testing socket-residual limb interface stiffness of above-elbow prostheses. *IEEE Transactions on Neural Systems and Rehabilitation Engineering.* 2008;16(2):184-190. Accessed 13 May 2015.

Chapter 6. The application of thin film sensors in characterizing biomechanical interfaces

The majority of this chapter has been published as:

Schofield JS, Evans KR, Hebert JS, and Carey JP. (2016). The Effect of Biomechanical Variables on Force Sensitive Resistor Error: Implications for Calibration and Improved Accuracy. *Journal of Biomechanics*. 49(5): 786-792

6.1 Chapter Preface

Thin film sensors have many practical advantages when employed to empirically describe the force interactions between a medical device and human tissue. This affordable technology can be rapidly applied in many clinical settings as commercially available systems exist; reducing the need for specialized technical expertise. This technology was particularly attractive in our work as it did not require the fabrication of a custom sensor system, and sensors could be placed between the residual limb and prosthetic socket without modification. Employing such a system in a sensory integrated socket would allow for the mechanical evaluation of design decisions at the socket-limb interface. However, numerous works highlight limitations of this technology in sensing contact forces between substrates¹⁻³. Unavoidable conditions innate to many biological environments, such as increased temperatures, and curved or highly deformable surfaces, may impede sensor performance¹, yet few works suggest methods to mitigate the error induced by these factors. In this chapter we consolidate and characterize the impact of environmental-biomechanical factors with the intent of suggesting standard practices to address the deleterious effects. This work is presented in the broader context of ‘biomechanical environments,’ and was performed in preparation of employing this sensing technology to empirically characterize UL prosthetic socket-residual limb interface mechanics in Chapter 7.

6.2 Introduction

Quantifying biomechanical forces between medical devices and human soft tissue has important implications for comfort, reducing tissue injury and improving device design³⁻⁵. Typical measurement of these interactions requires a sensor positioned at the interface between the tissue

and medical device. Many biomechanical sensors are described in literature including those based on capacitance, fluid pressure, or optics⁴, with one of the more prevalent sensors being Force Sensitive Resistors (FSRs). FSRs are constructed of thin polymer films and change resistance with the application of pressure. With sensor thicknesses as little as 0.2 mm⁴, FSRs can be positioned between two contacting surfaces with little mechanical impact on the substrates. FSRs require minimal signal conditioning, and are easily integrated with hobbyist micro-controllers through advanced data acquisition systems. FSRs are inexpensive compared to similar technologies^{3,4}, making them an attractive option for research and clinical applications.

FSRs have been employed in numerous biomechanical applications from prosthetic control and pressure measurements⁶⁻⁸ through gait studies^{9,10} and telerobotics¹¹ among many other biomechanical applications quantifying interface mechanics^{12,13}.

However, FSRs have limitations; sensor drift and hysteresis have been shown to impact repeatability and accuracy in existing systems^{4,14}. Additionally, changes in accuracy and increases in drift error when curvature is applied to the sensors have been shown in prosthetic applications¹⁵, but can be minimized by calibration in the same curved configuration¹⁶.

FSR manufacturers often recommend calibration and operating conditions to include flat, rigid surfaces at room temperature^{17,18}. Yet the human body hosts unavoidable curvatures, soft tissue compliances, and temperature differentials. The error imparted by these variables has yet to be comprehensively investigated, preventing researchers and clinicians from understanding the implications of their biological testing environment on sensor accuracy.

This work investigates the effects of common biomechanical variables on FSR error with the intent of examining calibration practices and providing recommendations to improve accuracy in a clinical-research environment.

6.3 Methods

6.3.1 Experimental Variables

A full factorial design-of-experiments approach was used¹⁹. Twelve unique combinations of temperature, curvature and compliance were introduced to each FSR in a semi-randomized order

(Table 6-1). Temperature was evaluated at room (21°C) and body (37°C) temperature; curvature at the diameter of a 95th percentile male thigh (215 mm), diameter of a 5th percentile female wrist (44 mm)²⁰ and a flat surface; and material compliance of a human soft tissue analog (SynDaver Labs, Tampa, USA) and a rigid surface.

Table 6-1 Combinations of Biomechanical Variables Tested

Combination	Temperature (°C)	Curvature (Diameter mm)	Compliance
1	21°C	215 mm	Rigid
2	21°C	44 mm	Rigid
3	21°C	Flat	Rigid
4	21°C	215 mm	Soft
5	21°C	44 mm	Soft
6	21°C	Flat	Soft
7	37°C	215 mm	Rigid
8	37°C	44 mm	Rigid
9	37°C	Flat	Rigid
10	37°C	215 mm	Soft
11	37°C	44 mm	Soft
12	37°C	Flat	Soft

6.3.2 Setup and Procedure

Interlink FSRs were selected for testing due to their widespread usage^{6,11,21-24}. Two small round (5 mm diameter), two medium round (13 mm diameter) and two 38 mm square (Models 400, 402 and 406, respectively, Interlink Electronics, Camarillo, USA) FSRs were tested. Once calibrated, manufacturer specifications state force accuracy in a range of $\pm 6\%$ to $\pm 50\%$ (Interlink Electronics, 2015). FSRs were wired to a data acquisition system (PCI 6259, National Instruments, Austin, TX, USA) connected to a 10 k Ω resistor in a voltage divider configuration (Interlink Electronics, 2015). FSRs were placed in-line with a load cell calibrated to an accuracy of ± 0.02 N (LCM703, Omegadyne, Sunbury, USA) affixed to a micromanipulator (MM-3, Narishige Group, Tokyo JA) (Figure 6.1). Custom PLA-thermoplastic pushing heads were 3D printed to match the sensing surface dimensions of each FSR and introduce curvature as required

(Figure 6.1). During testing, FSRs were pressed between the pushing head and the test surface. The testing assembly was located inside an incubator (Air-Shields C100, Soma Technology Inc., Bloomfield USA) allowing for precise temperature control.

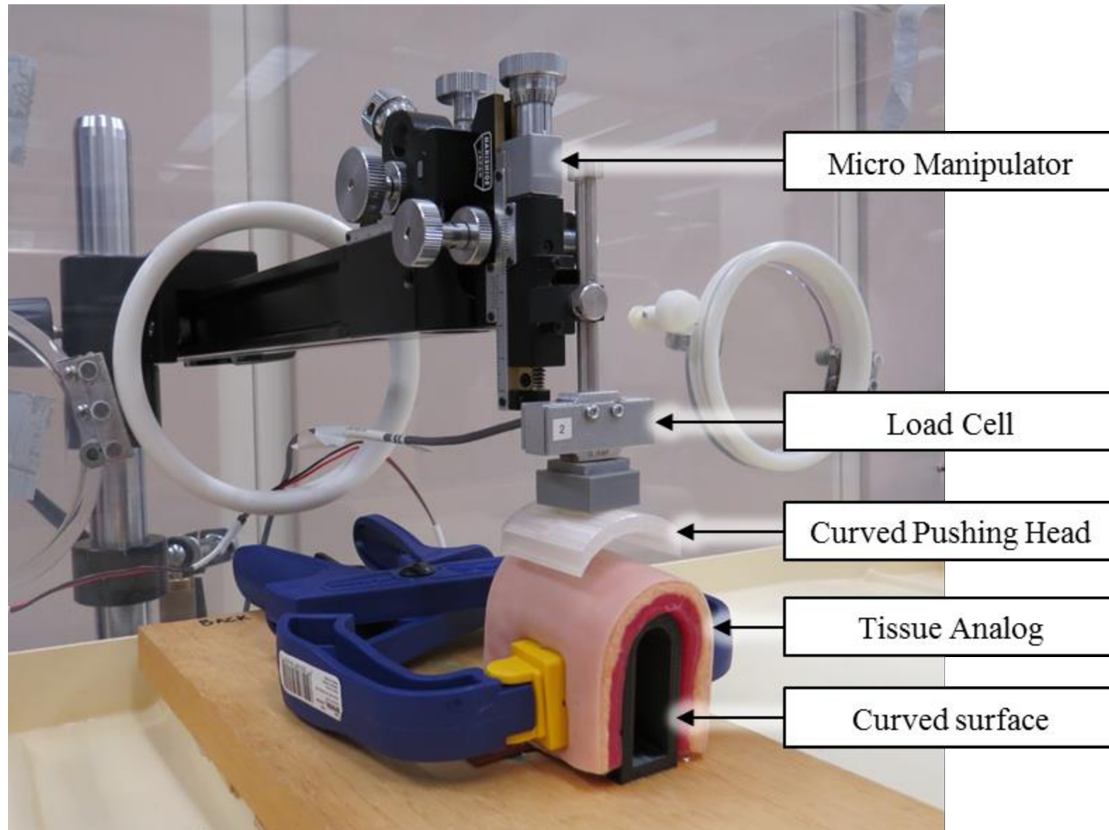


Figure 6.1 Experimental Setup. Experimental setup for testing of the 12 combinations of variables. Setup shown in the body temperature, 44 mm diameter, and soft compliance configuration.

Although the FSRs selected have a working range between 0 to 20 N of force¹⁷, a testing range of 0 to 10 N was used²⁵. The upper bound was limited to 10 N, as further force can cause discomfort if applied to human soft tissue over a small surface area^{26,27}. Data collection was conducted according to ANSI/ISA 51.1 Standards²⁸. Accordingly, FSRs were preconditioned and data logging was initiated mid-way through the force range. The FSRs were loaded to the maximum and minimum values three times at a consistent loading rate¹⁷ of 30 seconds/cycle. This loading rate was chosen to reflect a low frequency or static application and to avoid any

time dependent dynamic effects^{3,17}. FSR voltage and load cell forces were sampled at 100 Hz, low-pass filtered at 20 Hz and 10 Hz, respectively, and logged at 10 Hz.

For each FSR, calibration equations mapping FSR voltage to applied load (load cell reading) were determined through fitting an inverse logarithmic equation (6.1) as recommended¹⁷.

$$F = ae^{bV} + c \quad (6.1)$$

Where F represent the force predicted from the calibration equation, V measured voltage from the FSR and a , b , and c are constants to be solved for each sensor and combination of variables.

Twelve equations per FSR were determined corresponding to the twelve combinations of temperature, curvature and compliance introduced. The fitted-root-mean-squared-error (RMSE-F), mean absolute error (MAE), and maximum error were calculated and recorded for each combination ([Appendix A](#)).

Data for each combination of biomechanical conditions was evaluated under three calibration strategies: **self**-fit calibration, each sensor calibrated 12 times, once for each combination of variables; **baseline**-fit, often recommended by manufacturers¹⁸, each sensor is calibrated once under optimal conditions (flat, rigid, and room temperature); and **cross**-fit, one baseline calibration equation applied to all sensors of the same model. Mean differences in RMSE-F, MAE, and maximum error, corresponding to calibration fit strategy, were determined and statistically compared using paired t-tests, with $p < 0.05$ indicating significance.

The Baseline calibration equation for each sensor was defined as the flat, rigid, room temperature condition. At each of the remaining 11 combinations, calibration equations were compared to the baseline using root means squared error (RMSE-C). This procedure was performed for each sensor independently, yielding twelve RMSE-C values for each of the six sensors. A graphical example is illustrated in Figure 6.2.

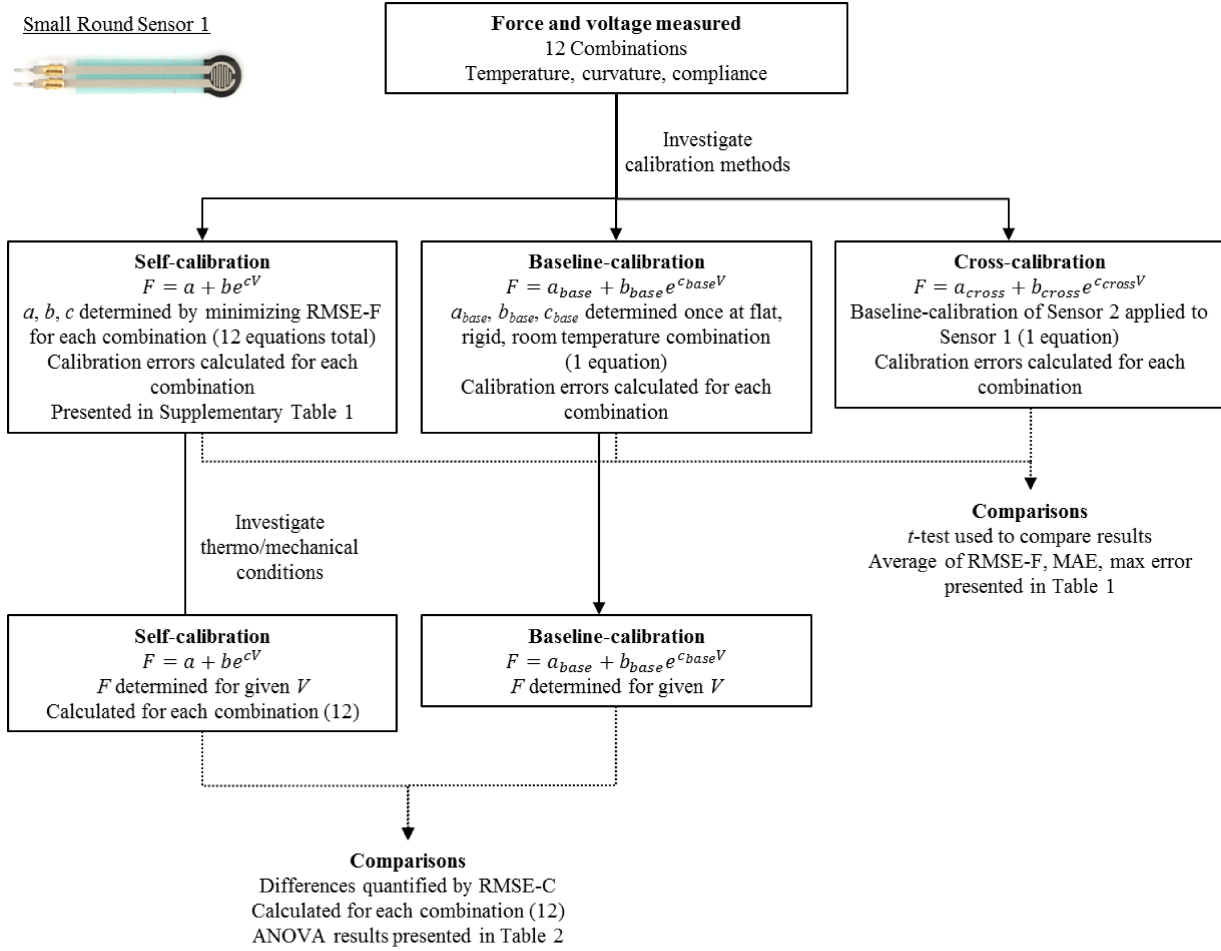


Figure 6.2 Example of the data treatment process for small round sensor 1

Three analyses of variance (ANOVAs) were performed, one for each sensor model. Since two sensors of each model were used, these data were treated as replicate measures in the statistical analysis. Temperature, curvature and compliance were held as input variables with RMSE-C evaluated as the output measure, and blocking performed by sensor number. Initially, all main effects, 2-way and 3-way interactions were evaluated with $p < 0.05$ indicating significance. Non-significant variables were then removed from the model. Significant main effects, significant 2-way interactions, and the main effects corresponding to any significant interactions were reported.

6.3.3 Participant Testing

Two healthy participants were recruited. Ethics approval was obtained through our institute's review board and participants gave written informed consent.

Participant testing closely paralleled the variable testing procedure described previously and was intended to simulate the implications of FSR usage in a biomechanical system. Participants' arms were secured using an adjustable arm rest. Each FSR was adhered directly to the participants' skin and given minimally 15 minutes to reach a stable temperature (approximately 32.5 – 34°C). Using the previously described preconditioning and loading procedures, the micromanipulator, load cell, and FSR pushing heads were then pressed tangentially onto each participant's forearm directly over the sensor (Figure 6.3). FSR and load cell data were captured over a 0 to 10 N range for each FSR (small round FSRs limited to 0 – 8 N to reduce discomfort).

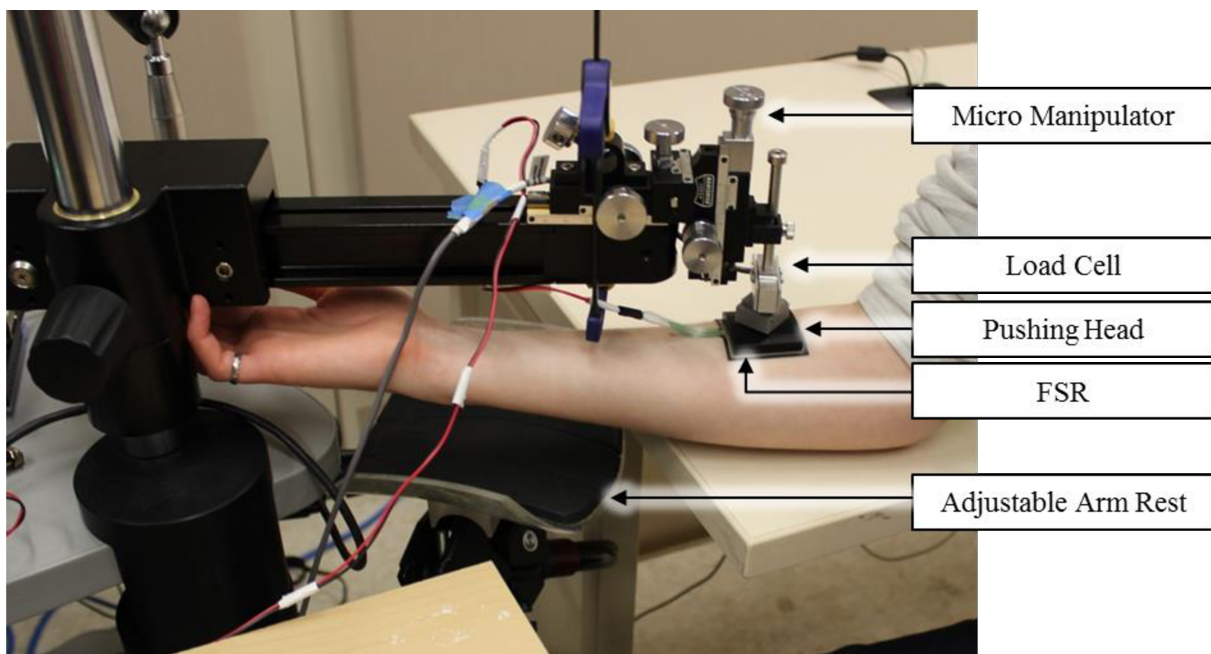


Figure 6.3 Experimental Setup for Participant Trials

From this data, calibration equations were derived for each FSR using the same inverse logarithmic equation described previously. Comparing participant data against each sensor's previously derived baseline equation; differences in mean RSME-C, MAE and Maximum error were evaluated using a paired t-test, with $p < 0.05$ indicating significance. Additionally, for each

FSR, the participant calibration equations were plotted against their previously-derived baseline equations.

6.4 Results

6.4.1 Variable Testing

Baseline calibration curves for each of the six sensors are shown in Figure 6.4 and graphically highlight differences across sensors of the same model.

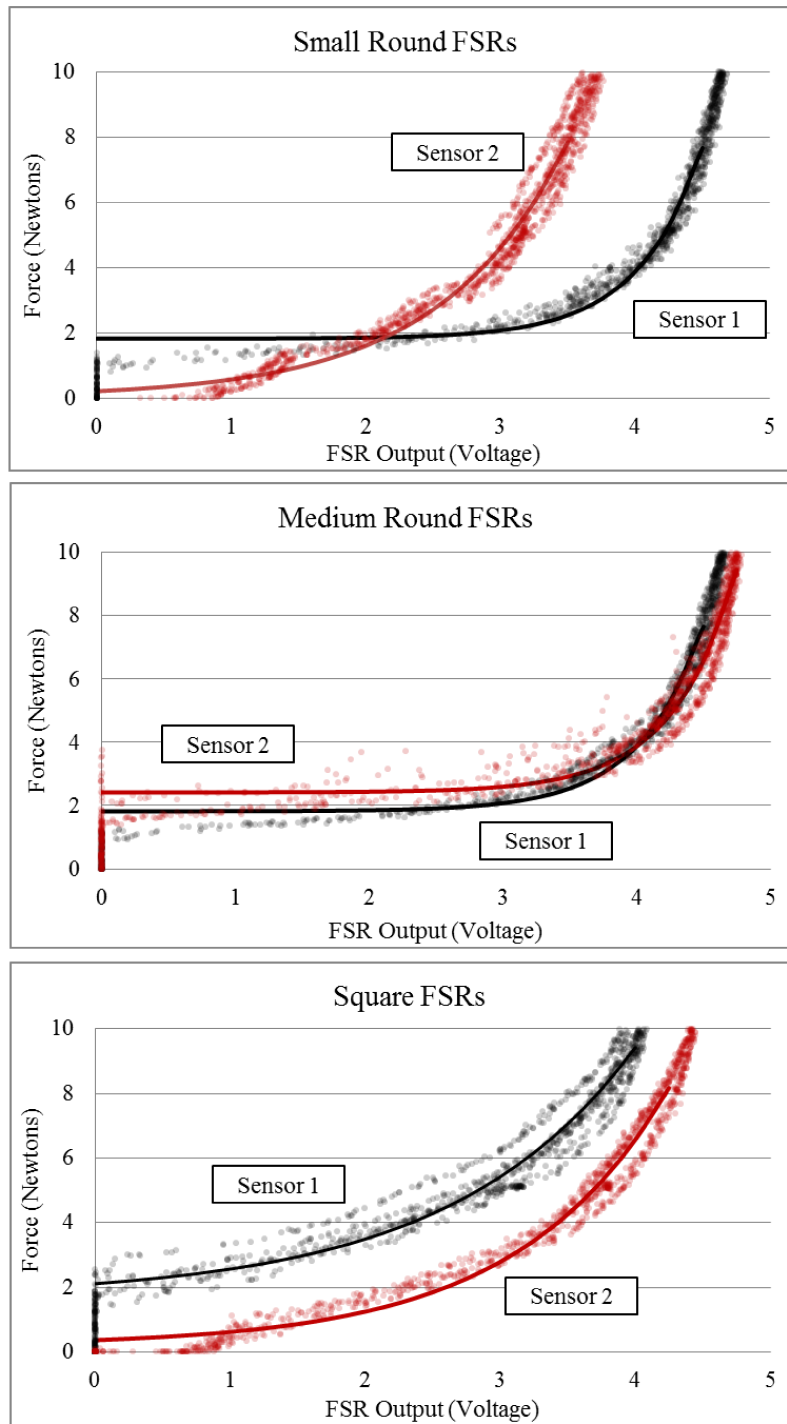


Figure 6.4 Baseline Calibration Curves. Calibration curves for each of the 6 sensors' force-voltage response in the room temperature, flat, rigid configuration (baseline). Calibration curves are transposed over the raw force-voltage data.

Mean RMSE-F, MAE and maximum error values categorized by sensor model are shown in Table 6-2. Over the tested 0 – 10 N range, all three error measures in all three sensor models were significantly lower when the *self*-fit calibration strategy was employed relative to the *baseline* and *cross*-fitting strategies.

Table 6-2 Mean error based on calibration curve used to fit data* Indicates significantly different from self-calibration ($p < 0.05$), Where RMSE-F denotes the root mean squared error for the calibration curve fit to experimental data, MAE and Max denote the mean absolute error and maximum error in force units of Newtons (N)

	Small			Medium			Square		
	Self	Baseline*	Cross*	Self	Baseline*	Cross*	Self	Baseline*	Cross*
RMSE-F	0.8±0.4	3.0±1.4	3.6±2.3	0.4±0.1	2.2±0.9	2.2±0.8	0.6±0.3	2.5±1.7	2.9±1.6
MAE (N)	0.6±0.3	2.5±1.2	3.0±2.1	0.3±0.1	1.9±0.7	1.8±0.7	0.5±0.3	2.2±1.6	2.6±1.6
Max (N)	2.3±1.2	6.1±2.5	6.7±3.1	1.3±0.3	4.5±1.3	4.4±1.7	1.6±0.8	4.2±2.2	4.8±2.2

Calibration equations were investigated to determine mechanical conditions responsible for differences from the baseline calibration equations (RMSE-C). The results of the ANOVA analyses (Table 6-3) and the means plots highlighting the effects of individual experimental variables with all others held constant are shown in Figure 6.5.

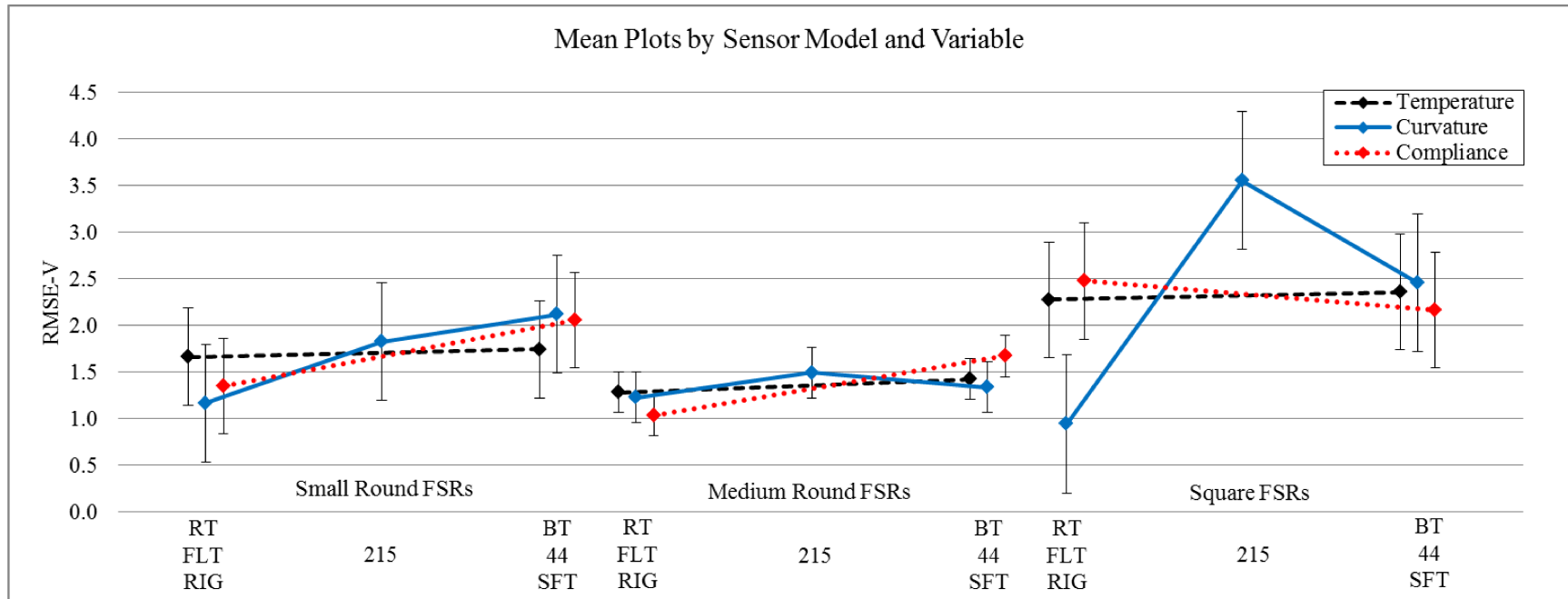


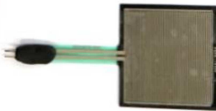


Figure 6.5 RMSE-C Mean Plots for each Experimental Variable according to Sensor Model. Plots highlight the effects of individual experimental variables with all others held constant. Where RMSE-V denotes the root mean squared error relative to the baseline equations. RT and BT signify room temperature and body temperature, respectively. 44, 215 and flat represent sensor curvature in millimeters and SFT and RIG denote soft tissue and rigid compliance, respectively. Error bars represent the ± 95 th confidence interval.

For the small round FSRs, ANOVA results suggested the presence of a significant linear effect of interactions between temperature and curvature as well as curvature and compliance. Blocking by sensor demonstrated a significant effect, with statistical differences in calibration equations across sensors of the same model. Medium round FSRs displayed a significant effect from tissue compliance, as well as an interaction effect between curvature and compliance. As curvature was tested at three values, both linear and quadratic main effects were evaluated. For the square FSRs, curvature was found to have both a linear and quadratic effect. Quadratic interaction effects were found between curvature and compliance.

Table 6-3 ANOVA Table and Effects Estimates for RMSE-C. *Indicates statistical significance ($p < 0.05$). Abbreviations Temp, Curve, and Comp denote temperature, curvature and compliance, respectively. As curvature was tested at 3 levels, Curve(Q) signifies quadratic (non-linear) effects, whereas the absence of (Q) signifies linear effects. Hyphenated variables (ex. Temp-Curve) denote two way interaction effects.

		RMSE-C				
	Variables	Effect Estimate	-95%	95%	p-value	
	Small FSR	Mean	1.92	1.62	2.22	-
		Sensor (blocked)	-0.84	-1.43	-0.24	<0.01*
		Temp	0.46	-0.14	1.05	0.12
		Curve	-0.40	-1.13	0.34	0.27
		Comp	-0.30	-0.90	0.30	0.31
		Temp-Comp	0.74	0.14	1.33	0.02*
		Curve-Comp	-1.03	-1.76	-0.30	<0.01*
R ² = 0.45						
	Medium FSR	Mean	1.38	1.22	1.54	-
		Sensor (blocked)	-0.28	-0.60	0.03	0.07
		Curve	-0.17	-0.56	0.22	0.38
		Comp	-0.68	-1.00	-0.37	<0.01*
		Curve-Comp	-0.75	-1.14	-0.36	<0.01*
R ² = 0.33						
	Square FSR	Mean	2.27	1.81	2.74	-
		Sensor (blocked)	0.44	-0.49	1.37	0.33
		Curve	-1.52	-2.66	-0.38	0.01*
		Curve(Q)	1.69	0.70	2.68	<0.01*
		Comp	0.43	-0.50	1.36	0.34
		Curve(Q)-Comp	1.57	0.58	2.56	<0.01*
R ² = 0.76						

6.4.2 Participant Testing

Participant data is plotted in Figure 6.6, highlighting differences in each FSRs force-voltage response at baseline conditions and on soft tissue. There were notable differences across sensors of the same model and between participants.

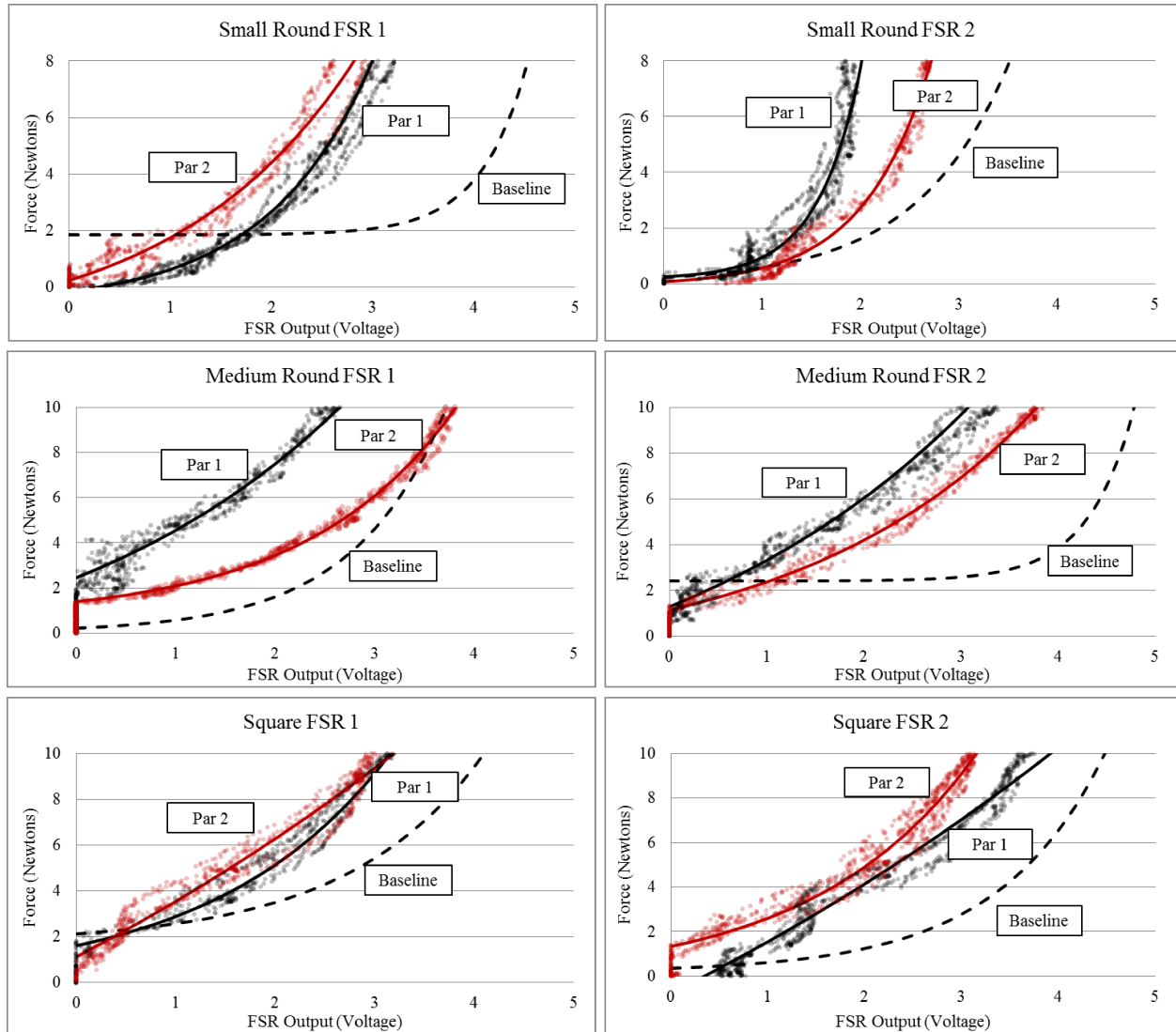


Figure 6.6 Participant Testing Data for Individual FSR Sensors. Calibration curves plotted for each sensor and participant against the previously determined baseline calibration curve (under room temperature, flat, rigid conditions), where Par 1 and Par 2 abbreviates participant 1 and participant 2, respectively. Participant calibration curves are transposed over the raw force-voltage data.

6.5 Discussion

FSRs are attractive sensors for biomechanical applications due to their versatility, small profile and low cost. Yet FSRs have limitations such as sensor drift and hysteresis^{4,14-16}. To achieve optimal performance it is recommended that these sensors be used on flat, rigid surfaces at approximately room temperature^{17,18}. Yet in many biomechanical environments temperature differentials, curvatures and compliant tissues are unavoidable. Therefore, investigation of the effect of these variables is necessary to understand how calibration and implementation of FSRs may impact sensor accuracy.

The data supports the use of a self-fit calibration scheme to reduce calibration error and yield more accurate readings. The raw force and voltage data, and calibration curves demonstrated varying force-voltage responses from sensors of the same model even under optimal operating conditions (room temperature, flat, rigid). These curves (Figure 6.4) paired with the significantly higher cross-fit error data (Table 6-2) suggest that in a system using multiple FSRs of the same model, independent calibration equations for each sensor are necessary to minimize calibration error and improve the accuracy of the sensor readings.

The individual impact of manipulating temperature, curvature and compliance on calibration equations (in terms of RMSE-C) were investigated. No single variable impacted calibration equations for all three sensor models. Rather, each sensor model illustrated a unique combination of significant main effects and interaction effects that influenced RMSE-C values (Table 6-3). These main effects and interactions, if not held constant at the baseline values, will significantly impact the individual sensor's calibration equation and force accuracy. Additionally, given that the self-fit calibration strategy yields significantly lower mean error values, error induced from biomechanical conditions of a sensor's environment should be minimized by calibrating the FSR in an environment as close to its intended use as possible.

Participant testing highlighted that two participants tested in the same location of the body yielded different calibration curves and that these calibration curves strayed from the baseline curves for each sensor. Additionally, Figure 6.6 highlights changes in the dead band of each FSR (the small force application required to initially register a voltage change). By introducing the varying curvatures of a human forearm, the sensor is forced into physical configurations known

to impact FSR performance such as mechanical deformation and shearing effects². These mechanical conditions can lower the dead band or induce an artificial preload into the sensor. In all, the biomechanical environment of a human forearm introduces inherent changes in temperature, curvature and tissue compliance relative to baseline conditions; these changes are clearly reflected in the calibration curves. These findings further illustrate the need to calibrate FSR sensors as close to their intended use as possible. In doing so, the resulting self-fit calibration equation will be specific to the participant and the individual set of mechanical variables they introduce to the sensing environment.

The results of this study highlight inherent advantages and disadvantages for each of the three calibration techniques evaluated: The self-fit strategy is a rigorous and more time consuming approach that significantly minimizes calibration error; The baseline-fit strategy is a time saving approach at the cost of increased error; The cross-fit strategy is the least time consuming approach yielding the highest calibration error.

Taken together, temperature, curvature and tissue compliance all have the potential to impact FSR calibration curves. The FSR models are sensitive to these three factors at varying levels, supporting two key recommendations:

- 1) Each FSR in a system should be calibrated independently. This may help reduce calibration error as multiple sensors of the same model demonstrated notable differences in force-voltage response.
- 2) FSRs must be calibrated in the environment of their intended use or as close as possible. This will ensure the corresponding calibration curve will account for the physical and mechanical variables affecting its force-voltage response. If the application of the FSR prohibits such a calibration strategy, the researcher or clinician must be aware of the implications on sensor accuracy.

6.6 Conclusions

The intent of this study was to identify biomechanical variables impacting FSR calibration and evaluate strategies to minimize calibration error. Expanding on this work and increasing the number of FSRs tested, would lend further confidence to the results discussed and provide the

ability to develop a statistical model for the prediction of FSR error based on the biomechanical environment. Additional limitations of this work may lie in the choice of loading rate (30sec/cycle). FSRs are sensitive to dynamic load rates. Further multivariate testing including load rate effects may be warranted. Finally, this work calibrates FSRs to a known force, as recommended by the manufacturer¹⁷ and standard practice in literature^{3,16}. Yet each sensor model has different sensing surface geometries. Calibration practices mapping FSR voltage to applied pressure may be more appropriate in future work as this would account for sensing surface geometry.

FSRs have been employed in numerous studies and biomechanical environments as these thin-profile, flexible, and affordable sensors are easily implement in clinical-research applications. This chapter contributes standard practices to help mitigate calibration error and accommodate biomechanical factors present in many sensing environments. The development of novel prostheses and prosthetic sockets require the evaluation of socket-limb interactions to appreciate the implications of design decisions on load bearing anatomy, socket fit, and comfort. Thin film sensors (such as FSRs) are ideal for this application as they can be positioned between the limb and socket with minimal impact on the substrate. Chapter 7 adapts the suggested calibration practices recommend in this chapter to establish a technique employing thin film sensors to evaluate prosthetic socket-limb interactions in preparation for the design/evaluation of a sensory integrated prosthesis in chapter 8.

6.7 References

1. Schofield JS, Evans KR, Hebert JS, Marasco PD, Carey JP. The effect of biomechanical variables on force sensitive resistor error: Implications for calibration and improved accuracy. *J Biomech.* 2016;49(5):786. doi: <http://dx.doi.org/10.1016/j.jbiomech.2016.01.022>.
2. Hall RS, Desmoulin GT, Milner TE. A technique for conditioning and calibrating force-sensing resistors for repeatable and reliable measurement of compressive force. *J Biomech.* 2008;41(16):3492-3495. Accessed 11 December 2015. doi: 10.1016/j.jbiomech.2008.09.031.

3. Lebosse C, Renaud P, Bayle B, De Mathelin M. Modeling and evaluation of low-cost force sensors. *IEEE Transactions on Robotics*. 2011;27(4):815-822. Accessed 22 April 2015.
4. Dabling JG, Filatov A, Wheeler JW. Static and cyclic performance evaluation of sensors for human interface pressure measurement. *Proceedings of the Annual International Conference of the IEEE Engineering in Medicine and Biology Society, EMBS*. 2012:162-165. Accessed 22 April 2015.
5. Mak AFT, Zhang M, Tam EWC, eds. *Biomechanics of pressure ulcer in body tissues interacting with external forces during locomotion*. ; 2010Annual Review of Biomedical Engineering; No. 12.
6. Hebert JS, Olson JL, Morhart MJ, et al. Novel targeted sensory reinnervation technique to restore functional hand sensation after transhumeral amputation. *IEEE Transactions on Neural Systems and Rehabilitation Engineering*. 2014;22(4):765.
7. Junaid AB, Tahir S, Rasheed T, et al. Low-cost design and fabrication of an anthropomorphic robotic hand. *Journal of Nanoscience and Nanotechnology*. 2014;14(10):7427-7431. Accessed 22 April 2015.
8. Silver-Thorn MB, Steege JW, Childress DS. A review of prosthetic interface stress investigations. *Journal of Rehabilitation Research and Development*. 1996;33(3):253-266. Accessed 9 February 2014.
9. Moon S-, Lee C-, Lee S-. A study of knee brace locking timing and walking pattern detected from an FSR and knee joint angle. *International Conference on Control, Automation and Systems*. 2011:1783-1787. Accessed 22 April 2015.
10. Rueterbories J, Spaich EG, Larsen B, Andersen OK. Methods for gait event detection and analysis in ambulatory systems. *Medical Engineering and Physics*. 2010;32(6):545-552. Accessed 22 April 2015.

11. Yun MH, Cannon D, Freivalds A, Thomas G. An instrumented glove for grasp specification in virtual-reality-based point-and-direct telerobotics. *IEEE Transactions on Systems, Man, and Cybernetics, Part B: Cybernetics*. 1997;27(5):835-846. Accessed 22 April 2015.
12. Cascioli V, Liu Z, Heusch AI, McCarthy PW. Settling down time following initial sitting and its relationship with comfort and discomfort. *J Tissue Viability*. 2011;20(4):121-129. Accessed 22 April 2015.
13. Di Fazio D, Lombardo L, Gracco A, D'Amico P, Siciliani G. Lip pressure at rest and during function in 2 groups of patients with different occlusions. *American Journal of Orthodontics and Dentofacial Orthopedics*. 2011;139(1):e1-e6. Accessed 22 April 2015.
14. Herbert-Copley AG, Sinitski EH, Lemaire ED, Baddour N. Temperature and measurement changes over time for F-scan sensors. *MeMeA 2013 - IEEE International Symposium on Medical Measurements and Applications, Proceedings*. 2013:265-267. Accessed 22 April 2015.
15. Polliack AA, Sieh RC, Craig DD, Landsberger S, McNeil DR, Ayyappa E. Scientific validation of two commercial pressure sensor systems for prosthetic socket fit. *Prosthet Orthot Int*. 2000;24(1):63-73. Accessed 22 April 2015.
16. Buis AWP, Convery P. Calibration problems encountered while monitoring stump/socket interface pressures with force sensing resistors: Techniques adopted to minimise inaccuracies. *Prosthet Orthot Int*. 1997;21(3):179-182. Accessed 22 April 2015.
17. Interlink Electronics. FSR integration guide. . 2015.
18. TekScan. Pressure mapping, force measurement & tactile sensors. <https://www.tekscan.com/pressure-mapping-sensors>. Updated 2015. Accessed Apr. 22, 2015, 2015.
19. Montgomery D.C. Factorials with mixed levels. In: *Design and analysis of experiments*. 8th ed. Wiley; 2012:412.

20. NASA. Volume I section 3: Anthropometry and biomechanics.
<http://msis.jsc.nasa.gov/sections/section03.htm>. Updated 2008. Accessed 04/22, 2015.
21. Jang E-, Cho Y-, Chi S-, Lee J-, Kang SS, Chun B-. Recognition of walking intention using multiple bio/kinesthetic sensors for lower limb exoskeletons. *ICCAS 2010 - International Conference on Control, Automation and Systems*. 2010:1802-1805. Accessed 22 April 2015.
22. More M, Lka O, eds. *Design of active feedback for rehabilitation robot*. ; 2014Applied Mechanics and Materials; No. 611.
23. Rogers B, Zhang W, Narayana S, Lancaster JL, Robin DA, Fox PT. Force sensing system for automated assessment of motor performance during fMRI. *J Neurosci Methods*. 2010;190(1):92-94. Accessed 22 April 2015.
24. Wang X, Zhao J, Yang D, Li N, Sun C, Liu H. Biomechatronic approach to a multi-fingered hand prosthesis. *2010 3rd IEEE RAS and EMBS International Conference on Biomedical Robotics and Biomechatronics, BioRob 2010*. 2010:209-214. Accessed 22 April 2015.
25. Hollinger A, Wanderley MM. Evaluation of commercial force-sensing resistors. . 2006.
26. Armiger RS, Tenore FV, Katyal KD, et al. Enabling closed-loop control of the modular prosthetic limb through haptic feedback. *Johns Hopkins APL Technical Digest (Applied Physics Laboratory)*. 2013;31(4):345-353. Accessed 29 April 2013.
27. Antfolk C, Balkenius C, Lundborg G, Rosén B, Sebelius F. A tactile display system for hand prostheses to discriminate pressure and individual finger localization. *Journal of Medical and Biological Engineering*. 2010;30(6):355-360. Accessed 5 April 2013.
28. ANSI. ANSI/ISA–51.1–1979 (R1993) process instrumentation terminology. . 1995.

Chapter 7. The characterization of socket-residual limb interface mechanics

The majority of this section has been published as:

Schofield JS, Schoepp KR, Williams HE, Carey JP, Marasco PD, Hebert JS. (2017). Characterization of interfacial socket pressure in transhumeral prostheses: a case series. PLOS one. <https://doi.org/10.1371/journal.pone.0178517>

7.1 Chapter preface

In Chapter 6 we developed an understanding of how common biomechanical factors may impact thin film sensor performance, and recommended practices to mitigate calibration induced measurement errors. Although Chapter 6 was provided in the broader context of biomechanical applications, the motivation was to translate the information and techniques to the measurement of prosthetic socket-residual limb (RL) contact pressures. In this chapter, we adapt these techniques to the use of a commercially available Tekscan measurement system. First, a baseline understanding of how the RL and prosthetic socket interact in traditional well-fit prostheses is provided. A case series is then presented in which the socket-RL contact pressures are quantified and mapped to anatomical locations on the users' residual limb. These results are discussed in the context of specific design choices made during socket fabrication. The techniques discussed in the chapter

With the motivation of integrating a kinesthetic sensory feedback system in a functional prosthesis, from data presented in this chapter, we can compare and contrast the mechanical implications of a sensory integrated prosthetic system relative to traditional sockets in later chapters.

7.2 Introduction

One of the most crucial factors for the successful use of an upper limb (UL) prosthesis is the design of the prosthetic socket¹. The socket encompasses the user's RL and functions as the point of attachment securing the prosthetic components to the user. It is at this crucial junction where the soft tissue of the user's RL must interface with the rigid materials of the prosthesis. Consequently, a prosthetic socket must be custom-designed to accommodate the individual's

morphology, achieve suspension of the prosthesis, and aid in control by securely and efficiently transmitting intended movements. This not only promotes the user's ability to move and manipulate the prosthesis, but in a system that is otherwise absent of direct sensory feedback, may help promote indirect feedback such as position of the prosthetic device. The term 'socket fit' broadly describes the quantitative and qualitative factors impacting prosthetic comfort, suspension and stability on the RL. Both fit and the corresponding comfort have substantial implications on user satisfaction; how long (or if) the user will tolerate wearing the prosthesis; and, ultimately, the success of an UL prosthetic prescription²⁻⁵. Clinically, the implications of fit are well acknowledged and much of a prosthetist's effort is specifically dedicated to the design and fabrication of the socket⁶.

The primary challenge in socket design and fabrication is achieving socket geometry that appropriately distributes pressure across the RL. The socket must couple the prosthesis to the user's underlying bony structure through deliberate compression and relief in appropriate areas of the surrounding soft tissues. As a physical consequence, some skeletal motion will inherently be lost due to the deformable nature of residual tissues and not fully translated to movement of the prosthesis⁷. This decreases the stability of the system and may result in a reduced range of motion and inappropriate loading of the residual anatomy⁷. Therefore, a technical design challenge exists: mechanical stability will increase with tissue compression and relief at physiologically and mechanically appropriate locations on the residual limb. The resulting contact pressures magnitudes and locations must therefore be strategically considered during socket fabrication to reduce the risk of discomfort, tissue irritation, and damage. This challenge becomes more relevant for those with more proximal amputations, as additional prosthetic components (elbows and shoulders) are required. This increases the weight and reduces the user's control over the device; ultimately amplifying the demand placed on the socket and the user's RL.

Adding to these challenges, Lake et al., describe a paradox which they refer to as "the upper extremity dilemma"⁸. The prevalence of lower limb amputations far outweighs that of UL⁹. As the field of UL prosthetics becomes increasingly technical and specialized, it becomes

challenging for many prosthetists to expand their UL knowledge as significantly fewer UL clients are seen¹⁰. This results in a group of affected individuals requiring highly specialized expertise from clinicians who have often limited practice in addressing their needs. This is further magnified for more proximal levels of UL amputation, such as transhumeral, as the demand on the prosthetic socket increases and prevalence further decreases⁹. When compared to those with more distal amputations, prosthetic users with transhumeral or shoulder level amputations are more likely to be dissatisfied and reject their prostheses³. Underlying reasons may include dissatisfaction with prosthetic functionality or appearance, however a chief contributor lays in prosthetic comfort^{5,11} specifically at the socket interface⁵.

In practice, socket fabrication relies heavily on experienced-based, heuristic techniques. Although literature does report novel socket designs for improved suspension and function^{7,8} very little analytical documentation and quantitative descriptions of UL socket-RL interactions have been published. This limits the understanding of the implications of socket design decisions. Daly et al. performed work with a group of participants with upper limb amputation (3 transradial, 3 transhumeral and 3 shoulder disarticulation participants)¹². They used a Tekscan sensor system for the measurement of contact pressure between the RL and prosthesis to investigate the relationship between maximum pressures and discomfort. They found a combination of weak and strong correlations and concluded that this relationship is variable and patient specific. However this study reported maximum pressures exclusively and did not report the anatomical locations at which these pressures occurred, limiting the translation of this work to aid informed socket design decisions.

In lower limb prostheses, measurements and mapping pressures to participants' anatomy are commonly performed using commercially available systems such as the Tekscan F-Socket or VersaTek^{13,14}. The accuracy and repeatability of such systems have been well documented¹⁵⁻¹⁷ and it has been suggested they are adequate in indicating areas of high pressure at the socket-RL interface¹⁶. Pressure measurement and mapping of lower-limb prosthetic sockets has improved the understanding of prosthetic fit at a very fundamental level and has helped facilitated objectively based socket designs¹⁸⁻²¹. Yet these techniques do not translate directly to the UL.

There is much complexity in the diverse set of movements performed with UL prostheses relative to the cyclical, high pressure loading patterns experienced in the lower limb. Therefore, applying pressure measurement and mapping to UL sockets holds the potential to characterize these unique physical differences and develop foundational knowledge to aid in socket design and fabrication processes.

This work describes empirical techniques enabling the analytical characterization of socket-RL interface pressures. We adapt lower-limb socket measurement methods to describe pressure distributions across the RL in terms of distribution patterns, load bearing anatomy, and relative magnitude of interfacial pressures. These techniques were employed to test four transhumeral participant wearing well-fit prosthetic sockets.

7.3 Methods

Four participants with transhumeral amputation were recruited. Participant demographics and RL geometries are reported in Figure 7.1. All participants wore a body-powered prosthesis with voluntary opening terminal device and prosthetic liner. A description of each participant's prosthetic components is included in Table 7-1. Ethics approval was obtained through the University of Alberta's institutional review board and participants provided informed consent prior to participation.

Gender	Height (m)	Weight (Kg)	Side of Amputation	Residual Limb Dimensions			
				Length (cm)		Circumference (cm)	
				a	b	(c) ₁	(c) ₂
Par 1 Male	1.75	103	Left	29.0	25.0	42.0	38.0
Par 2 Female	1.73	104	Right	27.0	23.0	40.5	35.5
Par 3 Female	1.70	52	Left	16.0	15.5	24.0	22.0
Par 4 Male	1.83	95	Left	28.0	26.0	33.0	29.0

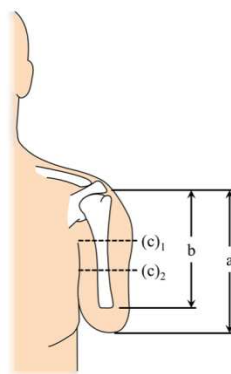


Figure 7.1 Participant demographics and residual limb characteristics. Par denotes the participant number, (c)1 and (c)2 denote circumference measurements taken at the axilla and mid-length of the limb, respectively, a denotes the residual limb length taken from the acromion to distal tip of the limb, and b represents the limb length from the acromion to the distal residual humeral tip.

Table 7-1 Descriptions of participants' prosthetic components

	Terminal Device	Elbow	Liner	Harness
Participant 1	Hosmer 555 Lyre Hook	Ottbock ErgoArm	WillowWood Alpha Medium	Figure-eight (bilaterally connected control cable)
Participant 2	Ottobock 8K23 Hand	Ottbock ErgoArm	WillowWood Alpha Medium	Figure-eight
Participant 3	Hosmer 555 Lyre Hook	Ottbock ErgoArm	Ossur Iceross Upper-X	Figure-eight
Participant 4	Hosmer 555 Lyre Hook	Ottbock ErgoArm	WillowWood Alpha Medium	Figure-eight

7.3.1 Socket fit

Participants were recruited through the Glenrose Rehabilitation Hospital's prosthetics department. Subjects were enrolled in the study within approximately 60 days following the delivery of a newly refit or adjusted prosthetic socket. Each participant's socket was evaluated by a certified prosthetist, and based on their clinical expertise, deemed a 'well-fit' socket prior to testing. To confirm the quality of socket fit, each participant completed an OPUS Satisfaction with Device survey modified to present questions relevant to prosthetic socket fit²². This survey and results are included in [Appendix B](#).

7.3.2 Socket pressure measurements

A Tekscan VersaTek system with 9811E sensors (Tekscan Inc., Boston, USA) was used to capture contact pressures acting on the RL within the prosthetic socket. Each sensor contained 96 sensels; therefore, being capable of capturing 96 simultaneous discrete readings. This system was selected as the thin flexible profile of the sensors permits socket-RL interface measurements without the need to modify the socket. Sensors were adhered directly to each participant's RL using double sided adhesive tape. One or two sensors, which were trimmed as necessary and positioned to maximize coverage over the residual limb, were used for each participant.

As required by the Tekscan VersaTek software, each sensor underwent an equilibration and calibration procedure. Typically these activities would be performed with the sensor on a flat, rigid surface at room temperature; however literature suggests improved accuracy with thin film-sensors if calibration occurs in an environment as close to their intended use as possible²³.

Therefore, custom apparatuses were fabricated to allow for these activities to be performed while the sensors were adhered to the participant's residual limb. The equilibration procedure required equal pressure to be distributed across the whole surface area of the sensor. This was achieved using an inflatable bladder system whereby the participants placed their RL into a chamber where a bladder is inflated around the RLs (Figure 7.2 a). Two equilibration points were captured in the software, baseline atmospheric and 10 kPa. Calibration was performed using a load cell affixed to a custom pushing head, and an apparatus allowing for the application of known loads to the sensors on the RLs (Figure 7.2 b). A two point calibration was employed in the Tekscan software which captured the sensor response to a baseline 0 Newton force and 10 Newton force.

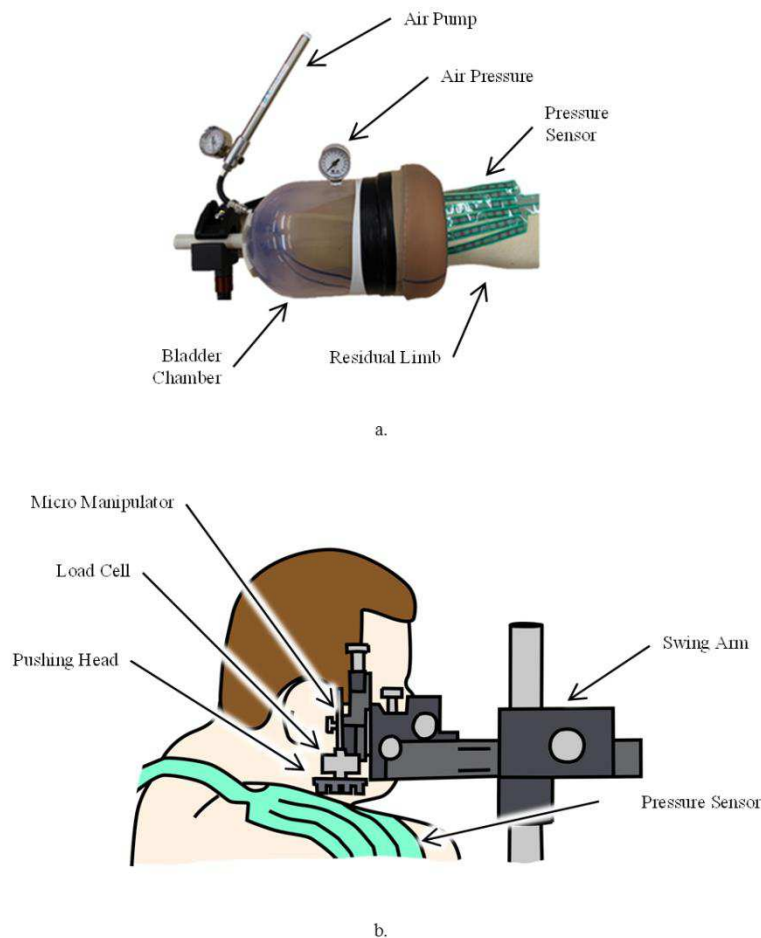


Figure 7.2 Equilibration and calibration apparatuses. Equilibration setup schematically described and demonstrated on a participant, b. calibration setup demonstrated on a participant

The location of each sensor relative to the anatomy of the participants was captured using a FaroArm Edge Coordinate Measurement Machine (FaroArm, Coventry, UK). Each participant's RL was supported by a stationary arm rest to prevent movement of the limb during this process. The three dimensional position of each sensor's sensels relative to a predefined coordinate system were logged. Additionally the coordinates of five anatomical landmarks were captured to geometrically register the relative position of each sensor to the participant's anatomy (acromion, lateral distal point of the residual humerus, mid-bicep muscle belly, mid-triceps muscle belly and most distal tip of the residual limb).

Pressure measurements were then performed. Participants first donned their prosthetic liners, and were instructed to "hold still" with the RL positioned neutral at their side. The pre-pressure introduced by the liner was recorded. Participants then donned their prosthesis and pressure measurements were recorded in four static positions: 90° prosthetic elbow flexion; 90° prosthetic elbow flexion with 1 kg weight at their terminal device; full prosthetic elbow extension with shoulder flexion in the plane of the scapula; and, full prosthetic elbow extension with shoulder flexion in the plane of the scapula with 1 kg weight at the terminal device (Depicted in Figure 7.3 to Figure 7.6). Note that the prosthetic elbow was locked in each position indicated. Participants held each position statically for 3 seconds while pressure data were logged at 50 Hz.

7.3.3 Data treatment

For each participant performing a static pose, 150 samples of pressure data were recorded for each sensel (3 seconds at 50 Hz). Each sensel's data (from the Tekscan system) was averaged and paired with its corresponding geometric location data (from the FARO arm system). This data set was then interpolated linearly to add two additional pressure values and corresponding coordinates between each sensel in preparation for creating surface pressure maps. Data were then imported into Paraview 5.0 software (Kitware Inc., Clifton Park, USA), where the '3D Delaunay Surface' filter was employed to reconstruct the 3D geometry of each participant's residual limb with overlaid pressure values. Pressure maps were scaled from 0 to 12.5 kPa, which was the lowest sensor saturation value of all the participants following sensor calibration; this value allows for a common scale for comparison of pressure maps across participants.

Threshold filtering was employed to isolate regions of maximum pressure, and the ‘Integrate Variables’ filter in Paraview was employed to estimate the corresponding surface areas of these regions on the RL. For each trial, the surface areas exceeding 12.5 kPa and exceeding the saturation pressure of each participant’s sensors were calculated.

7.4 Results

7.4.1 Participant 1

Participant 1 had a left side transhumeral amputation (the tested limb) and right side transradial amputation. It was approximately 11 years since the injury at the time of testing and the participant wore a transhumeral prosthesis between 12 to 15 hours a day. It was noted that participant 1’s RL was more abundant in soft tissue at the end of the RL, with less muscle tone relative to the other participants. Investigators noted redness and minor skin irritation near the posterior-proximal areas of the limb close to the axilla. However, the participant’s prosthetist evaluated the socket as being well-fit and the participant confirmed the satisfaction with the modified OPUS survey ([Appendix B](#)).

Two pressure sensors were used to cover the residual limb resulting in 148 sensels capturing discrete pressure measurements. Pressure maps and analysis results are highlighted in Figure 7.3. After calibration activities, sensor saturation occurred at 16.6 kPa. With the liner donned (Figure 7.3- Position 1) no area on the RL exceeded this threshold value. There was an area of higher pressure on the proximal posterior-medial aspect of the RL (near the posterior axilla) that may be an indication of the soft tissue contacting the thorax in this area. With the prosthesis donned and the elbow positioned at 90° (Figure 7.3- Position 2), the posterior-proximal region near the axilla registered the highest pressure. Surface areas on the RL exceeding 12.5 kPa were approximately 575 mm² and those exceeding sensor saturation (16.6 kPa) were approximately 225 mm². With a 1 kg load added to the terminal device (Figure 7.3- Position 3), the surface areas indicating more than 12.5 kPa or saturation increased to 1220 mm² and 1065 mm², respectively. Locations developing local pressure maximums included the posterior-proximal region near the axilla, the posterior-distal RL, and an anterior-distal region near the humeral tip. With the shoulder in flexion (Figure 7.3- Position 4), a large posterior-proximal region near the axilla and a smaller lateral-distal region near the humeral tip demonstrated local pressure maximums. The surface

areas of the RL that exceeded 12.5 kPa or saturation were 2765 mm² and 1695 mm², respectively. This loading pattern was further amplified with the addition of a 1 kg load to the terminal device with the shoulder flexed (Figure 7.3- Position 5). Both local maximums grew in size with the areas that exceeded 12.5 kPa or saturation pressure were now 3990 mm² and 3710 mm², respectively.

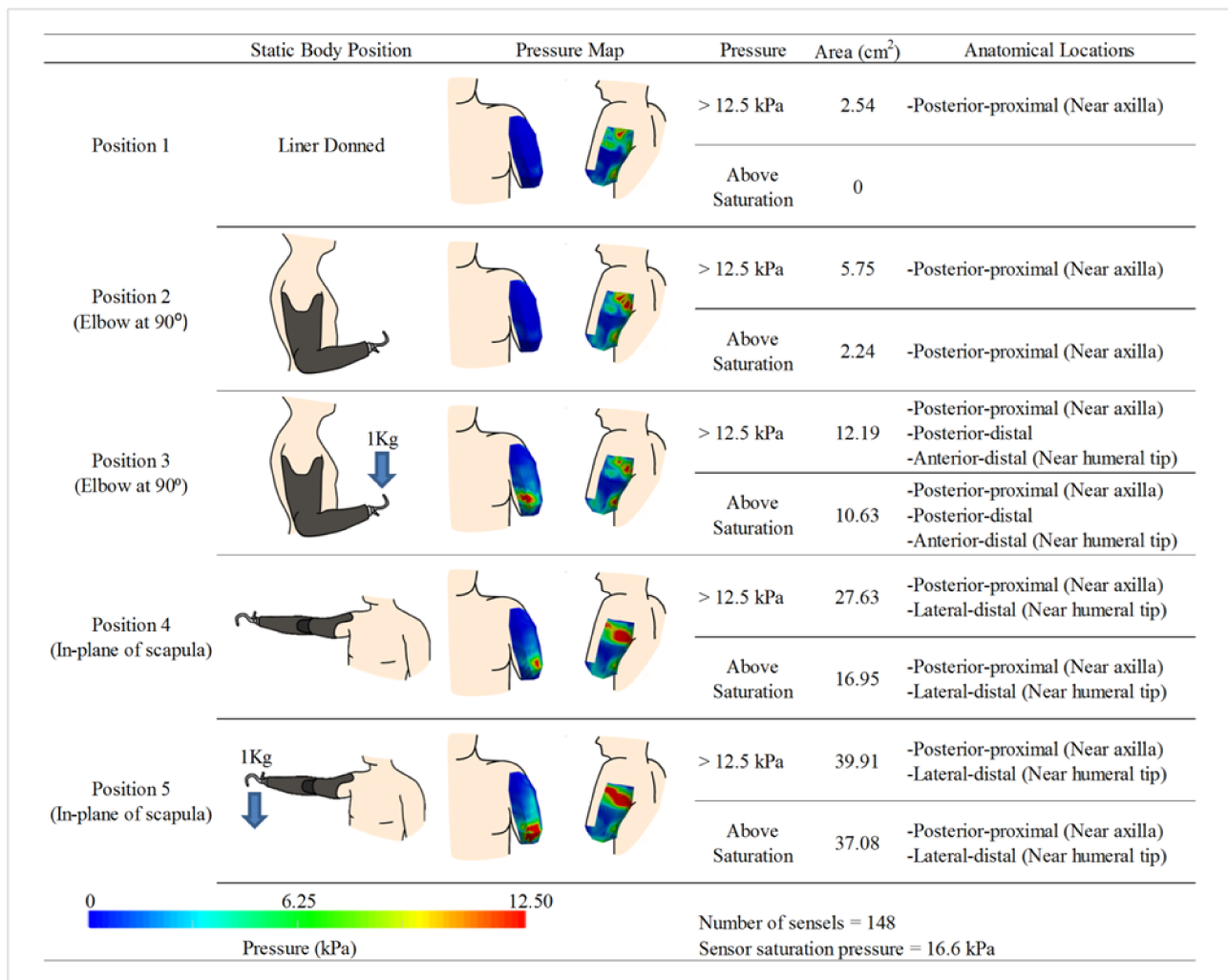


Figure 7.3 Experimental results for Participant 1. kPa denotes units of pressure in kilopascals. Note: The posterior pressure maps are shown with the view in slight rotation to reveal pressures around the curve of the posterior axilla.

7.4.2 Participant 2

Participant 2 had a right transhumeral amputation approximately 1 year prior to testing, and wore their prosthesis infrequently during the course of a day. The participant and the prosthetist confirmed that this was a well-fit socket; however, they noted that the prosthetic harness was “too tight” and caused irritation. However, above average device satisfaction was indicated by the modified OPUS survey ([Appendix B](#)).

Two pressures sensors were used to cover the residual limb resulting in 148 sensels capturing discrete pressure measurements. Pressure maps and analysis results are highlighted in Figure 7.4. After calibration, sensor saturation occurred at 15.1 kPa. With the liner donned (Figure 7.4- Position 1), no area on the RL exceeded 12.5 kPa. When the prosthesis was worn with elbow positioned at 90° (Figure 7.4- Position 2), a small area of 190 mm² in the posterior medial-proximal area of the RL (near the axilla) exceeded 12.5 kPa, but did not exceed sensor saturation values (15.1 kPa). This area increased to 625 mm² with the addition of a 1 kg load on the terminal device (Figure 7.4- Position 3). Similar to Participant 1, with shoulder flexion (Figure 7.4- Position 4), posterior-medial regions of the RL increased in pressure. Additionally more of the posterior RL showed increased pressures, and a small area near the anterior humeral tip presented as a local pressure maximum. Surface areas exceeding 12.5 kPa or sensor saturation were 2500 mm² and 1953 mm², respectively. Participant 1 was uncomfortable lifting a 1 kg load in abduction; therefore, a 500 g load was substituted (Figure 7.4- Position 5). This resulted in the areas that exceeded 12.5 kPa or saturation pressure growing to 2825 mm² and 145 mm², respectively.

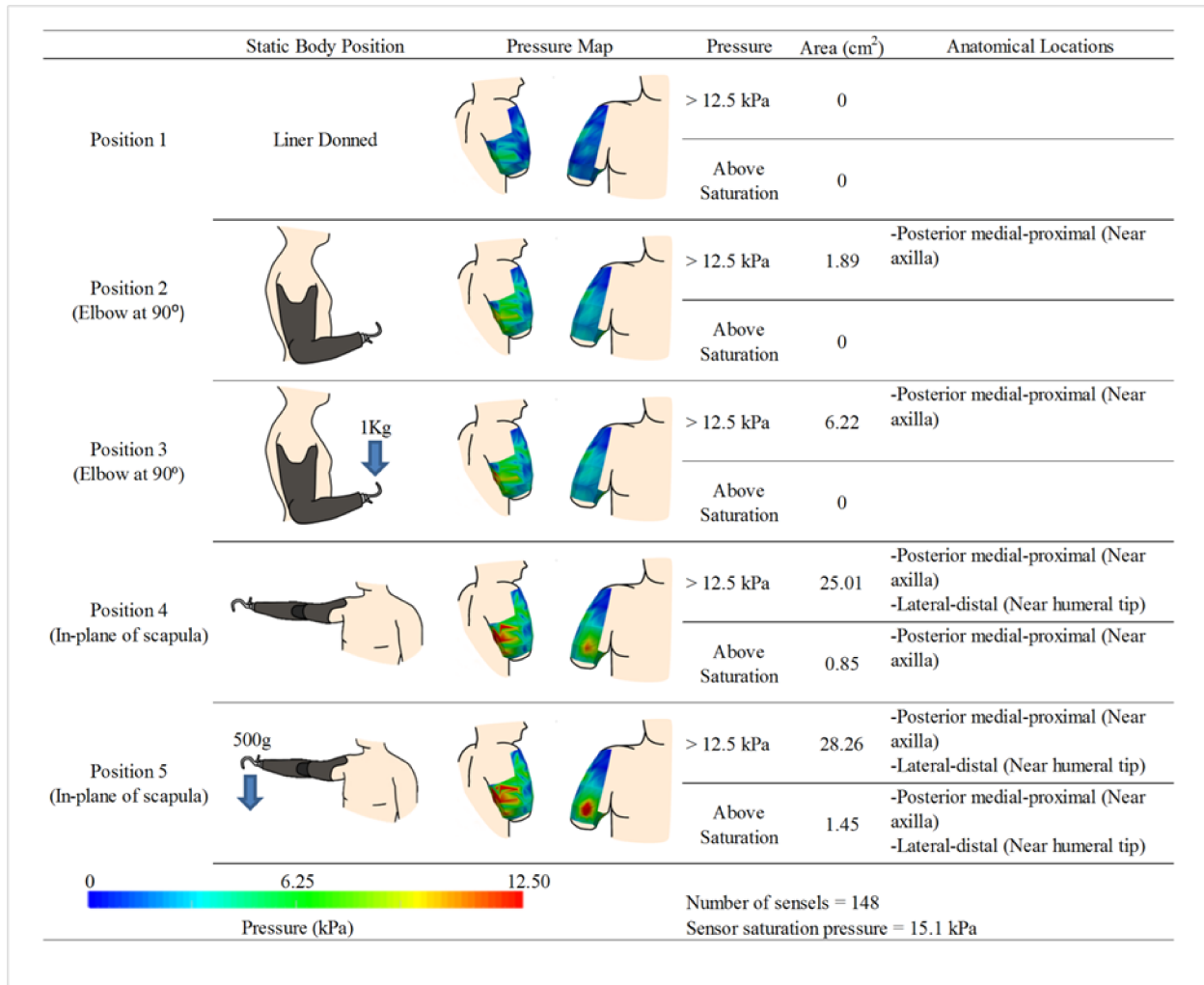


Figure 7.4 Experimental results for Participant 2. kPa denotes units of pressure in kilopascals. Note: The posterior pressure maps view are shown with slight medial rotation to reveal pressures around curve of the posterior axilla.

7.4.3 Participant 3

Participant 3 had a left transhumeral amputation approximately 1 year prior to testing, and wore their prosthesis between 1 to 2 hours a day. Their prosthetist noted that special consideration was given during socket fabrication to accommodate sensitivity to pressure on the distal RL. During testing, Participant 3 noted that their harness may require readjustment as it was too tight and limited their range of motion. However, above average satisfaction was indicated upon completion of the modified OPUS survey ([Appendix B](#)).

Due to the small size of Participant 3's RL, one pressure sensor was trimmed and adhered to the limb resulting in 72 sensels capturing discrete pressure measurements. Pressure maps and analysis results are highlighted in Figure 7.5. After calibration, sensor saturation occurred at 21.1 kPa. With the prosthetic liner donned (Figure 7.5- Position 1), no area of the RL limb exceeded 12.5 kPa. Similarly, while the prosthesis was donned with the elbow at 90° (Figure 7.5- Position 2), no area of the RL exceeded 12.5 kPa, however a local maximum developed on the anterior-proximal side of the RL near the axilla. With the addition of a 1 kg load at the terminal device (Figure 7.5- Position 3), this local maximum increased to a 1715 mm² area that exceeded 12.5 kPa, but no other area exceeded the sensor saturation value. When the prosthesis was held abducted (Figure 7.5- Position 4) the same anterior proximal area, the middle portions of the anterior RL, as well as the posterior-proximal area near the axilla demonstrated local pressure maximums. The areas that exceeded 12.5 kPa or saturation pressure were 6220 mm² and 1945 mm², respectively. When a 1 kg load was added to the terminal device (Figure 7.5- Position 5) the area that exceeded 12.5 kPa was reduced to 5120 mm² while the area that exceeded saturation pressure grew to 3090 mm².

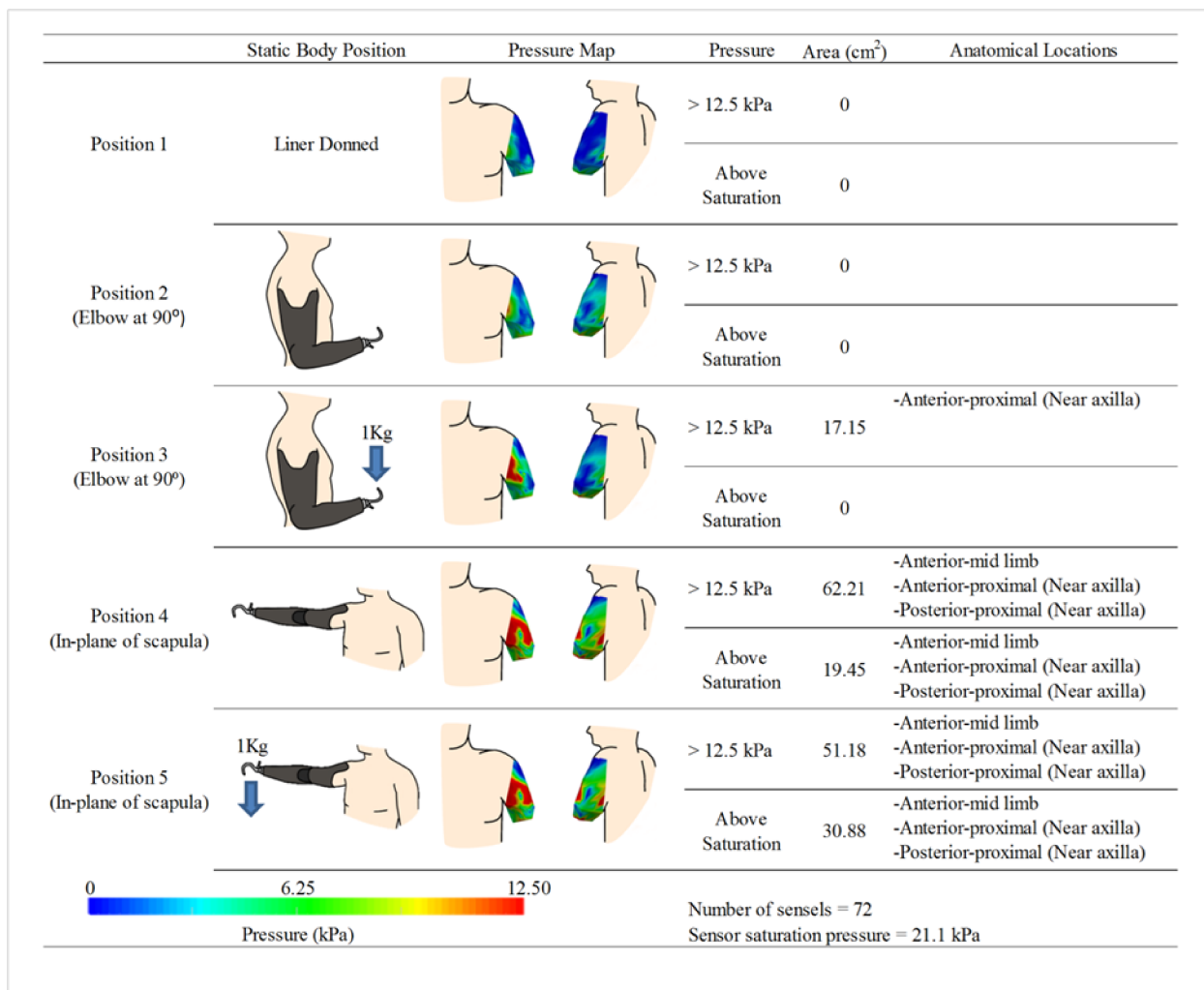


Figure 7.5 Experimental results for Participant 3. kPa denotes units of pressure in kilopascals. Note: The posterior pressure maps view are shown with slight medial rotation to reveal pressures around curve of the posterior axilla.

7.4.4 Participant 4

Participant 4 had a left transhumeral amputation. It was approximately 10 years since their injury at the time of testing and they wore their prosthesis between 6 to 10 hours a day. Above average prosthetic satisfaction was indicated through the results of the modified OPUS survey ([Appendix B](#)).

Two pressures sensors were used to cover the residual limb resulting in 172 sensels capturing discrete pressure measurements. Pressure maps and analysis results are highlighted in Figure 7.6.

After calibration, sensor saturation occurred at 12.5 kPa. With the liner donned (Figure 7.6- Position 1) no area of the RL limb exceeded 12.5 kPa. With the prosthesis donned and elbow at 90°, both with and without the 1 kg load, no area of the limb exceeded 12.5 kPa (Figure 7.6- Position 2 and 3). In these positions a local maximum (although low in magnitude) was observed in the posterior-proximal area of the RL near the axilla as well as anterior proximal region. With the shoulder flexion (Figure 7.6- Position 4), a local pressure maximum was observed on the lateral-distal region of the limb near the humeral tip with an approximate surface area of 875 mm². This area expanded to 1530 mm² with the introduction of a 1 kg load at the terminal device (Figure 7.6- Position 5).

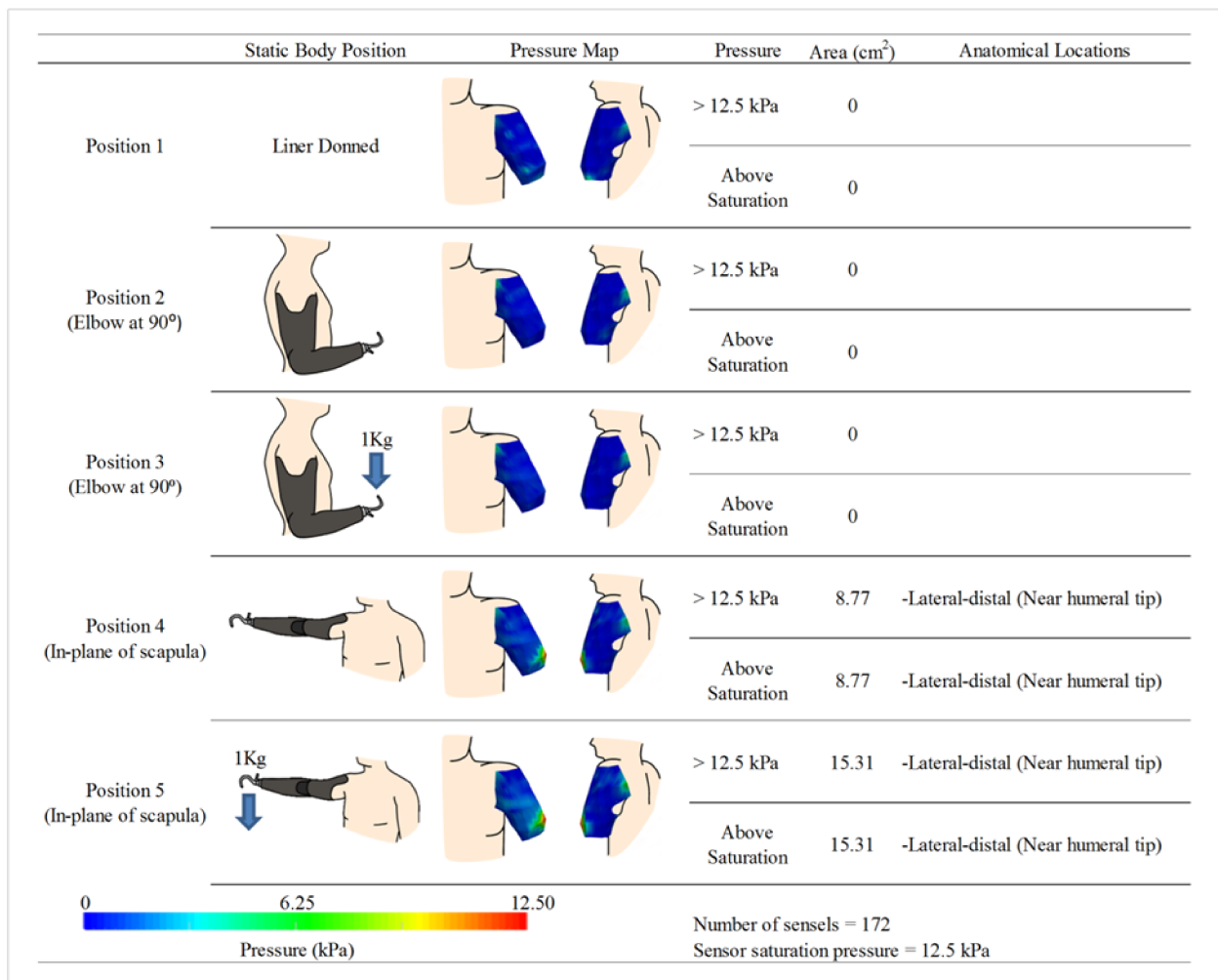


Figure 7.6 Experimental results for Participant 4 kPa denotes units of pressure in kilopascals. Note: The posterior pressure maps view are shown with slight medial rotation to reveal pressures around curve of the posterior axilla.

7.5 Discussion

One of the most influential factors for the use of upper limb prostheses is the socket, which must be custom designed to accommodate the individual's morphology and to distribute the pressures resulting from the weight of the prosthesis appropriately across the RL. Socket fabrication currently relies heavily on heuristic practice. This work presents a first step toward incorporating a quantitative-empirical tool into UL prosthetic socket evaluation. In a fabrication context, one of the most useful methods presented in this work is the ability to characterize pressure distribution patterns and identify anatomical locations bearing local pressure maximums, to further understanding of what constitutes a "well-fit" socket.

For each participant, individual socket design considerations were reflected in the surface pressure distribution across their RLs. Proximal areas of the RL near the axilla were a common area of high pressure in Participants 1, 2, and 3. During socket fabrication, this area was specifically targeted by the prosthetist for tissue compression as a method of avoiding socket contact with the user's thorax. This technique allows increased mobility of the shoulder joint and the additional tissue compression helps stabilize the socket in the coronal plane; however, as a result, it leads to higher pressures while the prosthesis is worn and a possible destabilizing effect in the sagittal plane. Investigators noted mild tissue irritation in this area on Participant 1. Being a user who has undergone bilateral amputation, their dependency on the prosthesis is greatly increased, which is reflected in typical daily use (12-15 hours/day). Therefore, the increased pressure in this area coupled with high usage time, and the noted abundance of soft tissue, likely increases the risk of tissue irritation. However, it was also noted that Participant 1 reported no discomfort while wearing the device and confirmed that the socket was in fact well-fit.

Participant 3's socket was unique relative to the other participant's as it was fabricated to accommodate sensitivity of the distal RL. The prosthetist specifically targeted middle regions of the anterior RL for tissue compression, thereby relieving distal load bearing. This is evident in the location of local pressure maximums in the resulting pressure maps. When the prosthesis was positioned with the shoulder in an abducted position, an anterior region at the mid-length of the limb, as well as a posterior area near the axilla, exhibited local pressure maximums. When a 1 kg load was added in this position, the surface area exceeding saturation pressure (21.2kPa)

increased, yet the area exceeding 12.5kPa decreased. This suggests that with further loading of the terminal device, the socket continued to concentrate its application of pressure over the high pressure areas rather than further redistributing the load, thereby successfully avoiding excess pressure onto the distal limb.

Tissue deformation around skeletal structures was evident in the pressure maps of Participants 1, 2, and 4; especially with the prosthetic elbow and participant's shoulder extended. Local pressure maximums near the distal tip of the residual humerus were observed, with the formation of high pressure areas posterior-medially on the RL in Participants 1 and 2. These patterns were further intensified and grew in surface area with a load applied to the terminal device. In this position, the prosthesis' center of gravity is distal-lateral to the socket. This results in a fulcrum by which the rigid prosthetic socket pivots about the humeral tip which is counter balanced by the posterior medial regions of the RL. In more extreme cases, this action may result in lateral gapping, whereby a void is created as the socket loses contact with the RL in some areas while concentrating pressure on opposing locations. This phenomenon can increase discomfort, and reduce the desire to use the device in greater ranges of motion. Less severe forms of this loading pattern are nearly unavoidable due to the physics of encapsulating soft deformable tissue between a rigid socket and skeletal structure. Some novel socket designs attempt to minimize lateral gapping effects through strategic patterns of tissue compression and release⁷, with follow up imaging and user satisfaction studies being conducted to evaluate the efficacy of their design²⁴. The analytical techniques presented in this work would enable the evaluation of the tissue loading mechanism proposed in these novel socket designs, through the identification of the affected anatomical areas as well as a description of the size and relative magnitude of the pressure in these areas.

The techniques presented in this work demonstrate a number of encouraging potential benefits if incorporated for socket evaluation. Implemented clinically, these techniques can help the prosthetist further refine socket geometry by specifically and accurately targeting regions of a patient's anatomy for load bearing. Beyond this, the data also highlights anatomical areas bearing little or no load. As prosthetic weight, internal socket temperature, and resulting perspiration are often highlighted as major contributors to discomfort, tissue damage, and

prosthetic abandonment²⁵, there exists the possibility that the corresponding non-loaded areas of the socket may be removed. This may help reduce some the undesirable effects of wearing a traditional prosthetic socket, by providing a lighter more breathable device that maintains the interfacial mechanics necessary for suspension and control.

As novel sockets continue to be developed for improved comfort, stability and suspension, this work presents a tool that can be implemented to analytically evaluate new approaches. By quantitatively documenting socket designs to understand the effect on the underlying interfacial mechanics, UL socket fabrication might begin to be more approachable by those less experienced in the highly specialized techniques. However, adoption into a clinical setting will require further development with regards to ease of use and technical accessibility. The Tekscan VersaTek system used to capture contact pressure data is commercially available and designed specifically for the clinic. The procedures presented for capturing RL geometry could be modified to use commercially available laser scanners that are already present in many prosthetic workshops and computer aided design (CAD) systems. However, a gap currently exists in the technical knowledge required to easily pair this data and assemble pressure maps relative to the anatomy. Therefore the development of automated software capable of quickly and accurately assembling pressure maps, with reduced requirement for technical expertise, will be necessary to promote clinical adoption.

Upper limb socket design and fabrication is a process that must accommodate and optimize numerous considerations specific to a patient's morphology, anatomy, and comfort, among many other factors. This work highlights four participants, all with clinically deemed "well-fit" prosthetic sockets, who demonstrated similar and unique load bearing characteristics at the interface of their RL and socket. Although the results were individual to each participant, the presented techniques provided a quantitative understanding of the implications of some of the major design decisions made during socket fabrication. Therefore, this work can help provide a foundation for techniques aimed at leveraging analytically-based design practices, by furthering our understanding of transhumeral socket interface mechanics.

7.5.1 Limitations

A well-documented limitation of Tekscan measurement systems is the measurement accuracy. The Tekscan VersaTek system and 9811E sensor used in our study have been reported to have measurement error of 8.5% on flat surfaces and 11.2% on curved surfaces¹⁶. To help mitigate sensor error, it has been suggested that calibration activities be performed in an environment as close to its intended use as possible²³ (in this case directly affixed to the RL). In doing so, the sensors must be bent to conform to the RL prior to calibration. The physical bending of the sensors introduces an unavoidable initial change in sensel resistance that reduces their working range and results in earlier sensor saturation. Therefore, the technique used in our approach allows a more accurate representation of how pressure distributes across the RL and identification of maximum pressure locations. However, we are unable to infer the magnitude of the pressure in the localized areas of sensor saturation.

One or two sensors were placed on each participant's RL. The investigator attempted to maximize coverage; however full coverage of the limb was not physically possible. Although we could discriminate between 72 to 172 discrete pressure readings (depending on the participant), values occurring in-between sensors and sensels are still unknown. Future work with more densely packed sensor arrays and sensors more adaptable to RL geometry could help improve this resolution.

Finally, two body positions representing a neutral position (arm at the side) and the maximum range of motion for the shoulder were performed by participants under two loading conditions. However, this does not represent the full range of uses for transhumeral prostheses. Although this work provides a preliminary understanding of RL-socket interaction in relation to body position, further work with dynamic movements or other functional static body positions may be warranted.

7.6 Conclusions

This work describes techniques, adapted from lower limb prosthetic research, to empirically characterize the pressure distribution occurring between the residual limb and well-fit transhumeral prosthetic sockets. We demonstrated that the techniques developed in this chapter were capable of characterizing unique pressure distribution patterns that could be traced to

individual socket design considerations. This work represents some of the first fundamental first step toward improved socket designs developed through informed, analytically-based design by allowing visualization and evaluation of socket-RL interactions. In the context of sensory integrated prosthetic sockets, this work establishes a baseline understanding of how a traditional prosthetic socket interacts with the RL. It may be further applied to appreciate the implications of novel prostheses and sockets on load bearing anatomy, socket fit, and comfort. In subsequent chapters developing sockets that incorporate kinesthetic feedback systems, the data presented in this chapter allows for a point of comparison between a traditional and sensory integrated prosthesis.

7.7 References

1. Lake C. The evolution of upper limb prosthetic socket design. *Journal of Prosthetics and Orthotics*. 2008;20(3):85-92. Accessed 20 December 2013.
2. Resnik L, Patel T, Cooney SG, Crisco JJ, Fantini C. Comparison of transhumeral socket designs utilizing patient assessment and in vivo skeletal and socket motion tracking: A case study. *Disabil Rehabil Assistive Technol*. 2016;11(5):423-432. Accessed 29 November 2016. doi: 10.3109/17483107.2014.981876.
3. Mcfarland LV, Winkler SLH, Heinemann AW, Jones M, Esquenazi A. Unilateral upper-limb loss: Satisfaction and prosthetic-device use in veterans and servicemembers from vietnam and OIF/OEF conflicts. *J Rehabil Res Dev*. 2010;47(4):299-316. Accessed 29 November 2016. doi: 10.1682/JRRD.2009.03.0027.
4. Biddiss E, Chau T. Upper limb prosthesis use and abandonment: A survey of the last 25 years. *Prosthet Orthot Int*. 2007;31(3):236-257. Accessed 24 January 2014.
5. Schultz AE, Baade SP, Kuiken TA. Expert opinions on success factors for upper-limb prostheses. *Journal of Rehabilitation Research and Development*. 2007;44(4):483-489. Accessed 5 April 2013.

6. Sanders J. Stump-socket interface conditions. In: *Pressure ulcer research: Current and future perspectives*. Heidelberg Germany: Springer-Verlag Berlin; 2005:129-147. Accessed 25 January 2016.
7. Alley RD, Williams TW, Albuquerque MJ, Altobelli DE. Prosthetic sockets stabilized by alternating areas of tissue compression and release. *Journal of Rehabilitation Research and Development*. 2011;48(6):679-696. Accessed 5 April 2013.
8. Lake C, Dodson R. Progressive upper limb prosthetics. *Phys Med Rehabil Clin N Am*. 2006;17(1):49-72. Accessed 5 April 2013.
9. Ziegler-Graham K, MacKenzie EJ, Ephraim PL, Travison TG, Brookmeyer R. Estimating the prevalence of limb loss in the united states: 2005 to 2050. *Arch Phys Med Rehabil*. 2008;89(3):422-429. doi: <http://dx.doi.org/10.1016/j.apmr.2007.11.005>.
10. Brenner CD. Wrist disarticulation and transradial amputation: Prosthetic management. In: Smith DG, Michael JW, Bowker JH, ed. *Atlas of amputations and limb deficienciesd surgical, prosthetic and rehabilitation principles*. 3rd ed. Rosemont: American Academy of Orthopaedic Surgeons; 2004:223-230.
11. Biddiss E, Beaton D, Chau T. Consumer design priorities for upper limb prosthetics. *Disability and Rehabilitation: Assistive Technology*. 2007;2(6):346-357. Accessed 5 April 2013.
12. Daly W, Voo L, Rosenbaum-Chou T, Arabian A, Boone D. Socket pressure and discomfort in upper-limb prostheses: A preliminary study. *Journal of Prosthetics and Orthotics*. 2014;26(2):99-106. Accessed 22 April 2014.
13. Silver-Thorn MB, Steege JW, Childress DS. A review of prosthetic interface stress investigations. *Journal of Rehabilitation Research and Development*. 1996;33(3):253-266. Accessed 9 February 2014.
14. Sanders JE. Interface mechanics in external prosthetics: Review of interface stress measurement techniques. *Med Biol Eng Comput*. 1995;33(4):509-516. Accessed 13 May 2015.

15. Herbert-Copley AG, Sinitski EH, Lemaire ED, Baddour N. Temperature and measurement changes over time for F-scan sensors. *MeMeA 2013 - IEEE International Symposium on Medical Measurements and Applications, Proceedings*. 2013:265-267. Accessed 22 April 2015.
16. Polliack AA, Sieh RC, Craig DD, Landsberger S, McNeil DR, Ayyappa E. Scientific validation of two commercial pressure sensor systems for prosthetic socket fit. *Prosthet Orthot Int*. 2000;24(1):63-73. Accessed 22 April 2015.
17. Buis AWP, Convery P. Calibration problems encountered while monitoring stump/socket interface pressures with force sensing resistors: Techniques adopted to minimise inaccuracies. *Prosthet Orthot Int*. 1997;21(3):179-182. Accessed 22 April 2015.
18. Pirouzi G, Abu Osman NA, Eshraghi A, Ali S, Gholizadeh H, Wan Abas WAB. Review of the socket design and interface pressure measurement for transtibial prosthesis. *Scientific World Journal*. 2014;2014. Accessed 22 April 2015.
19. Kahle JT, Jason Highsmith MJ. Transfemoral sockets with vacuum-assisted suspension comparison of hip kinematics, socket position, contact pressure, and preference: Ischial containment versus brimless. *Journal of Rehabilitation Research and Development*. 2013;50(9):1241-1252. Accessed 2 February 2016.
20. Dumbleton T, Buis AWP, McFadyen A, et al. Dynamic interface pressure distributions of two transtibial prosthetic socket concepts. *Journal of Rehabilitation Research and Development*. 2009;46(3):405-415. Accessed 2 February 2016.
21. Rogers B, Bosker G, Faustini M, Walden G, Neptune RR, Crawford R. Case report: Variably compliant transtibial prosthetic socket fabricated using solid freeform fabrication. *Journal of Prosthetics and Orthotics*. 2008;20(1):1-7. Accessed 2 February 2016.
22. Heinemann AW, Bode RK, O'Reilly C. Development and measurement properties of the orthotics and prosthetics user's survey (OPUS): A comprehensive set of clinical outcome instruments. *Prosthet Orthot Int*. 2003;27(3):191-206. Accessed 24 February 2014.

23. Schofield JS, Evans KR, Hebert JS, Marasco PD, Carey JP. The effect of biomechanical variables on force sensitive resistor error: Implications for calibration and improved accuracy. *J Biomech*. 2016;49(5):786. doi: <http://dx.doi.org/10.1016/j.jbiomech.2016.01.022>.
24. Resnik L, Patel T, Cooney SG, Crisco JJ, Fantini C. Comparison of transhumeral socket designs utilizing patient assessment and in vivo skeletal and socket motion tracking: A case study. *Disabil Rehabil Assistive Technol*. 2016;11(5):423-432. Accessed 8 January 2017. doi: 10.3109/17483107.2014.981876.
25. Biddiss E, Chau T. Upper-limb prosthetics: Critical factors in device abandonment. *Am J Phys Med Rehabil*. 2007;86(12):977-987. Accessed 16 March 2017. doi: 10.1097/PHM.0b013e3181587f6c.

Chapter 8. The integration of kinesthetic feedback in a functional prosthetic system

8.1 Chapter Preface

In chapter 4, we presented a novel sensory feedback technique with the potential to provide movement information from the prosthesis to the user through matched movement sensations experienced in the missing limb. Although we have demonstrated the use of our techniques with physical prosthetic components, the feedback system and prosthesis were separate from the user and mounted to a desktop. A significant step in the development of our kinesthetic technique was the integration of the feedback componentry into a prosthetic arm without compromising comfort or function. This crucial step is often overlooked in sensory feedback literature, yet is a fundamental step in demonstrating a feedback system is capable of being translated beyond the laboratory. In this chapter we describe a novel solution to this challenge by highlighting a prosthetic socket design capable of achieving this task. We further analyze the mechanical implications of our design using the empirical techniques developed in chapters 6 and 7.

8.2 Introduction

Movement of an intact upper limb (UL) returns rich streams of sensory information. This is vital to volitional control of the limb, and is responsible for detecting limb position, touch, and grip force, among others¹. This information is largely unavailable to those relying on (UL) prostheses, forcing a reliance on visual cues and increasing the cognitive burden required for effective operation². While advanced prostheses have been developed with the aim of improved dexterity, function, and control, 23-39% of electric prosthetic users still reject their device³. The absence of sensory feedback, comfort, and functionality are often highlighted as some of the top contributors to prosthetic rejection^{3,4}. In response to the challenges associated with the lack of sensory feedback, numerous sensors, haptic systems, and feedback strategies have been developed to detect and translate prosthetic sensory information to the user^{2,5}. Yet practical barriers still exist in translating many of these systems beyond the benchtop into clinical prosthetic applications².

In chapter 4, we demonstrated a kinesthetic sensory feedback technique capable of intuitively informing the user of prosthetic movement. Our technique, like most non-invasive feedback approaches, employ mechanical/electrical haptic devices (tactors) that encode sensory information through stimulation of strategic locations on the user's residual limb (RL)²⁻⁵. However, traditional prostheses rely on the socket to encapsulate the residual limb (RL) and strategically target areas of soft tissue to compress and relieve in order to maintain suspension and socket security^{6,7}. Integration of sensory feedback systems into functional prostheses will require that tactors pass through the prosthetic socket to access the limb. Therefore, it must be insured that the additional socket modifications, inherent to installing a feedback system, do not compromise the traditional requirements of comfort, suspension, or security. Furthermore consideration must be given to the spacing of tactors and additional feedback componentry as to not interfere with other necessary devices such as the electromyography (EMG) control system. Therefore a major practical barrier for many sensory feedback systems lays in the development of non-traditional sockets capable of facilitating access of the tactors to the RL, while accommodating the traditional requirements for socket fit and prosthetic function.

A basic requirement of both sensory integrated prosthesis and traditional EMG controlled prostheses is accurate electrode placement and contact. To efficiently control myoelectric prostheses, it is imperative that control electrodes maintain consistent contact with the muscle control site on the RL both in terms of contact pressure and location^{8,9}. Surface electrodes are separated from the muscle (the biological signal generator) by intermediate layers of skin, fat, and other soft tissues. A decrease in contact pressure can lead to changes in impedance as the electrode is moved further from the muscle. This action may decrease the signal amplitude and often increases the signal's noise⁹. This may result in the user needing to increase muscle contraction effort to control the device, or in the event that a gap forms between the electrode and skin, a loss of control over the corresponding degree of freedom. In contrast, if pressure is increased the sensor may register higher amplitude signals and may trigger unintentional movement of the prosthesis. Location also plays a key role in EMG recordings and prosthetic control^{8,9}. Slippage or displacement of the prosthetic socket can result in the electrode no longer

contacting the appropriate location on the muscle control site. This may result in intermittent or poor control over the prosthetic components. These challenges may be amplified in sensory integrated prostheses as a result of the additional weight of feedback components and the socket modifications required for access to the RL.

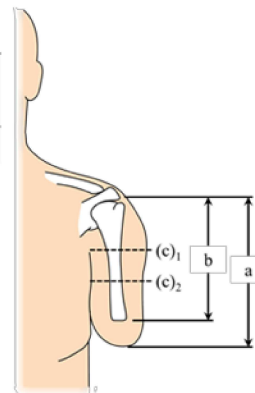
In this chapter we present a case study that describes a novel myoelectric transhumeral prosthetic socket designed to integrate a custom kinesthetic-vibration tactor with consideration given to maintaining good socket fit and electrode contact. A quantitative analysis was performed to evaluate the impact of the novel prototype socket on the interface pressures between the socket and residual limb (RL).

8.3 Methods

A single participant with left side transhumeral amputation, who had previously received targeted reinnervation surgery, was recruited. The participant had four 4 muscle control sites (hand close- medial bicep, elbow flex- lateral bicep, hand open- lateral triceps, elbow extend- medial triceps). Additional participant information is included in Table 8-1. Informed consent was obtained prior to participation and ethic approval was obtained through the University of Alberta's Institutional Review Board.

Table 8-1 Participant demographics and residual limb characteristics, where (c)1 and (c)2 denote circumference measurements taken at the axilla and mid-length of the limb, respectively, 'a' denotes the residual limb length taken from the acromion to distal tip of the limb, and 'b' represents the limb length from the acromion to the distal residual humeral tip.

Gender	Height (m)	Weight (Kg)	Side of Amputation
Male	1.75	103	Left
Residual Limb Dimensions			
Length (mm)		Circumference (mm)	
a	b	(c) ₁	(c) ₂
290	250	420	380



8.3.1 Design criteria

The prosthetic socket design had to be capable of mounting standard prosthetic components as well as allowing a kinesthetic tactor (HDT Global, Solon, Oh, USA) access to the anterior distal region of the RL (Figure 8.1). A myoelectric prosthetic hand (Bebionic, Ottobock, Duderstandt, Germany), body powered elbow (Ergo Arm, Ottobock, Duderstandt, Germany), and prosthetic harnessing were to be used in conjunction with the prototype socket, as per a traditional transhumeral socket fitting. As we demonstrated in Chapter 4, the kinesthetic illusion is location dependent and may require minor adjustment of the stimulus location to achieve strong consistent movement illusions, therefore the socket had to accommodate this requirement. The socket design also had to maintain the traditional requirements for fit, suspension, and secure attachment of the prosthetic components. Additional criteria to facilitate myoelectric control included firm electrode contact, and spatial flexibility (with regard to electrode and tactor contact) in the event of minor socket slip or displacement. Table 8-2 summarizes these design criteria.

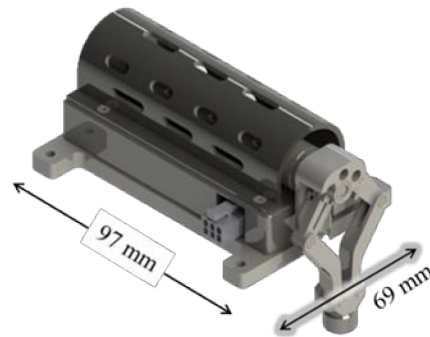


Figure 8.1 Vibration factor and stimulus location. Top: The anterior distal location targeted to provide kinesthetic feedback. Bottom: The kinesthetic factor and its footprint dimensions

Table 8-2 Summary of design criteria

Design Criteria
Utilize standard prosthetic componentry
Mount preexisting tactor
Minor adjustments of tactor stimulus location
Maintain socket fit
Firm electrode contact
Flexibility in event of minor socket displacement

8.3.2 Socket Design

At the Glenrose Rehabilitation Hospital's Prosthetics Department, a traditional transhumeral myoelectric check socket was fabricated for the participant. The socket was intended to be worn in conjunction with a prosthetic gel liner (Alpha Classic, Willow Wood, Mt. Sterling, OH, USA). As is standard in TR - EMG controlled prosthesis using gel liners, 4 pairs of dome style electrode buttons (Cavity-Back, Liberating Technologies Inc., Holliston, MA, USA) were installed

through the liner to contact the skin above the 4 muscle control sites for elbow and hand operation (Figure 8.2). Additionally, at the location on the participant's liner that corresponded to the vibration stimulus location on the participant's RL, the silicone was removed using a scalpel knife, leaving only the fabric at this area (Figure 8.2). This was intended to reduce any damping effect of the silicone on the vibration feedback while still allowing the prosthetic liner to be worn. Depressions were added to the socket with the aim of compressing soft tissues around the four electrode control sites. These depressions were strategically cut out of the socket, creating windows at these locations. The geometric foot prints of these windows were filled with conductive panels that were electrically tied to the EMG control system of the prosthesis. A BOA cable tensioning system (RevoFit, Denver, CO, USA) was passed through the four panels, such that tensioning of the cable would allow adjustable compression of the underlying tissue (Figure 8.3). As the conductive panels were located over the muscle control sites, they would contact the dome electrodes. The conductive portions of these panels that contacted individual electrodes were physically split and electrically isolated as necessary in achieving two active electrodes and a ground (when required) for each muscle control site¹⁰. This design served two purposes. First the adjustable compression provided by the BOA system allowed for adjustable contact pressure of the electrodes. Second the larger foot print and contact area of the conductive panels would maintain electrical contact with the liner's electrodes in the event of minor socket slip or displacement (Figure 8.3).

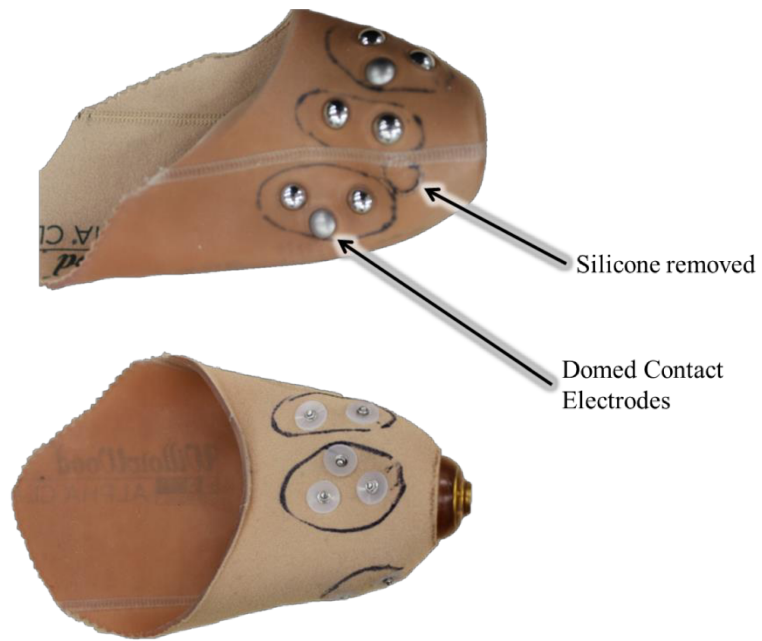


Figure 8.2 Prosthetic liner and electrode contacts. Top: The prosthetic liner inverted to the interior and domed electrode contacts. Bottom: Exterior view of the prosthetic liner with the footprint of the corresponding conductive panel traced on the surface.

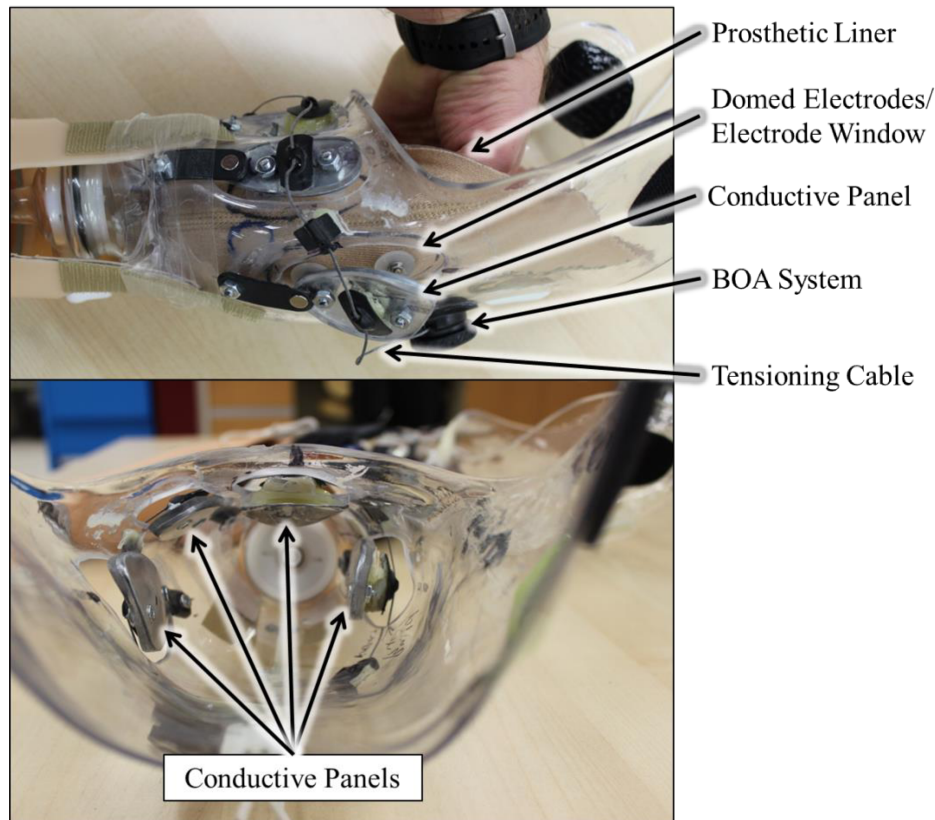


Figure 8.3 Prototype socket design. Top: Schematic diagram of the main components involved in the adjustable compression mechanism over the electrode contacts. Bottom: Interior view of the socket with the conductive panels in the position of maximum compression (maximum cable tension in the BOA system).

A schematic diagram of the tactor integration can be seen in Figure 8.4. Tactor integration was achieved by adding a flat posterior build up distal to the prosthetic socket. This surface was coated in a layer of Silicone sealant (GE Silicone ii sealant, Boston, MA, USA) to provide a ‘tacky’ slip resistant mounting surface. The remainder of the buildup was upholstered with adhesive hook and loop tape. 3D printed brackets were created to mount with the pre-tapped holes on the tactor base. Hook and loop strapping was affixed to these brackets. A 19mm diameter hole was drilled through the prosthetic socket at a location anticipated to align with the predefined stimulus location on the participant’s RL. This hole was strategically oversized from the 13.75mm required to allow the tactor head access to the RL. Therefore, this design allowed the tactor to be securely mounted to the prosthesis. The hook and loop design provide flexibility in positioning the tactor. By slightly oversizing the access hole in the socket, minor adjustment

could be made to ensure the appropriate stimulus location was being reached. Finally, by removing a portion of the silicone from the prosthetic liner, we ensured that the vibration stimulus could be introduced to the RL with minimal attenuation from the prosthetic liner.

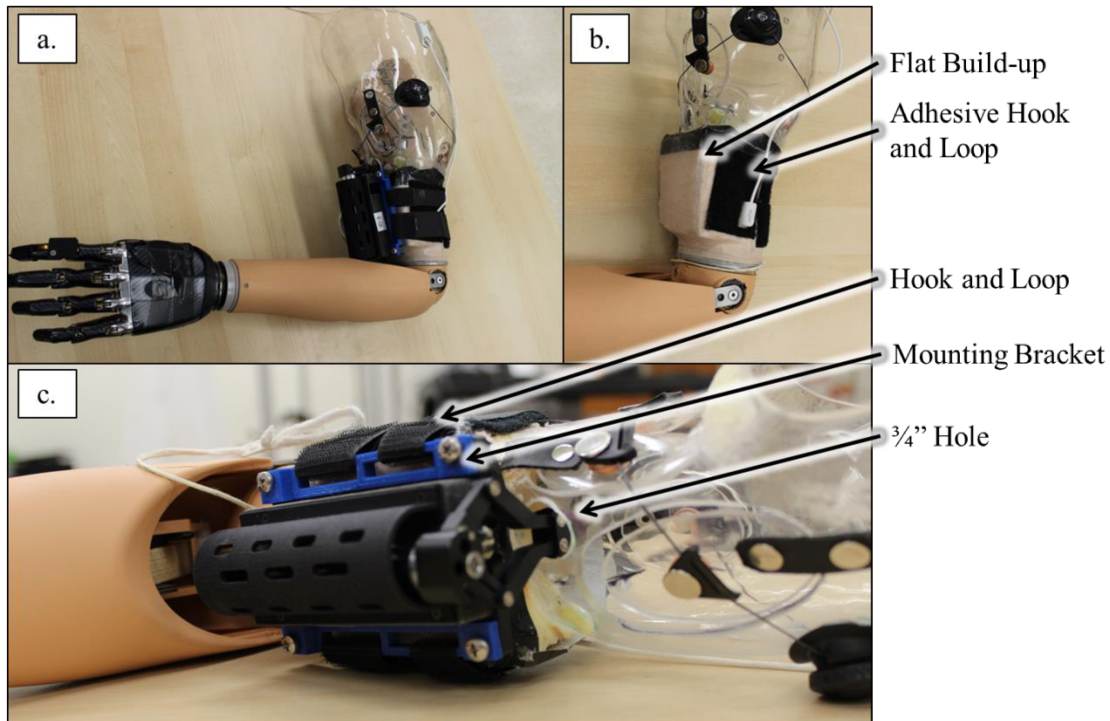


Figure 8.4 Kinesthetic tactor integration and assembly. (a.) An overall view of the prosthesis with kinesthetic tactor installed. (b.) A magnified view of the distal anterior buildup. (c.) A magnified view of the tactor installed on the prosthesis and prosthetic modifications

With this final design, the movement of the prosthetic components was nearly unaffected. As the vibration tactor was required to be positioned on the distal anterior side of the RL, interference with the prosthetic elbow was an initial concern. The final design permitted elbow flexion in excess of 90°, resulting in minor (if any) functional impact of the tactor's presence (Figure 8.5). When donned, the participant subjectively reported the prosthesis as being “comfortable,” with no concerns expressed in regard to socket fit. During the course of testing the investigators did not note any restrictions or movement impairment in the prosthesis range of motion beyond what would be anticipated in a traditional prosthesis.

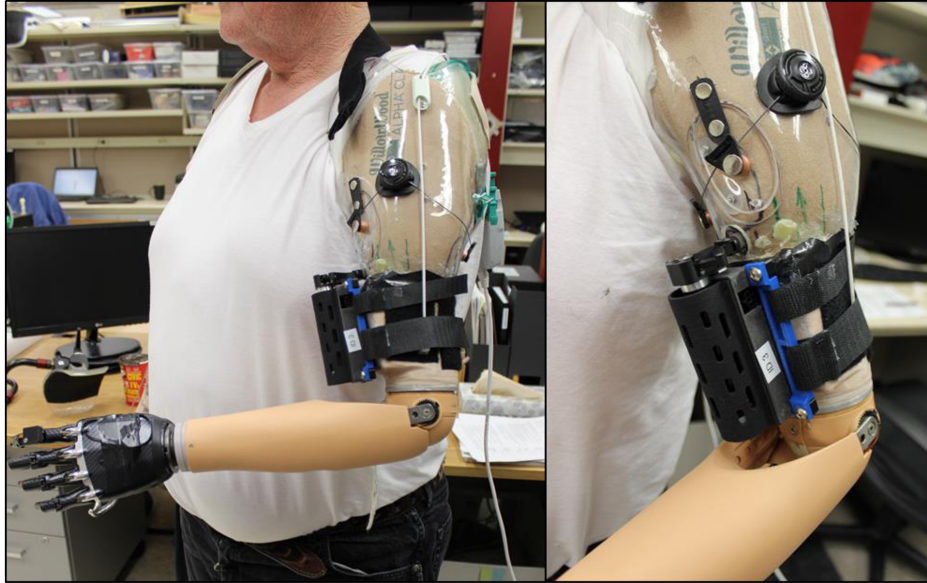


Figure 8.5 The donned prototype prosthesis. Left: The prototype prosthesis worn by the participant with prosthetic elbow at 90°. Right: A magnified view of the integrated kinesthetic tactor.

8.4 Evaluation

8.4.1 Pressure measurement methods

Once a socket that met the design criteria was fabricated, the prosthetic components installed, and the kinesthetic tactor integrated, a quantitative analysis of the socket interface was performed. The intent was to evaluate the mechanical implications of the novel socket design on interface contact pressures, a correlate of fit and comfort^{6,11,12}. As previously reported by Schofield et al.⁶ (Chapter 7), a Tekscan VersaTek system with 9811E sensors (Tekscan Inc., Boston, USA) was employed. Two sensors were adhered directly to the participant's RL using double sided adhesive tape. Sensors were positioned and cropped on the limb to best maximize surface coverage.

Using a FaroArm Edge Coordinate Measurement Machine (FaroArm, Coventry, UK), the location of each sensor relative to the participant's residual anatomy was captured. The participant placed their RL in a rigidly fixed arm rest to prevent movement during this process. Relative to a predefined coordinate system, the three dimensional location of each sensor's sensels was registered. Five additional anatomical landmarks were captured during this process

(acromion, lateral distal point of the residual humerus, mid-bicep muscle belly, mid-triceps muscle belly and most distal tip of the residual limb) allowing for the relative registration of the sensors to these points in space.

Once the geometric data were collected, the sensors were calibrated and equilibrated directly on the participant's RL^{6,13}. Using the custom apparatus and calibration/equilibration techniques described in chapter 7, the participant placed their RL into a chamber where a bladder was inflated around the RL (Figure 8.6 a). Two equilibration points were captured in the software, baseline atmospheric and 10 kPa. Calibration was performed using a load cell affixed to a custom pushing head, and an apparatus allowing for the application of known loads to the sensors on the RL (Figure 8.6 b). A two point calibration was employed in the Tekscan software which captured the sensor response to a baseline 0 Newton force and 10 Newton force.

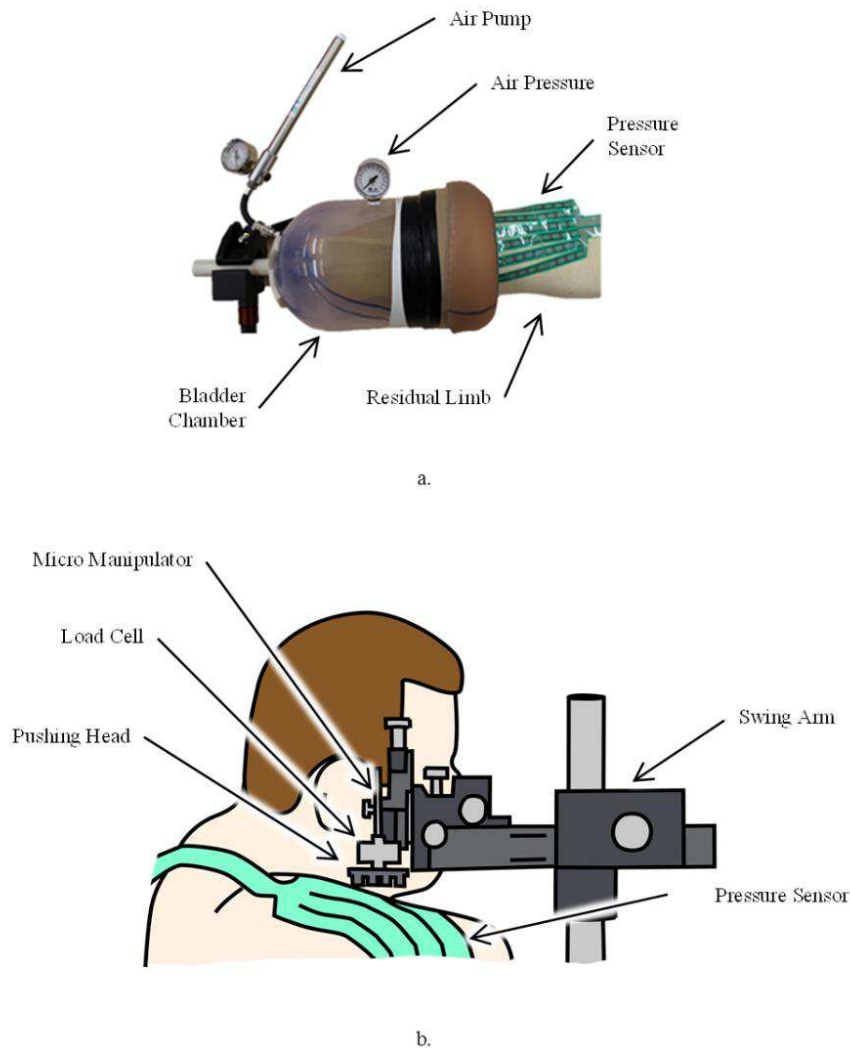


Figure 8.6 Equilibration and calibration apparatuses. Equilibration setup schematically described and demonstrated on a participant, b. calibration setup demonstrated on a participant

The participant then donned the liner and prosthesis. The BOA tensioning system was adjusted by the participant to a ‘comfortable’ level that they would anticipate being able to wear throughout an average day. The tactor stimulus head was pressed into the residual limb with 5N forces (as measured by its integrated load cell), the upper working limit of the tactor. Pressure measurements were then recorded in 4 static positions: 90° prosthetic elbow flexion, 90° prosthetic elbow flexion with 1kg weight, full prosthetic elbow extension with shoulder flexion in the plane of the scapula, and full prosthetic elbow extension with shoulder flexion in the plane

of the scapula with 1kg weight (Figure 8.7). Note that the prosthetic elbow was locked in each position. Pressure data were recorded at 50Hz over a 3 second capture window⁶.

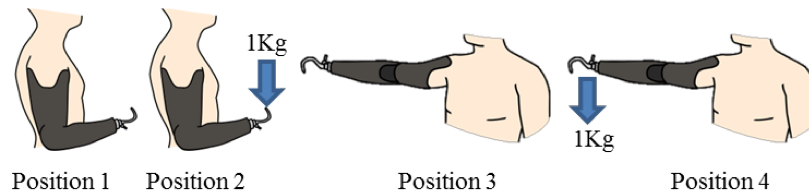


Figure 8.7 The four static testing positions

Employing the techniques developed in Schofield et al.⁶ (Chapter 7), pressure measurement and geometric data were paired in Paraview 5.0 software (Kitware Inc., Clifton Park, USA). In this software, 3D surface pressure maps of the participant's RL were constructed using the '3D Delaunay Surface' filter tool. Threshold filtering was employed to isolate regions of maximum pressure, and the 'Integrate Variables' filter was employed to estimate the corresponding surface areas of these regions on the RL.

As our participant was previously enrolled in the study presented in Schofield et al.⁶ (Chapter 7), interface pressures of the prototype socket with the tactor could be compared and contrasted to the pressures of his traditional socket without the tactor integrated. This analysis allowed an understanding of the mechanical implications of the prototype socket with integrated tactor at the RL-socket interface.

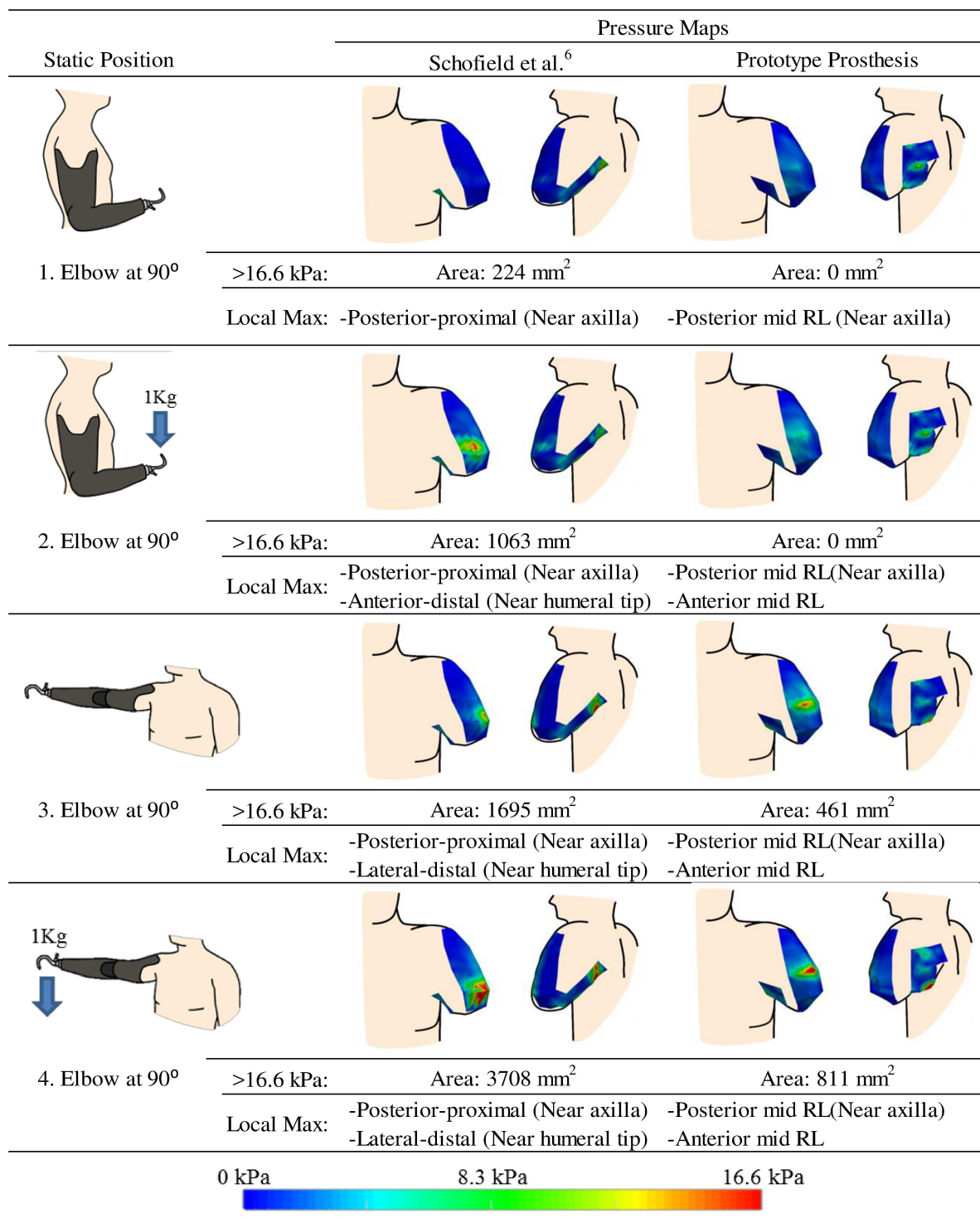
8.4.2 Pressure Measurement Results

Two pressure sensors were used to cover the residual limb resulting in 156 sensels capturing discrete pressure measurements. Pressure maps and analysis results are highlighted in Table 8-3. After calibration activities, sensor saturation occurred at 16.6 kPa. With the prosthesis donned and the elbow positioned at 90° (Table 8-3- Position 1), a posterior region approximately mid-length of the RL registered the highest pressure. However, no measured contact pressure exceeded saturation (16.6 kPa). With a 1kg load added to the terminal device (Table 8-3- Position 2), no measured contact pressure exceeded 16.6 kPa. On both the posterior and anterior

sides of the residual limb, local pressures maximums developed approximately mid-length of the RL. With the shoulder in flexion (Table 8-3- Position 3), an anterior region mid-length of the RL exceeded sensor saturation. The surface area of this area was estimated to be 640mm². An additional local maximum on the posterior side near the axilla also developed a local pressure maximum. This loading pattern was further amplified with the addition of a 1kg load to the terminal device with the shoulder flexed (Table 8-3- Position 4). Both local maximums grew in size with the areas that exceeded 16.6 kPa and saturation pressure now 811 mm².

When comparing and contrasting these results to the traditional prosthetic socket of our participant studied in Schofield et al.⁶ (Chapter 7) notable differences in contact pressure were present. In the prototype socket, local pressure maximums were more proximal (typically mid-length of the RL) than the traditional socket. Additionally, areas exceeding the sensor threshold value were reduced in the prototype socket such that no measured pressure exceeded 16.6 kPa in both positions where the prosthetic elbow was held at 90°. With the elbow in extension these areas reduced from 1695mm² to 461mm² (27 % of the original area), and 3708mm² to 811mm² (22 % of the original area), without and with a 1kg load at the prehensor, respectively.

Table 8-3 Contact pressure results. Contact pressure results from the prototyped socket (right column) next to Schofield et al.⁶ results for comparison. kPa denotes units of pressure in kilopascals. . Note: The posterior pressure maps are shown with the view in slight rotation to reveal pressures around the curve of the posterior axilla.



8.5 Discussion

In this chapter we present a unique solution to practical integration challenges associated with the development of functional prostheses with sensory feedback devices. Furthermore, the techniques presented hold applicability to traditional myoelectric prosthetic socket design. The prototype socket described in this chapter is capable of integrating a kinesthetic tactor for prosthetic movement feedback, as well as aimed to improve electrode contact and maintain prosthetic fit, with adjustability.

The final prototyped design was able to successfully integrate our preexisting kinesthetic tactor. The design allowed for secure affixment of the tactor to the prosthesis while providing adjustability to optimize the stimulus location. An additional challenge presented itself as the length of the participant's RL was a short for a transhumeral amputation. When considering that the four pairs of control electrodes also required access to specific areas on the RL, the physical space available for the tactor was quite limited. This issue required careful consideration to avoid interference of prosthetic components. It was possible to position the bulk of the tactor distal to the socket to accommodate this challenge. However, this solution now placed the tactor near the prosthetic elbow, so specific consideration had to be given to locate the tactor such that it did not interfere with the elbow's range of motion. Beyond the scope of this thesis, a miniaturized kinesthetic tactor is currently in development. By implementing a smaller tactor, space considerations challenges may be partially alleviated in follow up work. In practice, prosthetic sockets and stimulus locations will be unique to each prosthetic user. This chapter presents an encouraging case study demonstrating the integration of kinesthetic sensory feedback in a functional prosthesis; a necessary step in achieving sensory-motor integrated artificial limbs.

The prototype socket used a BOA tensioning system allowing the user adjustability in electrode contact and tissue compression. By employing the pressure measurement techniques previously described in Schofield et al.⁶ (Chapter 7), the mechanical implications of this design could be analytically evaluated. Compared to the traditional socket, the prototyped yielded a shift in location of local pressure maximums toward the mid-length of the RL. It can be inferred that this shift was likely a result of the strategic compression provided by the conductive panels and BOA

tensioning system. This helps validate that the intent of the design was in fact being achieved (firm electrode contact). Additionally, this demonstrates a potential remedying effect for the pressure patterns presented in Chapter 7 that suggested early indicators of lateral gapping. As contact pressure is moved away from the humeral tip, the fulcrum effect and corresponding gapping effect should be reduced. Not only did the locations bearing local pressure maximums change, but so did the surface area of the RL experiencing pressures in excess of sensor saturation. In all four tested positions the area exceeding 16.6kPa were reduced. This result is encouraging as it indicates that the contact pressures are less extreme and more distributed in the prototyped socket. Coupled with the fact that these areas were typically located in close vicinity to the electrode control sites, these data demonstrates that the prototype socket is capable of strategically targeting areas on the RL that require higher contact pressures while alleviating the contact pressure in non-dependent areas. Taken together, and paired with the subjective feedback of the participant, we are confident that we successfully designed and fabricated a single sensory integrated prosthesis that is comfortable, as well as accommodates the challenges of factor and electrode placement.

This work presents a case study with a single participant. Follow up work with additional participants will broaden our approach and identify further unique challenges and solutions. The design described in this chapter relies on a prosthetic liner; however, our approach would not be successful in linerless socket designs that require suction for suspension. To broaden the application of our design, investigation into suction based sockets and prevention of slippage or vacuum loss is warranted. Finally, the static tasks performed in this chapter provide insightful design evaluation information; however, they do not represent the multitude of active movements that may be performed during daily living. Future testing during dynamic functional tasks may provide information to further understand and evaluate the interaction between socket and RL.

8.6 Conclusions

In moving toward functional sensory integrated UL prostheses, techniques facilitating the integration of feedback devices will become crucial. This chapter presents a single case study achieving this task. As the field continues to progress, other challenges and unique solutions will

emerge. A key strength to our approach was the quantitative analysis of our design. It allowed for verifications of driving criteria, such as tissue contact near muscle control sites, as well as highlighted a reduction in areas bearing high contact pressure; a correlate to fit and comfort. Although successful design approaches may be achieved without this level of rigor, it is necessary to truly understand the implications of a design at the socket interfaces, and help evaluate the efficacy of design decisions.

8.7 References

1. Kim K, Colgate JE, Santos-Munné JJ, Makhlin A, Peshkin MA. On the design of miniature haptic devices for upper extremity prosthetics. *IEEE/ASME Transactions on Mechatronics*. 2010;15(1):27-39. Accessed 5 April 2013.
2. Schofield JS, Evans KR, Carey JP, Hebert JS. Applications of sensory feedback in motorized upper extremity prosthesis: A review. *Expert Review of Medical Devices*. 2014;11(5):499-511. Accessed 8 April 2015.
3. Biddiss E, Chau T. Upper limb prosthesis use and abandonment: A survey of the last 25 years. *Prosthet Orthot Int*. 2007;31(3):236-257. Accessed 24 January 2014.
4. Biddiss E, Chau T. Upper-limb prosthetics: Critical factors in device abandonment. *Am J Phys Med Rehabil*. 2007;86(12):977-987. Accessed 16 March 2017. doi: 10.1097/PHM.0b013e3181587f6c.
5. Antfolk C, D'alonzo M, Rosén B, Lundborg G, Sebelius F, Cipriani C. Sensory feedback in upper limb prosthetics. *Expert Review of Medical Devices*. 2013;10(1):45-54. Accessed 2 December 2013.
6. Schofield JS, Schoepp KR, Williams HE, Carey JP, Marasco PD, Hebert J.S. Characterization of interfacial socket pressure in transhumeral prostheses: A case series. *PLoS ONE*. 2017.

7. Alley RD, Williams TW, Albuquerque MJ, Altobelli DE. Prosthetic sockets stabilized by alternating areas of tissue compression and release. *Journal of Rehabilitation Research and Development*. 2011;48(6):679-696. Accessed 5 April 2013.
8. Stegeman DF, Hermens HJ. Standards for surface electromyography. *The European Project Surface EMG for Non-Invasive Assessment of Muscles (SENIAM)*. 2007.
9. Day S. Important factors in surface EMG measurement. Bortec biomedical ltd. .
10. Liberating Technologies Inc. Remote electrode system installation guide. .
11. Daly W, Voo L, Rosenbaum-Chou T, Arabian A, Boone D. Socket pressure and discomfort in upper-limb prostheses: A preliminary study. *Journal of Prosthetics and Orthotics*. 2014;26(2):99-106. Accessed 22 April 2014.
12. Lake C. The evolution of upper limb prosthetic socket design. *Journal of Prosthetics and Orthotics*. 2008;20(3):85-92. Accessed 20 December 2013.
13. Schofield JS, Evans KR, Hebert JS, Marasco PD, Carey JP. The effect of biomechanical variables on force sensitive resistor error: Implications for calibration and improved accuracy. *J Biomech*. 2016;49(5):786. doi: <http://dx.doi.org/10.1016/j.jbiomech.2016.01.022>.

Chapter 9. The prediction and modelling of socket-residual limb interface mechanics

9.1 Chapter Preface

In this chapter we present a numerical tool with the aim of predicting contact forces at the interface of a transhumeral prosthetic socket and residual limb (RL), as well as compare predicted results to empirically derived values. Our work adapts numerical modelling techniques implemented in studies of lower limb prostheses. Herein we demonstrate a proof concept for the application of finite element analysis (FEA) as a tool to predict and forecast upper limb (UL) socket-RL contact pressures. Foundational techniques are presented that may help further the understanding of mechanical contributors to successful socket fit. Further applications include the evaluation of design decisions prior to the creation of the physical socket, and providing a mechanical basis to guide socket design decisions toward improved fit.

In the context of this thesis, in chapter 7 and 8, we empirically characterized the RL-socket contact interactions of both traditional and sensory integrated prostheses. The empirical data collected necessitated the fabrication of a physical prosthesis. As the field of sensory integrated prostheses continues to advance, so will the need for advanced non-traditional prosthetic sockets to facilitate the integration of prosthetic feedback systems. As such, unique, patient-specific challenges will present themselves and tools to evaluate, refine and iterate solutions will become necessary. In this chapter we demonstrate the feasibility of a numerical model that, with refinement, could forecast the effect of sensory integrated socket design on contact pressures; a mechanical correlate of fit, comfort, and prosthetic use^{1,2}.

9.2 Introduction

Upper limb (UL) loss is a significant injury that has a permanent impact on daily lives of those affected. Following amputation, a prosthesis is commonly prescribed to help restore the lost function of the hand and arm. Yet prosthetic abandonment remains high with literature reporting 20%¹ to 39%³ of UL prosthetic users rejecting their prosthesis. Among the top contributing

factors and priorities for improvement are comfort^{2,4}, function^{2,4}, sensory feedback⁴ and cosmesis².

The prosthetic socket is a key component with substantial influence on prosthetic comfort and function. The socket encompasses the RL and functions as the point of attachment between the user and the prosthesis. At this critical interface, the rigid materials of the prosthesis meet the soft tissue of the residual limb. While prosthetic components come in standard sizes and forms, the prosthetic socket must be custom fit to strategically compress and relieve the soft tissues at targeted anatomical locations on the limb. The term ‘socket fit’ broadly describes the quantitative and qualitative factors impacting prosthetic comfort, suspension and stability on the RL⁵. A well fit socket is largely a product of the socket geometry achieved during fabrication. Clinically, the implications of fit are well acknowledged and much of a prosthetist’s effort is specifically dedicated to the design and fabrication of the socket⁶.

Designing and manufacturing a socket of appropriate geometry is a technically challenging practice as it must result in a suitable, patient specific distribution of surface contact pressures between the socket and RL. The socket interfaces with the exterior surface of the RL and must couple the prosthesis to the user’s underlying skeletal structure through an intermediate layer of highly deformable soft tissue. Inherent to the mechanics of such a system, intended motion driven by the skeletal structure is attenuated by the soft tissue before being translated to the prosthesis⁷. As skeletal motion is lost to the deformation of the soft tissues, it impedes the users’ ability to precisely control or position their prostheses and encumbers prosthetic function. One method of compensating for this during socket fabrication is to strategically compress or relieve soft tissue to stabilize the prostheses and maintain suspension on the RL. This must be completed with consideration given to minimizing the risks of tissue irritation or damage, and patient specific requirements for comfort. This challenge becomes amplified with more proximal amputations, as additional prosthetic components increase the weight and reduce the users’ control over their devices; ultimately increasing the demand placed on the socket and the RL⁵. When compared to those with more distal amputations, prosthetic users with transhumeral or shoulder level amputations are more likely to be dissatisfied and reject their prostheses⁸.

Current UL socket fabrication techniques are largely experience-based, and heuristic in nature. Unique solutions for improved fit are rarely analytically evaluated and often are not documented in scientific literature. Although a limited number of novel UL socket designs aiming to improve fit, function, or control have been reported in literature^{7,9}, the underlying mechanical understanding of how these sockets influence the crucial interface at the RL has yet to be analytically reported. To date, only two quantitative studies report the contact pressure occurring between an UL socket and RL. The first reports maximum pressures as a correlate to discomfort¹⁰, and the second describes anatomical location bearing maximum pressure during transhumeral prosthetic use⁵. These two works provide a foundation on which to build a quantitative understanding of the interactions between socket and limb, by retroactively evaluating the mechanical determinates of socket fit following the fabrication of a physical prosthesis.

Finite element analysis is a predictive numerical technique for solving systems of differential equations that mathematically approximate a system's behavior. Applied in the context of UL prostheses, these computer models hold the potential to help inform and guide quantitatively based socket design decisions. Unlike empirical studies employing instrumentation to measure contact pressures at discrete locations on the RL, FEA holds the advantage of predicting intermediate values that would occur in between sensors. As this modelling technique is performed virtually, once the initial model building is complete, it does not require physical sensors, prosthetic components, or a participant to be present to extract data. In the lower limb FEA modelling has been applied to predict the interactions between the prosthetic socket and residual limb^{11,12}. Typically these studies aim to understand how the socket loads the RL during activities of daily living such as ambulation¹³⁻¹⁷, or aim to predict socket pressures for fabrication purposes^{15,18}. These quantitative models have helped improve the understanding of lower limb prosthetic fit at a very fundamental level and have facilitated objectively based design practices^{11,18}. Yet these techniques do not translate directly to the UL. There is much complexity in dexterous UL movement in contrast to the highly cyclical loading in the lower limb. This creates unique and specific requirements for prostheses to interact with the UL anatomy. Taken

together, applying and adapting FEA modeling techniques to UL sockets holds the potential to develop foundational knowledge to aid in UL socket design for improved fit.

In this chapter we present an UL FEA model intended to predict contact pressures occurring between the prosthetic socket and RL in transhumeral prostheses. We adapted lower limb FEA techniques to build and validate the model's prediction with data from two transhumeral amputee participants. The model and results are presented as a proof of concept with a focus on the clinical implications of our technique and barriers to its potential adoption.

9.3 Methods

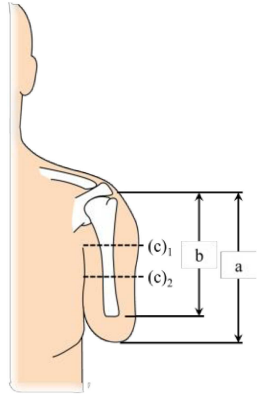
9.3.1 Participants

Two participants with transhumeral amputation were recruited. Participant demographics, RL geometry and a description of each participant's prosthetic components are provided in Table 9-1. Participants provided written informed consent prior to participation and research ethics were approved through the University of Alberta's institutional review board.

Table 9-1 Participant Information. Par denotes the participant number, (c)₁ and (c)₂ denote circumference measurements taken at the axilla and mid-length of the limb, respectively, a denotes the residual limb length taken from the acromion to distal tip of the limb, and b represents the limb length from the acromion to the distal residual humeral tip.

					Residual Limb Dimensions			
					Length (mm)		Circumference (mm)	
	Gender	Height (m)	Weight (Kg)	Side of Amputation	a	b	(c) ₁	(c) ₂
Par 1	Male	1.75	103	Left	290	250	420	380
Par 2	Female	1.73	104	Right	270	230	405	355

	Terminal Device	Elbow	Liner	Harness
Par 1	Hosmer 555 Lyre Hook	Ottobock ErgoArm	WillowWood Alpha Medium	Figure-eight (bilaterally connected)
Par 2	Ottobock 8K23 Hand	Ottobock ErgoArm	WillowWood Alpha Medium	Figure-eight



9.3.2 Model Geometry

Participant recruitment was performed through the Glenrose Rehabilitation Hospital's Prosthetics department. To ensure our work modelled well fit prosthetic sockets, data were collected upon the delivery of a newly refit or adjusted socket. Socket fit was evaluated by a senior certified prosthetist specializing in UL prostheses, and deemed 'well-fit' based on their subjective expertise prior to data collection. To further confirm the quality of socket fit, each participant completed an OPUS Satisfaction with Device survey modified to present questions relevant to prosthetic socket fit¹⁹. This survey and results are included in [Appendix C](#).

For each participant, three main geometric components were modelled, the prosthetic socket, the residual soft tissue, and the residual humerus (bone). Following the initial collection and preparation of the 3D geometry files, the data were imported into ANSYS Workbench 17.1 (ANSYS Inc. Canonsburg, PA, USA) Finite Element Software.

Prosthetic socket geometry was created from each participants existing well fit socket. Similar to standard socket duplicating procedures, plaster casting material was poured into each participant's well-fit socket to create a positive mold. The exterior 3D surface geometries of these molds were digitized using a scanGogh II optical laser scanner (Vorum, Vancouver, Canada) yielding a virtual representation of each participant's prosthetic socket. Additional refinement of these files was performed in SolidWorks 2016 software (Dassault Systemes, Velizy-Villacoublay, France), where excess scanned geometry was removed along the socket trim lines, and a flare was added to the trim line edges to reduce possible stress concentrations and improve contact conditions between the socket and RL. The final geometry was imported into ANSYS Workbench.

A digital scan of an anthropometric humerus (Sawbones, Vashon, WA, USA) was imported into SolidWorks software. Here, the bone geometry was scaled to meet the anthropometric proportion of each participant²⁰ and cropped to match the length of the residual humerus (Figure 9.1), similar to the techniques highlighted by Goh et al.¹⁵.

Soft tissue geometry was created from 3D laser scan geometry¹⁵. Consistent with clinical laser scanning practices, participants were instructed to don their prosthetic liners, abduct their RLs

such that it was not in contact with their thorax, and hold as still as possible. The scanGogh II optical laser scanner was then used to capture the 3D surface geometries distal of the acromion and axilla. These surface files were imported into SolidWorks to be smoothed, patched and refined as necessary. The final surface geometry was converted into a solid and exported into an assembly. Here the residual humerus and soft tissue were virtually positioned relative to each other. To ensure accurate placement, colocations of these two components were dictated through alignment of anatomical landmarks (the acromion, and distal humeral tip) consistent with clinical measurements of each participant's RL. A cavity was then created in the residual soft tissue to exactly match the dimensions of the intersecting bone. Figure 9.1 schematically depicts the process by which the soft tissue geometry was created. Through the application of rigid boundary conditions this bone cavity would serve to model the behavior of the residual humerus (further discussed in the Boundary Conditions section).

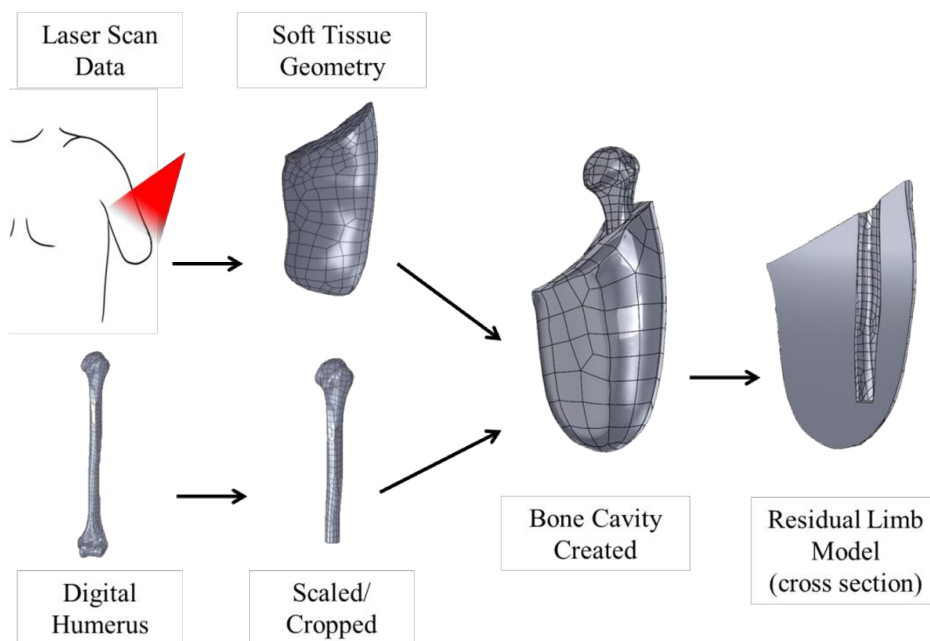


Figure 9.1 Creation of the residual limb model

The final geometry files were imported into ANSYS Workbench. Where the socket and soft tissue were aligned and position such that the surfaces just contacted each other without any initial deformation.

9.3.3 Material Definitions

Consistent with tissue mechanics literature, soft tissue can be expected to demonstrate large deformations and a non-linear force response²¹. An incompressible Mooney-Rivlin hyper-elastic material model was used to define the soft tissue response to loading (9.1)^{12,22}, where W denotes strain energy and I_1 and I_2 represent the first two stress invariants. C_{01} and C_{10} were defined according to the flaccid muscle tissue values of 21.38 MPa and 85.5 MPa, respectively²².

$$W = C_{01}(I_2 - 3) + C_{10}(I_1 - 3) \quad (9.1)$$

Homopolymer polypropylene, a traditional material used in socket fabrication, and mechanical testing on human bone have yielded Young's modulus values of 1.3 GPa²³ and 15GPa¹², respectively. Literature reports linear soft tissue models with Young's modulus values of 1.5×10^{-4} GPa¹². Due to the magnitude of difference in stiffness, the sockets and bones, were modelled as a non-deformable rigid bodies^{15,18} as their deformations were anticipated to be negligible relative to the highly deformable soft tissue.

9.3.4 Meshing

All modelled components were meshed in ANSYS Workbench. The soft tissue was discretized using quadratic tetrahedral elements^{14,15} to facilitate the components irregular shape and the anticipated large deformations. An initial seed constraint limiting elements to a maximum of 9mm was implemented. Refinement of the region surrounding the distal tip of the humeral bone cavity and edges of the soft tissue was performed in which a maximum element size of 4.5mm was implemented. Due to the large surface area, thin profile, and irregular shape of the prosthetic socket, the rigid geometry was discretized using non-linear triangular elements^{18,24}. This resulted in 91,826 elements (137,413 nodes) used for participant 1, and 114348 elements (168070 nodes) for participant 2. Additionally, a mesh sensitivity analysis was performed to ensure the stability

of predicted results to the mesh geometry. A description of the analysis and results are included in [Appendix E](#).

9.3.5 Contact, Loading, and Boundary Conditions

A frictionless pure-penalty contact was applied between the exterior surface of the soft tissue and socket surfaces. A penetration tolerance of 1mm and normal contact stiffness factor of 10 were used to further define the contact formulation.

Loading and boundary conditions were applied to reflect to two loading steps: 1) the physical act of the RL being pressed into the socket (donning the prosthesis), 2) the loading imparted as a result of the prosthetic weight and the user's posture (prosthetic loading).

1) Donning the prosthesis was modelled through a rigid zero-displacement boundary condition applied to the surface nodes of the bone cavity. A displacement boundary condition was defined about the rigid surface of the socket such that it would slide over and compress the soft tissue to reach its donned positioned (Figure 9.2).

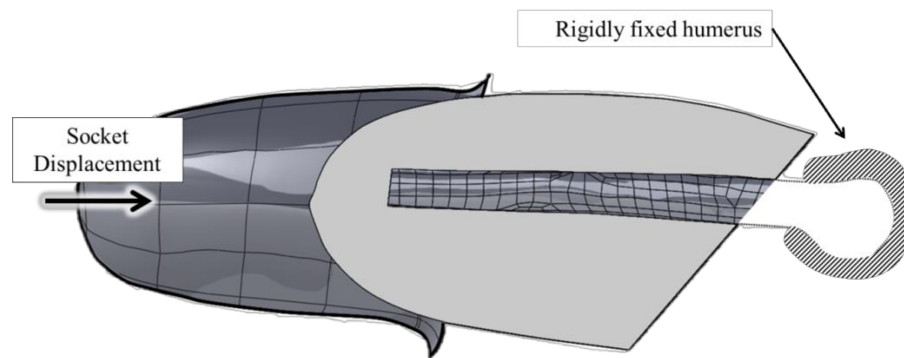

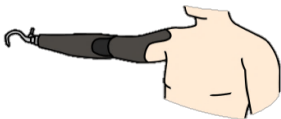


Figure 9.2 Boundary conditions employed to simulate socket donning. Where the rigidly fixed humerus was represented by rigidly tying surface nodes of the bone cavity to a fixed remote point located at the center of the humeral head.

2) Prosthetic loading was modelled through the application of boundary and loading conditions to simulate two physical loading conditions: Position 1 (90° prosthetic elbow flexion), and

Position 2 (full prosthetic elbow extension with shoulder flexion in the plane of the scapula) (Table 9-2). These positions were selected to represent a neutral position and a mechanically demanding position (at the extreme of the prosthetic's range of motion), respectively⁵. Once the socket donning step was complete, displacement and force boundary conditions were applied to represent the residual skeletal structure supporting the weight of the prosthesis. A zero displacement boundary condition was applied to the rigid socket to fix it in place. A remote displacement boundary condition was applied to tie the surface nodes of the bone cavity to a remote proximal point representative of the shoulder's approximate center of rotation (as physically measured on the participants, 250mm and 230mm proximal of the humeral tip for Participant 1 and 2, respectively). This point was fixed from translation and allowed to rotate in the plane of the prosthetic reaction force describe below. Force was applied to the distal tip of the rigid bone cavity to simulate the reaction forces at the humerus as a result of prosthetic loading. This reaction force was calculated from the weight and dimensions of the participants' prosthetic components ([Appendix D](#)). Forces applied to participant 1 were 5.76N and 8.60N for positions 1 and 2, respectively, while participant 2 had forces applied of 7.48N and 9.35N for positions 1 and 2, respectively (Table 9-2). Boundary and loading conditions are schematically depicted in Figure 9.3.

Table 9-2 Modelled positions and applied reaction forces

	Prosthetic Reaction Forces	
		
	Position 1	Position 2
Participant 1	5.76 N	8.60 N
Participant 2	7.48 N	9.35 N

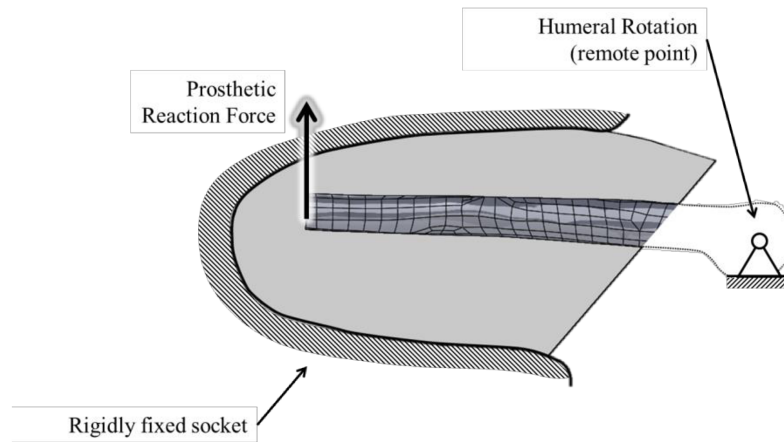


Figure 9.3 Boundary and loading conditions employed to simulate prosthetic loading. The humerus was represented by rigidly tying surface nodes of the bone cavity to a remote point located at the center of the humeral head. This point was fixed in translation and allowed to rotate on the axis of the plane of the prosthetic reaction force.

9.3.6 Model Evaluation

Our work used two empirical RL-socket interface studies to evaluate the model's ability to predict contact pressures and locations. The first work was a study in which our same 2 participants and their modelled prosthetic components were previously studied⁵ (chapter 7). The aim of this study was to evaluate socket-RL interface contact pressure by identifying anatomical locations in which local maximums occurred. Therefore, we compared and contrasted the locations of local pressure maximums predicted by our FEA model with the empirically measured results reported for our participants in the previous study⁵. Secondly, we compared and contrasted the maximum contact pressure values to those reported in a separate study of transhumeral prostheses¹⁰. Although our participants were not directly involved in this second study, it served to verify that our model's predicted values were within the same magnitude as reported in other transhumeral prosthetic users.

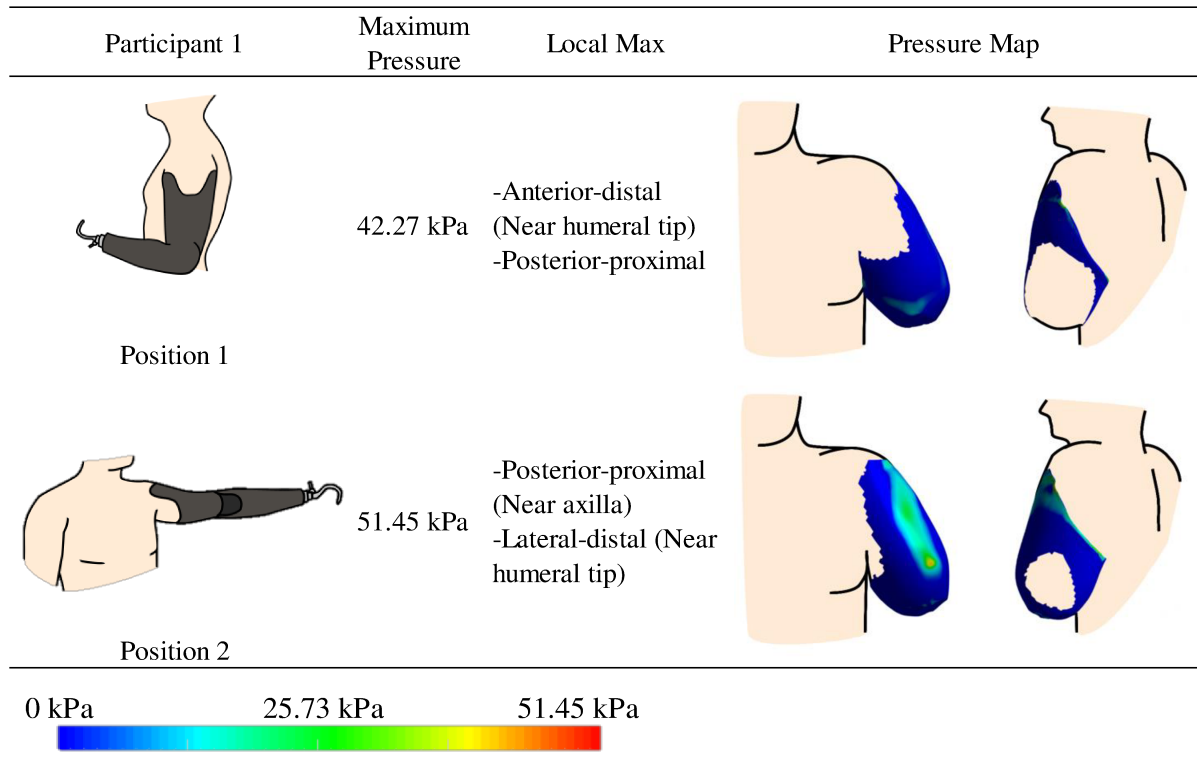
9.4 Results

9.4.1 Participant 1

Participant 1 had a left side transhumeral amputation (the tested limb) and right side transradial amputation. The participant reported that they wore the prosthesis for 12 to 15 hours each day. Investigators noted that the RL was abundant in soft tissue, with less muscle tissue than a typical patient with transhumeral amputation. Additionally, investigators noted redness and minor skin irritation near the proximal aspects of the RL close to the axilla. However, when asked about the comfort of the socket and the irritation on the limb, the participant confirmed his satisfaction with socket fit. The research prosthetist further verified that the socket was in fact well-fit prior to data collection. OPUS Satisfaction with Device survey results can be found in [Appendix C](#).

Modelling the prosthesis at 90° elbow flexion (position 1) resulted in a maximum predicted contact pressure of 42.47kPa. The location of this global maximum was at a small, concentrated location on the posterior proximal side of the RL in close proximity to the axilla. Additional local maximums were predicted on the anterior distal regions of the RL near the tip of the residual humerus and along the posterior socket trim lines. In this position, the model predicted minimal to no contact at the distal posterior region of the RL. When modelling the prosthesis in full elbow extension with shoulder flexion in the plane of the scapula (position 2), a maximum predicted contact pressure of 51.45kPa was determined. Again a global maximum was predicted in the same concentrated location on the posterior proximal side of the RL near the axilla. A second local maximum presented itself on a lateral distal region of the RL near the humeral tip. Again, minimal to no contact was predicted at the distal posterior region of the RL. Results are presented in Table 9-3.

Table 9-3 Participant 1 predicted contact pressure results. Pressure values are provided in units of kilopascals (kPa). Note areas on the residual limb not in contact with the socket are indicated in beige.



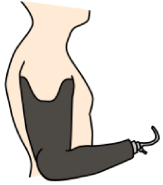
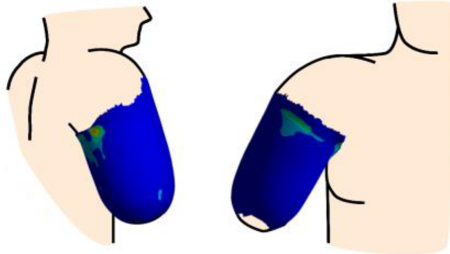
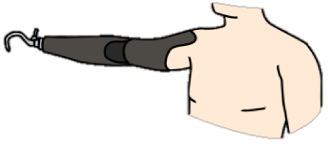
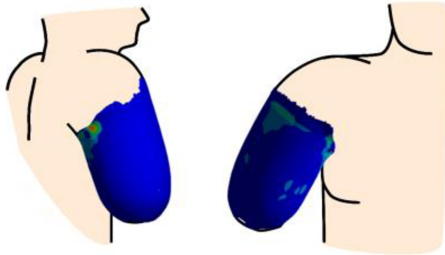

9.4.2 Participant 2

Participant 2 had a right transhumeral amputation. They reported using their prosthesis infrequently during the course of an average day. Investigators did not note any visible redness or irritation on the participant RL. Both the research prosthetist and participant confirmed their satisfaction with socket fit prior to data collection. OPUS Satisfaction with Device survey results can be found in [Appendix C](#).

Modelling the prosthesis at 90° elbow flexion (position 1) resulted in a maximum predicted contact pressure of 45.43kPa. The location of this global maximum was confined to a concentrated location on the medial proximal RL near the axilla. An additional local maximum

was predicted on the anterior proximal regions of the RL along the sockets anterior trip line. When modelling the prosthesis in full elbow extension with shoulder flexion in the plane of the scapula (position 2), a maximum predicted contact pressure of 47.71kPa was determined. Again, the global maximum was predicted in the same concentrated location on the posterior proximal side of the RL near the axilla. Additional local maximums were predicted near the socket's anterior trim lines and on a medial distal region of the RL near the humeral tip. Results are presented in Table 9-4.

Table 9-4 Participant 2 contact pressure results. Pressure values are provided in units of kilopascals (kPa). Note areas on the residual limb not in contact with the socket are indicated in beige.

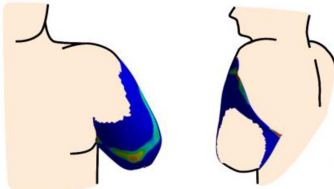
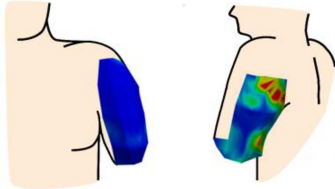
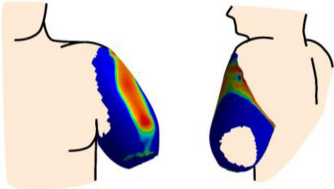
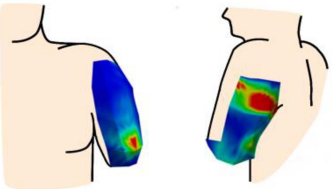
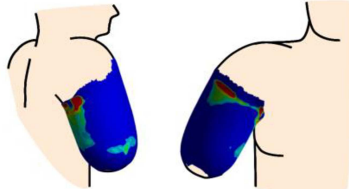
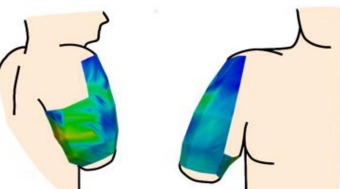
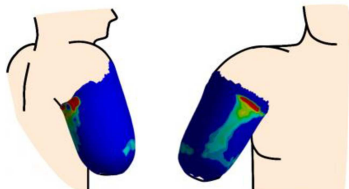
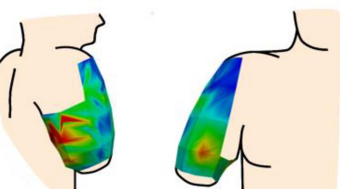

Participant 2	Maximum Pressure	Local Max	Pressure Map
 Position 1	45.43 kPa	-Anterior proximal -Medial-proximal (Near axilla)	
 Position 2	47.71 kPa	-Anterior proximal -Medial-proximal (Near axilla) -Medial-distal	
<div> <div>0 kPa</div> <div>25.73 kPa</div> <div>51.45 kPa</div>  </div>			

9.4.3 Model Evaluation

The ability of the model to accurately predict and represent the physics of the UL socket-RL interface was evaluated by comparing its output to physical measurements of interface pressures. Both participants were previously involved in a study that placed thin film sensors between the

RL and prosthetic liner prior to donning their prosthesis and characterized contact pressure distributions across the RL⁵. Table 9-5 presents descriptions of the local maximums predicted through our finite element model next to the results of the empirical Schofield et al. study⁵ (chapter 7). Predicted anatomical locations bearing local pressure maximums demonstrated some congruency with the locations of local maximums reported by Schofield et al. This helps provide confidence to the models ability to predict key load bearing locations on the RL; however, differences were also present. For participant 1, an area of no contact was predicted on the distal posterior region of the RL that was not present in the empirical data. Additionally for participant 2 a local maximum was predicted on the anterior proximal RL that was not presented in the empirical data. Explanations for this divergence are provided in the discussion section. In a separate study that empirically quantified contact pressure occurring in three participants' transhumeral prostheses, maximum pressures values in a range of 2.8psi (19.31kPa) to 7.6psi (54.40kPa) across a variety of limb positions including shoulder flexion, shoulder transverse abduction, elbow flexion, and shoulder internal rotation¹⁰. The maximum values reported in our work ranged from 42.27kPa to 51.45kPa, well within this previously reported range.

Table 9-5 Validation of predicted locations of high contact pressure. Pressure values are provided in units of kilopascals (kPa). Note predicted pressure values were scaled to a maximum of 12.5 kPa to allow for comparison to the empirical data presented in Schofield et al.⁵ (Chapter 7), in the ‘Predicted contact pressure column’ areas on the residual limb not in contact with the socket are indicated in beige. In the ‘Schofield et al.’ column areas on the residual limb in beige did not receive sensor coverage.

Predicted contact pressures			Schofield et al. study ⁵		
Pressure Map		Local Maximums	Pressure Map		Local Maximums
Participant 1					
		-Anterior-distal (Near humeral tip) -Posterior-proximal			- Posterior-proximal (Near axilla)
Position 1			Position 1		
		-Posterior-proximal (Near axilla) -Lateral-distal (along residual humerus)			- Posterior-proximal (Near axilla) -Lateral-distal (Near humeral tip)
Position 2			Position 2		
Participant 2					
		-Anterior proximal -Medial-proximal (Near axilla) -Medial-distal			-Posterior medial-proximal (Near axilla)
Position 1			Position 1		
		-Anterior proximal -Medial-proximal (Near axilla)			-Posterior medial-proximal (Near axilla) -Lateral-distal (Near humeral tip)
Position 2			Position 2		
<div>0 kPa6.25 kPa12.50 kPa</div> 					

9.5 Discussion

In this chapter we described a numerical model intended to predict contact pressure development between transhumeral prosthetic sockets and RL. Here we retrospectively evaluated the well-fit socket designs of two transhumeral prosthetic users as a demonstration of the application of FEA in predicting socket-RL contact pressures.

In both participants, proximal areas near the axilla were predicted to experience local contact pressure maximums. This result is likely a reflection of socket geometry derived through a very specific design consideration. During socket fabrication this area is often targeted for higher tissue compression as it provides increased shoulder mobility, socket stabilization in the coronal plane, and helps avoid socket contact with the thorax⁵. Although it may lead to possible destabilizing affects in the sagittal plane and higher local contact pressures, the functional benefits often out way these drawbacks. For participant 1, the investigators noted mild tissue irritation in this same area, although both the research prosthetist and participant expressed satisfaction with the socket's fit. As an individual with bilateral amputation the daily use of the prostheses (12-15 hours per day) and dependency is amplified. At this location it is likely that the combination of higher contact pressures, high prosthetic usage, and noted abundance in soft tissue resulted in tissue irritation. This observation provided further confidence in our model, as this area exhibiting tissue irritation was also identified in our model as a key location bearing high contact pressures.

In both participants, especially with the prosthetic elbow extended and participants' shoulders flexed (position 2), the model predicted local areas of high contact pressure anterior near the distal humeral tip and posterior in proximal regions near socket trim lines and the axilla. This predicted loading pattern likely resulted from the prosthetic's center of gravity being positioned distal to the RL. As the RL soft tissue deformed under the weight of the prosthesis, a loading moment was introduced as the underlying boney tip of the residual humerus acted as a fulcrum. This action was counterbalanced by the posterior proximal regions of the RL. This is nearly unavoidable due to the physics of the prosthetic socket encapsulating the RL. In more extreme cases, this action results in proximal gapping, a phenomenon by which the socket loses contact with portions of the RL while counterbalancing and concentrating prosthetic loads on other

locations. This may promote discomfort or limit the range of motion achieved by the prosthesis⁵. Our data suggests that the model was able to predict this well-known prosthetic fitting challenge.

Model evaluation was a key piece of the data presented in this chapter. This crucial step helped establish an understanding of the potential errors, and inherent limitations of our model. Yet, in previous prosthetic literature this important step as it is often overlooked^{18,24,25}. Therefore, a strength of our work is the comparison of our predicted pressure data to the contact pressure maps derived from our same participants in a prior study⁵ (chapter 7). Most of the predicted anatomical locations bearing high contact pressures are in agreement with those derived empirically, including the presences of high contact pressures near the axilla, and the local pressure maximums near the distal humeral tip in position 2 of both participants. However, differences in in the predicted pressures and empirical data were also present.

For participant 1 our model predicted a region of no contact on the distal posterior RL that was not present in the empirical data. A possible explanation is that we represented the RL and liner as one single component in our model, and the empirical data were derived by placing pressure sensors between the RL and liner. As the intent of a liner is to pre-shape/ pre-compress the RL limb and more evenly distribute contact pressure, the true contact pressure occurring on the limb was not predicted in our model. The pre-compression of residual soft tissue, resulting from the liner, may explain the presence of empirically measured pressure on the distal posterior RL; yet, these measurements would not be able to capture separation of the liner from the socket wall, as predicted by our model. This is further supported by the data presented in chapter 7 (Figure 7.3), where an initial pressure was measured in this same distal posterior region with just the prosthetic liner donned (prior to donning the prosthesis).

For participant 2, the model predicted a proximal anterior region of the RL forming a local pressure maximum that was not consistent with the empirical data. When collecting the empirical data, it is possible that sensor coverage was not complete in this region especially in the results of position 2 (Table 9-5). Further empirical data collection may provide additional confidence in the modelled results. However, this region also falls near a socket trim line. Mathematically, in the model, this trim line would form an edge that is in contact with the soft tissue surface. This type of interaction often results in stress concentrations that may lead to an increase in the

predicted contact pressure. Further refinement of local meshes and contact definitions in this area may help mitigate these effects and warrant further investigation.

As a final evaluation of the model, we compared the maximum contact pressures measured in previous literature with those predicted by our model. The maximum pressure values predicted in our work fall within the reported values in past literature; however, socket fit is unique to the individual patient's morphology, prosthetic componentry, and comfort preferences. As our model did not validate the predicted maximum pressure values against empirically derived maximum values specifically from the participants recruited in our study, we cannot speak to the true accuracy of predicted values. Yet, this test provides subjective confidence in the relative magnitude of our predicted values.

As computer aided manufacturing techniques continue to see growth in prosthetic shops, the potential application of numerical predictive techniques is evident. With further refinement of our technique, there is the potential to pair with the output of these virtual systems and provide socket fit analysis prior to the fabrication of a physical socket^{11,15,18}. Although encouraging results are presented, substantial barriers must first be addressed to translate these techniques into a clinical socket fabrication setting. For clinical staff to adopt FEA, and our model, as a design tool, the need for specialized technical expertise must be minimized. User friendly interfaces must be developed to parametrically adjust simplified models incorporating the RL, prosthetic componentry, and load applications. Further refinement to achieve simplified, validated and arcuate models for this task will be necessary to reduce technical complexity and computation time; from hours to minutes or less. Confidence in the predicted result will also play a pivotal role in clinical adoption. Further large scale studies that develop stable accurate models, and validate the models through empirically collected data will be necessary. Validation is crucial to the confidence of predicted results and often not performed in current literature^{18,24,25}. In our work, comparing model output to empirical measurements was fundamental to understanding the specific limitations of our modelling choices, and helped identify inconsistencies between predicted values and those measured empirically. This information is crucial to the future development toward clinical applications.

Inherent to any numerical model are mathematical assumptions and limitations. The soft tissue of our model is represented as a single component with a single hyper-elastic material definition. The effects of individual tissues such as skin, muscle and fat may slightly change resulting contact pressures. Further investigations around tissue material properties and geometry defining individual tissues may be warranted. Finite element analysis can allow for the prediction of internal stress and strain development within the RL. This may provide insight into tissue injury mechanisms or further information with regard to socket stability and security. Although our model can predict internal stress and strain values, it would not be possible to validate the results given our current data set. Further modelling studies that validate internal tissue mechanics with imaging data may provide additional insight into socket fit and function.

9.6 Conclusions

In this chapter we present a numerical technique that aims to predict and potentially forecast socket-RL contact pressures. These first foundational steps hold the potential to inform socket fabrication practices, and help guide design decisions for improved socket fit. Yet, many practical barriers still exist such as improved runtimes, simplified user interfacing, and further model validation; however the powerful utility of numerical predictive techniques warrant the refinement and investigation necessary. A refined, user friendly, predictive model holds the potential to help shift socket fabrication away from purely experience based practices, and deliver well-fit prostheses with fewer revisions of the physical socket. The overall implication of which is the delivery of more comfortable and functional sockets. In the context of sensory integrated prosthesis, FEA holds the potential to forecast the mechanical impact of installing sensory feedback systems into prostheses. As sensory integrated prostheses continue to be developed, unique socket solutions will inherently be required. This work can help unlock the evaluation of the necessary non-traditional sockets prior to fabricating the physical device. This may result in reduced prototype iterations, and fabrication time prior to arriving at a successful sensory integrated prosthesis. The work presented in this chapter demonstrates the feasibility of FEA in traditional prosthetic design, and builds the foundations for novel socket design in a virtual iterative environment.

References

1. Biddiss E, Chau T. Upper-limb prosthetics: Critical factors in device abandonment. *Am J Phys Med Rehabil*. 2007;86(12):977-987. Accessed 16 March 2017. doi: 10.1097/PHM.0b013e3181587f6c.
2. Schultz AE, Baade SP, Kuiken TA. Expert opinions on success factors for upper-limb prostheses. *Journal of Rehabilitation Research and Development*. 2007;44(4):483-489. Accessed 5 April 2013.
3. Biddiss E, Chau T. Upper limb prosthesis use and abandonment: A survey of the last 25 years. *Prosthet Orthot Int*. 2007;31(3):236-257. Accessed 24 January 2014.
4. Biddiss E, Beaton D, Chau T. Consumer design priorities for upper limb prosthetics. *Disability and Rehabilitation: Assistive Technology*. 2007;2(6):346-357. Accessed 5 April 2013.
5. Schofield JS, Schoepp KR, Williams HE, Carey JP, Marasco PD, Hebert J.S. Characterization of interfacial socket pressure in transhumeral prostheses: A case series. *PLoS ONE*. 2017.
6. Sanders J. Stump-socket interface conditions. In: *Pressure ulcer research: Current and future perspectives*. Heidelberg Germany: Springer-Verlag Berlin; 2005:129-147. Accessed 25 January 2016.
7. Alley RD, Williams TW, Albuquerque MJ, Altobelli DE. Prosthetic sockets stabilized by alternating areas of tissue compression and release. *Journal of Rehabilitation Research and Development*. 2011;48(6):679-696. Accessed 5 April 2013.
8. Mcfarland LV, Winkler SLH, Heinemann AW, Jones M, Esquenazi A. Unilateral upper-limb loss: Satisfaction and prosthetic-device use in veterans and servicemembers from vietnam and OIF/OEF conflicts. *J Rehabil Res Dev*. 2010;47(4):299-316. Accessed 29 November 2016. doi: 10.1682/JRRD.2009.03.0027.

9. Lake C, Dodson R. Progressive upper limb prosthetics. *Phys Med Rehabil Clin N Am*. 2006;17(1):49-72. Accessed 5 April 2013.
10. Daly W, Voo L, Rosenbaum-Chou T, Arabian A, Boone D. Socket pressure and discomfort in upper-limb prostheses: A preliminary study. *Journal of Prosthetics and Orthotics*. 2014;26(2):99-106. Accessed 22 April 2014.
11. Zachariah SG, Sanders JE. Interface mechanics in lower-limb external prosthetics: A review of finite element models. *IEEE Trans Rehabil Eng*. 1996;4(4):288-302. Accessed 26 January 2016. doi: 10.1109/86.547930.
12. Zhang M, Mak AFT, Roberts VC. Finite element modelling of a residual lower-limb in a prosthetic socket: A survey of the development in the first decade. *Medical Engineering and Physics*. 1998;20(5):360-373. Accessed 31 January 2014.
13. Peng H-, Hsu LH, Huang GF, Hong DY. The analysis and measurement of interface pressures between stump and rapid prototyping prosthetic socket coated with a resin layer for transtibial amputee. *IFMBE Proceedings*. 2009;23:1720-1723. Accessed 22 April 2014.
14. Faustini MC, Neptune RR, Crawford RH. The quasi-static response of compliant prosthetic sockets for transtibial amputees using finite element methods. *Medical Engineering and Physics*. 2006;28(2):114-121. Accessed 23 February 2016.
15. Goh JCH, Lee PVS, Toh SL, Ooi CK. Development of an integrated CAD-FEA process for below-knee prosthetic sockets. *Clin Biomech*. 2005;20(6):623-629. Accessed 2 February 2014.
16. Jia X, Zhang M, Wang R, Jin D. Dynamic investigation of interface stress on below-knee residual limb in a prosthetic socket. *Tsinghua Science and Technology*. 2004;9(6):680-683. Accessed 23 February 2016.
17. Lee WCC, Zhang M, Jia X, Cheung JTM. Finite element modeling of the contact interface between trans-tibial residual limb and prosthetic socket. *Medical Engineering and Physics*. 2004;26(8):655-662. Accessed 23 February 2016.

18. Colombo G, Facchetti G, Morotti R, Rizzi C. Physically based modelling and simulation to innovate socket design. *Computer-Aided Design and Applications*. 2011;8(4):617-631. Accessed 9 February 2014.
19. Heinemann AW, Bode RK, O'Reilly C. Development and measurement properties of the orthotics and prosthetics user's survey (OPUS): A comprehensive set of clinical outcome instruments. *Prosthet Orthot Int*. 2003;27(3):191-206. Accessed 24 February 2014.
20. Winter DA. *Biomechanics and motor control of human movement*. Hoboken, N.J.: John Wiley & Sons; 2005.
21. Tönük E, Silver-Thorn MB. Nonlinear viscoelastic material property estimation of lower extremity residual limb tissues. *J Biomech Eng*. 2004;126(2):289-300. Accessed 6 October 2013.
22. Zhang L, Zhu M, Shen L, Zheng F. Finite element analysis of the contact interface between trans-femoral stump and prosthetic socket. *Proceedings of the Annual International Conference of the IEEE Engineering in Medicine and Biology Society, EMBS*. 2013:1270-1273. Accessed 2 March 2014.
23. INEOS Global. Typical engineering properties of polypropylene.
<http://www.ineos.com/Global/Olefins%20and%20Polymers%20USA/Products/Technical%20information/Engineering%20Properties%20of%20PP.pdf>. Updated 20102014.
24. Nehme G, Dib M. Impact of pressure distribution on the relief areas of prosthetic sockets for transtibial amputees using design of experiment and finite element analysis. *Journal of Prosthetics and Orthotics*. 2011;23(4):170-183. Accessed 23 February 2016.
25. Lenka P, Choudhury A. Analysis of trans tibial prosthetic socket materials using finite element method. *J. Biomedical Science and Engineering*. 2011;4:762.

Chapter 10. Conclusions and Future Directions

Upper limb (UL) amputation is one of the most difficult challenges for prosthetic replacement given the dexterous capabilities of a healthy hand and the complexity of its fine sensory input. In recent years, UL prostheses have undergone substantial technological development to improve their function, and utility^{1,2}, yet abandonment remains high for electric prostheses with 23% to 39% of users rejecting their devices³. Among the top contributors to rejection lays the lack of sensory feedback^{3,4}. In healthy intact limbs, feedback mechanisms relay touch and movement information to higher control centers that are responsible for planning and actuating limb movement^{5,6}. In an UL prosthesis, this information is unavailable to the user, forcing a heavy reliance on visual feedback and other indirect measures to infer the state of the prosthesis^{7,8}. The cognitive demand placed on the user is greatly increased as operation of the prosthesis requires high and continuous attention⁹. This often leaves the user overwhelmed, frustrated and more prone to abandon the device.

In this thesis we explore and develop a novel sensory feedback technique allowing prosthetic movement to be experienced as though it occurred in the missing limb. This work presents a complete arc beginning with the exploration and refinement of our feedback technique in an able-bodied population in chapter 1, through the translation to an amputee population in chapter 4, and finally the integration into a functional prosthesis in chapter 8. Furthermore, in chapter 7 and chapter 9 we developed empirical and predictive tools to build an understanding of prosthetic socket interface mechanics to facilitate the development of non-traditional sockets for the incorporation of sensory feedback devices. These techniques allow for a departure from current heuristic clinical practices by providing a quantitative visual tool set to understand how specific design decisions may impact load bearing anatomy, socket fit and comfort.

Part I: Development of our feedback approach

Kinesthesia, the sense of limb movement, is vital to UL motor control. Through the development of the novel necessary background information and translation into amputee trials, we demonstrate in chapter 4 that it is possible to leverage the anatomy of participants who have

previously undergone targeted reinnervation surgery, and the kinesthetic illusion, to purposefully elicit the perception of missing hand movement. We further established that these movement percepts can be matched to the movement of a multi-dexterous prosthetic hand through a demonstration of real-time bidirectional control of commercially available prosthetic components. Addressing a challenge faced by many sensory feedback techniques, our approach provided intuitive, relevant information to the user, and was readily interpreted as movement sensation in the missing hand.

Part II: Translation into functional prostheses

To fully realize the functional utility of our technique, it was necessary to transition our kinesthetic feedback system from a desktop setup into a functional prosthesis. This crucial step is often overlooked in literature, and is a substantial barrier in the development of sensate prostheses. Achieving this task required the development of a non-traditional prosthesis that integrated feedback componentry without compromising the traditional requirements of prosthetic fit and comfort. This task necessitated the mechanical understanding of how traditional prostheses interact with the RL developed in chapter 7. In chapter 8 a novel sensory integrated prosthesis was developed. As this system employed a non-traditional prosthetic socket, the interaction between the RL and socket were empirically evaluated to appreciate the mechanical implications of the design. Beyond integration, as a proof-of-concept, in chapter 9, we demonstrated the feasibility of a numerical model capable of forecasting the contact mechanics at the RL-socket interface in transhumeral prosthesis. With further refinement, this model could enable the evaluation of how novel sensory integrated sockets interact with the RL prior to fabrication of the physical socket. Together this work delivers a design and evaluation tool-set capable of informing the fabrication practices of both traditional and sensory integrated prosthetic sockets.

This work provides an encouraging non-invasive technique to establish kinesthetic feedback in functional prostheses. The strengths of this work lay in the translation of techniques beyond the benchtop with a translational focus on integration with commercially available myoelectric prosthesis. The engineering nature of these integration tasks necessitated the development of

foundational information that is largely absent in previous literature, such as understanding the socket interfaces mechanics of transhumeral prostheses. The conceptualization and fabrication of sensory-integrated prosthetic sockets is fundamentally a design-based challenge. As such, analytical and quantitative design approaches, as well as traditional experience based fabrication techniques must be implemented to arrive at informed, effective solutions. Although advanced sensory feedback techniques will continue to be developed, it is only once integration challenges are addressed and sensory feedback systems are installed in functional prostheses, that the true efficacy can be evaluated. This work provides foundational tools to enable these necessary integration and evaluation activities.

10.1 Future Directions

In moving forward, investigations with a larger participant group will be necessary. Integrating kinesthetic feedback in multiple participants' individual prosthetic sockets will likely uncover a number of unique design challenges. Documenting and disseminating socket designs, solutions to integration challenges, and the resulting contact mechanics will further establish the foundations necessary for development of fully functional sensory-motor prostheses. Furthermore, functional testing remains a key component of evaluation that needs to be addressed. Once a sensory feedback strategy, such as our kinesthetic technique, is implemented in a functioning prosthesis, evaluating users' performance with and without feedback is essential. The development of meaningful tests, representative of daily activities, and sensitive to changes when sensory information is provided, will be required to fully evaluate the practical efficacy of our kinesthetic feedback strategy.

The kinesthetic illusion is a phenomenon that has been documented in intact upper limbs and lower limbs at all joint levels. Therefore, it can be hypothesized that it is possible to elicit illusions of missing joints in both lower and upper limb amputees with varying levels of amputation. In these populations it would be anticipated that vibration of residual muscles may introduce percepts of movement in the joint that the muscles once actuated; for example vibration of the residual gastrocnemius in transtibial amputees may introduce percepts of the missing ankle or foot movement. This would dramatically expand the application of our

techniques to most levels of limb amputation without the requirement of targeted reinnervation surgery. This thesis lays the foundation for the continued application of our kinesthetic feedback technique beyond targeted reinnervation populations.

Continuing to quantify the interactions between socket and RL will become important as novel socket will need to be developed to incorporate sensory feedback systems. When a unique socket solution is achieved it is important to quantitatively analyze and document what makes it successful, and how it mechanically interacts with the RL. To this end, the utility of numerical predictive models can play a key role. The model presented in Chapter 9 demonstrates the feasibility of predicting interface contact pressure in traditional transhumeral socket. However, this work can be expanded to forecast and evaluate both traditional and novel sensory-motor prosthetic sockets. Refinement is necessary to translate the modelling into clinical use; however, with refinement, such a forecasting tool can be tremendously advantageous during socket conceptualization and design as it can evaluate contact pressures virtually before a socket is fabricated. To arrive at this stage, efforts to simplify the model, parameterizes variables, decrease computation time, and develop user friendly interfaces are necessary. This is a significant undertaking; however the implications of such a tool could potentially shift fabrication practice toward analytically based design decisions. This may result in reduced fabrication times, better fit prosthetic sockets, and ultimately an improved quality of patient care.

10.2 References

1. Belter JT, Segil JL, Dollar AM, Weir RF. Mechanical design and performance specifications of anthropomorphic prosthetic hands: A review. *Journal of Rehabilitation Research and Development*. 2013;50(5):599-618. Accessed 27 February 2014.
2. Zlotolow DA, Kozin SH. Advances in upper extremity prosthetics. *Hand Clin*. 2012;28(4):587-563. Accessed 8 April 2015.
3. Biddiss E, Chau T. Upper limb prosthesis use and abandonment: A survey of the last 25 years. *Prosthet Orthot Int*. 2007;31(3):236-257. Accessed 24 January 2014.

4. Biddiss E, Chau T. Upper-limb prosthetics: Critical factors in device abandonment. *Am J Phys Med Rehabil*. 2007;86(12):977-987. Accessed 16 March 2017. doi: 10.1097/PHM.0b013e3181587f6c.
5. Gordon J, Ghilardi MF, Ghez C. Impairments of reaching movements in patients without proprioception. I. spatial errors. *J Neurophysiol*. 1995;73(1):347-360. Accessed 24 May 2017.
6. Ghez C, Gordon J, Ghilardi MF. Impairments of reaching movements in patients without proprioception. II. effects of visual information on accuracy. *J Neurophysiol*. 1995;73(1):361-372. Accessed 24 May 2017.
7. Schofield JS, Evans KR, Carey JP, Hebert JS. Applications of sensory feedback in motorized upper extremity prosthesis: A review. *Expert Review of Medical Devices*. 2014;11(5):499-511. Accessed 8 April 2015.
8. Lundborg G, Rosen B, Lindstrom K, Lindberg S. Artificial sensibility based on the use of piezoresistive sensors. *J Hand Surg*. 1998;23 B(5):620-626. Accessed 3 December 2013.
9. Gonzalez J, Soma H, Sekine M, Yu W. Auditory display as a prosthetic hand biofeedback. *Journal of Medical Imaging and Health Informatics*. 2011;1(4):325-333. Accessed 3 December 2013.

References

Chapter 1

1. Biddiss E, Chau T. Upper limb prosthesis use and abandonment: A survey of the last 25 years. *Prosthet Orthot Int.* 2007;31(3):236-257. Accessed 24 January 2014.
2. Biddiss E, Chau T. Upper-limb prosthetics: Critical factors in device abandonment. *Am J Phys Med Rehabil.* 2007;86(12):977-987. Accessed 16 March 2017. doi: 10.1097/PHM.0b013e3181587f6c.
3. Kuiken TA, Dumanian GA, Lipschutz RD, Miller LA, Stubblefield KA. The use of targeted muscle reinnervation for improved myoelectric prosthesis control in a bilateral shoulder disarticulation amputee. *Prosthet Orthot Int.* 2004;28(3):245-253. Accessed 20 December 2013.
4. Hebert J.S., Elzinga K., Chan M., Olson J., Morhart M. Updates in targeted sensory reinnervation for upper limb amputation. *Current Surgery Reports.* 2014;2(45).
5. Kuiken TA, Marasco PD, Lock BA, Harden RN, Dewald JPA. Redirection of cutaneous sensation from the hand to the chest skin of human amputees with targeted reinnervation. *Proc Natl Acad Sci U S A.* 2007;104(50):20061-20066. Accessed 20 December 2013.
6. Schofield JS, Evans KR, Carey JP, Hebert JS. Applications of sensory feedback in motorized upper extremity prosthesis: A review. *Expert Review of Medical Devices.* 2014;11(5):499-511. Accessed 8 April 2015.
7. Goodwin GM, McCloskey DI, Matthews PBC. The contribution of muscle afferents kinaesthesia shown by vibration induced illusions of movement and by the effects of paralyzing joint afferents. *J Physiol (Lond).* 1972;536:635-647. Accessed 24 May 2013.

Chapter 2

1. Ziegler-Graham K, MacKenzie EJ, Ephraim PL, Travison TG, Brookmeyer R. Estimating the prevalence of limb loss in the united states: 2005 to 2050. *Arch Phys Med Rehabil.* 2008;89(3):422-429. doi: <http://dx.doi.org/10.1016/j.apmr.2007.11.005>.
2. Lake C, Dodson R. Progressive upper limb prosthetics. *Phys Med Rehabil Clin N Am.* 2006;17(1):49-72. Accessed 5 April 2013.
3. A.M.R.Agur MJL. *Grant's atlas of anatomy.* 10th ed. Lippincott Williams and Wilkins; 1999.
4. Belter JT, Segil JL, Dollar AM, Weir RF. Mechanical design and performance specifications of anthropomorphic prosthetic hands: A review. *Journal of Rehabilitation Research and Development.* 2013;50(5):599-618. Accessed 27 February 2014.
5. Cloutier A, Yang J. Design, control, and sensory feedback of externally powered hand prostheses: A literature review. *Crit Rev Biomed Eng.* 2013;41(2):161-181. Accessed 27 February 2014.
6. Lundborg G, Rosén B. Sensory substitution in prosthetics. *Hand Clin.* 2001;17(3):481-488. Accessed 24 May 2013.

7. Kim K, Colgate JE, Santos-Munné JJ, Makhlin A, Peshkin MA. On the design of miniature haptic devices for upper extremity prosthetics. *IEEE/ASME Transactions on Mechatronics*. 2010;15(1):27-39. Accessed 5 April 2013.
8. Vallbo AB, Johansson RS. Properties of cutaneous mechanoreceptors in the human hand related to touch sensation. *Hum Neurobiol*. 1984;3(1):3-14. Accessed 3 December 2013.
9. Johansson RS. Sensory and memory information in the control of dexterous manipulation. In: *Neural basis of motor behaviour*. Kluwer Academic Publishers; 1996:205.
10. Biddiss E, Chau T. Upper limb prosthesis use and abandonment: A survey of the last 25 years. *Prosthet Orthot Int*. 2007;31(3):236-257. Accessed 24 January 2014.
11. Wright TW, Hagen AD, Wood MB. Prosthetic usage in major upper extremity amputations. *J Hand Surg*. 1995;20(4):619-622. Accessed 24 May 2013.
12. Biddiss E, Beaton D, Chau T. Consumer design priorities for upper limb prosthetics. *Disability and Rehabilitation: Assistive Technology*. 2007;2(6):346-357. Accessed 5 April 2013.
13. Panarese A, Edin BB, Vecchi F, Carrozza MC, Johansson RS. Humans can integrate force feedback to toes in their sensorimotor control of a robotic hand. *IEEE Transactions on Neural Systems and Rehabilitation Engineering*. 2009;17(6):560-567. Accessed 2 December 2013.
14. Gonzalez J, Soma H, Sekine M, Yu W. Psycho-physiological assessment of a prosthetic hand sensory feedback system based on an auditory display: A preliminary study. *Journal of NeuroEngineering and Rehabilitation*. 2012;9(1). Accessed 27 March 2013.
15. Antfolk C, D'Alonzo M, Rosén B, Lundborg G, Sebelius F, Cipriani C. Sensory feedback in upper limb prosthetics. *Expert Review of Medical Devices*. 2013;10(1):45-54. Accessed 2 December 2013.
16. Bach-y-Rita P. Tactile sensory substitution studies. *Annals of the New York Academy of Sciences*. 2004;1013:83-91. Accessed 3 December 2013.
17. Cipriani C, Dalonzo M, Carrozza MC. A miniature vibrotactile sensory substitution device for multifingered hand prosthetics. *IEEE Transactions on Biomedical Engineering*. 2012;59(2):400-408. Accessed 5 April 2013.
18. Jones LA, Sarter NB. Tactile displays: Guidance for their design and application. *Hum Factors*. 2008;50(1):90-111. Accessed 30 October 2013.
19. Pylatiuk C, Kargov A, Schulz S. Design and evaluation of a low-cost force feedback system for myoelectric prosthetic hands. *Journal of Prosthetics and Orthotics*. 2006;18(2):57-61. Accessed 30 October 2013.
20. Chatterjee A, Chaubey P, Martin J, Thakor N. Testing a prosthetic haptic feedback simulator with an interactive force matching task. *Journal of Prosthetics and Orthotics*. 2008;20(2):27-34. Accessed 30 October 2013.
21. Stepp CE, Matsuoka Y. Vibrotactile sensory substitution for object manipulation: Amplitude versus pulse train frequency modulation. *IEEE Transactions on Neural Systems and Rehabilitation Engineering*. 2012;20(1):31-37. Accessed 20 December 2013.
22. Saunders I, Vijayakumar S. The role of feed-forward and feedback processes for closed-loop prosthesis control. *Journal of NeuroEngineering and Rehabilitation*. 2011;8(1). Accessed 3 December 2013.

23. Tejeiro C, Stepp CE, Malhotra M, Rombokas E, Matsuoka Y. Comparison of remote pressure and vibrotactile feedback for prosthetic hand control. *Proceedings of the IEEE RAS and EMBS International Conference on Biomedical Robotics and Biomechatronics*. 2012:521-525. Accessed 20 December 2013.
24. Cipriani C, Zaccone F, Micera S, Carrozza MC. On the shared control of an EMG-controlled prosthetic hand: Analysis of user-prosthesis interaction. *IEEE Transactions on Robotics*. 2008;24(1):170-184. Accessed 3 December 2013.
25. Shannon GF. A comparison of alternative means of providing sensory feedback on upper limb prostheses. *Med.Biol.Engineering*. 1976;14(3):289-294. Accessed 3 December 2013.
26. Antfolk C, D'Alonzo M, Controzzi M, et al. Artificial redirection of sensation from prosthetic fingers to the phantom hand map on transradial amputees: Vibrotactile versus mechanotactile sensory feedback. *IEEE Transactions on Neural Systems and Rehabilitation Engineering*. 2013;21(1):112-120. Accessed 27 March 2013.
27. Patterson PE, Katz JA. Design and evaluation of a sensory feedback system that provides grasping pressure in a myoelectric hand. *Journal of Rehabilitation Research and Development*. 1992;29(1):1-8. Accessed 2 December 2013.
28. Brown JD, Paek A, Syed M, et al. Understanding the role of haptic feedback in a teleoperated/prosthetic grasp and lift task. *2013 World Haptics Conference, WHC 2013*. 2013:271-276. Accessed 20 December 2013.
29. Lundborg G, Rosen B, Lindstrom K, Lindberg S. Artificial sensibility based on the use of piezoresistive sensors. *J Hand Surg*. 1998;23 B(5):620-626. Accessed 3 December 2013.
30. Wang G, Zhang X, Zhang J, Gruver WA. Gripping force sensory feedback for a myoelectrically controlled forearm prosthesis. *Proceedings of the IEEE International Conference on Systems, Man and Cybernetics*. 1995;1:501-504. Accessed 3 December 2013.
31. Tupper CN, Gerhard GC. Improved prosthesis control via high resolution electro-tactile feedback. *Bioengineering, Proceedings of the Northeast Conference*. 1989:39-40. Accessed 3 December 2013.
32. Shannon GF. A myoelectrically-controlled prosthesis with sensory feedback. *Medical and Biological Engineering and Computing*. 1979;17(1):73-80. Accessed 20 December 2013.
33. Rohland TA. Sensory feedback for powered limb prostheses. *Med.Biol.Engineering*. 1975;13(2):300-301. Accessed 20 December 2013.
34. Kaczmarek KA, Webster JG, Bach-y-Rita P, Tompkins WJ. Electrotactile and vibrotactile displays for sensory substitution systems. *IEEE Transactions on Biomedical Engineering*. 1991;38(1):1-16. Accessed 30 October 2013.
35. Zafar M, Van Doren CL. Effectiveness of supplemental grasp-force feedback in the presence of vision. *Medical and Biological Engineering and Computing*. 2000;38(3):267-274. Accessed 3 December 2013.
36. Buma DG, Buitenweg JR, Veltink PH. Intermittent stimulation delays adaptation to electrocutaneous sensory feedback. *IEEE Transactions on Neural Systems and Rehabilitation Engineering*. 2007;15(1):435-441. Accessed 3 December 2013.
37. Lundborg G, Rosén B, Lindberg S. Hearing as substitution for sensation: A new principle for artificial sensibility. *J Hand Surg*. 1999;24(2):219-224. Accessed 2 December 2013.

38. Gonzalez J, Soma H, Sekine M, Yu W. Auditory display as a prosthetic hand biofeedback. *Journal of Medical Imaging and Health Informatics*. 2011;1(4):325-333. Accessed 3 December 2013.
39. Gonzalez J, Yu W. Multichannel audio aided dynamical perception for prosthetic hand biofeedback. *2009 IEEE International Conference on Rehabilitation Robotics, ICORR 2009*. 2009:240-245. Accessed 3 December 2013.
40. Gillespie RB, Contreras-Vidal JL, Shewokis PA, et al. Toward improved sensorimotor integration and learning using upper-limb prosthetic devices. *2010 Annual International Conference of the IEEE Engineering in Medicine and Biology Society, EMBC'10*. 2010:5077-5080. Accessed 20 December 2013.
41. Wheeler J, Bark K, Savall J, Cutkosky M. Investigation of rotational skin stretch for proprioceptive feedback with application to myoelectric systems. *IEEE Transactions on Neural Systems and Rehabilitation Engineering*. 2010;18(1):58-66. Accessed 20 December 2013.
42. Childress DS. Closed-loop control in prosthetic systems: Historical perspective. *Ann Biomed Eng*. 1980;8(4-6):293-303. Accessed 2 December 2013.
43. Antfolk C, Björkman A, Frank S-, Sebelius F, Lundborg G, Rosen B. Sensory feedback from a prosthetic hand based on airmediated pressure from the hand to the forearm skin. *J Rehabil Med*. 2012;44(8):702-707. Accessed 2 December 2013.
44. Meek SG, Jacobsen SC, Goulding PP. Extended physiologic tactation: Design and evaluation of a proportional force feedback system. *Journal of Rehabilitation Research and Development*. 1989;26(3):53-62. Accessed 2 December 2013.
45. Antfolk C, Cipriani C, Carrozza MC, et al. Transfer of tactile input from an artificial hand to the forearm: Experiments in amputees and able-bodied volunteers. *Disability and Rehabilitation: Assistive Technology*. 2013;8(3):249-254. Accessed 2 December 2013.
46. Antfolk C, Balkenius C, Lundborg G, Rosén B, Sebelius F. A tactile display system for hand prostheses to discriminate pressure and individual finger localization. *Journal of Medical and Biological Engineering*. 2010;30(6):355-360. Accessed 5 April 2013.
47. Stepp CE, Matsuoka Y. Relative to direct haptic feedback, remote vibrotactile feedback improves but slows object manipulation. *Conference proceedings : ...Annual International Conference of the IEEE Engineering in Medicine and Biology Society.IEEE Engineering in Medicine and Biology Society.Conference*. 2010;2010:2089-2092. Accessed 3 December 2013.
48. Armiger RS, Tenore FV, Katyal KD, et al. Enabling closed-loop control of the modular prosthetic limb through haptic feedback. *Johns Hopkins APL Technical Digest (Applied Physics Laboratory)*. 2013;31(4):345-353. Accessed 29 April 2013.
49. HDT Robotics. Robotics research. <http://www.hdtglobal.com/services/robotics/Research/>. Updated 2013. Accessed 12/2013, 2013.
50. Kim K, Colgate JE, Peshkin MA, Santos-Munné JJ, Makhlin A. A miniature tactor design for upper extremity prosthesis. *Proceedings of the Frontiers in the Convergence of Bioscience and Information Technologies, FBIT 2007*. 2007:537-542. Accessed 5 April 2013.

51. Kim K, Colgate JE. Haptic feedback enhances grip force control of sEMG-controlled prosthetic hands in targeted reinnervation amputees. *IEEE Transactions on Neural Systems and Rehabilitation Engineering*. 2012;20(6):798-805. Accessed 18 December 2013.
52. Micera S, Carpaneto J, Raspopovic S. Control of hand prostheses using peripheral information. *IEEE Reviews in Biomedical Engineering*. 2010;3:48-68. Accessed 30 December 2013.
53. Clippinger FW, Avery R, Titus BR. A sensory feedback system for an upper-limb amputation prosthesis. *Bull Prosthet Res*. 1974;247-258. Accessed 30 December 2013.
54. Benvenuto A, Raspopovic S, Hoffmann KP, et al. Intrafascicular thin-film multichannel electrodes for sensory feedback: Evidences on a human amputee. *2010 Annual International Conference of the IEEE Engineering in Medicine and Biology Society, EMBC'10*. 2010:1800-1803. Accessed 20 December 2013.
55. Horch K, Meek S, Taylor TG, Hutchinson DT. Object discrimination with an artificial hand using electrical stimulation of peripheral tactile and proprioceptive pathways with intrafascicular electrodes. *IEEE Transactions on Neural Systems and Rehabilitation Engineering*. 2011;19(5):483-489. Accessed 27 March 2013.
56. Rossini PM, Micera S, Benvenuto A, et al. Double nerve intraneural interface implant on a human amputee for robotic hand control. *Clinical Neurophysiology*. 2010;121(5):777-783. Accessed 20 December 2013.
57. Dhillon GS, Horch KW. Direct neural sensory feedback and control of a prosthetic arm. *IEEE Transactions on Neural Systems and Rehabilitation Engineering*. 2005;13(4):468-472. Accessed 27 March 2013.
58. Dhillon GS, Krüger TB, Sandhu JS, Horch KW. Effects of short-term training on sensory and motor function in severed nerves of long-term human amputees. *J Neurophysiol*. 2005;93(5):2625-2633. Accessed 30 December 2013.
59. Davis TS, Wark HAC, Hutchinson DT, et al. Restoring motor control and sensory feedback in people with upper extremity amputations using arrays of 96 microelectrodes implanted in the median and ulnar nerves. *J Neural Eng*. 2016;13(3). Accessed 8 August 2017. doi: 10.1088/1741-2560/13/3/036001.
60. Clark GA, Wendelken S, Page DM, et al. Using multiple high-count electrode arrays in human median and ulnar nerves to restore sensorimotor function after previous transradial amputation of the hand. *Conf Proc IEEE Eng Med Biol Soc*. 2014;2014:1977-1980. Accessed 8 August 2017. doi: 10.1109/EMBC.2014.6944001.
61. Tan DW, Schiefer MA, Keith MW, Anderson JR, Tyler DJ. Stability and selectivity of a chronic, multi-contact cuff electrode for sensory stimulation in human amputees. *J Neural Eng*. 2015;12(2). Accessed 8 August 2017. doi: 10.1088/1741-2560/12/2/026002.
62. Riso RR. Strategies for providing upper extremity amputees with tactile and hand position feedback - moving closer to the bionic arm. *Technology and Health Care*. 1999;7(6):401-409. Accessed 27 March 2013.
63. Anani A, Korner L. Discrimination of phantom hand sensations elicited by afferent electrical nerve stimulation in below-elbow amputees. *Med Prog Technol*. 1979;6(3):131-135. Accessed 2 January 2014.
64. Micera S, Citi L, Rigosa J, et al. Decoding information from neural signals recorded using intraneural electrodes: Toward the development of a neurocontrolled hand prosthesis. *Proc IEEE*. 2010;98(3):407-417. Accessed 30 December 2013.

65. Polasek KH, Huyen HA, Keith MW, Kirsch RF, Tyler DJ. Stimulation stability and selectivity of chronically implanted multicontact nerve cuff electrodes in the human upper extremity. *IEEE Transactions on Neural Systems and Rehabilitation Engineering*. 2009;17(5):428-437. Accessed 30 December 2013.
66. Alles DS. Information transmission by phantom sensations. *IEEE Trans Man-Mach Syst*. 1970;MMS-11(1):85-91. Accessed 15 January 2014.
67. Kooijman CM, Dijkstra PU, Geertzen JHB, Elzinga A, Van Der Schans CP. Phantom pain and phantom sensations in upper limb amputees: An epidemiological study. *Pain*. 2000;87(1):33-41. Accessed 14 January 2014.
68. Kuiken TA, Dumanian GA, Lipschutz RD, Miller LA, Stubblefield KA. The use of targeted muscle reinnervation for improved myoelectric prosthesis control in a bilateral shoulder disarticulation amputee. *Prosthet Orthot Int*. 2004;28(3):245-253. Accessed 20 December 2013.
69. Hijjawi JB, Kuiken TA, Lipschutz RD, Miller LA, Stubblefield KA, Dumanian GA. Improved myoelectric prosthesis control accomplished using multiple nerve transfers. *Plast Reconstr Surg*. 2006;118(7):1573-1578. Accessed 20 December 2013.
70. Hebert JS, Olson JL, Morhart MJ, et al. Novel targeted sensory reinnervation technique to restore functional hand sensation after transhumeral amputation. *IEEE Transactions on Neural Systems and Rehabilitation Engineering*. 2014;22(4):765.
71. Kuiken TA, Marasco PD, Lock BA, Harden RN, Dewald JPA. Redirection of cutaneous sensation from the hand to the chest skin of human amputees with targeted reinnervation. *Proc Natl Acad Sci U S A*. 2007;104(50):20061-20066. Accessed 20 December 2013.
72. Kuiken TA, Miller LA, Lipschutz RD, et al. Targeted reinnervation for enhanced prosthetic arm function in a woman with a proximal amputation: A case study. *Lancet*. 2007;369(9559):371-380. Accessed 20 December 2013.
73. Sensinger JW, Schultz AE, Kuiken TA. Examination of force discrimination in human upper limb amputees with reinnervated limb sensation following peripheral nerve transfer. *IEEE Transactions on Neural Systems and Rehabilitation Engineering*. 2009;17(5):438-444. Accessed 5 April 2013.
74. Dawson MR, Fahimi F, Carey JP. The development of a myoelectric training tool for above-elbow amputees. *Open Biomedical Engineering Journal*. 2012;6(1):5-15. Accessed 20 December 2013.
75. Kung TA, Bueno RA, Alkhalefah GK, Langhals NB, Urbanchek MG, Cederna PS. Innovations in prosthetic interfaces for the upper extremity. *Plast Reconstr Surg*. 2013;132(6):1515-1523. Accessed 14 January 2014.
76. Johansson RS, Westling G. Signals in tactile afferents from the fingers eliciting adaptive motor responses during precision grip. *Experimental Brain Research*. 1987;66(1):141-154. Accessed 30 December 2013.
77. Westling G, Johansson RS. Responses in glabrous skin mechanoreceptors during precision grip in humans. *Experimental Brain Research*. 1987;66(1):128-140. Accessed 30 December 2013.
78. Hernandez-Arieta A, Dermitzakis K, Damian D, Langarella M, Pfeifer R. Sensory-motor coupling in rehabilitation robotics. In: Takahashi Y, ed. *Service robot applications*. Rijeka: InTech Europe; 2008:21-36.
79. Mann RW, Reimers SD. Kinesthetic sensing for the EMG controlled "Boston arm". *IEEE Trans Man-Mach Syst*. 1970;MMS-11(1):110-115. Accessed 30 October 2013.

80. Goodwin GM, McCloskey DI, Matthews PBC. The contribution of muscle afferents kinaesthesia shown by vibration induced illusions of movement and by the effects of paralyzing joint afferents. *J Physiol (Lond)*. 1972;536:635-647. Accessed 24 May 2013.
81. Eklund G. Position sense and state of contraction: The effects of vibration. *J Neurol Neurosurg Psychiatr*. 1972;35:606-611. Accessed 24 May 2013.
82. Proske U, Gandevia SC. The proprioceptive senses: Their roles in signaling body shape, body position and movement, and muscle force. *Physiol Rev*. 2012;92(4):1651-1697. Accessed 30 September 2013.
83. Lake C. The evolution of upper limb prosthetic socket design. *Journal of Prosthetics and Orthotics*. 2008;20(3):85-92. Accessed 20 December 2013.
84. Daly W. Upper extremity socket design options. *Phys Med Rehabil Clin N Am*. 2000;11(3):627-638. Accessed 20 December 2013.
85. Moran CW. Revolutionizing prosthetics 2009 modular prosthetic limb-body interface: Overview of the prosthetic socket development. *Johns Hopkins APL Technical Digest (Applied Physics Laboratory)*. 2011;30(3):240-249. Accessed 5 April 2013.
86. Hargrove L, Englehart K, Hudgins B. A training strategy to reduce classification degradation due to electrode displacements in pattern recognition based myoelectric control. *Biomedical Signal Processing and Control*. 2008;3(2):175-180. Accessed 4 February 2014.

Chapter 3

1. Ackerley R, Kavounoudias A. The role of tactile afference in shaping motor behaviour and implications for prosthetic innovation. *Neuropsychologia*. 2015;79:192-205. Accessed 10 February 2017. doi: 10.1016/j.neuropsychologia.2015.06.024.
2. Bays PM, Wolpert DM. Computational principles of sensorimotor control that minimize uncertainty and variability. *J Physiol*. 2007;578(2):387-396. Accessed 13 February 2017. doi: 10.1113/jphysiol.2006.120121.
3. Johansson RS, Flanagan JR. Coding and use of tactile signals from the fingertips in object manipulation tasks. *Nat Rev Neurosci*. 2009;10(5):345-359. Accessed 24 January 2017. doi: 10.1038/nrn2621.
4. Kandel ER, Schwartz JH, Jessell TM. Ch.23 touch. In: *Principles of neuroscience*. 4th ed. McGraw-Hill, Health Professions Division; 2000.
5. Proske U, Gandevia SC. The proprioceptive senses: Their roles in signaling body shape, body position and movement, and muscle force. *Physiol Rev*. 2012;92(4):1651-1697. Accessed 30 September 2013.
6. Collins DF, Refshauge KM, Gandevia SC. Sensory integration in the perception of movements at the human metacarpophalangeal joint. *J Physiol*. 2000;529(2):505-515. Accessed 14 February 2017. doi: 10.1111/j.1469-7793.2000.00505.x.
7. Cooper S. The responses of the of the primary and secondary endings of muscle spindles with intact motor innervation during applied stretch. *Exp Physiol*. 1961;46(4):389-398. Accessed 14 February 2017. doi: 10.1113/expphysiol.1961.sp001558.

8. Goodwin GM, McCloskey DI, Matthews PBC. The contribution of muscle afferents kinaesthesia shown by vibration induced illusions of movement and by the effects of paralyzing joint afferents. *J Physiol (Lond)*. 1972;536:635-647. Accessed 24 May 2013.
9. Jones LA. Motor illusions: What do they reveal about proprioception? *Psychol Bull*. 1988;103(1):72-86. Accessed 5 April 2013.
10. Craske B. Perception of impossible limb positions induced by tendon vibration. *Science*. 1977;196(4285):71-73. Accessed 16 December 2013.
11. Lackner JR. Some proprioceptive influences on the perceptual representation of body shape and orientation. *Brain*. 1988;111(2):281-297. Accessed 18 December 2013.
12. Kandel ER. Part VI: Movement. In: *Principles of neural science*. 5th ed. New York: McGraw-Hill; 2013:743.
13. Rinderknecht MD, Kim Y, Santos-Carreras L, Bleuler H, Gassert R. Combined tendon vibration and virtual reality for post-stroke hand rehabilitation. 2013 World Haptics Conference, WHC 2013. 2013:277-282. Accessed 20 December 2013.
14. Rinderknecht MD. Device for a novel hand and wrist rehabilitation strategy for stroke patients based on illusory movements induced by tendon vibration. *Proceedings of the Mediterranean Electrotechnical Conference - MELECON*. 2012:926-931. Accessed 20 December 2013.
15. Redon-Zouiteni, C. Roll, JP. Lacert, P. Proprioceptive postural reprogramming in childhood cerebral palsy validation of tendon vibration as a therapeutic tool. *Motricité cérébrale*. 1994;15(2):57.
16. Krueger-Beck E, Nogueira-Neto GN, Nohama P. Vibrational stimulus in spasticity - A perspective of treatment. *Revista Neurociencias*. 2010;18(4):523-530. Accessed 29 January 2014.
17. Gay A, Parratte S, Salazard B, et al. Proprioceptive feedback enhancement induced by vibratory stimulation in complex regional pain syndrome type I: An open comparative pilot study in 11 patients. *Joint Bone Spine*. 2007;74(5):461-466. Accessed 16 December 2013.
18. Willigenburg NW, Kingma I, Hoozemans MJM, van Dieën JH. Precision control of trunk movement in low back pain patients. *Human Movement Science*. 2013;32(1):228-239. Accessed 20 December 2013.
19. Frima N, Nasir J, Grünewald RA. Abnormal vibration-induced illusion of movement in idiopathic focal dystonia: An endophenotypic marker? *Movement Disorders*. 2008;23(3):373-377. Accessed 5 February 2014.
20. Frima N, Grünewald RA. Abnormal vibration induced illusion of movement in essential tremor: Evidence for abnormal muscle spindle afferent function. *Journal of Neurology, Neurosurgery and Psychiatry*. 2005;76(1):55-57. Accessed 5 February 2014.
21. Frima N, Rome SM, Grünewald RA. The effect of fatigue on abnormal vibration induced illusion of movement in idiopathic focal dystonia. *Journal of Neurology Neurosurgery and Psychiatry*. 2003;74(8):1154-1156. Accessed 5 February 2014.
22. Rome S, Grünewald RA. Abnormal perception of vibration-induced illusion of movement in dystonia. *Neurology*. 1999;53(8):1794-1800. Accessed 5 February 2014.

23. Han J, Jung J, Lee J, Kim E. Effects of vibration stimuli on the knee joint reposition error of elderly women. *Journal of Physical Therapy Science*. 2013;25(1):93-95. Accessed 20 December 2013.
24. Roll R, Kavounoudias A, Albert F, et al. Illusory movements prevent cortical disruption caused by immobilization. *Neuroimage*. 2012;62(1):510-519. Accessed 29 January 2014.
25. Quercia P, Demougeot L, Dos Santos M, Bonnetblanc F. Integration of proprioceptive signals and attentional capacity during postural control are impaired but subject to improvement in dyslexic children. *Experimental Brain Research*. 2011;209(4):599-608. Accessed 5 February 2014.
26. Vaugoyeau M, Hakam H, Azulay J-. Proprioceptive impairment and postural orientation control in parkinson's disease. *Human Movement Science*. 2011;30(2):405-414. Accessed 5 February 2014.
27. Roll JP, Vedel JP, Ribot E. Alteration of proprioceptive messages induced by tendon vibration in man: A microneurographic study. *Experimental Brain Research*. 1989;76(1):213-222. Accessed 16 December 2013.
28. Gilhodes JC, Roll JP, Tardy-Gervet MF. Perceptual and motor effects of agonist-antagonist muscle vibration in man. *Experimental Brain Research*. 1986;61(2):395-402. Accessed 16 December 2013.
29. Roll JP, Vedel JP. Kinaesthetic role of muscle afferents in man, studied by tendon vibration and microneurography. *Experimental Brain Research*. 1982;47(2):177-190. Accessed 16 December 2013.
30. Clark FJ, Matthews PB, Muir RB. Effect of the amplitude of muscle vibration on the subjectively experienced illusion of movement [proceedings]. *J Physiol (Lond)*. 1979;296:14P-15P. Accessed 18 December 2013.
31. Meek SG, Jacobsen SC, Goulding PP. Extended physiologic taction: Design and evaluation of a proportional force feedback system. *Journal of Rehabilitation Research and Development*. 1989;26(3):53-62. Accessed 2 December 2013.
32. Eklund G. Position sense and state of contraction: The effects of vibration. *J Neurol Neurosurg Psychiatr*. 1972;35:606-611. Accessed 24 May 2013.
33. Verschueren SMP, Brumagne S, Swinnen SP, Cordo PJ. The effect of aging on dynamic position sense at the ankle. *Behav Brain Res*. 2002;136(2):593-603. Accessed 16 December 2013.
34. Calvin-Figuière S, Romaiguère P, Roll J-. Relations between the directions of vibration-induced kinesthetic illusions and the pattern of activation of antagonist muscles. *Brain Res*. 2000;881(2):128-138. Accessed 5 April 2013.
35. Kito T, Hashimoto T, Yoneda T, Katamoto S, Naito E. Sensory processing during kinesthetic aftereffect following illusory hand movement elicited by tendon vibration. *Brain Res*. 2006;1114(1):75-84. Accessed 20 December 2013.
36. White O, Proske U. Illusions of forearm displacement during vibration of elbow muscles in humans. *Experimental Brain Research*. 2009;192(1):113-120. Accessed 18 December 2013.
37. Seizova-Cajic T, Smith JL, Taylor JL, Gandevia SC. Proprioceptive movement illusions due to prolonged stimulation: Reversals and aftereffects. *PLoS ONE*. 2007;2(10). Accessed 20 December 2013.
38. Lackner J. Human sensory-motor adaptation to the terrestrial force environment. *Brain Mechanisms and Spatial Vision*. 1985;21:175.

39. Capaday C, Cooke JD. The effects of muscle vibration on the attainment of intended final position during voluntary human arm movements. *Experimental Brain Research*. 1981;42(2):228-230. Accessed 18 December 2013.
40. McCloskey DI. Differences between the senses of movement and position shown by the effects of loading and vibration of muscles in man. *Brain Res*. 1973;61:119-131. Accessed 23 December 2013.
41. Guerraz M, Provost S, Narison R, Brugnon A, Virolle S, Bresciani J-. Integration of visual and proprioceptive afferents in kinesthesia. *Neuroscience*. 2012;223:258-268. Accessed 5 April 2013.
42. Seizova-Cajic T, Azzi R. Conflict with vision diminishes proprioceptive adaptation to muscle vibration. *Experimental Brain Research*. 2011;211(2):169-175. Accessed 5 February 2014.
43. Izumizaki M, Tsuge M, Akai L, Proske U, Homma I. The illusion of changed position and movement from vibrating one arm is altered by vision or movement of the other arm. *J Physiol (Lond)*. 2010;588(15):2789-2800. Accessed 5 April 2013.
44. Lackner JR, Taublieb AB. Influence of vision on vibration-induced illusions of limb movement. *Exp Neurol*. 1984;85(1):97-106. Accessed 18 December 2013.
45. Blanchard C, Roll R, Roll J-, Kavounoudias A. Combined contribution of tactile and proprioceptive feedback to hand movement perception. *Brain Res*. 2011;1382:219-229. Accessed 5 April 2013.
46. Rabin E, Gordon AM. Prior experience and current goals affect muscle-spindle and tactile integration. *Experimental Brain Research*. 2006;169(3):407-416. Accessed 5 February 2014.
47. Eklund G. HK. Motor effects of vibratory muscle stimuli in man. *Electroenceph clin Neurophysiol*. 1965;19:619.

Chapter 4

1. Gordon J, Ghilardi MF, Ghez C. Impairments of reaching movements in patients without proprioception. I. spatial errors. *J Neurophysiol*. 1995;73(1):347-360. Accessed 24 May 2017.
2. Ghez C, Gordon J, Ghilardi MF. Impairments of reaching movements in patients without proprioception. II. effects of visual information on accuracy. *J Neurophysiol*. 1995;73(1):361-372. Accessed 24 May 2017.
3. Biddiss E, Chau T. Upper-limb prosthetics: Critical factors in device abandonment. *Am J Phys Med Rehabil*. 2007;86(12):977-987. Accessed 16 March 2017. doi: 10.1097/PHM.0b013e3181587f6c.
4. Childress DS. Control strategy for upper-limb prostheses. *Annu Int Conf IEEE Eng Med Biol Proc*. 1998;5:2273-2275. Accessed 23 May 2017.
5. Schofield JS, Evans KR, Carey JP, Hebert JS. Applications of sensory feedback in motorized upper extremity prosthesis: A review. *Expert Review of Medical Devices*. 2014;11(5):499-511. Accessed 8 April 2015.
6. Antfolk C, D'alonzo M, Rosén B, Lundborg G, Sebelius F, Cipriani C. Sensory feedback in upper limb prosthetics. *Expert Review of Medical Devices*. 2013;10(1):45-54. Accessed 2 December 2013.
7. Raspopovic S, Capogrosso M, Petrini FM, et al. Bioengineering: Restoring natural sensory feedback in real-time bidirectional hand prostheses. *Sci Transl Med*. 2014;6(222). Accessed 24 May 2017. doi: 10.1126/scitranslmed.3006820.

8. Hebert JS, Olson JL, Morhart MJ, et al. Novel targeted sensory reinnervation technique to restore functional hand sensation after transhumeral amputation. *IEEE Transactions on Neural Systems and Rehabilitation Engineering*. 2014;22(4):765.
9. Kuiken TA, Marasco PD, Lock BA, Harden RN, Dewald JPA. Redirection of cutaneous sensation from the hand to the chest skin of human amputees with targeted reinnervation. *Proc Natl Acad Sci U S A*. 2007;104(50):20061-20066. Accessed 20 December 2013.
10. Kuiken TA, Dumanian GA, Lipschutz RD, Miller LA, Stubblefield KA. The use of targeted muscle reinnervation for improved myoelectric prosthesis control in a bilateral shoulder disarticulation amputee. *Prosthet Orthot Int*. 2004;28(3):245-253. Accessed 20 December 2013.
11. Marasco PD, Kim K, Colgate JE, Peshkin MA, Kuiken TA. Robotic touch shifts perception of embodiment to a prosthesis in targeted reinnervation amputees. *Brain*. 2011;134(3):747-758. Accessed 24 May 2017. doi: 10.1093/brain/awq361.
12. Schofield JS, Dawson MR, Carey JP, Hebert JS. Characterizing the effects of amplitude, frequency and limb position on vibration induced movement illusions: Implications in sensory-motor rehabilitation. *Technology and Health Care*. 2015;23(2):129-141. Accessed 8 April 2015.
13. Goodwin GM, McCloskey DI, Matthews PBC. The contribution of muscle afferents kinaesthesia shown by vibration induced illusions of movement and by the effects of paralyzing joint afferents. *J Physiol (Lond)*. 1972;536:635-647. Accessed 24 May 2013.
14. McCloskey DI. Differences between the senses of movement and position shown by the effects of loading and vibration of muscles in man. *Brain Res*. 1973;61:119-131. Accessed 23 December 2013.
15. Montgomery D.C. Factorials with mixed levels. In: *Design and analysis of experiments*. 8th ed. Wiley; 2012:412.
16. Proske U, Gandevia SC. The proprioceptive senses: Their roles in signaling body shape, body position and movement, and muscle force. *Physiol Rev*. 2012;92(4):1651-1697. Accessed 30 September 2013.
17. Clark FJ, Matthews PB, Muir RB. Effect of the amplitude of muscle vibration on the subjectively experienced illusion of movement [proceedings]. *J Physiol (Lond)*. 1979;296:14P-15P. Accessed 18 December 2013.

Chapter 5

1. Schofield JS, Evans KR, Carey JP, Hebert JS. Applications of sensory feedback in motorized upper extremity prosthesis: A review. *Expert Review of Medical Devices*. 2014;11(5):499-511. Accessed 8 April 2015.
2. Pirouzi G, Abu Osman NA, Eshraghi A, Ali S, Gholizadeh H, Wan Abas WAB. Review of the socket design and interface pressure measurement for transtibial prosthesis. *Scientific World Journal*. 2014;2014. Accessed 22 April 2015.
3. Owings MF, Kozak LJ. Ambulatory and inpatient procedures in the united states, 1996. Vital and health statistics.Series 13, Data from the National Health Survey. 1998(139):1-119. Accessed 25 January 2016.
4. Adams PF, Hendershot GE, Marano MA, eds. Current estimates from the national health interview survey, 1996. ; 1999; No. 10.

5. Ziegler-Graham K, MacKenzie EJ, Ephraim PL, Travison TG, Brookmeyer R. Estimating the prevalence of limb loss in the united states: 2005 to 2050. *Arch Phys Med Rehabil.* 2008;89(3):422-429. doi: <http://dx.doi.org/10.1016/j.apmr.2007.11.005>.
6. Lake C, Dodson R. Progressive upper limb prosthetics. *Phys Med Rehabil Clin N Am.* 2006;17(1):49-72. Accessed 5 April 2013.
7. Biddiss E, Chau T. Upper limb prosthesis use and abandonment: A survey of the last 25 years. *Prosthet Orthot Int.* 2007;31(3):236-257. Accessed 24 January 2014.
8. Biddiss E, Beaton D, Chau T. Consumer design priorities for upper limb prosthetics. *Disability and Rehabilitation: Assistive Technology.* 2007;2(6):346-357. Accessed 5 April 2013.
9. Schultz AE, Baade SP, Kuiken TA. Expert opinions on success factors for upper-limb prostheses. *Journal of Rehabilitation Research and Development.* 2007;44(4):483-489. Accessed 5 April 2013.
10. Sanders J. Stump-socket interface conditions. In: *Pressure ulcer research: Current and future perspectives.* Heidelberg Germany: Springer-Verlag Berlin; 2005:129-147. Accessed 25 January 2016.
11. Hachisuka K, Dozono K, Ogata H, Ohmine S, Shitama H, Shinkoda K. Total surface bearing below-knee prosthesis: Advantages, disadvantages, and clinical implications. *Arch Phys Med Rehabil.* 1998;79(7):783-789. Accessed 25 January 2016.
12. Li W, Pang Q, Lu M, Liu Y, Zhou ZR. Rehabilitation and adaptation of lower limb skin to friction trauma during friction contact. *Wear.* 2015;332-333:725-733. Accessed 25 January 2016. doi: 10.1016/j.wear.2015.01.045.
13. Levy W. Chapter 26: Skin problems of the amputee. In: Bowker JH, Michael JW, eds. *Atlas of limb prosthetics: Surgical, prosthetic, and rehabilitation principles.* 2nd ed. Mosby Year Book; 1992.
14. Knapik JJ, Reynolds KL, Duplantis KL, Jones BH. Friction blisters: Pathophysiology, prevention and treatment. *Sports Med.* 1995;20(3):136-147. Accessed 25 January 2016. doi: 10.2165/00007256-199520030-00002.
15. Mak AFT, Zhang M, Tam EWC, eds. *Biomechanics of pressure ulcer in body tissues interacting with external forces during locomotion.* ; 2010Annual Review of Biomedical Engineering; No. 12.
16. Salawu A, Middleton C, Gilbertson A, Kodavali K, Neumann V. Stump ulcers and continued prosthetic limb use. *Prosthet Orthot Int.* 2006;30(3):279-285. Accessed 26 January 2016.
17. Portnoy S, Siev-Ner I, Shabshin N, Gefen A. Effects of sitting postures on risks for deep tissue injury in the residuum of a transtibial prosthetic-user: A biomechanical case study. *Comput Methods Biomech Biomed Engin.* 2011;14(11):1009-1019. Accessed 26 January 2016.
18. Dillingham TR, Pezzin LE, MacKenzie EJ, Burgess AR. Use and satisfaction with prosthetic devices among persons with trauma-related amputations: A long-term outcome study. *American Journal of Physical Medicine and Rehabilitation.* 2001;80(8):563-571. Accessed 31 January 2014.
19. Silver-Thorn MB, Steege JW, Childress DS. A review of prosthetic interface stress investigations. *Journal of Rehabilitation Research and Development.* 1996;33(3):253-266. Accessed 9 February 2014.
20. Sanders JE. Interface mechanics in external prosthetics: Review of interface stress measurement techniques. *Med Biol Eng Comput.* 1995;33(4):509-516. Accessed 13 May 2015.

21. Al-Fakih EA, Abu Osman NA, Mahmad Adikan FR. Techniques for interface stress measurements within prosthetic sockets of transtibial amputees: A review of the past 50 years of research. *Sensors*. 2016;16(7). Accessed 13 September 2016. doi: 10.3390/s16071119.
22. Zachariah SG, Sanders JE. Interface mechanics in lower-limb external prosthetics: A review of finite element models. *IEEE Trans Rehabil Eng*. 1996;4(4):288-302. Accessed 26 January 2016. doi: 10.1109/86.547930.
23. Zhang M, Mak AFT, Roberts VC. Finite element modelling of a residual lower-limb in a prosthetic socket: A survey of the development in the first decade. *Medical Engineering and Physics*. 1998;20(5):360-373. Accessed 31 January 2014.
24. Mak AFT, Zhang M, Boone DA. State-of-the-art research in lower-limb prosthetic biomechanics-socket interface: A review. *Journal of Rehabilitation Research and Development*. 2001;38(2):161-173. Accessed 9 February 2014.
25. Schofield JS, Evans KR, Hebert JS, Marasco PD, Carey JP. The effect of biomechanical variables on force sensitive resistor error: Implications for calibration and improved accuracy. *J Biomech*. 2016;49(5):786. doi: <http://dx.doi.org/10.1016/j.jbiomech.2016.01.022>.
26. El-Sayed AM, Hamzaid NA, Tan KYS, Abu Osman NA. Detection of prosthetic knee movement phases via in-socket sensors: A feasibility study. *Sci World J*. 2015;2015. Accessed 2 February 2016. doi: 10.1155/2015/923286.
27. Mai A, Commuri S, Dionne CP, Day J, Ertl WJJ, Regens JL. Effect of prosthetic foot on residuum-socket interface pressure and gait characteristics in an otherwise healthy man with transtibial osteomyoplastic amputation. *J Prosthet Orthot*. 2012;24(4):211-220. Accessed 2 February 2016. doi: 10.1097/JPO.0b013e31826fdaf8.
28. Beil TL, Street GM, Covey SJ. Interface pressures during ambulation using suction and vacuum-assisted prosthetic sockets. *J Rehabil Res Dev*. 2002;39(6):693-700. Accessed 3 February 2016.
29. Kahle JT, Jason Highsmith MJ. Transfemoral sockets with vacuum-assisted suspension comparison of hip kinematics, socket position, contact pressure, and preference: Ischial containment versus brimless. *Journal of Rehabilitation Research and Development*. 2013;50(9):1241-1252. Accessed 2 February 2016.
30. Dumbleton T, Buis AWP, McFadyen A, et al. Dynamic interface pressure distributions of two transtibial prosthetic socket concepts. *Journal of Rehabilitation Research and Development*. 2009;46(3):405-415. Accessed 2 February 2016.
31. Rogers B, Bosker G, Faustini M, Walden G, Neptune RR, Crawford R. Case report: Variably compliant transtibial prosthetic socket fabricated using solid freeform fabrication. *Journal of Prosthetics and Orthotics*. 2008;20(1):1-7. Accessed 2 February 2016.
32. Rajtukova V, Hudak R, Zivcak J, Halfarova P, Kudrikova R. Pressure distribution in transtibial prostheses socket and the stump interface. *Procedia Engineering*. 2014;96:374-381. Accessed 2 February 2016.
33. Polliack AA, Sieh RC, Craig DD, Landsberger S, McNeil DR, Ayyappa E. Scientific validation of two commercial pressure sensor systems for prosthetic socket fit. *Prosthet Orthot Int*. 2000;24(1):63-73. Accessed 22 April 2015.
34. Boutwell E, Stine R, Hansen A, Tucker K, Gard S. Effect of prosthetic gel liner thickness on gait biomechanics and pressure distribution within the transtibial socket. *Journal of Rehabilitation Research and Development*. 2012;49(2):227-240. Accessed 22 April 2014.

35. Wolf SI, Alimusaj M, Fradet L, Siegel J, Braatz F. Pressure characteristics at the stump/socket interface in transtibial amputees using an adaptive prosthetic foot. *Clin Biomech.* 2009;24(10):860-865. Accessed 3 February 2016. doi: 10.1016/j.clinbiomech.2009.08.007.
36. Dabbling JG, Filatov A, Wheeler JW. Static and cyclic performance evaluation of sensors for human interface pressure measurement. *Proceedings of the Annual International Conference of the IEEE Engineering in Medicine and Biology Society, EMBS.* 2012:162-165. Accessed 22 April 2015.
37. Lebosse C, Renaud P, Bayle B, De Mathelin M. Modeling and evaluation of low-cost force sensors. *IEEE Transactions on Robotics.* 2011;27(4):815-822. Accessed 22 April 2015.
38. Herbert-Copley AG, Sinitski EH, Lemaire ED, Baddour N. Temperature and measurement changes over time for F-scan sensors. *MeMeA 2013 - IEEE International Symposium on Medical Measurements and Applications, Proceedings.* 2013:265-267. Accessed 22 April 2015.
39. Polliack AA, Sieh RC, Craig DD, Landsberger S, McNeil DR, Ayyappa E. Scientific validation of two commercial pressure sensor systems for prosthetic socket fit. *Prosthet Orthot Int.* 2000;24(1):63-73. Accessed 22 April 2015.
40. Hall RS, Desmoulin GT, Milner TE. A technique for conditioning and calibrating force-sensing resistors for repeatable and reliable measurement of compressive force. *J Biomech.* 2008;41(16):3492-3495. Accessed 11 December 2015. doi: 10.1016/j.jbiomech.2008.09.031.
41. Buis AWP, Convery P. Calibration problems encountered while monitoring stump/socket interface pressures with force sensing resistors: Techniques adopted to minimise inaccuracies. *Prosthet Orthot Int.* 1997;21(3):179-182. Accessed 22 April 2015.
42. Patterson RP, Fisher SV. The accuracy of electrical transducers for the measurement of pressure applied to the skin. *IEEE Trans Biomed Eng.* 1979;BME-26(8):450-456. Accessed 10 February 2016. doi: 10.1109/TBME.1979.326570.
43. Sonck WA, Cockrell JL, Koepke GH. Effect of liner materials on interface pressures in below-knee prostheses. *Arch Phys Med Rehabil.* 1970;51(11):666-669. Accessed 10 February 2016.
44. Rae JW, Cockrell JL. Interface pressure and stress distribution in prosthetic fitting. *U S, Veterans Adm, Dep Med Surg.* 1971(10-16):64-111. Accessed 10 February 2016.
45. Pearson JR, Holmgren G, March L, Oberg K. Pressures in critical regions of the below knee patellar tendon bearing prosthesis. *Bull Prosthet Res.* 1973;No.19:52-76. Accessed 10 February 2016.
46. Williams RB, Porter D, Roberts VC, Regan JF. Triaxial force transducer for investigating stresses at the stump/socket interface. *Med Biol Eng Comput.* 1992;30(1):89-96. Accessed 10 February 2016. doi: 10.1007/BF02446199.
47. Smith LM, Sanders JE, Spelman FA. Portable signal conditioning and data acquisition system for prosthetic triaxial force transducers. *Proc Annu Conf Eng Med Biol.* 1993;15(pt 3):1288-1289. Accessed 10 February 2016.
48. Sanders JE, Smith LM, Spelman FA, Warren DJ. A portable measurement system for prosthetic triaxial force transducers. *IEEE Trans Rehab Eng.* 1995;3(4):366-373. Accessed 10 February 2016. doi: 10.1109/86.481977.

49. Sanders JE, Miller RA, Berglund DN, Zachariah SG. A modular six-directional force sensor for prosthetic assessment: A technical note. *Journal of Rehabilitation Research and Development*. 1997;34(2):195-202. Accessed 9 February 2014.
50. Goh JCH, Lee PVS, Chong SY. Stump/socket pressure profiles of the pressure cast prosthetic socket. *Clin Biomech*. 2003;18(3):237-243. Accessed 3 February 2016. doi: 10.1016/S0268-0033(02)00206-1.
51. Goh JCH, Lee PVS, Sook YC. Comparative study between patellar-tendon-bearing and pressure cast prosthetic sockets. *J Rehabil Res Dev*. 2004;41(3 B):491-501. Accessed 3 February 2016.
52. Xin Z. Design of a new type six-axis force sensor. *Int Conf Intelligent Comput Technol Autom , ICICTA*. 2009;2:446-449. Accessed 10 February 2016. doi: 10.1109/ICICTA.2009.343.
53. Zhang X. Development of a novel three-axis force sensor. *IET Conf Publ*. 2009;2009(556 CP). Accessed 10 February 2016. doi: 10.1049/cp.2009.1440.
54. Abu Osman NA, Spence WD, Solomonidis SE, Paul JP, Weir AM. Transducers for the determination of the pressure and shear stress distribution at the stump-socket interface of trans-tibial amputees. *Proc Inst Mech Eng Part B J Eng Manuf*. 2010;224(8):1239-1250. Accessed 10 February 2016. doi: 10.1243/09544054JEM1820.
55. Neumann ES, Yalamanchili K, Brink J, Lee JS. Transducer-based comparisons of the prosthetic feet used by transtibial amputees for different walking activities: A pilot study. *Prosthet Orthot Int*. 2012;36(2):203-216. Accessed 10 February 2016. doi: 10.1177/0309364612436408.
56. Sanders JE, Jacobsen AK, Fergason JR. Effects of fluid insert volume changes on socket pressures and shear stresses: Case studies from two trans-tibial amputee subjects. *Prosthet Orthot Int*. 2006;30(3):257-269. Accessed 10 February 2016. doi: 10.1080/03093640600810266.
57. Siegel DM, Drucker SM, Garabieta I. Performance analysis of a tactile sensor. . 1987:1493-1499. Accessed 10 February 2016.
58. Zheng E, Wang L, Wei K, Wang Q. A noncontact capacitive sensing system for recognizing locomotion modes of transtibial amputees. *IEEE Transactions on Biomedical Engineering*. 2014;61(12):2911-2920. Accessed 2 February 2016.
59. Vandeparre H, Watson D, Lacour SP. Extremely robust and conformable capacitive pressure sensors based on flexible polyurethane foams and stretchable metallization. *Appl Phys Lett*. 2013;103(20). Accessed 12 February 2016. doi: 10.1063/1.4832416.
60. Sundara-Rajan K, Bestick A, Rowe GI, et al. An interfacial stress sensor for biomechanical applications. *Measurement Science and Technology*. 2012;23(8). Accessed 2 February 2016.
61. Sundara-Rajan K, Rowe GI, Simon AJ, Klute GK, Ledoux WR, Mamishev AV. Shear sensor for lower limb prosthetic applications. 2009 1st Annual ORNL Biomedical Science and Engineering Conference, BSEC 2009. 2009. Accessed 2 February 2016.
62. Polliack AA, Craig DD, Sieh RC, Landsberger S, McNeal DR. Laboratory and clinical tests of a prototype pressure sensor for clinical assessment of prosthetic socket fit. *Prosthet Orthot Int*. 2002;26(1):23-34. Accessed 2 February 2016.

63. Laszczak P, Jiang L, Bader DL, Moser D, Zahedi S. Development and validation of a 3D-printed interfacial stress sensor for prosthetic applications. *Med Eng Phys.* 2015;37(1):132-137. Accessed 13 September 2016. doi: 10.1016/j.medengphy.2014.10.002.
64. Tiwana MI, Redmond SJ, Lovell NH. A review of tactile sensing technologies with applications in biomedical engineering. *Sens Actuators A Phys.* 2012;179:17-31. Accessed 22 September 2016. doi: 10.1016/j.sna.2012.02.051.
65. Meltz G, Dunphy JR, Glenn WH, Farina JD, Leonberger FJ. Fiber optic temperature and strain sensors. *Proc SPIE Int Soc Opt Eng.* 1987;798:104-114. Accessed 10 February 2016. doi: 10.1117/12.941093.
66. Tsiokos D, Kanellos G, Papaioannou G, Pissadakis S. Fiber optic-based pressure sensing surface for skin health management in prosthetic and rehabilitation interventions. In: *Biomedical engineering - technical applications in medicine.* InTech; 2012. 10.5772/50574.
67. Mishra V, Singh N, Tiwari U, Kapur P. Fiber grating sensors in medicine: Current and emerging applications. *Sens Actuators A Phys.* 2011;167(2):279-290. Accessed 12 February 2016. doi: 10.1016/j.sna.2011.02.045.
68. Mignani AG, Baldini F. Fibre-optic sensors in health care. *Phys Med Biol.* 1997;42(5):967-979. Accessed 12 February 2016. doi: 10.1088/0031-9155/42/5/015.
69. Mignani AG, Baldini F. Biomedical sensors using optical fibres. *Rep Prog Phys.* 1996;59(1):1-28. Accessed 12 February 2016. doi: 10.1088/0034-4885/59/1/001.
70. Al-Fakih EA, Osman NA, Eshraghi A, Adikan FR. The capability of fiber bragg grating sensors to measure amputees' trans-tibial stump/socket interface pressures. *Sensors (Basel).* 2013;13(8):10348-10357. Accessed 10 February 2016.
71. Wheeler JW, Dabling JG, Chinn D, et al. MEMS-based bubble pressure sensor for prosthetic socket interface pressure measurement. *Proc Annu Int Conf IEEE Eng Med Biol Soc EMBS.* 2011:2925-2928. Accessed 2 February 2016. doi: 10.1109/IEMBS.2011.6090805.
72. Sanders JE, Lam D, Dralle AJ, Okumura R. Interface pressures and shear stresses at thirteen socket sites on two persons with transtibial amputation. *J Rehabil Res Dev.* 1997;34(1):19-43. Accessed 12 February 2016.
73. Goh JCH, Lee PVS, Toh SL, Ooi CK. Development of an integrated CAD-FEA process for below-knee prosthetic sockets. *Clin Biomech.* 2005;20(6):623-629. Accessed 2 February 2014.
74. Lacroix D, Ramírez Patiño JF. Finite element analysis of donning procedure of a prosthetic transfemoral socket. *Ann Biomed Eng.* 2011;39(12):2972-2983. Accessed 23 February 2016.
75. Ramírez JF, Vélez JA. Incidence of the boundary condition between bone and soft tissue in a finite element model of a transfemoral amputee. *Prosthet Orthot Int.* 2012;36(4):405-414. Accessed 23 February 2016.
76. Zhang L, Zhu M, Shen L, Zheng F. Finite element analysis of the contact interface between trans-femoral stump and prosthetic socket. *Proceedings of the Annual International Conference of the IEEE Engineering in Medicine and Biology Society, EMBS.* 2013:1270-1273. Accessed 2 March 2014.
77. Colombo G, Facoetti G, Morotti R, Rizzi C. Physically based modelling and simulation to innovate socket design. *Computer-Aided Design and Applications.* 2011;8(4):617-631. Accessed 9 February 2014.

78. Peng H-, Hsu LH, Huang GF, Hong DY. The analysis and measurement of interface pressures between stump and rapid prototyping prosthetic socket coated with a resin layer for transtibial amputee. IFMBE Proceedings. 2009;23:1720-1723. Accessed 22 April 2014.
79. Faustini MC, Neptune RR, Crawford RH. The quasi-static response of compliant prosthetic sockets for transtibial amputees using finite element methods. Medical Engineering and Physics. 2006;28(2):114-121. Accessed 23 February 2016.
80. Jia X, Zhang M, Li X, Lee WCC. A quasi-dynamic nonlinear finite element model to investigate prosthetic interface stresses during walking for trans-tibial amputees. Clin Biomech. 2005;20(6):630-635. Accessed 13 May 2015.
81. Jia X, Zhang M, Wang R, Jin D. Dynamic investigation of interface stress on below-knee residual limb in a prosthetic socket. Tsinghua Science and Technology. 2004;9(6):680-683. Accessed 23 February 2016.
82. Jia X, Zhang M, Lee WCC. Load transfer mechanics between trans-tibial prosthetic socket and residual limb - dynamic effects. J Biomech. 2004;37(9):1371-1377. Accessed 2 February 2014.
83. Lee WCC, Zhang M, Jia X, Cheung JTM. Finite element modeling of the contact interface between trans-tibial residual limb and prosthetic socket. Medical Engineering and Physics. 2004;26(8):655-662. Accessed 2 February 2014.
84. Portnoy S, Yizhar Z, Shabshin N, et al. Internal mechanical conditions in the soft tissues of a residual limb of a trans-tibial amputee. J Biomech. 2008;41(9):1897-1909. Accessed 23 February 2016.
85. Portnoy S, Yarnitzky G, Yizhar Z, et al. Real-time patient-specific finite element analysis of internal stresses in the soft tissues of a residual limb: A new tool for prosthetic fitting. Ann Biomed Eng. 2007;35(1):120-135. Accessed 23 February 2016.
86. Sengeh DM, Herr H. A variable-impedance prosthetic socket for a transtibial amputee designed from magnetic resonance imaging data. Journal of Prosthetics and Orthotics. 2013;25(3):129-137. Accessed 11 March 2014.
87. Lee WCC, Zhang M. Using computational simulation to aid in the prediction of socket fit: A preliminary study. Medical Engineering and Physics. 2007;29(8):923-929. Accessed 23 February 2016.
88. Jia X, Zhang M, Li X, Lee WCC. A quasi-dynamic nonlinear finite element model to investigate prosthetic interface stresses during walking for trans-tibial amputees. Clin Biomech. 2005;20(6):630-635. Accessed 23 February 2016.
89. Lenka P, Choudhury A. Analysis of trans tibial prosthetic socket materials using finite element method. J. Biomedical Science and Engineering. 2011;4:762.
90. Nehme G, Dib M. Impact of pressure distribution on the relief areas of prosthetic sockets for transtibial amputees using design of experiment and finite element analysis. Journal of Prosthetics and Orthotics. 2011;23(4):170-183. Accessed 23 February 2016.
91. Lee WCC, Zhang M, Jia X, Cheung JTM. Finite element modeling of the contact interface between trans-tibial residual limb and prosthetic socket. Medical Engineering and Physics. 2004;26(8):655-662. Accessed 23 February 2016.

92. Tönük E, Silver-Thorn MB. Nonlinear viscoelastic material property estimation of lower extremity residual limb tissues. *J Biomech Eng.* 2004;126(2):289-300. Accessed 6 October 2013.
93. Tonuk E, Silver-Thorn MB. Nonlinear viscoelastic material property estimation for lower extremity residual limbs. *Annual International Conference of the IEEE Engineering in Medicine and Biology - Proceedings.* 1999;1:645. Accessed 6 October 2013.
94. Daly W, Voo L, Rosenbaum-Chou T, Arabian A, Boone D. Socket pressure and discomfort in upper-limb prostheses: A preliminary study. *Journal of Prosthetics and Orthotics.* 2014;26(2):99-106. Accessed 22 April 2014.
95. Sensinger JW, Weir RFF. Modeling and preliminary testing socket-residual limb interface stiffness of above-elbow prostheses. *IEEE Transactions on Neural Systems and Rehabilitation Engineering.* 2008;16(2):184-190. Accessed 13 May 2015.

Chapter 6

1. Schofield JS, Evans KR, Hebert JS, Marasco PD, Carey JP. The effect of biomechanical variables on force sensitive resistor error: Implications for calibration and improved accuracy. *J Biomech.* 2016;49(5):786. doi: <http://dx.doi.org/10.1016/j.jbiomech.2016.01.022>.
2. Hall RS, Desmoulin GT, Milner TE. A technique for conditioning and calibrating force-sensing resistors for repeatable and reliable measurement of compressive force. *J Biomech.* 2008;41(16):3492-3495. Accessed 11 December 2015. doi: 10.1016/j.jbiomech.2008.09.031.
3. Lebosse C, Renaud P, Bayle B, De Mathelin M. Modeling and evaluation of low-cost force sensors. *IEEE Transactions on Robotics.* 2011;27(4):815-822. Accessed 22 April 2015.
4. Dabling JG, Filatov A, Wheeler JW. Static and cyclic performance evaluation of sensors for human interface pressure measurement. *Proceedings of the Annual International Conference of the IEEE Engineering in Medicine and Biology Society, EMBS.* 2012:162-165. Accessed 22 April 2015.
5. Mak AFT, Zhang M, Tam EWC, eds. *Biomechanics of pressure ulcer in body tissues interacting with external forces during locomotion.* ; 2010Annual Review of Biomedical Engineering; No. 12.
6. Hebert JS, Olson JL, Morhart MJ, et al. Novel targeted sensory reinnervation technique to restore functional hand sensation after transhumeral amputation. *IEEE Transactions on Neural Systems and Rehabilitation Engineering.* 2014;22(4):765.
7. Junaid AB, Tahir S, Rasheed T, et al. Low-cost design and fabrication of an anthropomorphic robotic hand. *Journal of Nanoscience and Nanotechnology.* 2014;14(10):7427-7431. Accessed 22 April 2015.
8. Silver-Thorn MB, Steege JW, Childress DS. A review of prosthetic interface stress investigations. *Journal of Rehabilitation Research and Development.* 1996;33(3):253-266. Accessed 9 February 2014.
9. Moon S-, Lee C-, Lee S-. A study of knee brace locking timing and walking pattern detected from an FSR and knee joint angle. *International Conference on Control, Automation and Systems.* 2011:1783-1787. Accessed 22 April 2015.
10. Rueterbories J, Spaich EG, Larsen B, Andersen OK. Methods for gait event detection and analysis in ambulatory systems. *Medical Engineering and Physics.* 2010;32(6):545-552. Accessed 22 April 2015.

11. Yun MH, Cannon D, Freivalds A, Thomas G. An instrumented glove for grasp specification in virtual-reality-based point-and-direct telerobotics. *IEEE Transactions on Systems, Man, and Cybernetics, Part B: Cybernetics*. 1997;27(5):835-846. Accessed 22 April 2015.
12. Cascioli V, Liu Z, Heusch AI, McArthur PW. Settling down time following initial sitting and its relationship with comfort and discomfort. *J Tissue Viability*. 2011;20(4):121-129. Accessed 22 April 2015.
13. Di Fazio D, Lombardo L, Gracco A, D'Amico P, Siciliani G. Lip pressure at rest and during function in 2 groups of patients with different occlusions. *American Journal of Orthodontics and Dentofacial Orthopedics*. 2011;139(1):e1-e6. Accessed 22 April 2015.
14. Herbert-Copley AG, Sinitski EH, Lemaire ED, Baddour N. Temperature and measurement changes over time for F-scan sensors. *MeMeA 2013 - IEEE International Symposium on Medical Measurements and Applications, Proceedings*. 2013:265-267. Accessed 22 April 2015.
15. Polliack AA, Sieh RC, Craig DD, Landsberger S, McNeil DR, Ayyappa E. Scientific validation of two commercial pressure sensor systems for prosthetic socket fit. *Prosthet Orthot Int*. 2000;24(1):63-73. Accessed 22 April 2015.
16. Buis AWP, Convery P. Calibration problems encountered while monitoring stump/socket interface pressures with force sensing resistors: Techniques adopted to minimise inaccuracies. *Prosthet Orthot Int*. 1997;21(3):179-182. Accessed 22 April 2015.
17. Interlink Electronics. FSR integration guide. . 2015.
18. TekScan. Pressure mapping, force measurement & tactile sensors. <https://www.tekscan.com/pressure-mapping-sensors>. Updated 2015. Accessed Apr. 22, 2015, 2015.
19. Montgomery D.C. Factorials with mixed levels. In: *Design and analysis of experiments*. 8th ed. Wiley; 2012:412.
20. NASA. Volume I section 3: Anthropometry and biomechanics. <http://msis.jsc.nasa.gov/sections/section03.htm>. Updated 2008. Accessed 04/22, 2015.
21. Jang E-, Cho Y-, Chi S-, Lee J-, Kang SS, Chun B-. Recognition of walking intention using multiple bio/kinesthetic sensors for lower limb exoskeletons. *ICCAS 2010 - International Conference on Control, Automation and Systems*. 2010:1802-1805. Accessed 22 April 2015.
22. More M, Lka O, eds. *Design of active feedback for rehabilitation robot*. ; 2014Applied Mechanics and Materials; No. 611.
23. Rogers B, Zhang W, Narayana S, Lancaster JL, Robin DA, Fox PT. Force sensing system for automated assessment of motor performance during fMRI. *J Neurosci Methods*. 2010;190(1):92-94. Accessed 22 April 2015.
24. Wang X, Zhao J, Yang D, Li N, Sun C, Liu H. Biomechatronic approach to a multi-fingered hand prosthesis. *2010 3rd IEEE RAS and EMBS International Conference on Biomedical Robotics and Biomechatronics, BioRob 2010*. 2010:209-214. Accessed 22 April 2015.
25. Hollinger A, Wanderley MM. Evaluation of commercial force-sensing resistors. . 2006.

26. Armiger RS, Tenore FV, Katyal KD, et al. Enabling closed-loop control of the modular prosthetic limb through haptic feedback. *Johns Hopkins APL Technical Digest (Applied Physics Laboratory)*. 2013;31(4):345-353. Accessed 29 April 2013.
27. Antfolk C, Balkenius C, Lundborg G, Rosén B, Sebelius F. A tactile display system for hand prostheses to discriminate pressure and individual finger localization. *Journal of Medical and Biological Engineering*. 2010;30(6):355-360. Accessed 5 April 2013.
28. ANSI. ANSI/ISA-51.1-1979 (R1993) process instrumentation terminology. . 1995.

Chapter 7

1. Lake C. The evolution of upper limb prosthetic socket design. *Journal of Prosthetics and Orthotics*. 2008;20(3):85-92. Accessed 20 December 2013.
2. Resnik L, Patel T, Cooney SG, Crisco JJ, Fantini C. Comparison of transhumeral socket designs utilizing patient assessment and in vivo skeletal and socket motion tracking: A case study. *Disabil Rehabil Assistive Technol*. 2016;11(5):423-432. Accessed 29 November 2016. doi: 10.3109/17483107.2014.981876.
3. Mcfarland LV, Winkler SLH, Heinemann AW, Jones M, Esquenazi A. Unilateral upper-limb loss: Satisfaction and prosthetic-device use in veterans and servicemembers from vietnam and OIF/OEF conflicts. *J Rehabil Res Dev*. 2010;47(4):299-316. Accessed 29 November 2016. doi: 10.1682/JRRD.2009.03.0027.
4. Biddiss E, Chau T. Upper limb prosthesis use and abandonment: A survey of the last 25 years. *Prosthet Orthot Int*. 2007;31(3):236-257. Accessed 24 January 2014.
5. Schultz AE, Baade SP, Kuiken TA. Expert opinions on success factors for upper-limb prostheses. *Journal of Rehabilitation Research and Development*. 2007;44(4):483-489. Accessed 5 April 2013.
6. Sanders J. Stump-socket interface conditions. In: *Pressure ulcer research: Current and future perspectives*. Heidelberg Germany: Springer-Verlag Berlin; 2005:129-147. Accessed 25 January 2016.
7. Alley RD, Williams TW, Albuquerque MJ, Altobelli DE. Prosthetic sockets stabilized by alternating areas of tissue compression and release. *Journal of Rehabilitation Research and Development*. 2011;48(6):679-696. Accessed 5 April 2013.
8. Lake C, Dodson R. Progressive upper limb prosthetics. *Phys Med Rehabil Clin N Am*. 2006;17(1):49-72. Accessed 5 April 2013.
9. Ziegler-Graham K, MacKenzie EJ, Ephraim PL, Travison TG, Brookmeyer R. Estimating the prevalence of limb loss in the united states: 2005 to 2050. *Arch Phys Med Rehabil*. 2008;89(3):422-429. doi: <http://dx.doi.org/10.1016/j.apmr.2007.11.005>.
10. Brenner CD. Wrist disarticulation and transradial amputation: Prosthetic management. In: Smith DG, Michael JW, Bowker JH, ed. *Atlas of amputations and limb deficienciesd surgical, prosthetic and rehabilitation principles*. 3rd ed. Rosemont: American Academy of Orthopaedic Surgeons; 2004:223-230.
11. Biddiss E, Beaton D, Chau T. Consumer design priorities for upper limb prosthetics. *Disability and Rehabilitation: Assistive Technology*. 2007;2(6):346-357. Accessed 5 April 2013.

12. Daly W, Voo L, Rosenbaum-Chou T, Arabian A, Boone D. Socket pressure and discomfort in upper-limb prostheses: A preliminary study. *Journal of Prosthetics and Orthotics*. 2014;26(2):99-106. Accessed 22 April 2014.
13. Silver-Thorn MB, Steege JW, Childress DS. A review of prosthetic interface stress investigations. *Journal of Rehabilitation Research and Development*. 1996;33(3):253-266. Accessed 9 February 2014.
14. Sanders JE. Interface mechanics in external prosthetics: Review of interface stress measurement techniques. *Med Biol Eng Comput*. 1995;33(4):509-516. Accessed 13 May 2015.
15. Herbert-Copley AG, Sinitski EH, Lemaire ED, Baddour N. Temperature and measurement changes over time for F-scan sensors. *MeMeA 2013 - IEEE International Symposium on Medical Measurements and Applications, Proceedings*. 2013:265-267. Accessed 22 April 2015.
16. Polliack AA, Sieh RC, Craig DD, Landsberger S, McNeil DR, Ayyappa E. Scientific validation of two commercial pressure sensor systems for prosthetic socket fit. *Prosthet Orthot Int*. 2000;24(1):63-73. Accessed 22 April 2015.
17. Buis AWP, Convery P. Calibration problems encountered while monitoring stump/socket interface pressures with force sensing resistors: Techniques adopted to minimise inaccuracies. *Prosthet Orthot Int*. 1997;21(3):179-182. Accessed 22 April 2015.
18. Pirouzi G, Abu Osman NA, Eshraghi A, Ali S, Gholizadeh H, Wan Abas WAB. Review of the socket design and interface pressure measurement for transtibial prosthesis. *Scientific World Journal*. 2014;2014. Accessed 22 April 2015.
19. Kahle JT, Jason Highsmith MJ. Transfemoral sockets with vacuum-assisted suspension comparison of hip kinematics, socket position, contact pressure, and preference: Ischial containment versus brimless. *Journal of Rehabilitation Research and Development*. 2013;50(9):1241-1252. Accessed 2 February 2016.
20. Dumbleton T, Buis AWP, McFadyen A, et al. Dynamic interface pressure distributions of two transtibial prosthetic socket concepts. *Journal of Rehabilitation Research and Development*. 2009;46(3):405-415. Accessed 2 February 2016.
21. Rogers B, Bosker G, Faustini M, Walden G, Neptune RR, Crawford R. Case report: Variably compliant transtibial prosthetic socket fabricated using solid freeform fabrication. *Journal of Prosthetics and Orthotics*. 2008;20(1):1-7. Accessed 2 February 2016.
22. Heinemann AW, Bode RK, O'Reilly C. Development and measurement properties of the orthotics and prosthetics user's survey (OPUS): A comprehensive set of clinical outcome instruments. *Prosthet Orthot Int*. 2003;27(3):191-206. Accessed 24 February 2014.
23. Schofield JS, Evans KR, Hebert JS, Marasco PD, Carey JP. The effect of biomechanical variables on force sensitive resistor error: Implications for calibration and improved accuracy. *J Biomech*. 2016;49(5):786. doi: <http://dx.doi.org/10.1016/j.jbiomech.2016.01.022>.
24. Resnik L, Patel T, Cooney SG, Crisco JJ, Fantini C. Comparison of transhumeral socket designs utilizing patient assessment and in vivo skeletal and socket motion tracking: A case study. *Disabil Rehabil Assistive Technol*. 2016;11(5):423-432. Accessed 8 January 2017. doi: 10.3109/17483107.2014.981876.
25. Biddiss E, Chau T. Upper-limb prosthetics: Critical factors in device abandonment. *Am J Phys Med Rehabil*. 2007;86(12):977-987. Accessed 16 March 2017. doi: 10.1097/PHM.0b013e3181587f6c.

Chapter 8

1. Kim K, Colgate JE, Santos-Munné JJ, Makhlin A, Peshkin MA. On the design of miniature haptic devices for upper extremity prosthetics. *IEEE/ASME Transactions on Mechatronics*. 2010;15(1):27-39. Accessed 5 April 2013.
2. Schofield JS, Evans KR, Carey JP, Hebert JS. Applications of sensory feedback in motorized upper extremity prosthesis: A review. *Expert Review of Medical Devices*. 2014;11(5):499-511. Accessed 8 April 2015.
3. Biddiss E, Chau T. Upper limb prosthesis use and abandonment: A survey of the last 25 years. *Prosthet Orthot Int*. 2007;31(3):236-257. Accessed 24 January 2014.
4. Biddiss E, Chau T. Upper-limb prosthetics: Critical factors in device abandonment. *Am J Phys Med Rehabil*. 2007;86(12):977-987. Accessed 16 March 2017. doi: 10.1097/PHM.0b013e3181587f6c.
5. Antfolk C, D'alonzo M, Rosén B, Lundborg G, Sebelius F, Cipriani C. Sensory feedback in upper limb prosthetics. *Expert Review of Medical Devices*. 2013;10(1):45-54. Accessed 2 December 2013.
6. Schofield JS, Schoepp KR, Williams HE, Carey JP, Marasco PD, Hebert J.S. Characterization of interfacial socket pressure in transhumeral prostheses: A case series. *PLoS ONE*. 2017.
7. Alley RD, Williams TW, Albuquerque MJ, Altobelli DE. Prosthetic sockets stabilized by alternating areas of tissue compression and release. *Journal of Rehabilitation Research and Development*. 2011;48(6):679-696. Accessed 5 April 2013.
8. Stegeman DF, Hermens HJ. **Standards for surface electromyography**. *The European Project Surface EMG for Non-Invasive Assessment of Muscles (SENIAM)*. 2007.
9. Day S. Important factors in surface EMG measurement. Bortec biomedical ltd. .
10. Liberating Technologies Inc. Remote electrode system installation guide. .
11. Daly W, Voo L, Rosenbaum-Chou T, Arabian A, Boone D. Socket pressure and discomfort in upper-limb prostheses: A preliminary study. *Journal of Prosthetics and Orthotics*. 2014;26(2):99-106. Accessed 22 April 2014.
12. Lake C. The evolution of upper limb prosthetic socket design. *Journal of Prosthetics and Orthotics*. 2008;20(3):85-92. Accessed 20 December 2013.
13. Schofield JS, Evans KR, Hebert JS, Marasco PD, Carey JP. The effect of biomechanical variables on force sensitive resistor error: Implications for calibration and improved accuracy. *J Biomech*. 2016;49(5):786. doi: <http://dx.doi.org/10.1016/j.jbiomech.2016.01.022>.

Chapter 9

1. Biddiss E, Chau T. Upper-limb prosthetics: Critical factors in device abandonment. *Am J Phys Med Rehabil*. 2007;86(12):977-987. Accessed 16 March 2017. doi: 10.1097/PHM.0b013e3181587f6c.
2. Schultz AE, Baade SP, Kuiken TA. Expert opinions on success factors for upper-limb prostheses. *Journal of Rehabilitation Research and Development*. 2007;44(4):483-489. Accessed 5 April 2013.

3. Biddiss E, Chau T. Upper limb prosthesis use and abandonment: A survey of the last 25 years. *Prosthet Orthot Int*. 2007;31(3):236-257. Accessed 24 January 2014.
4. Biddiss E, Beaton D, Chau T. Consumer design priorities for upper limb prosthetics. *Disability and Rehabilitation: Assistive Technology*. 2007;2(6):346-357. Accessed 5 April 2013.
5. Schofield JS, Schoepp KR, Williams HE, Carey JP, Marasco PD, Hebert J.S. Characterization of interfacial socket pressure in transhumeral prostheses: A case series. *PLoS ONE*. 2017.
6. Sanders J. Stump-socket interface conditions. In: *Pressure ulcer research: Current and future perspectives*. Heidelberg Germany: Springer-Verlag Berlin; 2005:129-147. Accessed 25 January 2016.
7. Alley RD, Williams TW, Albuquerque MJ, Altobelli DE. Prosthetic sockets stabilized by alternating areas of tissue compression and release. *Journal of Rehabilitation Research and Development*. 2011;48(6):679-696. Accessed 5 April 2013.
8. McFarland LV, Winkler SLH, Heinemann AW, Jones M, Esquenazi A. Unilateral upper-limb loss: Satisfaction and prosthetic-device use in veterans and servicemembers from vietnam and OIF/OEF conflicts. *J Rehabil Res Dev*. 2010;47(4):299-316. Accessed 29 November 2016. doi: 10.1682/JRRD.2009.03.0027.
9. Lake C, Dodson R. Progressive upper limb prosthetics. *Phys Med Rehabil Clin N Am*. 2006;17(1):49-72. Accessed 5 April 2013.
10. Daly W, Voo L, Rosenbaum-Chou T, Arabian A, Boone D. Socket pressure and discomfort in upper-limb prostheses: A preliminary study. *Journal of Prosthetics and Orthotics*. 2014;26(2):99-106. Accessed 22 April 2014.
11. Zachariah SG, Sanders JE. Interface mechanics in lower-limb external prosthetics: A review of finite element models. *IEEE Trans Rehabil Eng*. 1996;4(4):288-302. Accessed 26 January 2016. doi: 10.1109/86.547930.
12. Zhang M, Mak AFT, Roberts VC. Finite element modelling of a residual lower-limb in a prosthetic socket: A survey of the development in the first decade. *Medical Engineering and Physics*. 1998;20(5):360-373. Accessed 31 January 2014.
13. Peng H-, Hsu LH, Huang GF, Hong DY. The analysis and measurement of interface pressures between stump and rapid prototyping prosthetic socket coated with a resin layer for transtibial amputee. *IFMBE Proceedings*. 2009;23:1720-1723. Accessed 22 April 2014.
14. Faustini MC, Neptune RR, Crawford RH. The quasi-static response of compliant prosthetic sockets for transtibial amputees using finite element methods. *Medical Engineering and Physics*. 2006;28(2):114-121. Accessed 23 February 2016.
15. Goh JCH, Lee PVS, Toh SL, Ooi CK. Development of an integrated CAD-FEA process for below-knee prosthetic sockets. *Clin Biomech*. 2005;20(6):623-629. Accessed 2 February 2014.
16. Jia X, Zhang M, Wang R, Jin D. Dynamic investigation of interface stress on below-knee residual limb in a prosthetic socket. *Tsinghua Science and Technology*. 2004;9(6):680-683. Accessed 23 February 2016.
17. Lee WCC, Zhang M, Jia X, Cheung JTM. Finite element modeling of the contact interface between trans-tibial residual limb and prosthetic socket. *Medical Engineering and Physics*. 2004;26(8):655-662. Accessed 23 February 2016.

18. Colombo G, Facoetti G, Morotti R, Rizzi C. Physically based modelling and simulation to innovate socket design. *Computer-Aided Design and Applications*. 2011;8(4):617-631. Accessed 9 February 2014.
19. Heinemann AW, Bode RK, O'Reilly C. Development and measurement properties of the orthotics and prosthetics user's survey (OPUS): A comprehensive set of clinical outcome instruments. *Prosthet Orthot Int*. 2003;27(3):191-206. Accessed 24 February 2014.
20. Winter DA. *Biomechanics and motor control of human movement*. Hoboken, N.J.: John Wiley & Sons; 2005.
21. Tönük E, Silver-Thorn MB. Nonlinear viscoelastic material property estimation of lower extremity residual limb tissues. *J Biomech Eng*. 2004;126(2):289-300. Accessed 6 October 2013.
22. Zhang L, Zhu M, Shen L, Zheng F. Finite element analysis of the contact interface between trans-femoral stump and prosthetic socket. *Proceedings of the Annual International Conference of the IEEE Engineering in Medicine and Biology Society, EMBS*. 2013:1270-1273. Accessed 2 March 2014.
23. INEOS Global. Typical engineering properties of polypropylene. <http://www.ineos.com/Global/Olefins%20and%20Polymers%20USA/Products/Technical%20information/Engineering%20Properties%20of%20PP.pdf>. Updated 20102014.
24. Nehme G, Dib M. Impact of pressure distribution on the relief areas of prosthetic sockets for transtibial amputees using design of experiment and finite element analysis. *Journal of Prosthetics and Orthotics*. 2011;23(4):170-183. Accessed 23 February 2016.
25. Lenka P, Choudhury A. Analysis of trans tibial prosthetic socket materials using finite element method. *J. Biomedical Science and Engineering*. 2011;4:762.

Chapter 10


1. Belter JT, Segil JL, Dollar AM, Weir RF. Mechanical design and performance specifications of anthropomorphic prosthetic hands: A review. *Journal of Rehabilitation Research and Development*. 2013;50(5):599-618. Accessed 27 February 2014.
2. Zlotolow DA, Kozin SH. Advances in upper extremity prosthetics. *Hand Clin*. 2012;28(4):587-563. Accessed 8 April 2015.
3. Biddiss E, Chau T. Upper limb prosthesis use and abandonment: A survey of the last 25 years. *Prosthet Orthot Int*. 2007;31(3):236-257. Accessed 24 January 2014.
4. Biddiss E, Chau T. Upper-limb prosthetics: Critical factors in device abandonment. *Am J Phys Med Rehabil*. 2007;86(12):977-987. Accessed 16 March 2017. doi: 10.1097/PHM.0b013e3181587f6c.
5. Gordon J, Ghilardi MF, Ghez C. Impairments of reaching movements in patients without proprioception. I. spatial errors. *J Neurophysiol*. 1995;73(1):347-360. Accessed 24 May 2017.
6. Ghez C, Gordon J, Ghilardi MF. Impairments of reaching movements in patients without proprioception. II. effects of visual information on accuracy. *J Neurophysiol*. 1995;73(1):361-372. Accessed 24 May 2017.
7. Schofield JS, Evans KR, Carey JP, Hebert JS. Applications of sensory feedback in motorized upper extremity prosthesis: A review. *Expert Review of Medical Devices*. 2014;11(5):499-511. Accessed 8 April 2015.

8. Lundborg G, Rosen B, Lindstrom K, Lindberg S. Artificial sensibility based on the use of piezoresistive sensors. *J Hand Surg.* 1998;23 B(5):620-626. Accessed 3 December 2013.
9. Gonzalez J, Soma H, Sekine M, Yu W. Auditory display as a prosthetic hand biofeedback. *Journal of Medical Imaging and Health Informatics.* 2011;1(4):325-333. Accessed 3 December 2013.

Appendix A: Error data for the fitting of calibration equations

For each FSR, calibration equations mapping FSR voltage to applied load were determined through the fitting of an inverse logarithmic equation. In total, twelve equations per FSR were determined corresponding to the twelve combinations of temperature, curvature and compliance introduced. The fitted-root-mean-squared-error (RMSE-F), mean absolute error (MAE), and maximum error were calculated and recorded for each combination. These error values are reported for each sensor tested in Table A-1 below.

Table A-1 The fitting error for the determined calibration equations for each of the 6 sensors under the 12 unique temperature, curvature and compliance conditions are reported. Curvature is reported in terms of diameter and denoted in millimetres. RMSE, MAE abbreviates root mean square error and mean absolute error, respectively. MAE and Max (maximum) error are report in force units of Newton as denoted by N.



Sensor	Temperature (°C)	Curvature (mm)	Compliance	Small			Medium			Square		
				RMSE	MAE (N)	Max Error (N)	RMSE	MAE (N)	Max Error (N)	RMSE	MAE (N)	Max Error (N)
1	22	Flat	Rigid	0.4	0.3	1.3	0.4	0.3	1.4	0.5	0.4	1.4
1	22	Flat	Soft	0.7	0.5	1.6	0.3	0.3	0.8	0.3	0.3	1.0
1	22	44	Rigid	0.6	0.5	1.6	0.4	0.3	1.3	1.6	1.2	3.9
1	22	44	Soft	0.4	0.3	1.1	0.3	0.3	1.1	0.5	0.5	1.5
1	22	214	Rigid	0.8	0.6	2.0	0.4	0.3	1.3	0.6	0.5	1.4
1	22	214	Soft	0.8	0.6	2.5	0.4	0.4	1.2	0.3	0.2	0.9
1	37	Flat	Rigid	0.4	0.4	1.1	0.3	0.3	0.9	0.3	0.2	0.8
1	37	Flat	Soft	1.3	1.0	2.9	0.4	0.3	1.3	0.4	0.3	1.2
1	37	44	Rigid	0.5	0.4	1.3	0.4	0.4	1.1	0.9	0.7	2.3
1	37	44	Soft	0.5	0.3	1.7	-	-	-	0.9	0.8	2.3
1	37	214	Rigid	1.0	0.8	2.9	0.4	0.3	1.1	0.7	0.6	1.4
1	37	214	Soft	0.8	0.6	2.9	0.4	0.3	1.4	0.3	0.3	0.9
2	22	Flat	Rigid	0.5	0.4	1.5	0.6	0.4	2.3	0.4	0.4	1.1
2	22	Flat	Soft	1.1	0.7	3.9	0.4	0.3	1.0	0.3	0.2	1.0
2	22	44	Rigid	0.5	0.4	1.3	0.5	0.4	1.7	1.2	1.0	2.8
2	22	44	Soft	0.5	0.4	1.9	0.4	0.3	1.3	0.9	0.8	2.7
2	22	214	Rigid	0.7	0.6	1.8	0.4	0.3	1.3	0.7	0.5	2.1
2	22	214	Soft	1.2	0.9	3.7	0.3	0.3	0.9	0.3	0.2	0.7
2	37	Flat	Rigid	0.5	0.4	1.5	0.4	0.4	1.1	0.5	0.4	1.4
2	37	Flat	Soft	0.9	0.7	2.8	0.4	0.3	1.0	0.4	0.3	1.1
2	37	44	Rigid	1.4	1.2	3.7	0.6	0.5	1.9	0.5	0.4	1.9
2	37	44	Soft	0.6	0.5	2.0	0.5	0.4	1.6	0.7	0.6	1.9
2	37	214	Rigid	0.5	0.4	1.5	0.4	0.4	1.4	0.4	0.3	1.2
2	37	214	Soft	2.2	1.7	6.3	0.5	0.4	1.6	0.3	0.2	0.9

Appendix B: Modified OPUS survey results

To confirm the socket worn by each participant was in fact a ‘well-fit’ socket, sockets were evaluated by a certified prosthetist. To further confirm the quality of socket fit, each participant completed an OPUS Satisfaction with Device survey modified to present questions relevant to prosthetic socket fit. Survey result are includes in Table B-1 below.

Table B-1. Modified OPUS survey results. Note: 50th percentile (average) results in the *Satisfaction with Device Survey* has a Measure of approximately 45 and Score of 22

		Scoring Categories						Comments
		Strongly agree	Agree	Neither agree nor disagree	Disagree	Strongly disagree	N/A	
Participant 1								
My prosthesis fits well			X					Requires assistance due to bilateral amputation Investigators noted irritation near axilla
My prosthesis is comfortable throughout the day	X							
It is easy to put on my prosthesis							X	
My skin is free of abrasions and irritations			X					
My prosthesis is pain free to wear	X							
OPUS Score	38	OPUS Measure			72	Percentile		99
Participant 2								
My prosthesis fits well	X							Participant noted the harness required readjustment
My prosthesis is comfortable throughout the day				X				
It is easy to put on my prosthesis				X				Irritation around neck due to harness
My skin is free of abrasions and irritations		X						
My prosthesis is pain free to wear		X						
OPUS Score	34	OPUS Measure			65	Percentile		99
Participant 3								
My prosthesis fits well		X						Participant noted the harness required readjustment
My prosthesis is comfortable throughout the day					X			
It is easy to put on my prosthesis				X				
My skin is free of abrasions and irritations				X				
My prosthesis is pain free to wear					X			
OPUS Score	25	OPUS Measure			51	Percentile		71
Participant 4								
My prosthesis fits well		X						
My prosthesis is comfortable throughout the day		X						
It is easy to put on my prosthesis		X						
My skin is free of abrasions and irritations		X						
My prosthesis is pain free to wear		X						
OPUS Score	36	OPUS Measure			68	Percentile		99

Appendix C: OPUS survey results prior to modelling

To confirm the socket worn by each participant was in fact a ‘well-fit’ socket, sockets were evaluated by a certified prosthetist. To further confirm the quality of socket fit, each participant completed an OPUS Satisfaction with Device survey modified to present questions relevant to prosthetic socket fit. Survey results are included in Table C-1 below.

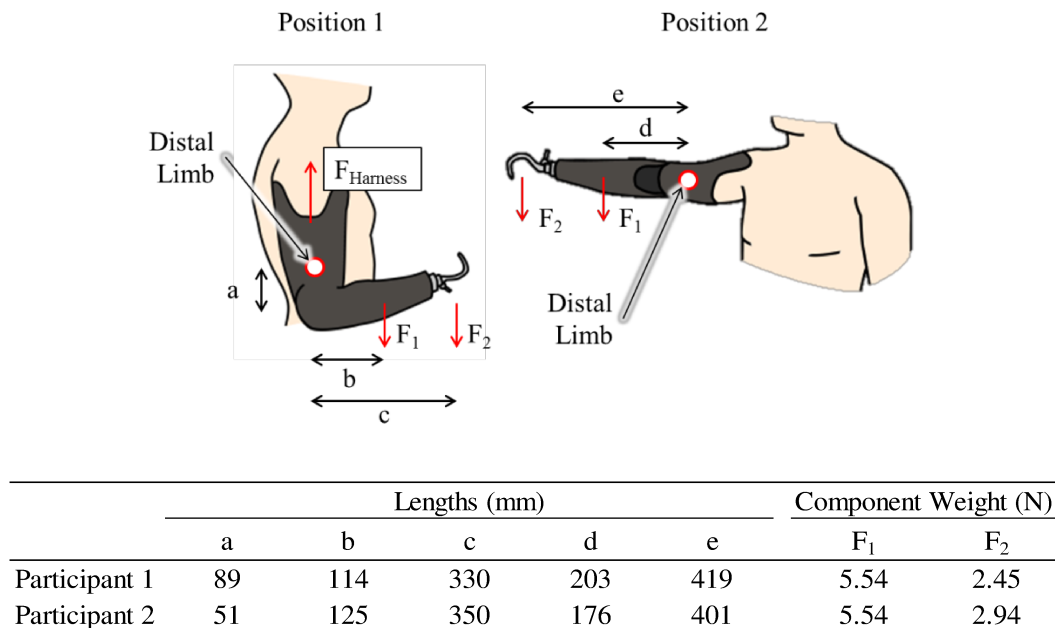
Table C-1. Modified OPUS survey results. Note: 50th percentile (average) results in the *Satisfaction with Device Survey* has a Measure of approximately 45 and Score of 22

		Scoring Categories						Comments
		Strongly agree	Agree	Neither agree nor disagree	Disagree	Strongly disagree	N/A	
Participant 1								
My prosthesis fits well			X					
My prosthesis is comfortable throughout the day		X						
It is easy to put on my prosthesis							X	Requires assistance due to bilateral amputation
My skin is free of abrasions and irritations			X					Investigators noted irritation near axilla
My prosthesis is pain free to wear		X						
OPUS Score		38	OPUS Measure			72	Percentile 99	
Participant 2								
My prosthesis fits well		X						
My prosthesis is comfortable throughout the day				X				Participant noted the harness required readjustment
It is easy to put on my prosthesis				X				
My skin is free of abrasions and irritations			X					Irritation around neck due to harness
My prosthesis is pain free to wear			X					
OPUS Score		34	OPUS Measure			65	Percentile 99	

Appendix D: Model loading calculations

Prosthetic loading conditions were calculated from the prosthetic geometry, component weight and body position for each participant. A force was applied in the model to the distal tip of the rigid bone cavity to simulate the reaction forces at the humerus as a result of prosthetic loading. Participant 1 used a Hosmer 555 Lyre hook (250g) and an Ottobock ErgoArm (565g). Participant 2 used an Ottobock 8k23 hand (300g) and an Ottobock ErgoArm (565g). Calculations to arrive at the modelled reaction forces F_{reac1} and F_{reac2} are provided in Figure D-1 and Figure D-2 below.

Figure D-1 Dimensions and forces used to calculate model loading. Calculations assumed a loading moment in close proximity to the distal tip of the residual limb. The center of gravity of the prosthetic components was assumed to occur at mid length. (a) Denotes the length from the elbow center of rotation to the distal end of the limb. (b) Is the distance from the elbow center of rotation to the forearm center of gravity. (c) The distance from the elbow center of rotation to the prehensor center of gravity. (d) Distance from the distal tip of the limb to forearm center of gravity. (e) Distance from the distal tip of the limb to the prehensor center of gravity. F_1 and F_2 represent the component weight of the forearm/elbow, and prehensor, respectively.

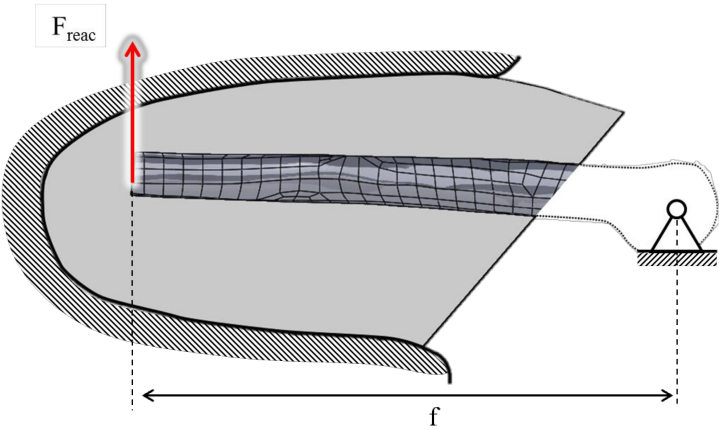


Equations used to determine the reaction moments introduced to the residual limb as a result of prosthetic component weight. Where M_{90} and M_{extn} denote the reaction moments with the prosthetic elbow at 90° degrees and fully extended, respectively.

$$\text{Position 1: } M_{90} = (b)F_1 + (c)F_2$$

$$\text{Position 2: } M_{\text{extn}} = (d)F_1 + (e)F_2$$

Figure D-2 The dimensions and equations used to calculate the reaction forces to be modelled. Where F_{reac1} and F_{reac2} denote the modelled reaction forces. f represents the approximate length to the humeral head.



Position 1: $F_{\text{reac1}} = M_{90}/f$

Position 2: $F_{\text{reac2}} = M_{\text{extn}}/f$

	Reaction Moments (Nm)		Length (mm)	Reaction Force (N)	
	M_{90}	M_{extn}	f (mm)	F_{reac1}	F_{reac2}
Participant 1	1.44	2.15	250	5.76	8.60
Participant 2	1.72	2.15	230	7.48	9.37

Appendix E: Mesh Sensitivity Analysis

To evaluate the sensitivity of the model's results to mesh size, a prosthetic reaction force of 8N was applied to the modelled geometry of participant 1. This loading condition, as well as all other boundary, and contact condition definitions were consistent with those described in Chapter 9. The soft tissue was meshed using quadratic tetrahedral elements. An initial seed constraint limiting elements to a maximum of 6mm was implemented. Refinement of the region surrounding the distal tip of the humeral bone cavity and edges of the soft tissue was performed in which a maximum element size of 3mm was implemented. Once the model solved, the maximum predicted contact pressure was recorded, as well as the corresponding anatomical location and the time required for the model to solve. The mesh seed values (6mm and 3mm) were then scaled by a multiplying factor. For example, with a scale factor of 2.00 the 6mm and 3mm initial seed size values would become 12mm and 6mm, respectively. The model was then rerun and the Maximum contact pressure, the location, and the time to solve were recorded. This procedure was repeated for scaling factors from 0.75 through 2.00 in increments of 0.25. Results are highlighted in the Table E-1 below.

Table E-1 Mesh sensitivity analysis. Note: a Dell Precision T5610 Computer with Intel Xeon E5-2670 processors was used to run the model.

Scale Factor	Number of Elements	Number of Nodes	Time to Solve	Max Contact Pressure	Location of Max
0.75	336957	489543	89h 45min	42.94 kPa	Axilla
1.00	183073	268662	19h 04min	42.34 kPa	Axilla
1.25	126059	186981	10h 59min	42.19 kPa	Axilla
1.50	91826	137413	6h 06min	42.26 kPa	Axilla
1.75	67399	101855	03h 11min	39.78 kPa	Proximal anterior near trim line
2.00	Mesh quality errors -- Mesh too large				

A scale factor of 1.50 was selected for all subsequent modelling yielding a 9mm seed size constraint and a 4.5mm size constraint in areas requiring refinement. The scale factor of 1.50 was selected as when compared to the values predicted using the original seed size values (factor of

1.00), it maintain less than 0.2% difference in the maximum contact pressure value, predicted the maximum value as occurring in the same anatomical location, and reduced computation time from 19h 04min to 6h 06min.